

# Classification of Fischer type metal carbenes

**Tsibela German Tebello Mofokeng**

**Student number: 20907729**

BSc. Honours in Chemistry

Dissertation submitted in partial fulfilment of the requirements for the degree *Magister Scientiae* in Chemistry at the Potchefstroom Campus of the North-West University

Supervisor: Dr CGCE van Sittert

Co-supervisor: Dr M Landman

Assistant Supervisor: Dr JI du Toit

May 2016



## Table of contents

<b>Abbreviations .....</b>	<b>vi</b>
<b>Summary .....</b>	<b>vii-viii</b>
<b>Preface.....</b>	<b>ix</b>
<b>Chapter 1: Introduction and objectives .....</b>	<b>1-2</b>
1.1. Aim of study .....	2
1.2. Objectives .....	2-3
<b>References.....</b>	<b>4-5</b>
<b>Chapter 2: Literature review on Fischer type metal carbenes .....</b>	<b>7</b>
2.1. Introduction.....	7-9
2.2. Reactivity profile of Fischer type carbene complexes .....	9-10
2.3. Reactions of Fischer type metal carbenes .....	10-12
2.3.1. Nucleophilic attack on the carbene carbon .....	12-14
2.3.2. Benzannulation reaction.....	14-15
2.3.3. Metathesis .....	16-17
2.3.4. Cyclopropanation.....	17-18
2.3.5. Nucleophilic attack on the $\alpha$ -carbon (reaction with imines) .....	18-19
2.4. Computational investigations of Fischer carbenes .....	19-20
2.4.1. Mono-metallic Fischer carbenes .....	20-22

2.4.2. Bi-metallic Fischer carbenes.....	22-23
2.5. Summary .....	23-24
<b>References.....</b>	<b>25-28</b>
<b>Chapter 3: Research methodology .....</b>	<b>29</b>
3.1. Introduction to principal component analysis (PCA) .....	29
3.1.1. Definitions.....	29
3.1.2. From eigenvalues to principal components .....	29-32
3.1.3. Example of a principal component analysis with a larger dataset .....	33
3.2. Example of how a statistical software can be used for PCA .....	34
3.2.1. Table of chemical properties.....	34
3.2.2. Correlation matrix and redundant chemical properties.....	35-39
3.2.3. % Total variance and eigenvalues.....	40-42
3.2.4. Loadings and scores plots .....	42-46
3.3. Computational method.....	46
3.3.1. Geometry optimization .....	46-48
3.3.2. Single-point energy and property calculation .....	49-50
3.3.3. Natural bond orbital (NBO) .....	50
3.3.4. Shielding .....	50-51
3.3.5. Multivariable data analysis .....	51-52
<b>References.....</b>	<b>53-54</b>



<b>Chapter 4: Results and Discussion .....</b>	<b>55</b>
4.1. Method validation .....	55-58
4.2. Principal component analysis (PCA).....	59-66
4.3. Complexes which are candidates for nucleophilic attack reactions.....	66-67
4.3.1. Electrophilicity indices .....	67-68
4.3.2. NPA charges .....	68-70
4.3.3. Intra-molecular $ E_{\text{HOMO}}-E_{\text{LUMO}} $ energy gap .....	70-72
4.3.4. Polarization and hybridization within the TM-C and $\text{TM}^1\text{-C}^1$ bonds .....	72-74
4.3.5. Inter-molecular $ E_{\text{HOMO}}-E_{\text{LUMO}} $ energy gap .....	75
4.3.6. Atomic orbital coefficients .....	76-78
4.4. Complexes which are candidates for metathesis and benzannulation reactions.....	79-84
4.4.1. Electrophilicity indices .....	84-85
4.4.2. NPA charges and Atomic orbital coefficients .....	85-91
4.4.3. Intra-molecular $ E_{\text{HOMO}}-E_{\text{LUMO}} $ energy gap .....	91-93
4.4.4. Polarization and hybridization within the TM-C and $\text{TM}^1\text{-C}^1$ bonds .....	93-96
4.4.5. Donor-acceptor interactions of natural bonding orbitals (NBO) in TM-C and $\text{TM}^1\text{-C}^1$ bonds .....	97-98
4.4.6. Shielding .....	99-100
4.5. Conclusion .....	100

4.5.1. Principal component analysis .....	100-101
4.5.2. Mono-and bi-metallic complexes with all ligands attached .....	101
4.5.3. Mono-and bi-metallic complexes with a trans-CO dissociated from TM or TM <sup>1</sup> ....	101-102
4.5.4. Complexes identified for nucleophilic attack, benzannulation and metathesis reactions .....	102
<b>References .....</b>	<b>103-104</b>
<b>Chapter 5: Conclusions and recommendations .....</b>	<b>105</b>
5.1. Conclusions.....	105
5.1.1. A comprehensive literature review on metal carbene complexes, especially Fischer type metal carbene complexes .....	105
5.1.2. Verification of the molecular modelling method with the aid of crystal data and statistical techniques.....	106
5.1.3. Evaluating the influence of various transition metals (single or double; the same or different) and various ligands on chemical properties .....	106-107
5.1.4. Employing multivariate statistical analysis to identify chemical properties that can be used to classify these Fischer type metal carbenes.....	107
5.1.5. Identifying complexes that can be used for various reactions, <i>i.e.</i> nucleophilic attack reactions, benzannulation and metathesis, based on their chemical properties .....	107-108
5.2. Recommendations.....	108
<b>References .....</b>	<b>109</b>
<b>Acknowledgements .....</b>	<b>111</b>
<b>Supplementary material .....</b>	<b>113</b>

<b>Supplementary document S1:</b> List of Complexes .....	114-117
<b>Supplementary document S2:</b> Method validation, bond lengths(Å) and angles (°) .....	118-126
<b>Supplementary document S3:</b> Eigenvalues and %Total variance for PCA 1 to PCA 5..	127-130
<b>Supplementary document S4:</b> Frontier orbital energies .....	131-132
<b>Supplementary document S5:</b> Intra-molecular $E_{\text{HOMO}}-E_{\text{LUMO}}$ energy gap and electrophilicity index ( $\omega$ ) .....	133-134
<b>Supplementary document S6:</b> Pictorial representation of HOMO and LUMO.....	135-143
<b>Supplementary document S7:</b> Fragment contribution to HOMO and LUMO .....	144-154
<b>Supplementary document S8:</b> Natural Population Charges .....	155-159
<b>Supplementary document S9:</b> Sheilding Parameters.....	160-161
<b>Supplementary document S10:</b> Hydridization of the transition metal-carbene bond (NBO analysis) .....	162-170
<b>Supplementary document S11:</b> Donor-Acceptor interactions (NBO analysis).....	171-172
<b>Supplementary document S12:</b> PCA worksheets .....	173-181

## **Abbreviations**

DFT	Density Function Theory
NBO	Natural bond orbital
NPA	Natural population analysis
PCA	Principal component analysis
PC	Principal component
TM-C	Transition metal-carbene carbon bond

## Summary

**Keywords:** DFT, PCA, NBO, NPA charges, Electrophilicity index, Fischer type carbenes

---

Fischer type metal carbene complexes are used as catalysts in various organic synthesis reactions, e.g. metathesis, cyclopropanation and benzannulation. Nevertheless, the mechanisms of the above-mentioned reactions are not properly understood, especially with regard to frontier orbital interactions.

Therefore, the focus of this study is on the classification of various Fischer type metal carbene complexes based on their catalytic activity for various reactions. A modified molecular modelling method used to classify these complexes was developed in previous studies in the Catalysis and Synthesis Group at the North-West University. The Fischer type carbene complexes with heteroaromatic groups investigated in this study were synthesised by a research group at the University of Pretoria. The heteroaromatic groups of interest in this study are furan, bithiophene, N-methyl-thieno[3,2-b]pyrrole, 2-(2'-thienyl)furan and N-methyl-2-(2'-thienyl)-pyrrole.

Twenty five Fischer carbene complexes were optimized using Materials Studio 6.0 DMol<sup>3</sup> density functional theory (DFT) module with the GGA/PW91 functional and the DNP basis set. Electronic and steric parameters were calculated for each Fischer carbene complex using Gaussian09, Chemissian and Solid-G. The data obtained from these calculations were analysed using principal component analysis within Statistica version 12 in order to establish trends.

Therefore, computational techniques such as NBO analysis, NPA charges, shielding, frontier orbital analysis and multivariate analysis were used to classify these Fischer type carbene complexes according to their chemical properties. Results obtained from NPA charge analysis of the TM-C bonds indicate that the carbene carbons attached to chromium have a higher positive charge than those attached to tungsten. This explains the preference for chromium based Fischer type carbene complexes for benzannulation reactions.

Furthermore based on electrophilicity indices we conclude from this study that complexes **A3** (furyl-substituted), **B9** (N-methyl-thieno[3,2-b]pyrrolyl-substituted) and **C15** (bithienyl-

substituted) (**Chapter 4**) are suitable candidates for nucleophilic attack reactions; while complexes **C12** (bithienyl-substituted), **C13** (bithienyl-substituted) and **D23** (2-(2'-thienyl)furyl-substituted) (**Chapter 4**) are suitable for benzannulation and metathesis reactions. Complexes **A4** (furyl-substituted) and **B6** (N-methyl-thieno[3,2-b]pyrrolyl-substituted) are suitable for both nucleophilic attack, metathesis and benzannulation reactions.

## Preface

**Chapter 1** provides a general overview of Fischer type metal carbene complexes, the aim of this study and objectives that will be used to guide this study. A literature study is included in **Chapter 2**, which focuses on the chemical properties of the following complexes; furyl, bithienyl, N-methyl-thieno[3,2-b]pyrrolyl, 2-(2'-thienyl)furyl and N-methyl-2-(2'-thienyl)-pyrrolyl substituted Fischer type metal carbenes, reactions of these Fischer type metal carbenes and computational methods that were previously used to investigate these Fischer type metal carbene complexes.

**Chapter 3** outlines the computational techniques and software used to analyse these complexes.

Computational investigations of the previously mentioned five-membered heteroaromatic ring substituted Fischer type carbene complexes are provided in **Chapter 4**. The focus of this chapter is to employ various computational methods in order to classify these Fischer type metal carbene complexes with regard to their chemical properties. After classifying these complexes, molecular orbital interaction studies are conducted in order to suggest possible reactions for these complexes.

Finally, conclusions and recommendations derived from the knowledge obtained from the literature study and computational investigations are provided in **Chapter 5**.





## Chapter 1: Introduction and objectives

Geuther and Hermann were the first to propose the existence of a neutral carbene species in 1855.<sup>1</sup> However, transition metal carbenes only became popular after the synthesis of  $(\text{CO})_5\text{W}=\text{C}(\text{Ph})(\text{OMe})$  by Fischer and Maasböl in 1964.<sup>2,3,4</sup> Fischer type carbene complexes are low valent, 18-electron complexes and have electron donating substituents bonded to the carbene carbon;<sup>2-6</sup> furthermore, the carbene carbon is known to be electrophilic. The metal fragment is usually from the middle or late transition metal group, *i.e.* W(0), Cr(0), Mo(0), Fe(0) and Co(0).

Alkynyl- or alkenyl substituted Fischer type metal carbenes are more reactive towards nucleophiles than their analogues of  $\alpha,\beta$ -unsaturated thioesters, amides and esters.<sup>2-4,7(a),(b)</sup> This increased reactivity can be ascribed to the strong  $\pi$ -electron withdrawing carbonyl ligands of the metal moiety, which results in an increased acidity of the  $\alpha$ -carbon and hydrogen.<sup>2</sup> Therefore, these Fischer type carbene complexes are exceptional candidates for nucleophilic substitutions,<sup>2,8,9</sup> benzannulation,<sup>2,9(a),(b)</sup> cyclopropanation<sup>10</sup> and Diels-Alder cycloaddition<sup>11</sup> reactions, among others.

The synthesis of mono-nuclear Fischer type carbenes of the form  $[(\text{CO})_5\text{Cr}=\text{C}(\text{X})\text{Z}]$  where X is an ethoxy or amino group and Z is a heteroaromatic substituent has been explored since the 1970s.<sup>12,13</sup> In recent years, the synthesis of mono- and bi-nuclear 5-membered heteroaromatic (furyl, bithienyl, N-methyl-thieno[3,2-b]pyrrolyl, 2-(2'-thienyl)furyl and N-methyl-2-(2'-thienyl)pyrrolyl) substituted Fischer type carbene complexes with carbonyl and 1,2-bis(diphenylphosphino)ethane metal ligands have been reported.<sup>13-21</sup> This was followed by a series of structural<sup>12,16</sup> and electrochemical investigations of these complexes using DFT, X-ray crystallography and cyclic voltammetry.<sup>16-21</sup> Density function theory (DFT) and cyclic voltammetry studies of these complexes confirmed that the oxidation of these complexes occurs on the HOMO while reduction occurs on the LUMO.<sup>19,21</sup> Furthermore, natural bond orbital (NBO) analysis was used to analyse the possible orbital interactions between the metal fragments, the carbonyl ligands and the heteroaromatic ring.<sup>22</sup>

The application of these 5-membered heteroaromatic Fischer type carbene complexes (as shown in Table 1.1) for benzannulation,<sup>22,27</sup> carbene-carbene coupling<sup>22</sup> between two Fischer type carbene complexes and substitution<sup>21-25</sup> reactions was also investigated.

**Table 1.1:** 5-membered heteroaromatic complexes used for various reactions<sup>21-27</sup>

Complexes	Reaction
$(\text{CO})_5\text{M}=\text{C}(\text{X})\text{Z}$ ; M = W or Mo, X= ethoxy, Z = furyl, thienyl	Ethoxy substitution and carbonyl-ligand substitution reactions
$\text{CO}_5\text{M}=\text{C}(\text{X})-\text{Z}-(\text{X})\text{C}=\text{M}^1(\text{CO})_5$ ; M/M <sup>1</sup> = Cr or W, X= ethoxy, Z = furyl, bithienyl or 2-(2'-thienyl)furyl	Carbene-carbene coupling and benzannulation reactions reactions

Nevertheless the reaction mechanisms of these reactions is still not properly understood especially with regards to frontier orbital interaction. Therefore this study will highlight the research that has been done in previous studies on furyl-, bithienyl-, N-methyl-thieno[3,2-b]pyrrolyl-, 2-(2'-thienyl)furyl- and N-methyl-2-(2'-thienyl)pyrrolyl-substituted Fischer type carbene complexes. This will be followed by identifying work that still needs to be done in order to understand the reaction mechanisms of these Fischer type metal carbene complexes.

### 1.1. Aim of study

The aim of this study is to identify and investigate factors that influence the activity of Fischer type metal carbene complexes for various catalytic reactions with the aid of molecular modelling techniques.

### 1.2. Objectives

The following objectives are proposed as part of the research methodology:

1. A comprehensive literature review on metal carbene complexes, especially Fischer type metal carbene complexes.
2. Verify molecular modelling method with the aid of crystal data and statistical techniques.

3. Evaluate the influence of various transition metals (single or double; the same or different) and various ligands on chemical properties.
4. Employ multivariate statistical analysis to identify chemical properties that can be used to classify these Fischer type metal carbenes.
5. Identify complexes that can be used for various reactions, *i.e.* nucleophilic attack reactions, benzannulation and metathesis, based on their chemical properties.

## References

1. Geuther, A.; Hermann, M. *Liebigs Ann. Chem.* **1855**, 95, 211.
2. Dorwald, F. Z. *Metal Carbenes in Organic Synthesis*, Wiley-VCH (Weinheim), **1999**.
3. Fischer, E. O.; Maasböl, A. *Angew. Chem. Int. Ed. Engl.* **1964**, 3, 580.
4. Schrock, R. R. *J. Am. Chem. Soc.* **1974**, 96, 6796-6767.
5. Brookhart, M.; Studabaker, W. B. *Chem. Rev.* **1907**, 87, 411-432.
6. Mathey, F.; Sevin, A. *Molecular chemistry of the transition elements – An introduction course*, Wiley: Chichester, **1996**. (a) Wu, Y. T.; Kurahashi, T.; de Meijere, A. *J. Organomet. Chem.* **2005**, 690, 5900-5911. (b) Hoffmann, R. *Angew. Chem.* **1982**, 94, 725.
7. (a) Casey, C. P.; Anderson, R. L. *J. Am. Chem. Soc.* **1974**, 96, 1230. (b) Wulff, W. D.; Liebeskind, L. S. *Advances in Metal–Organic Chemistry*, JAI Press: London, **1989**, 1, 209.
8. Crabtree, R. H. *The organometallic chemistry of the transition metals*; John Wiley and Sons, 4<sup>th</sup> ed, **2005**.
9. (a) Minatti, A.; Dötz, K. H. *Topics in organomet chem.* **2004**, 13, 123-156. (b) Casey, C. P.; Jones, M. Jr.; Moss, R. A. *Reactive Intermediates*; Wiley: New York, **1981**, 2, 152.
10. Dötz, K. H. *Metal carbenes in organic synthesis, Topics in Organometallic Chemistry*, Springer: **2004**, 13.
11. Inukai, T.; Kojima, T. *J. Org. Chem.* **1965**, 30, 3567.
12. Thompson, S.; Wessels, H. R.; Fraser, R.; van Rooyen, P. H.; Liles, D. C.; Landman, M. J. *Mol. Struct.* **2014**, 1060, 111-118.
13. Crause, C. *Synthesis and application of carbene complexes with heteroaromatic substituents*, PhD, University of Pretoria, **2004**.
14. Lotz, S.; Landman, M.; Görls, H.; Crause, C.; Nienaber, H.; Olivier, A. *Naturforsch.* **2007**, 62b, 419-426.

15. Lotz, S.; van Jaarsveld, N. A.; Liles, D. C.; Crause, C.; Görls, H.; Terblans, Y. M. *Organometallics*. **2012**, *31*, 5371-5383.
16. Van Jaarsveld, N. A.; Liles, D. C.; Lotz, S. *Dalton Trans.* **2010**, *39*, 5777-5779.
17. Landman, M.; Görls, H.; Lotz, S. *J. Organomet. Chem.* **2001**, 617-618, 280-287.
18. Landman, M.; Liu, R.; van Rooyen, P. H.; Conradie, J. *Electrochim. Acta.* **2013**, *114*, 205-214.
19. Landman, M.; Liu, R.; Fraser, R.; van Rooyen, P. H.; Conradie, J. *J. Organomet. Chem.* **2014**, *752*, 171-182.
20. Landman, M.; Ramontja, J.; van Staden, M.; Bezuidenhout, D. I.; van Rooyen, P. H.; Liles, D. C.; Lotz, S. *Inorg. Chim. Acta.* **2010**, *363*, 705-717.
21. Landman, M.; Pretorius, R.; Buitendach, B. E.; van Rooyen, P. H.; Conradie, J. *Organometallics*. **2013**, *23*, 5491-5503.
22. Van der Westhuizen, B.; Swarts, P. J.; van Jaarsveld, L. M.; Liles, D. C.; Siegert, U.; Swarts, J. C.; Fernandez, I.; Bezuidenhout, D. I. *Inorg. Chem.* **2013**, *52*, 6674-6684.
23. Landman, M.; Pretorius, R.; Fraser, R.; Buitendach, B. E.; Conradie, M. M.; van Rooyen, P. H.; Conradie, J. *Electrochim. Acta.* **2014**, *130*, 104-118.
24. Crause, C. *Synthesis and application of carbene complexes with heteroaromatic substituents*, PhD, University of Pretoria, **2004**.
25. Levell, T. M. *Substituted Fischer carbene complexes of molybdenum(0)*, MSc, University of Pretoria, **2014**.
26. Ramontja, J. *Biscarbene Complexes of Bithiophene*, MSc, University of Pretoria, **2005**, 17.
27. Lotz, S.; Crause, C.; Olivier, A. J.; Liles, D. C.; Görls, H.; Landman, M.; Bezuidenhout, D. I. *Dalton Trans.*, **2009**, 697, 697-710.



## Chapter 2: Literature review

### 2.1. Introduction

Incorporating transition metals in organic complexes has been found to stabilize short-lived and reactive molecules.<sup>1</sup> Therefore, transition metal carbene complexes gained great interest for various reactions. Fischer type metal carbene complexes with low-valent group VI to VIII transition metals are known to have an electrophilic carbene carbon. This makes them great candidates for nucleophilic attack reactions.<sup>2</sup> Fischer and Maasböl suggested the synthesis of a metal carbene complex of the form  $(\text{CO})_5\text{W}=\text{CMe}(\text{OMe})$ .<sup>3</sup> According to Fischer and Maasböl, this complex could be formed by the reaction between  $\text{W}(\text{CO})_6$  and  $\text{LiMe}$ , followed by protonation and subsequent treatment with  $\text{CH}_2\text{N}_2$ . This was followed by the synthesis of a series of Fischer type mono-carbene complexes with other transition metals, *i.e.* chromium, molybdenum, iron and cobalt. Fischer then reported the synthesis of a bis-carbene complexes by reacting chromium hexacarbonyl with 1,2-dilithiobenzene.<sup>3</sup> The synthesis of arene-substituted Fischer type bis-carbene complexes requires the formation of two adjacent carbanions. This step is often challenging.<sup>4,5</sup> Five-membered mono-nuclear bis-carbene complexes can be synthesised without the formation of two adjacent carbanions. Therefore, the synthesis of Fischer type carbenes with five-membered heterocyclic substituents gained great interest as alternatives to the arene-substituted Fischer type complexes. Connor *et al.*<sup>6</sup> reported Fischer type carbene complexes with five-membered heterocyclic substituents as early as 1971.

Heteroaromatic rings can be used as spacers between two metal moieties in homo- or heteronuclear bi-metallic carbenes, as indicated by **Figure 2.1**. The incorporation of heteroaromatic spacers facilitates electron transfer between two metal fragments through the delocalization of  $\pi$ -electrons across the heteroaromatic spacer.

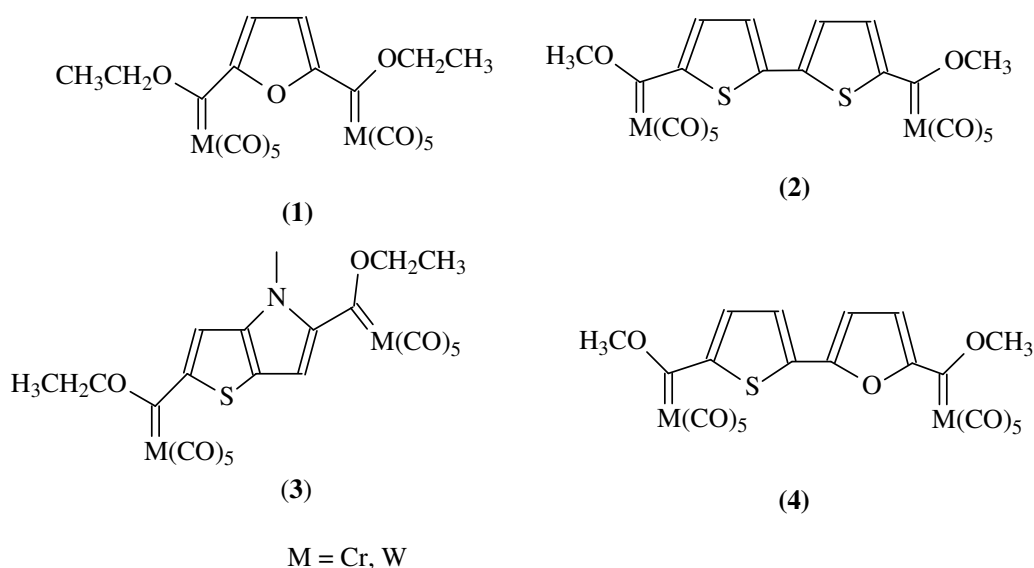


**Figure 2.1:** Bi-metallic Fischer type carbene complexes with heteroatomic substituents, *i.e.* furyl (1), bithienyl (2), N-methyl-thieno[3,2-b]pyrrolyl (3) and 2-(2'-thienyl)furyl (4)<sup>7,8</sup>

The reactivity of Fischer type metal carbenes is influenced by the presence of various heteroaromatic spacers. The five-membered heteroaromatic substituents of interest in this study are furyl, bithienyl, N-methyl-thieno[3,2-b]pyrrolyl, 2-(2'-thienyl)furyl and N-methyl-2-(2'-thienyl)pyrrolyl due to their stability in solid state and high reactivity in solution for nucleophilic attack at the carbene carbon.<sup>7,8</sup> Furthermore, regioselective template reactions at the carbene carbons could also be achieved.<sup>7</sup>

The route for synthesising N-methyl-2-(2'-thienyl)pyrrolyl substituted metal carbenes was suggested by Aoki<sup>9</sup> in a sequential lithiation method. This was followed by the synthesis of bis-carbene complexes of bithiophene as suggested by Lancellotti *et al.* in 1998.<sup>10</sup> The synthesis of some bithiophene carbene analogues were also reported by Landman<sup>8</sup> and Moeng<sup>11</sup> in 2001 and 2010, respectively. Fischer type carbene complexes with N,N'-dimethylbipyrrolyl substituents were reported by Olivier,<sup>12</sup> while Crause *et al.*<sup>13</sup> synthesised bis-carbene furyl complexes.

Investigating the influence of different transition metals, combinations of transition metals and different ligands on the reactivity of this type of metal carbenes via computational methods for different reactions could lead to the classification of these carbene complexes. Therefore, this review will focus on different computational methods that were used to investigate mono- and



bi-metallic (Cr and W) complexes with five-membered heteroaromatic substituents, namely furyl, 2-(2'-thienyl)furyl, N-methyl-2-(2'-thienyl)pyrrolyl, bithienyl and N-methyl-thieno[3,2-b]pyrrolyl that were synthesised by a research group at the University of Pretoria.<sup>4,7,8,13,14-20</sup> Reactions of Fischer type metal carbene complexes, *i.e.* nucleophilic substitution reactions, cyclopropanation, benzannulation and metathesis will also be investigated.<sup>14-23</sup>

## 2.2. Reactivity profile of Fischer type carbene complexes

The reactivity of metal carbenes is related to the extent to which the substituents donate electrons to the vacant p-orbital on the carbene carbon. The carbene carbon of Fischer type carbene complexes of the form  $(\text{CO})_5\text{Cr}=\text{C}(\text{Ph})\text{OMe}$  are poor  $\pi$ -acceptors and good  $\sigma$ -donors.<sup>5</sup> Bond formation in Fischer carbenes occurs between a singlet carbene and the vacant d-orbitals on the transition metal fragment (**Figure 2.2**).<sup>2,24,25</sup>

The transition metal-carbene orbital interaction in Fischer type carbenes is formally illustrated by the Dewar-Chatt-Duncanson (DCD) model.<sup>2</sup> This model suggests that the transition metal-carbene bond is formed as a result of  $\sigma$ -electron donation from the lone pair orbital on the carbene carbon to the vacant d-orbital of the transition metal. The second interaction occurs as a result of  $\pi$ -electron back-donation from the occupied d-atomic orbital of the transition metal to the vacant p orbital of the carbene carbon (**Figure 2.2**).<sup>2</sup> This donor-acceptor model was further investigated and proven to be valid by Marques.<sup>26</sup>

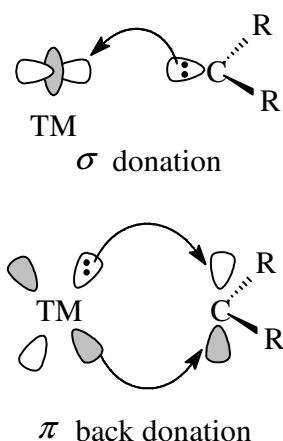


**Figure 2.2:** Dominant molecular orbital contributions towards the formation of the transition metal-carbene (TM-C bond) in Fischer type metal carbene complexes.<sup>2,24,25</sup>

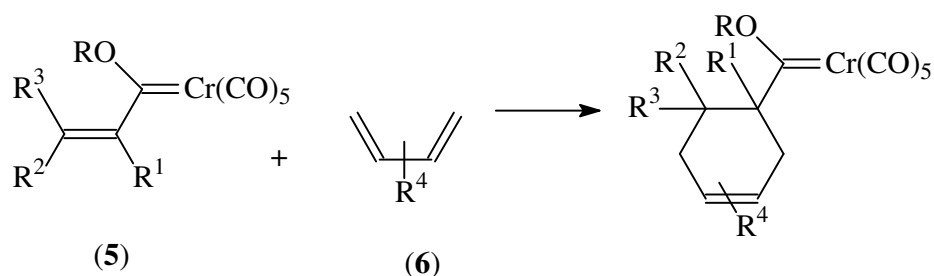
The transition metal-carbene bond of Fischer type carbene complexes has a partial double bond electronic character,<sup>27</sup> which can be attributed to the carbene substituents that stabilize the carbene carbon.<sup>28,29</sup> Fischer type carbenes are prone to nucleophilic attack on the carbene carbon, due to the electrophilic nature of the transition metal-carbene bond.<sup>29-31</sup> The  $\pi$ -electrons are polarized towards the metal; the electron deficient carbene carbon is usually stabilized by heteroatom substituents; while the metal is stabilized by a strong  $\pi$ -acceptor ligand, *i.e.* phosphine, cyclopentadienyl or carbonyl ligand.<sup>1</sup>

Recent studies suggest that the reactivity of the Fischer type metal carbenes of the form  $(\text{CO})_5\text{Cr}=\text{C}(\text{X})\text{R}$ ; with  $\text{X} = \text{NH}_2, \text{OCH}_3$  and  $\text{OCH}_2\text{CH}_3$  and  $\text{R} = \text{aryl, alkene}$  and the heteroaromatic ring, depends predominantly on the  $\pi$ -electron donation from the X group and resonance within the conjugated  $\pi$ -electron system of the R group.<sup>2,32-35</sup>

Incorporating heteroatoms in conjugated carbon chains enhances charge transfer properties within Fischer type carbene complexes. Metal moieties improve polarization of electron density by extending the conjugation of the  $\pi$ -electron system from one metal to another in bi-metallic Fischer type carbene complexes. The presence of different metals facilitates a ‘push-pull’ effect due to charge transfer properties.<sup>13</sup> This effect causes the length of the transition metal-carbene bonds within bi-metallic carbene complexes to differ in length when two different metal moieties are incorporated within these complexes, as evidenced by x-ray crystallographic studies.<sup>13</sup>

### 2.3. Reactions of Fischer type metal carbenes

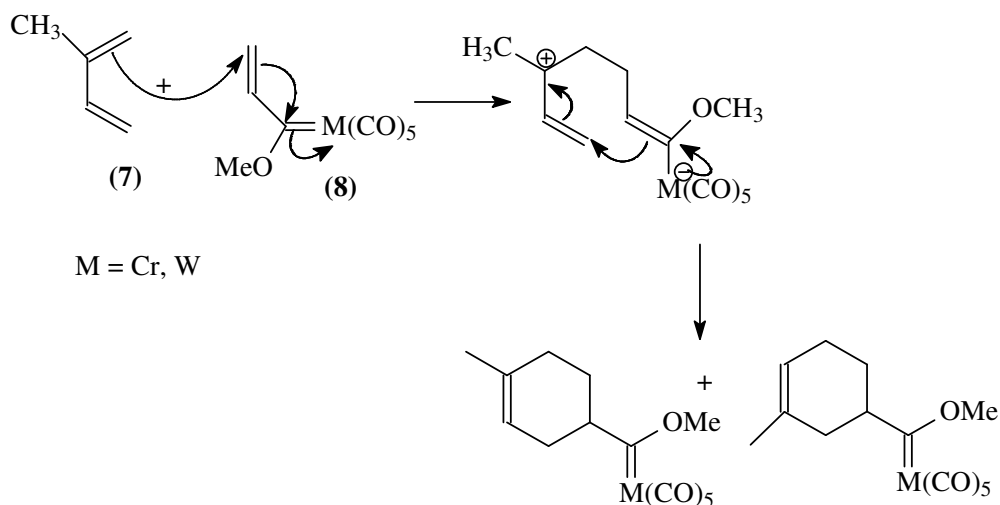
Fischer type carbene complexes are often referred to as isolobal analogues of esters.<sup>36-40</sup> This can be observed in [4+2] Diels–Alder cycloaddition reactions.<sup>41-43</sup> Fischer type metal carbenes can be used for reactions similar to the Diels–Alder cycloaddition reactions, as indicated in **Scheme 2.1**.



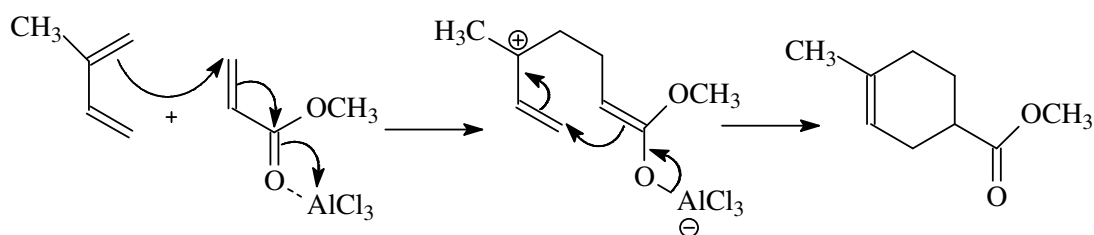
**Scheme 2.1:** Reaction similar to Diels-Alder cycloaddition reaction with Fischer type metal carbene<sup>43</sup>

The electron withdrawing properties of the pentacarbonyl metal fragment bestow these complexes with a reactivity profile similar to that of activated esters ( $\alpha,\beta$ -unsaturated esters).<sup>13</sup> This is evident in reactions such as nucleophilic substitution,<sup>13</sup> cyclopropanation,<sup>41-43</sup> deprotonation, methyl acrylate and isoprene reactions,<sup>43</sup> 1,3-dipolar cycloadditions with diazo complexes and benzannulation reactions, among others.<sup>44-46</sup>

A typical example of this concept is observed when the pentacarbonyl chromium(0) fragment activates the reaction between [(methoxy)(vinyl)pentacarbonyl]chromium(0) carbene (complex **8**) and isoprene (complex **7**) (**Scheme 2.2**), to a reaction rate that is comparable to that of isoprene and methyl acrylate in the presence of aluminium chloride (**Scheme 2.3**).<sup>43</sup> In the first step, the aluminium chloride activates the dienophile by increasing the polarization of the  $\alpha,\beta$ -double bond, thereby making it more susceptible to diene attack as observed in **Scheme 2.3**. The formed zwitterion undergoes an intra-molecular cyclization with the release of the aluminium chloride in order to form a cyclic hexene complex (**Scheme 2.3**).



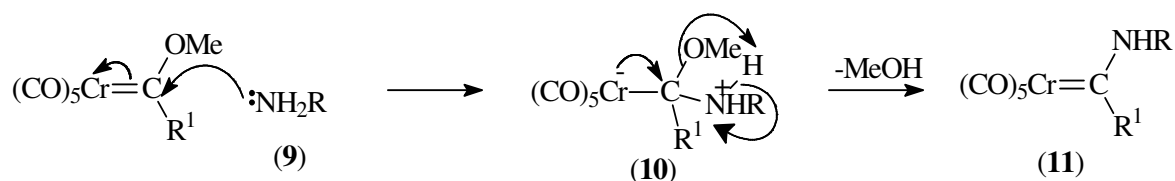
**Scheme 2.2:** Reaction between isoprene and Fischer carbene<sup>43</sup>



**Scheme 2.3:** Reaction between isoprene and methyl acrylate<sup>43</sup>

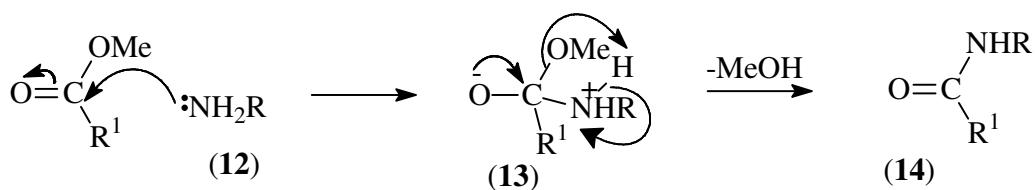
### 2.3.1. Nucleophilic attack on the carbene carbon

The transition metal-carbene bond is polarized, thereby leaving the carbene with a partial positive charge and the metal fragment with a partial negative charge.<sup>2</sup> Therefore, these complexes are more likely to undergo nucleophilic attack reactions on the carbene carbon or other reactions similar to those of  $\alpha,\beta$ -unsaturated esters. Amino Fischer type metal carbenes (complex **11**) can be synthesised by a nucleophilic attack of an amine's (complex **9**) lone pair on the carbene carbon in order to yield a zwitterionic intermediate (complex **10**). This is followed by the loss of methanol (**Scheme 2.4**).<sup>23,47</sup> This reaction resembles that of an ester and an amine (**Scheme 2.5**).



$\text{R}^1$  = aryl, alkene, alkane  
 $\text{R}$  = alkane

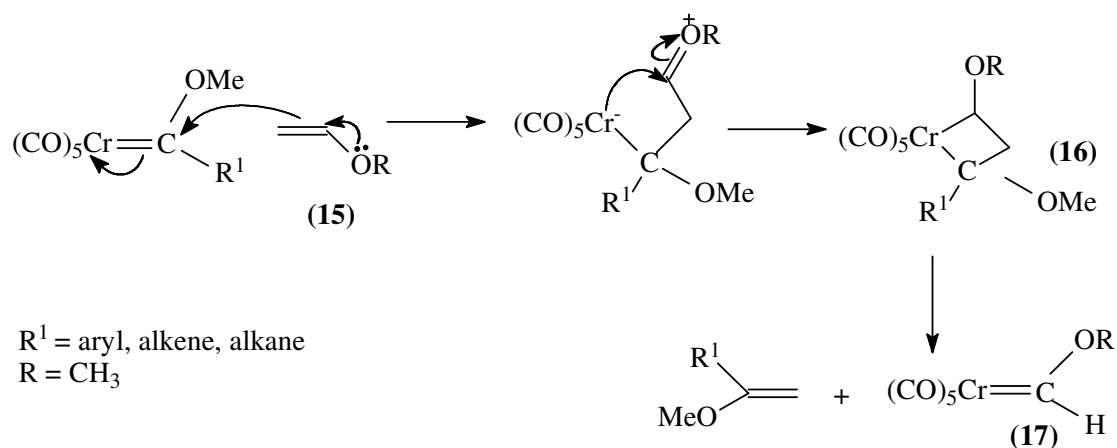
**Scheme 2.4:** Amino carbene synthesis from nucleophilic attack<sup>23,47</sup>



$\text{R}^1$  = aryl, alkene, alkane  
 $\text{R}$  = alkane

**Scheme 2.5:** Reaction of an ester and an amine<sup>47</sup>

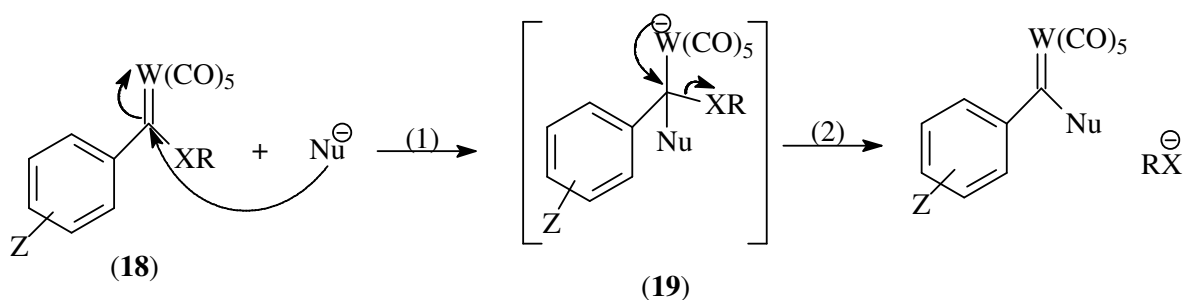
A nucleophilic attack with ethenyl methyl ether (complex **15**) will yield a zwitterion that leads to the production of a metallacycle (complex **16**). This cyclic complex dissociates to form a metal carbene (complex **17**) and an alkene (Scheme 2.6).<sup>47,48</sup>



$\text{R}^1$  = aryl, alkene, alkane  
 $\text{R} = \text{CH}_3$

**Scheme 2.6:** Nucleophilic attack reaction with ethenyl methyl ether<sup>40,47,48</sup>

Fischer and co-workers reported the first nucleophilic substitution reaction in 1967.<sup>52</sup> Fischer type carbenes containing good leaving groups, *i.e.* alkoxy, silyloxy or alkylthio, can easily be modified by nucleophilic attack on the carbene carbon.<sup>52</sup> Fischer carbenes containing amino groups do not readily undergo this type of substitution, since amines are poor leaving groups. Neutral or anionic nucleophiles, *i.e.* amines, hydrazines, oximes, alkyllithium,<sup>52</sup> malonitrile anion and alkoxides, among others, can be used in these S<sub>N</sub>2-type reactions. Anionic nucleophilic substitutions occur in two steps as indicated by **Scheme 2.7**; the first step involves a nucleophilic attack on the carbene carbon. This results in the formation of a tetrahedral intermediate (complex **19**). The negative charge on tungsten is finally stabilized by the formation of a double bond between the carbene carbon and the metal; this is accompanied by the elimination of the leaving group.<sup>52</sup>



R = Alkyl, aryl

X = S, O, OSi

Z = NMe<sub>2</sub>, MeO, Me, H, F, Cl, CF<sub>3</sub>

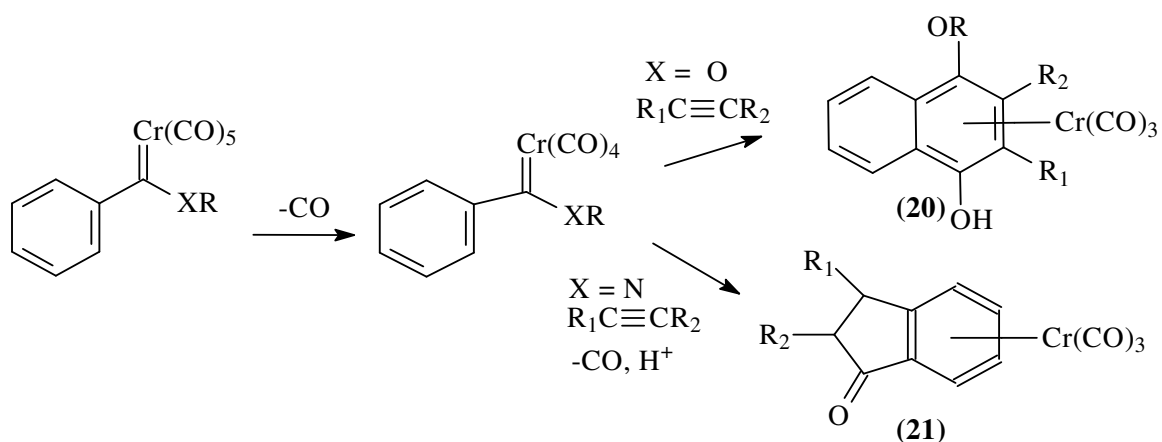
**Scheme 2.7:** Nucleophilic substitution with anionic nucleophile<sup>52</sup>

Benzannulation and metathesis reactions are both initiated by elimination of a carbonyl ligand, and therefore a metal moiety with a vacant coordination site is created in both cases.<sup>49-51</sup>

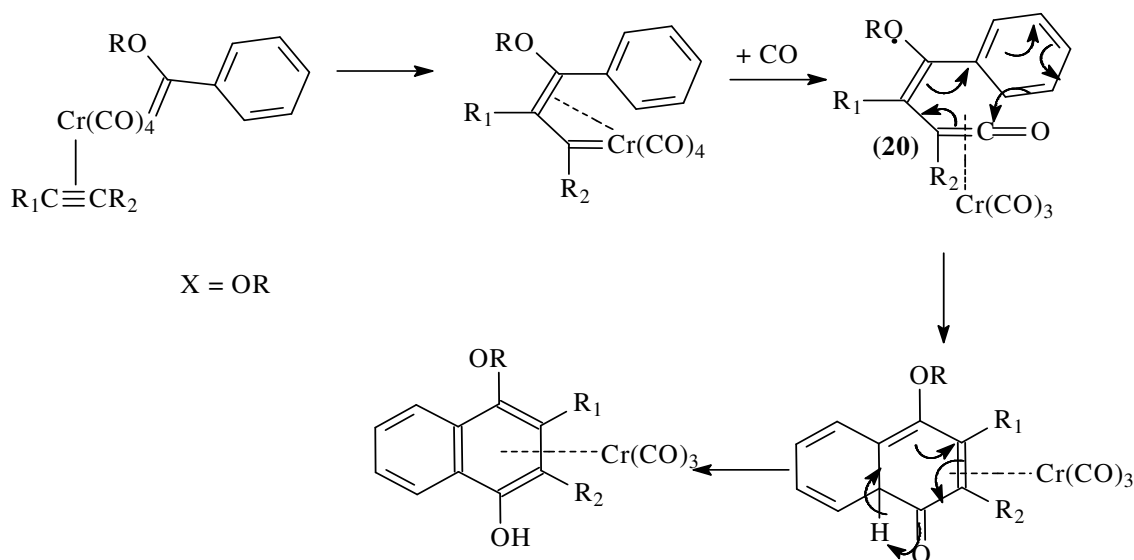
### 2.3.2. Benzannulation reaction

Benzannulation reactions of group 6 Fischer type carbenes are among a few well-developed reactions of Fischer type carbene complexes that have synthetic applications.<sup>53-56</sup> Six-membered ring benzannulation products are formed predominantly from chromium-based Fischer type carbene complexes, while molybdenum and tungsten Fischer type carbenes are more likely to form five-membered rings.<sup>16</sup> Investigations by Block *et al.*<sup>33</sup> confirmed that benzannulation with Fischer type carbenes prefers chromium-based carbenes. Therefore, these reactions often occur

between group 6 Fischer type carbenes (chromium alkoxy carbenes) and an alkyne to yield p-alkoxyphenol (complex **20**).<sup>2</sup> This reaction is initiated by the elimination of CO (**Scheme 2.8**), then incorporating a carbonyl and alkyne to form a vinylketene intermediate (complex **22**), followed by an electrocyclic ring closure (**Scheme 2.9**).<sup>2,57</sup> In contrast, amino carbene complexes yield indanones (complex **21**) instead of phenols because the CO insertion step does not occur (**Scheme 2.8**).



**Scheme 2.8:** Dötz benzannulation reaction<sup>2</sup>



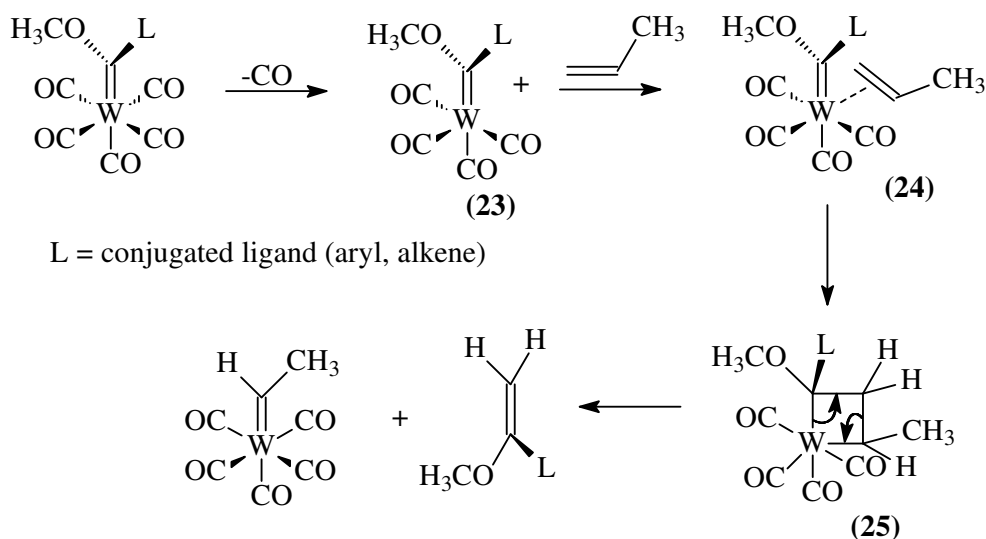
**Scheme 2.9:** Alkyne and CO insertion during benzannulation<sup>49</sup>

### 2.3.3. Metathesis

Fischer type metal carbenes can also be used in alkene metathesis even though they are not as popular as Grubbs or Schrock type carbenes for this type of reaction.<sup>21,22</sup> A typical example of a metathesis reaction involving Fischer type carbene complex occurs between an electron-rich alkene and a Fischer type carbene complex of tungsten, chromium or molybdenum. Chromium-based Fischer type metal carbenes are better candidates for metathesis reactions than tungsten- or molybdenum-based Fischer type carbenes.<sup>50,51</sup> This can be ascribed to the notion that the carbene carbon attached to chromium is more electrophilic than that attached to tungsten or molybdenum.<sup>7,33</sup> Block *et al.*<sup>33</sup> used Mulliken charges to validate this preference for chromium carbenes in metathesis and benzannulation reactions.

Metathesis can take place according to one of two mechanisms, namely a dissociative and an associative mechanism. Fischer type carbene complexes prefer a Chauvin dissociative mechanism.<sup>58</sup> This is supported by a study done by du Toit *et al.*<sup>21</sup> that indicates that the formation of the bond between the alkene and the Fischer type metal carbene in an associative mechanism requires a great deal of energy. This can be ascribed to the steric hindrance that the alkene experiences while approaching the metal.<sup>21</sup> The metathesis reaction is initiated by CO dissociation to yield a metal carbene complex with a vacant coordination site on the metal (complex **23**, **Scheme 2.10**). This step is followed by incorporating a propene in order to form a partial bond between the metal and propene (complex **24**).<sup>53</sup> Complex **24** rearranges to form a metallacyclobutane intermediate (complex **25**). This intermediate then goes on to form a secondary propene.

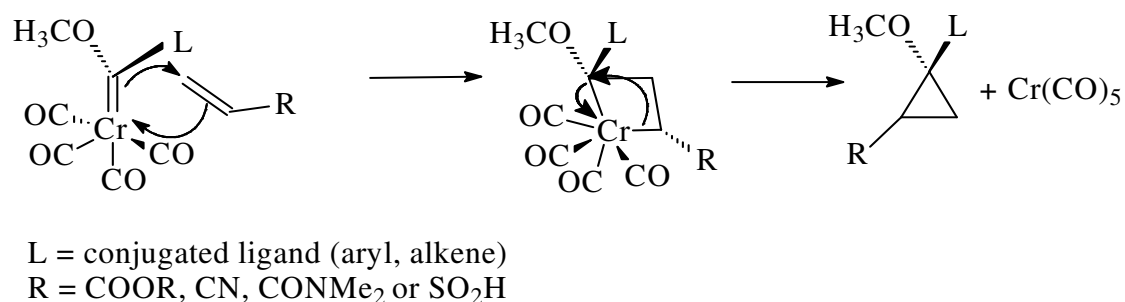




**Scheme 2.10:** Propene metathesis with Fischer carbenes<sup>43,56</sup>

#### 2.3.4. Cyclopropanation

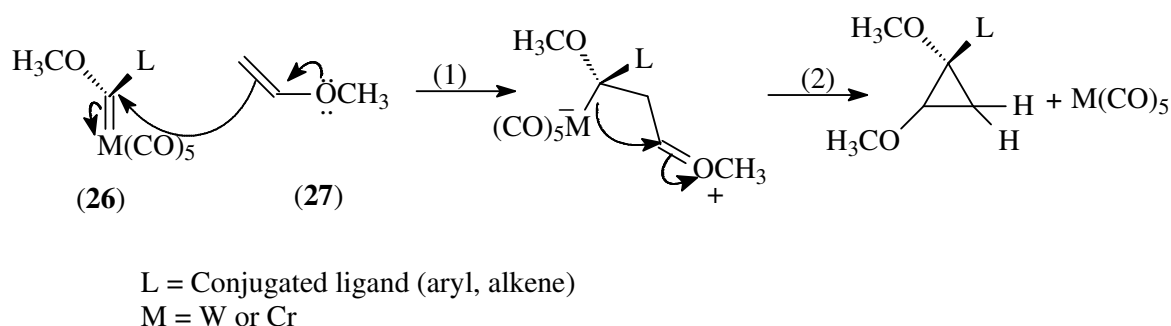
There are two routes for cyclopropanation with Fischer type carbenes depending on the substituents on the alkene. The first route (**Scheme 2.11**), which normally involves an alkene with an electron withdrawing group, *i.e.* R = COOR, CN, CONMe<sub>2</sub> or SO<sub>2</sub>H, usually follows cyclization via a metallacyclobutane intermediate.<sup>54-56</sup> This route is commenced by the dissociation of a CO ligand according to **Scheme 2.10**. The second step in this route leads to the formation of a metallacyclobutane, which eventually undergoes cyclization to form the cyclopropane (**Scheme 2.11**).



**Scheme 2.11:** Cyclopropanation via a metallacyclobutane intermediate<sup>54</sup>

The second route normally occurs with alkenes substituted with electron-donating groups, *i.e.* R = OCH<sub>3</sub>, OSiR<sub>3</sub> or NR<sub>2</sub>, where cyclization takes place via the formation of a zwitterionic intermediate.<sup>54,58</sup>

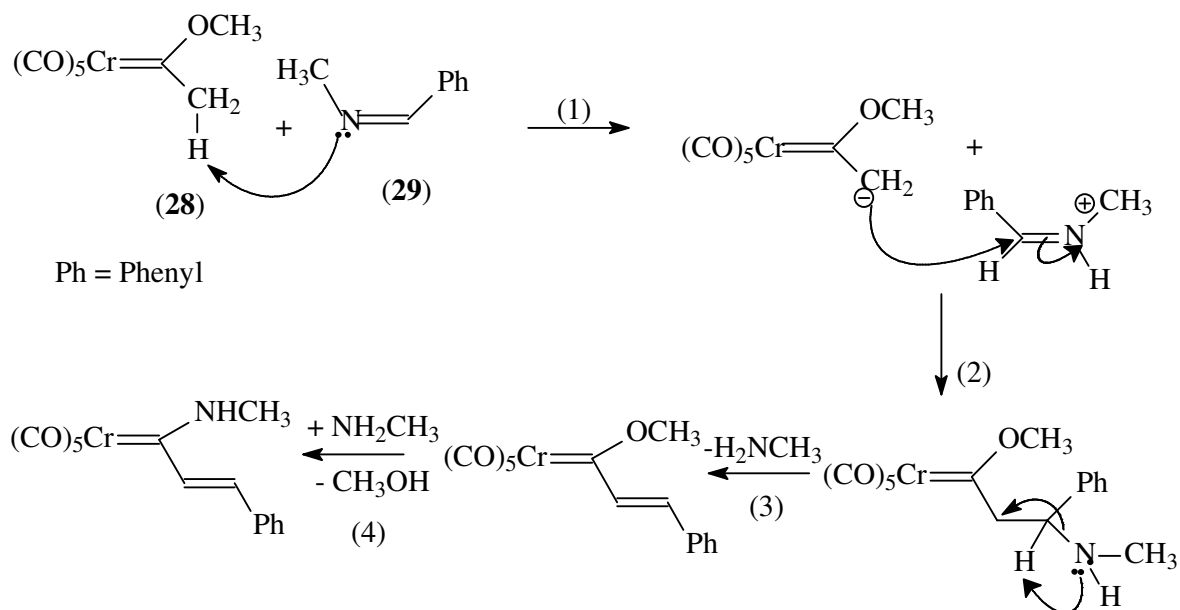
A nucleophilic attack by the  $\pi$  electrons of the ethenyl methyl ether (complex **27**) on the carbene carbon initiates this reaction (**Scheme 2.12**). This leaves the metal with a negative charge while the ether oxygen is left with a positive charge owing to its electron-donating properties. The TM-C bond breaks to form the cyclopropane as indicated by step (2) in **Scheme 2.12**.



**Scheme 2.12:** Cyclopropanation via a zwitterionic intermediate<sup>54</sup>

### 2.3.5. Nucleophilic attack on the $\alpha$ -carbon (reaction with imines)

Methyl substituents bonded to the carbene carbon can undergo a proton elimination reaction at elevated temperatures.<sup>59</sup> A typical example of such reactions occurs between pentacarbonyl-[methylmethoxycarbene]chromium (complex **28**) and N-benzylidene methylamine (complex **29**) (**Scheme 2.13**). This reaction is initiated through the abstraction of the acidic proton attached to the methyl substituent at the  $\alpha$ -position by a basic imine (complex **29**).<sup>59</sup> This leaves the  $\alpha$ -carbon with a negative charge while the N-benzylidene methylamine is left with a net positive charge. A nucleophilic attack on the tertiary carbon of benzylidene methylamine followed by the breaking of the double bond occurs in the second step to stabilize the imine. This is followed by the abstraction of hydrogen by the imine and subsequent removal of the primary amine to form a  $\alpha,\beta$ -unsaturated carbene complex. The final step is initiated by nucleophilic substitution with methylamine on the carbene carbon to yield an amine substituted Fischer type carbene complex.<sup>59</sup>



**Scheme 2.13:** Reaction of pentacarbonyl[methylmethoxycarbene]chromium and N-benzylidene methylamine<sup>59</sup>

## 2.4. Computational investigations of Fischer carbenes

The reactivity of an atom or complex is a measure of how readily that substance can interact with another reactant to produce a specific product. Therefore, the extent to which bonds are formed or broken in a particular reaction when using specific reactants and reagents can be used as a measure of reactivity. This general principle of chemical reactivity can be applied to examine the influence of heteroaromatic substituents and metal fragments on the reactivity of these Fischer type metal carbene complexes for certain reactions, *i.e.* benzannulation, cyclopropanation and metathesis, among others. Therefore, frontier orbital interactions between these Fischer type metal carbenes and other reactants can be used as an indicator of the extent to which certain products can be formed.

Extensive research has been done in order to determine the influence of the heteroatom, metal moiety and heteroaromatic substituent on the distribution of electron density throughout these metal carbene complexes.<sup>4,8,1-20</sup> Computational methods were mainly used to investigate the structure, conformations and electron density of group 6 Fischer carbenes.<sup>4,8,14-20</sup> Earlier computational methods used to differentiate between various types of metal carbenes were post-

HF,<sup>28,29,32,60,61</sup> semi-empirical<sup>2,33,34,61</sup> and Hartree-Fock(HF) methods.<sup>33,34</sup> Recent investigations focused on *ab initio* density function theory (DFT) calculations.<sup>2,32,61</sup> Modern techniques such as natural bond orbital (NBO) analysis,<sup>53-56</sup> energy decomposition analysis (EDA),<sup>36,39</sup> atoms in molecule (AIM)<sup>36,40</sup> and charge decomposition analysis (CDA)<sup>36</sup> offer valuable information on quantum chemical charge and energy partitioning of bonds in these complexes. In spite of these achievements, there is still a great gap in explaining the mechanism of reactions where Fischer type metal carbenes are involved, especially with regard to frontier orbital interactions.

The following sections will highlight some of the research on computational methods applied to mono- and bi-metallic Cr- or W-based Fischer carbenes with heteroaromatic substituents, *i.e.* furyl, 2-(2'-thienyl)furyl, N-methyl-2-(2'-thienyl)pyrrolyl, bithienyl and N-methylthieno[3,2-b]pyrrolyl. This will serve as a benchmark for further computational investigations with regard to the possible application of these carbenes in organic synthesis.

#### 2.4.1. Mono-metallic Fischer carbenes

Landman *et al.*<sup>18</sup> used DFT and electrochemical methods to evaluate oxidation and reduction in mono-metallic substituted ethoxy carbene complexes  $[(CO)_5Cr=C(OEt)R]$  where R = 2-thienyl, 2-(2'-thienyl)furyl, 2-furyl, 2-(N-thienyl)pyrrolyl and N-methyl-2-(2'-thienyl)pyrrolyl (**Figure 2.3**). They discovered that reduction occurred on the carbene carbon (LUMO) in all these complexes, while the first and second oxidations occurred on the HOMO of chromium, thereby leaving Cr with two unpaired electrons in the  $d_{xz}$  and  $d_{yz}$  orbitals, respectively. The third oxidation involves the heteroaromatic ring that leaves the complex paramagnetic with three unpaired electrons.<sup>18</sup> Therefore, the effect of the heteroaromatic substituent in a mono or dimer form was investigated with corresponding redox potentials. Oxidation results obtained from this study suggest that these carbenes have a spin multiplicity of one before oxidation, since the first and second oxidations leave two d-orbitals on chromium with two unpaired electrons.

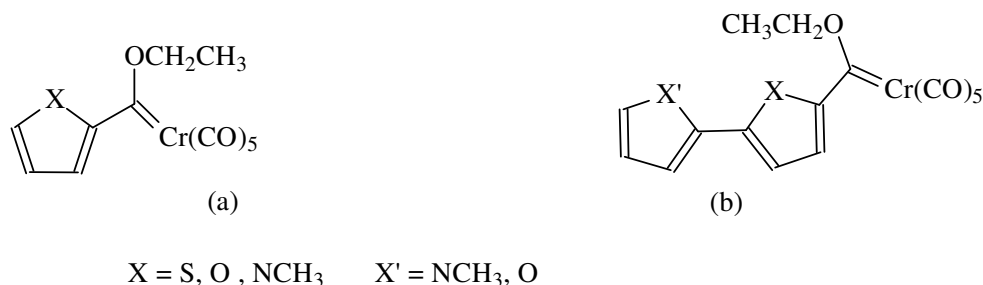


**Figure 2.3:** (a) Mono and (b) dimer form of the heteroaromatic substituted carbene complex<sup>18</sup>

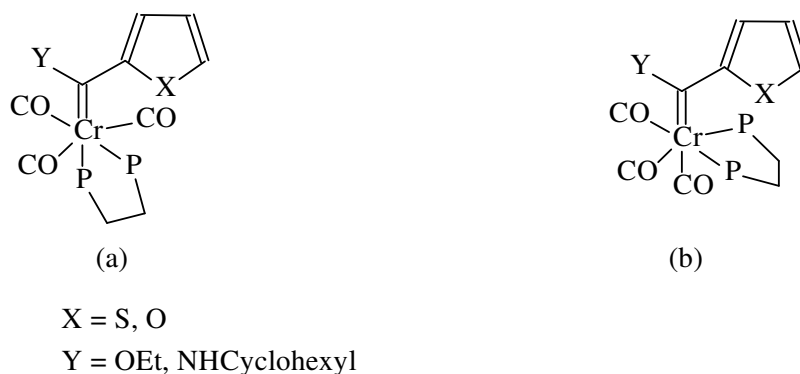


**Figure 2.4:** (a) *Mer* and (b) *fac* isomers of bis(diphenylphosphino)ethane substituted carbenes<sup>19</sup>

steric influence calculations. Therefore, this article illustrated the influence of both the heteroatom (X) and the heteroatom (Y) of the heteroaromatic ring on the conformation of these complexes.<sup>17</sup>

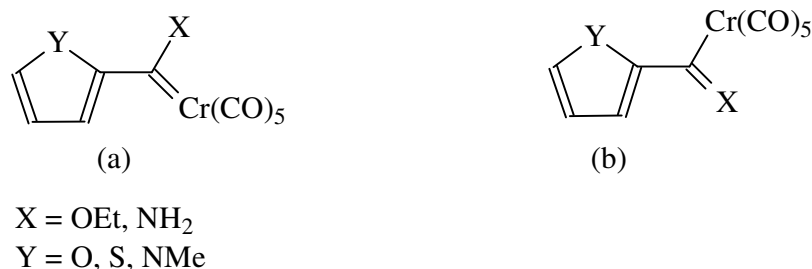


**Figure 2.5:** (a) *Syn*- and (b) *anti*-conformations of thienyl or furyl carbenes<sup>17</sup>

Landman *et al.*<sup>20</sup> investigated the oxidation and reduction properties of alkoxy and amino carbene complexes of tungsten (**Figure 2.6**). From this study it was concluded that oxidation occurs on the metal fragment, while reduction occurs on the carbene carbon. These findings were verified through the use of cyclic voltammetry and DFT calculations. The energy of the frontier orbitals indicates that the LUMO is predominantly located on the carbene carbon, while the HOMO is located on the metal fragment.

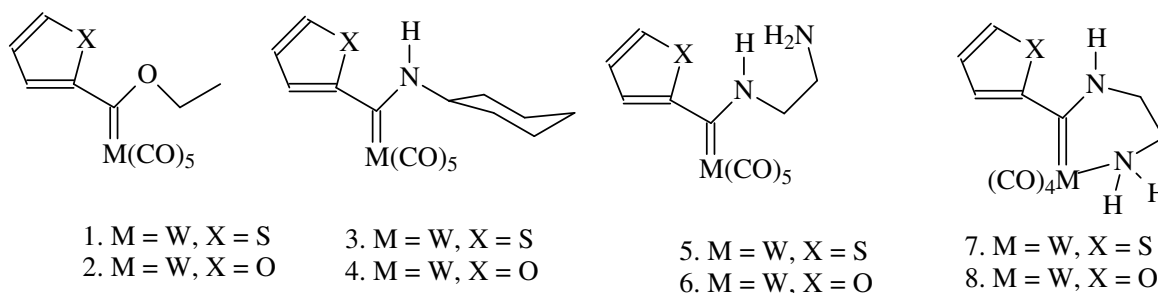


**Figure 2.6:** Mono-metallic alkoxy and amino carbene complexes of tungsten<sup>20</sup>

### 2.4.2. Bi-metallic Fischer carbenes

Van der Westhuizen *et al.*<sup>62</sup> reported the redox potentials of bi-metallic chromium Fischer carbenes of the form  $[(\text{CO})_5\text{Cr}=\text{C}(\text{OEt})-\text{X}-(\text{OEt})\text{C}=\text{Cr}(\text{CO})_5]$  and  $[(\text{CO})_5\text{Cr}=\text{C}(\text{NHBu})-\text{X}-(\text{NHBu})\text{C}=\text{Cr}(\text{CO})_5]$  where X = 2,5-furadiyl or 2,5-thiendiyl heteroaromatic rings (**Figure 2.7**).<sup>62</sup> By comparing the redox potentials of bis- and mono-carbenes of these complexes, patterns can

be established. From this investigation, it was found that the reduced complexes with an amino substituted (NHBu) carbene carbon are more reactive than the ethoxy-substituted carbenes. Furthermore, NHBu-substituted carbenes can donate electrons more easily to the Cr-C double bond as compared to the ethoxy carbene. It was found that the HOMO is mainly located on chromium, while the LUMO is located on the carbene carbon. The electrons within the C-H bond of the ethoxy substituents interact with the vacant d-orbital of the chromium atom, resulting in high stabilization energy. Furthermore, the influence of the heteroatom in stabilizing the Cr atom via a C-H agnostic interaction and the role of heteroatoms in redox potentials are clearly shown.<sup>62</sup>

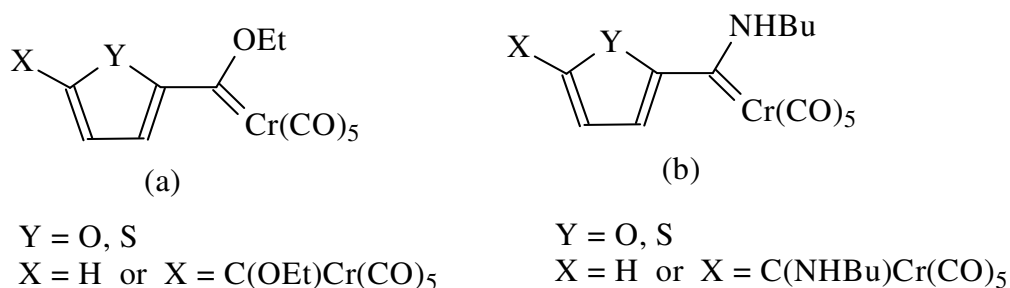


**Figure 2.7:** Ethoxy (a) and amino (b) substituted metal carbene<sup>63</sup>

## 2.5. Summary

The synthesis of mono- and bis-carbene complexes with the following heteroaromatic spacers, furan, 2-(2'-thienyl)furan, N-methyl-2-(2'-thienyl)pyrrole, bithiophene and N-methyl-thieno[3,2-b]pyrrole, has been well established.<sup>4,8,13-20</sup> Benzannulation reactions,<sup>4,8,14-20</sup> inter-molecular C-C coupling of two Fischer carbenes<sup>4,8,14-20</sup> and ligand substitution reactions have been studied by various analytical techniques and DFT methods. Electron density distribution through these carbene complexes was analysed by Mulliken charges, dipole moments, energy changes in frontier orbitals, steric interactions and redox potentials, among others. Donor-acceptor interactions were also analysed by using NBO analysis to determine dominant bond formation interactions between natural bond orbitals. Electrochemistry was used to investigate oxidation and reduction that occurred in these groups of Fischer type metal carbenes.<sup>13-20</sup> In these studies, electron transfer was also proven to occur predominantly from the metal fragment to the carbene carbon. Therefore, oxidation was observed to occur mainly on the metal moiety (HOMO), while reduction occurred on the carbene carbon (LUMO).

Even though great advances have been made in the synthesis, characterisation and application of these Fischer type metal carbenes, there is still much work that needs to be done in order to explain the reaction mechanisms, *i.e.* benzannulation, cyclopropanation and nucleophilic attack reactions among others, through frontier molecular orbital interactions,  $E_{\text{HOMO}}-E_{\text{LUMO}}$  energy gap, NBO analysis, metal shielding, NPA charges and electrophilicity indices.



## References

1. Jacobsen, H.; Ziegler, T. *Inorg. Chem.* **1996**, *35*, 775-783.
2. Cases, M.; Frenking, G.; Duran, M.; Sola, M. *Organometallics*. **2002**, *21*, 4182-4191.
3. Schubert, R. U.; Ackermann, K. *Angew. Chem. Int. Ed. Engl.* **1981**, *20*, 611-612.
4. Lotz, S.; van Jaarsveld, N. A.; Liles, D. C.; Crause, C.; Görls, H.; Terblans, Y. M. *Organometallics*. **2012**, *31*, 5371-5383.
5. Wittig, G.; Bickelhaupt, F. *Angew. Chem.* **1957**, *69*, 93; (b) Wittig, G.; Bickelhaupt, F. *Chem. Ber.* **1958**, *91*, 883-894.
6. Connor, J. A.; Jones, E. M. *J. Chem. Soc. A.* **1971**, 1974.
7. Crause, C.; Görls, H.; Lotz, S. *Dalton Trans.* **2005**, 1649-1657.
8. Landman, M.; Ramontja, J.; van Staden, M.; Bezuidenhout, D. I.; van Rooyen, P. H.; Liles, D. C.; Lotz, S. *Inorg. Chim. Acta.* **2010**, *363*, 705-717.
9. Aoki, A.; Fujimura, T.; Nakamura, E. *J. Am. Chem. Soc.* **1992**, *114*, 2985.
10. Lancellotti, L.; Tubino, R.; Luzzati, S.; Licandro, E.; Maiorana, S.; Papagni, A. *Synth. Met.* **1998**, *93*, 27.
11. Moeng, M. M. *Terthienyl carbene complexes*, PhD, University of Pretoria: South Africa, **2001**.
12. Olivier, A. J. *Novel carbene complexes with pyrrole ligands*, MSc, University of Pretoria: South Africa, **2001**.
13. Crause, C. *Synthesis and application of carbene complexes with heteroaromatic substituents*, PhD, University of Pretoria: South Africa, **2004**.
14. Lotz, S.; Landman, M.; Görls, H.; Crause, C.; Nienaber, H.; Olivier, A. *Naturforsch. B.* **2007**, *62b*, 419-426.
15. Van Jaarsveld, N. A.; Liles, D. C.; Lotz, S. *Dalton Trans.* **2010**, *39*, 5777-5779.

16. Landman, M.; Görls, H.; Lotz, S. *J. Organomet. Chem.* **2001**, 617-618, 280-287.
17. Thompson, S.; Wessels, H. R.; Fraser, R.; van Rooyen, P. H.; Liles, D. C.; Landman, M. *J. Mol. Struct.* **2014**, 1060, 111-118.
18. Landman, M.; Liu, R.; van Rooyen, P. H.; Conradie, J. *Electrochim. Acta.* **2013**, 114, 205-214.
19. Landman, M.; Liu, R.; Fraser, R.; van Rooyen, P. H.; Conradie, J. *J. Organomet. Chem.* **2014**, 752, 171-182.
20. Landman, M.; Pretorius, R.; Buitendach, B. E.; van Rooyen, P. H.; Conradie, J. *Organometallics.* **2013**, 23, 5491-5503.
21. Du Toit, J. I. 'n Modelleringsondersoek na die meganisme van die homogene alkeenmetatese reaksie, MSc, North-West University: South Africa, **2009**.
22. Du Toit, J. I. *On the mechanism of homogeneous alkene metathesis - a computational study*, PhD, North-West University: South Africa, **2012**.
23. Crabtree, R. H. *The organometallic chemistry of the transition metals*, John Wiley and Sons 4<sup>th</sup> ed. **2005**.
24. De Frémonta, P.; Marion, N.; Nolan, S. *Coord. Chem. Rev.* **2009**, 253, 862-892.
25. Schoeller, W. W.; Eisner, D.; Grigoleit, S.; Rozhenko, A. B.; Alijah, A. *J. Am. Chem. Soc.* **2000**, 122, 10115.
26. Marquez, A.; Fernandez, S. *J. Am. Chem. Soc.* **1992**, 114, 2903.
27. Ushio, J.; Nakatsuji, H.; Yonezawa, T. *J. Am. Chem. Soc.* **1984**, 106, 5892.
28. Canac, Y.; Soleilhavoup, M.; Conejero, S.; Bertrand, G. *J. Organomet. Chem.* **2004**, 689, 3857.
29. Taylor, T. E.; Hall, M. B. *J. Am. Chem. Soc.* **1984**, 106, 1576.
30. Lappert, M. F. *J. Organomet. Chem.* **1988**, 358, 185.

31. House, J. E. *Inorganic Chemistry*, Elsevier Inc: **2008**, 319.
32. Wang, C. C.; Wang, Y.; Liu, H. J.; Lin, K. J.; Chou, L. K.; Chan, K. S. *J. Phys. Chem.* **1997**, *101*, 8887.
33. Block, T. F.; Fenske, R. F.; Casey, C. P. *J. Am. Chem. Soc.* **1976**, *98*, 441.
34. Block, T. F.; Fenske, R. F. *J. Am. Chem. Soc.* **1977**, *99*, 4321.
35. Jacobsen, H.; Ziegler, T. *Organometallics*. **1995**, *14*, 224.
36. Sierra, M. A.; Fernandez, I.; Fernando, P. C. *Chem. Commun.* **2008**, 4671-4682.
37. Foster, J. P.; Weinhold, F. *J. Am. Chem. Soc.* **1980**, *102*, 7211.
38. Reed, A. E.; Weigend, F. *J. Chem. Phys.* **1985**, *83*, 1736.
39. Te Velde, G. F.; Bickelhaupt, M.; Baerends, E. J.; Guerra, F. C.; Van Gisbergen, S. J. A.; Snijders, J. G.; Ziegler, T. *J. Comput. Chem.* **2001**, *22*, 931.
40. Bader, R. F. W. *Atoms in Molecules: A Quantum Theory*. Oxford University Press, Oxford, **1990**.
41. Fischer, E. O.; Dötz, K. H. *Chem. Ber.* **1970**, *103*, 1273.
42. Barluenga, J.; Rodriguez, F.; Fananas, F. J.; Florez, J. *Topics Organomet. Chem.* **2004**, *13*, 59-121.
43. Inukai, T.; Kojima, T. *J. Org. Chem.* **1965**, *30*, 3567.
44. Semmelhack, M. F.; Lee, G. R. *Organometallics*. **1987**, *6*, 1839.
45. De Meijere, A.; Schirmer, H.; Deutsch, M. *Angew. Chem. Int. Ed. Engl.* **2000**, *39*, 3964.
46. Barluenga, J.; Florez, J.; Fananas, J. J. *J. Organomet. Chem.* **2001**, *624*, 5.
47. Werner, H.; Fischer E.O. *J. Organomet. Chem.* **1971**, *28*, 367.
48. Fischer, E. O. *Chem. Ber.* **1972**, *105*, 3966.

49. Dorwald, F. Z. *Metal Carbenes in Organic Synthesis*, Wiley-VCH (Weinheim), **1999**.
50. Dötz, K. H.; Tomuschat, P. *Chem. Soc. Rev.* **1999**, 28, 187.
51. Barluenga, J.; Aznar, F.; Martin, A. *Organometallics*. **1995**, 14, 1429.
52. Barluenga, J.; Moserrat, J. M.; Flórez, J. J. *Chem. Soc., Chem. Commun.* **1993**, 1068.
53. Tlenkopatchev, M.; Fomine, S. *J. Org. Chem.* **2001**, 603, 157-168.
54. Dötz, K. H. *Metal carbenes in organic synthesis, Topics in Organometallic Chemistry*, Springer: **2004**, Vol. 13.
55. Herndon, J. W.; Tumer, S. U. *J. Org. Chem.* **1991**, 56, 286.
56. Harvey, D. F.; Brown, M. F. *Tetrahedron Lett.* **1990**, 31, 1529.
57. Dötz, K. H. *J. Organomet. Chem.* **1977**, 140, 177.
58. Murray, C. K.; Yang, D. C.; Wulff, W. D. *J. Am. Chem. Soc.* **1990**, 112, 5660.
59. Hegedus, L. S.; McGuire, M. A.; Schultze, L. M.; Yijun, C.; Anderson, O. P. *J. Am. Chem. Soc.* **1984**, 106, 2680.
60. Carter, E. A.; Goddard, W. A. *J. Am. Chem. Soc.* **1986**, 108, 4746.
61. Marynick, D. S.; Kirkpatrick, C. M. *J. Am. Chem. Soc.* **1985**, 107, 1983.
62. Van der Westhuizen, B.; Swarts, P. J.; Van Jaarsveld, L. M.; Liles, D. C.; Siegert, U.; Swarts, J. C.; Fernandez, I.; Bezuidenhout, D. I. *Inorg. Chem.* **2013**, 52, 6674-6684.

## Chapter 3: Research methodology

### 3.1. Introduction to principal component analysis (PCA)

#### 3.1.1. Definitions

*Principal Component Analysis (PCA)*: A statistical technique used to reduce the number of variables (dimensions) in a dataset.

*Principal Component (PC)*: Principal components are orthogonal uncorrelated eigenvectors of a symmetric covariance matrix. The eigenvector with the largest eigenvalue can be referred to as a principal component.

*Eigenvector*: It is the dimension or direction that represents the variance within a dataset when variables are projected on it. The extent of variance is indicated by its corresponding eigenvalue.

*Eigenvalues*: Measures the amount of variance that is represented by the principal components.

*Covariance*: Measures the extent to which two random variables are correlated.

*Objects*: Individuals, chemical complexes, etc.

*Variables*: Size, length, entropy, enthalpy, etc.

#### 3.1.2. From eigenvalues to principal components

*General calculation of eigenvalues*:

The eigenvalues of matrix  $[A]$  can be obtained using the following equations<sup>1-3</sup>:

$$[A] \cdot [X] = \lambda [X] \dots \dots \dots (1)$$

Where  $[A]$  is the matrix of coefficients,  $[X]$  is the vector of unknowns,  $\lambda$  is a constant (eigenvalue). Equation (1) can also be written in the following form<sup>1,2</sup>:

$$([A] - \lambda [I]) \cdot [X] = 0 \dots \dots \dots (2)$$

Where  $[I]$  is the identity matrix:

$$\lambda [I] = \lambda \begin{bmatrix} 1 & 0 \\ 0 & 1 \end{bmatrix} = \begin{bmatrix} \lambda & 0 \\ 0 & \lambda \end{bmatrix}$$

Therefore:

$$([A] - \lambda [I]) \cdot [X] = 0$$

$$([A] - \lambda[I]) = 0$$

Where:

$$[A] = \begin{bmatrix} a_{11} & a_{12} \\ a_{21} & a_{22} \end{bmatrix} \text{ and } \lambda[I] = \begin{bmatrix} \lambda & 0 \\ 0 & \lambda \end{bmatrix} \dots\dots\dots(3)$$

It follows that:

$$\begin{aligned} ([A] - \lambda[I]) &= \begin{bmatrix} a_{11} - \lambda & a_{12} \\ a_{21} & a_{22} - \lambda \end{bmatrix} = 0 \\ (a_{11} - \lambda)(a_{22} - \lambda) - (a_{12}a_{21}) &= 0 \\ (a_{11}a_{22}) - (a_{12}a_{21}) - (a_{11}\lambda) - (a_{22}\lambda) + \lambda^2 &= 0 \\ \lambda^2 - (a_{11} + a_{22})\lambda + (a_{11}a_{22} - a_{12}a_{21}) &= 0 \dots\dots\dots(4) \end{aligned}$$

Equation (4)<sup>1,2</sup> is in the form of a quadratic equation *i.e.*

$$ax^2 + bx + c = 0$$

Therefore the solution for such an equation is:

$$x = \frac{-b \pm \sqrt{b^2 - 4ac}}{2a}$$

Thus:

$$\lambda = \frac{-(a_{11} + a_{22}) \pm \sqrt{(a_{11} + a_{22})^2 - 4(a_{11}a_{22} - a_{12}a_{21})}}{2}$$

The eigenvectors ( $x_i$ ) of the above-mentioned eigenvalues can be obtained from the following equation:

$$([A] - \lambda[I]) x_i = 0$$

Therefore:

$$([A] - \lambda[I])x_i = \begin{bmatrix} a_{11} - \lambda & a_{12} \\ a_{21} & a_{22} - \lambda \end{bmatrix} \begin{bmatrix} x_1 \\ x_2 \end{bmatrix} = 0$$

*Numeric example of calculation of eigenvalues:*

The following section illustrates a numeric example of how eigenvalues and eigenvectors of two variables are obtained.

[A] represents a matrix of two variables, each vector has two coordinates when plotted on a two dimensional scale *i.e.* (4, 7) and (7, 4) respectively. The eigenvalues of this matrix can be calculated from equations (1)-(4) as described in the previous section.

Therefore:

$$([A] - \lambda[I]) = 0 \dots\dots\dots(5)$$

Where:

$$[A] = \begin{bmatrix} 4 & 7 \\ 7 & 4 \end{bmatrix} \dots\dots\dots(6)$$

Combining equations (5) and (6):

$$([A] - \lambda[I]) = \begin{bmatrix} 4 - \lambda & 7 \\ 7 & 4 - \lambda \end{bmatrix} = 0$$

Then:

$$(4 - \lambda)^2 - (7 \times 7) = 0$$

$$16 - 8\lambda + \lambda^2 - 49 = 0$$

$$\lambda^2 - 8\lambda - 33 = 0$$

$$(\lambda - 11)(\lambda + 3) = 0$$

Therefore the two eigenvalues are  $\lambda_1 = 11$  and  $\lambda_2 = -3$ .

The eigenvectors with eigenvalues  $\lambda_1 = 11$  and  $\lambda_2 = -3$  can be calculated according to the following equation:

$$([A] - \lambda[I]) x_i = \begin{bmatrix} 4 - \lambda & 7 \\ 7 & 4 - \lambda \end{bmatrix} \begin{bmatrix} x_1 \\ x_2 \end{bmatrix} \dots\dots\dots (7)$$

where  $x_i$  is the eigenvector.

The eigenvector with the eigenvalue of  $\lambda_1 = 11$  is:

Substituting  $\lambda_1 = 11$  into equation (7) yields:

$$\begin{bmatrix} 4 - 11 & 7 \\ 7 & 4 - 11 \end{bmatrix} \begin{bmatrix} x_1 \\ x_2 \end{bmatrix} = 0$$

$$\begin{bmatrix} -7 & 7 \\ 7 & -7 \end{bmatrix} \begin{bmatrix} x_1 \\ x_2 \end{bmatrix} = 0$$

$$-7x_1 + 7x_2 = 0 \text{ and } 7x_1 - 7x_2 = 0$$

$$x_1 = \frac{7}{7} x_2 \text{ and } x_1 = \frac{7}{7} x_2$$

Therefore:

$$x_1 = x_2$$

The eigenvector of  $\lambda_1 = 11$  is  $\begin{bmatrix} x_1 \\ x_2 \end{bmatrix} = \begin{bmatrix} 1 \\ 1 \end{bmatrix}$

From trigonometry it follows that if  $\begin{bmatrix} y \\ x \end{bmatrix} = \begin{bmatrix} 1 \\ 1 \end{bmatrix}$  then  $\tan(45^\circ) = \frac{1}{1} \dots\dots\dots (8)$

The eigenvector with the eigenvalue of  $\lambda_2 = -3$  is:

$$\begin{bmatrix} 4 + 3 & 7 \\ 7 & 4 + 3 \end{bmatrix} \begin{bmatrix} x_1 \\ x_2 \end{bmatrix} = 0$$

$$\begin{bmatrix} 7 & 7 \\ 7 & 7 \end{bmatrix} \begin{bmatrix} x_1 \\ x_2 \end{bmatrix} = 0$$

$$7x_1 + 7x_2 = 0 \text{ and } 7x_1 + 7x_2 = 0$$

$$x_1 = -\frac{7}{7} x_2 \text{ and } x_1 = -\frac{7}{7} x_2$$

Therefore:

$$x_1 = -x_2$$

The eigenvector of  $\lambda_1 = -3$  is  $\begin{bmatrix} x_1 \\ x_2 \end{bmatrix} = \begin{bmatrix} -1 \\ 1 \end{bmatrix}$

From trigonometry it follows that if  $\begin{bmatrix} y \\ x \end{bmatrix} = \begin{bmatrix} -1 \\ 1 \end{bmatrix}$  then  $\tan(135^\circ) = -\frac{1}{1}$ .....(9)

**Figure 3.1** shows a graphic illustration of the eigenvectors (also called principal components) **PC 1** and **PC 2** with their respective eigenvalues *i.e.*  $\lambda_1 = 11$  and  $\lambda_2 = -3$ . The angles of the two eigenvectors as calculated in equations (8) and (9) are  $45^\circ$  and  $135^\circ$  from the x-axis. **PC 1** and **PC 2** are perpendicular to each other as observed in **Figure 3.1**. The first principal component **PC 1** represents the largest % variance in the dataset followed by **PC 2**.

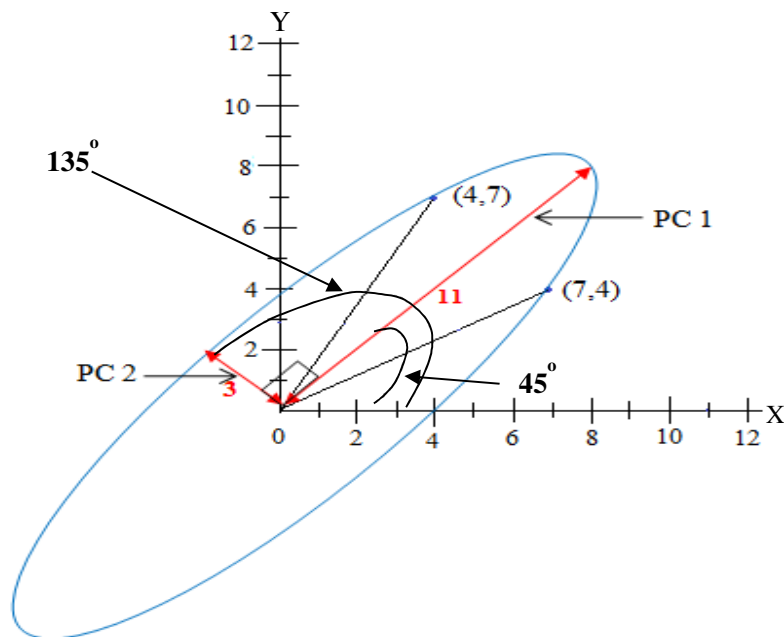


**Figure 3.1:** Graphic representation from eigenvalues to principal components<sup>1,2</sup>

The above basic representation of eigenvalues and eigenvectors becomes more complex with a dataset of more than two variables. Therefore statistical computation software packages such as Statistica which have a build in calculation algorithm can be used to obtain eigenvalues and eigenvectors for a larger dataset.<sup>4</sup>



### 3.1.3. Example of principal component analysis with a larger dataset

The best way to represent the variance between variables is by drawing a best fit line through the data points (**Figure 3.2**). This line can be drawn through the variables in a specific direction to ensure that the variables deviate most when projected on it. Therefore, this line represents the direction of the most variance when the data points are projected on it; we refer to these lines as principal components *i.e.* **PC 1** and **PC 2**. Principal components **PC 1** and **PC 2** can be rotated in such a way that they can be represented on a two dimensional axis.

The scores plot as illustrated in **Figure 3.2** shows the relation within the objects *i.e.* **A – H**. Objects **A** to **H** can be grouped into three sub-groups when projected along **PC 1** based on the variables. The first sub-group consists of objects **A** to **C**; the second sub-group consists of objects **D** and **E**; the last sub-group consists of objects **F**, **G** and **H**.

The loadings plot can be used to highlight variables which can be used to differential between the objects in the scores plot. Variables which are distributed towards the edges of the principal components describe the most variance within the objects. Therefore these variables can be used further to classify the objects in the scores plots. Variables **1** to **5** are distributed towards the edges of **PC 1**, therefore this variables can be used to distinguish between the objects in the scores plot.

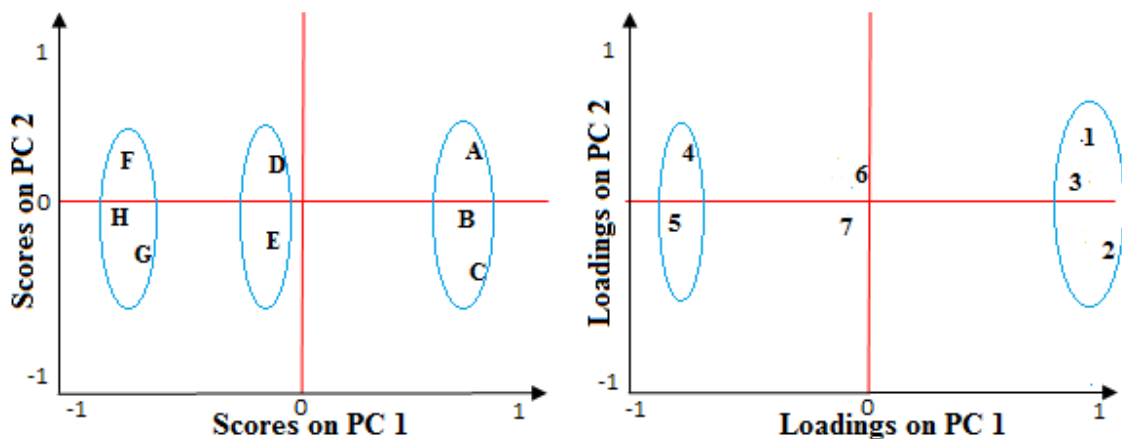


**Figure 3.2:** Example of scores and loadings plots

### 3.2. Example of how a statistical software can be used for PCA

#### 3.2.1. Table of chemical properties

A table that lists all the variables for each object must be compiled before multivariate analysis (PCA) can be computed. The values of the variables are listed in columns, while the corresponding objects are listed along the rows of this table.

Each row in **Table 3.1** is represented by a specific complex and the actual values of the chemical properties are listed in columns. Only eight hypothetical chemical properties and 12 complexes (A-L) are listed in **Table 3.1** as an example of how such a table is compiled.

The chemical properties listed in this table are ascribed a number as follows: 1 =  $E_{\text{HOMO}}$  (eV), 2 =  $E_{\text{HOMO}-1}$  (eV), 3 =  $E_{\text{LUMO}}$  (eV), 4 =  $E_{\text{LUMO}+1}$  (eV), 5 =  $|E_{\text{HOMO}} - E_{\text{LUMO}}|$  energy gap (eV), 6 = Electrophilicity index, 7 = TM% contribution to HOMO, 8 = C% contribution to LUMO.

**Table 3.1:** Chemical properties of the various complexes

Complexes	Chemical Properties							
	1	2	3	4	5	6	7	8
A	-5.695	-5.772	-2.536	-0.601	3.159	2.681	68	32
B	-5.663	-5.682	-2.333	-0.753	3.330	2.400	46	30
C	-4.986	-5.297	-2.807	-0.879	2.179	3.484	72	13
D	-5.485	-5.536	-2.474	-1.311	3.011	2.630	65	30
E	-4.665	-5.137	-2.949	-1.168	1.716	4.223	68	13
F	-5.836	-5.901	-2.747	-1.102	3.089	2.981	42	23
G	-5.662	-5.717	-2.844	-1.494	2.818	3.209	64	23
H	-5.758	-5.848	-2.674	-0.897	3.084	2.882	40	24
I	-5.581	-5.684	-2.650	-0.988	2.931	2.889	62	22
J	-5.594	-5.633	-2.779	-1.410	2.815	3.113	64	25
K	-5.516	-5.788	-2.461	-0.875	3.055	2.604	19	26
L	-5.462	-5.558	-2.562	-1.396	2.900	2.775	33	26

### 3.2.2. Correlation matrix and redundant chemical properties

Statistica version 12<sup>4(a)</sup> was used to compile a correlation matrix with the above listed chemical properties (**Table 3.1**). The coefficient of determination ( $R^2$  or  $r^2$ ) can be obtained from the correlation coefficient ( $r$ ), which represents the linear relationship between two variable values.  $R^2$  is the square of the correlation coefficient, which can be determined from a linear regression of variables. The correlation coefficient is usually expressed such that  $-1 \leq r \leq +1$ . When two variables have a negative linear relation, then  $r$  is usually a negative value. A positive linear relation is represented by a positive  $r$  value. If variables  $x$  and  $y$  are considered, then a positive  $r$  value means that as the value of variable  $x$  increases, the value of variable  $y$  will also increase. A negative  $r$  value means that as the value of variable  $x$  increases, the value of variable  $y$  will decrease. Where  $r = -1$  represents a strong negative linear relationship,  $r = 1$  represents a strong positive relationship and  $r = 0$  represents no linear relationship.<sup>4(a),(b),5</sup>

The value of  $R^2$  ranges from 0 to 1; therefore,  $R^2 = 1$  indicates that 100% of the variability in  $x$  can be explained by the variability in  $y$ . The opposite is also true: where  $R^2 = 0$ , this indicates that the variability in  $y$  cannot be explained by the variability in  $x$ .<sup>5</sup> Therefore, non-redundant chemical properties, *i.e.* chemical properties with a coefficient of determination [ $R^2 \leq 0.9$ ]<sup>6</sup> can be identified from the correlation matrix. Redundant chemical properties [ $R^2 \geq 0.9$ ] are properties that do not show much variance among all the other properties. Therefore, such properties can be discarded since they will not be useful in distinguishing among these twelve complexes. The correlation matrix of the above-mentioned properties, as calculated by Statistica version 12<sup>4(a)</sup>, is given in **Table 3.2**.

**Table 3.2:** Correlation matrix of the chemical properties (correlation coefficients (r))<sup>4</sup>

	2	3	4	5	6	7	8	
1	1.00	0.96	-0.47	-0.08	-0.93	0.79	0.38	-0.75
2	0.96	1.00	-0.43	-0.20	-0.88	0.73	0.51	-0.66
3	-0.47	-0.43	1.00	0.42	0.75	-0.90	-0.48	0.80
4	-0.08	-0.20	0.42	1.00	0.23	-0.29	-0.10	0.15
5	-0.93	-0.88	0.75	0.23	1.00	-0.95	-0.48	0.88
6	0.79	0.73	-0.90	-0.29	-0.95	1.00	0.49	-0.88
7	0.38	0.51	-0.48	-0.10	-0.48	0.49	1.00	-0.30
8	-0.75	-0.66	0.80	0.15	0.88	-0.88	-0.30	1.00

The following steps were followed in order to obtain the correlation matrix with Statistica version 12<sup>4</sup>:

- ❖ An Excel worksheet was imported in Statistica version 12, with the variables (chemical properties) obtained from the first row. The case names (name of complexes) are obtained from the first column of the Excel worksheet (**Table 3.1**). **Figure 3.3** shows how an Excel file is imported into Statistica version 12.

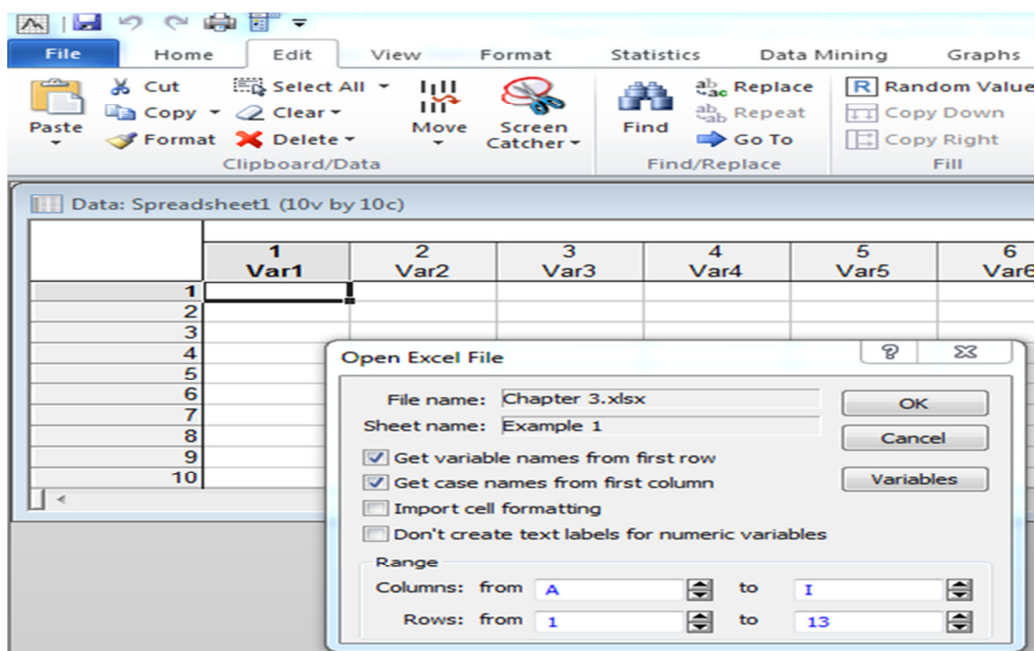
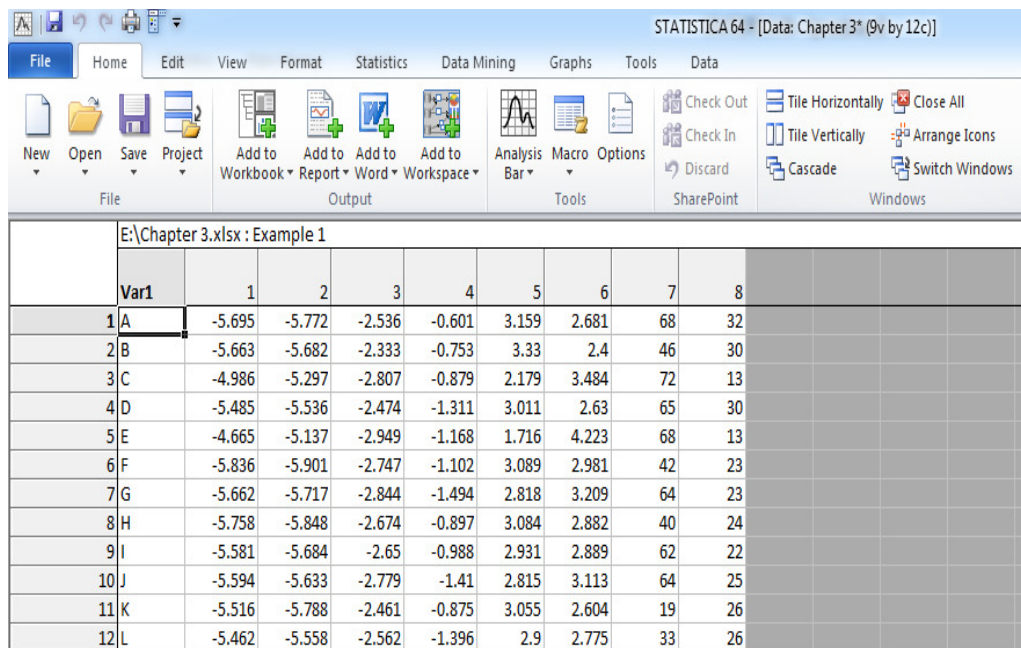


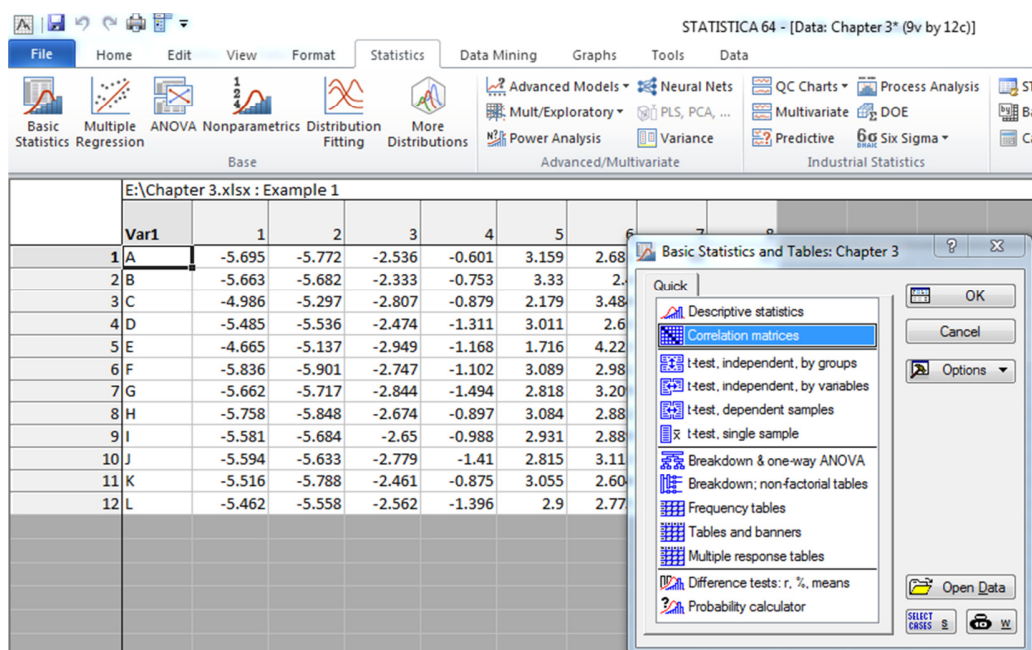
**Figure 3.3:** Opening an Excel worksheet in Statistica version 12<sup>4</sup>

- ❖ Once the above-mentioned boxes have been selected on the pop-up box (Open Excel File), OK was selected in order to import the worksheet to Statistica version 12. **Figure 3.4** shows how the worksheet appears on Statistica version 12.



	Var1	1	2	3	4	5	6	7	8		
1 A		-5.695	-5.772	-2.536	-0.601	3.159	2.681	68	32		
2 B		-5.663	-5.682	-2.333	-0.753	3.33	2.4	46	30		
3 C		-4.986	-5.297	-2.807	-0.879	2.179	3.484	72	13		
4 D		-5.485	-5.536	-2.474	-1.311	3.011	2.63	65	30		
5 E		-4.665	-5.137	-2.949	-1.168	1.716	4.223	68	13		
6 F		-5.836	-5.901	-2.747	-1.102	3.089	2.981	42	23		
7 G		-5.662	-5.717	-2.844	-1.494	2.818	3.209	64	23		
8 H		-5.758	-5.848	-2.674	-0.897	3.084	2.882	40	24		
9 I		-5.581	-5.684	-2.65	-0.988	2.931	2.889	62	22		
10 J		-5.594	-5.633	-2.779	-1.41	2.815	3.113	64	25		
11 K		-5.516	-5.788	-2.461	-0.875	3.055	2.604	19	26		
12 L		-5.462	-5.558	-2.562	-1.396	2.9	2.775	33	26		

**Figure 3.4:** Imported Excel file<sup>4</sup>



	Var1	1	2	3	4	5	6	7	8		
1 A		-5.695	-5.772	-2.536	-0.601	3.159	2.681	68	32		
2 B		-5.663	-5.682	-2.333	-0.753	3.33	2.4	46	30		
3 C		-4.986	-5.297	-2.807	-0.879	2.179	3.484	72	13		
4 D		-5.485	-5.536	-2.474	-1.311	3.011	2.63	65	30		
5 E		-4.665	-5.137	-2.949	-1.168	1.716	4.223	68	13		
6 F		-5.836	-5.901	-2.747	-1.102	3.089	2.981	42	23		
7 G		-5.662	-5.717	-2.844	-1.494	2.818	3.209	64	23		
8 H		-5.758	-5.848	-2.674	-0.897	3.084	2.882	40	24		
9 I		-5.581	-5.684	-2.65	-0.988	2.931	2.889	62	22		
10 J		-5.594	-5.633	-2.779	-1.41	2.815	3.113	64	25		
11 K		-5.516	-5.788	-2.461	-0.875	3.055	2.604	19	26		
12 L		-5.462	-5.558	-2.562	-1.396	2.9	2.775	33	26		

**Figure 3.5:** Basic Statistics and Tables tab<sup>4</sup>

- ❖ The Statistics tab was selected on the tool bar as shown in **Figure 3.5**, and then the Basic Statistics tab was selected in order to display a pop-up box (Basic Statistics and Tables). Correlation matrices was selected followed by OK on the dialog box as indicated.
- ❖ A dialog box (Product-Moment and Partial Correlations) was displayed as shown in **Figure 3.6**, and then one variable list was selected on the dialog box.
- ❖ The OK tab was chosen after all eight variables were selected.
- ❖ The Summary tab on the (Product-Moment and Partial Correlations) dialog box was selected to display the correlation matrix, mean and standard deviations of the dataset, as indicated in **Figure 3.7**.

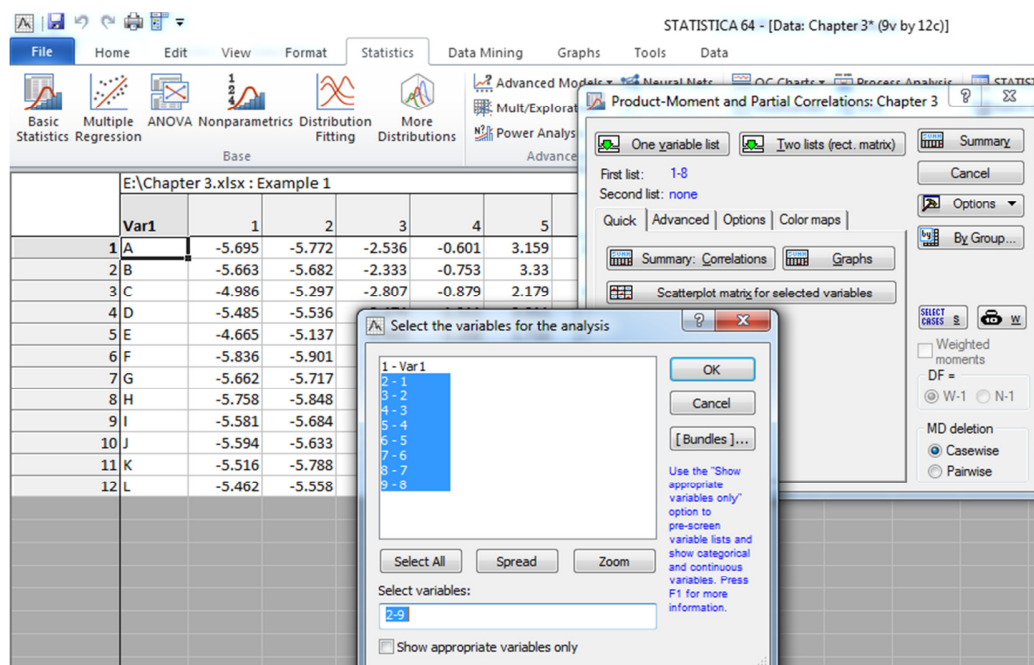


**Figure 3.6:** Variables (chemical properties) used to compile the correlation matrix<sup>4</sup>

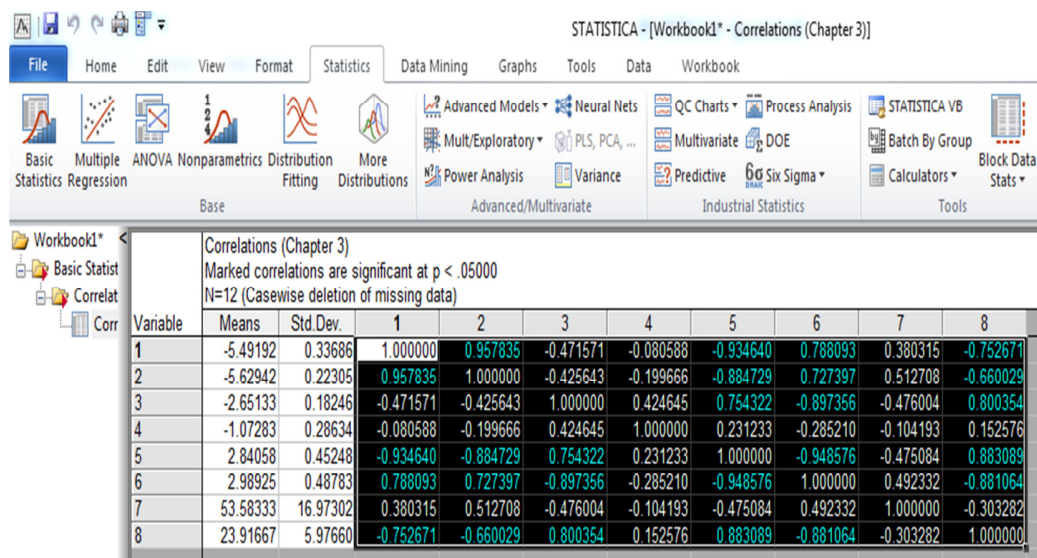


**Figure 3.7:** Correlation matrix as obtained from Statistica version 12<sup>4</sup>

The correlation coefficients (**Table 3.2, Figure 3.7**) were further copied into an Excel worksheet in order to calculate  $R^2$  values (**Table 3.3**). The cells with a coefficient of determination ( $R^2 > 0.9$ ) are highlighted, as indicated in **Table 3.3**. Chemical properties 1 =  $E_{\text{HOMO}}$  (eV) and 2 =  $E_{\text{HOMO}-1}$  (eV) have a coefficient of determination with a value of  $R^2 = 0.92$ , which is greater than  $R^2 = 0.9$  as indicated in **Table 3.3**. We can therefore consider one of the properties to be redundant in relation to the other. Since the energies of the highest occupied molecular orbital (HOMO) and that of the HOMO-1 show less variance, we consider the  $E_{\text{HOMO}-1}$  (eV) to be redundant. Therefore, chemical property 2 =  $E_{\text{HOMO}-1}$  (eV) can be removed from the dataset in order to further simplify our analysis.

**Table 3.3:** Table with coefficients of determination ( $R^2$ ) as calculated from **Table 3.2**

	1	2	3	4	5	6	7	8
1	1.00	0.92	0.22	0.01	0.86	0.62	0.14	0.56
2	0.92	1.00	0.18	0.04	0.77	0.53	0.26	0.44
3	0.22	0.18	1.00	0.18	0.56	0.81	0.23	0.64
4	0.01	0.04	0.18	1.00	0.05	0.08	0.01	0.02
5	0.86	0.77	0.56	0.05	1.00	0.90	0.23	0.77
6	0.62	0.53	0.81	0.08	0.90	1.00	0.24	0.77
7	0.14	0.26	0.23	0.01	0.23	0.24	1.00	0.09
8	0.56	0.44	0.64	0.02	0.77	0.77	0.09	1.00



### 3.2.3. % Total variance and eigenvalues

Statistica version 12<sup>4(a)</sup> can also be used to obtain % total variance and eigenvalues from the correlation matrix obtained previously. Eigenvalues and eigenvectors are obtained from a correlation or covariance matrix; the sum of all the eigenvalues is equal to the number of variables under investigation.<sup>4 (b)</sup>

The following steps were followed in order to obtain eigenvalues and % total variance:

- ❖ The Statistics tab was selected on the tool bar followed by the Mult/Exploratory tab and then (Principal Components and Classification) was selected on the list (**Figure 3.8**). The variables used to calculate eigenvalues and % total variance from a correlation matrix were then chosen, as indicated in **Figure 3.9**.

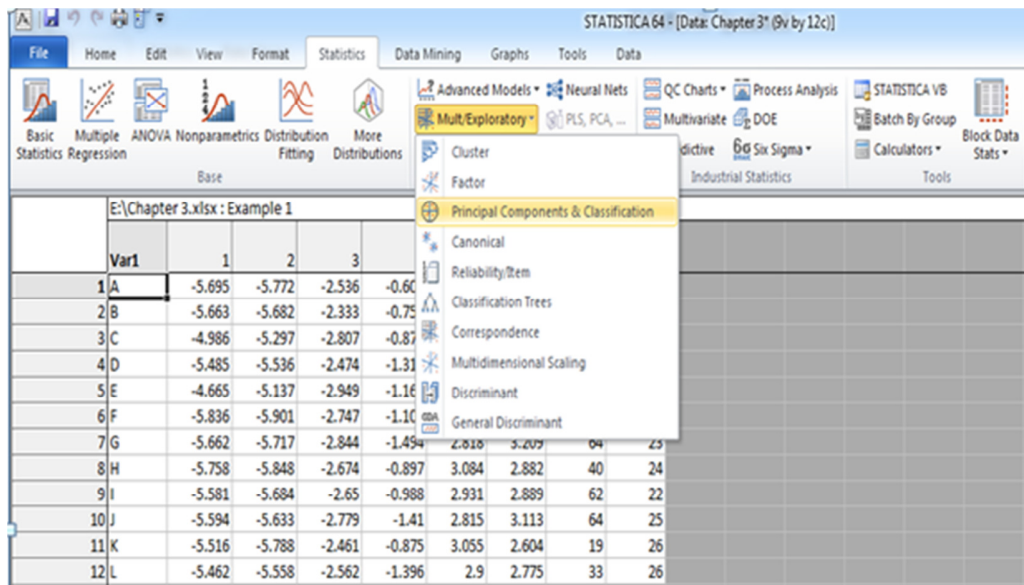


**Figure 3.8:** Principal component analysis with Statistica version 12<sup>4</sup>



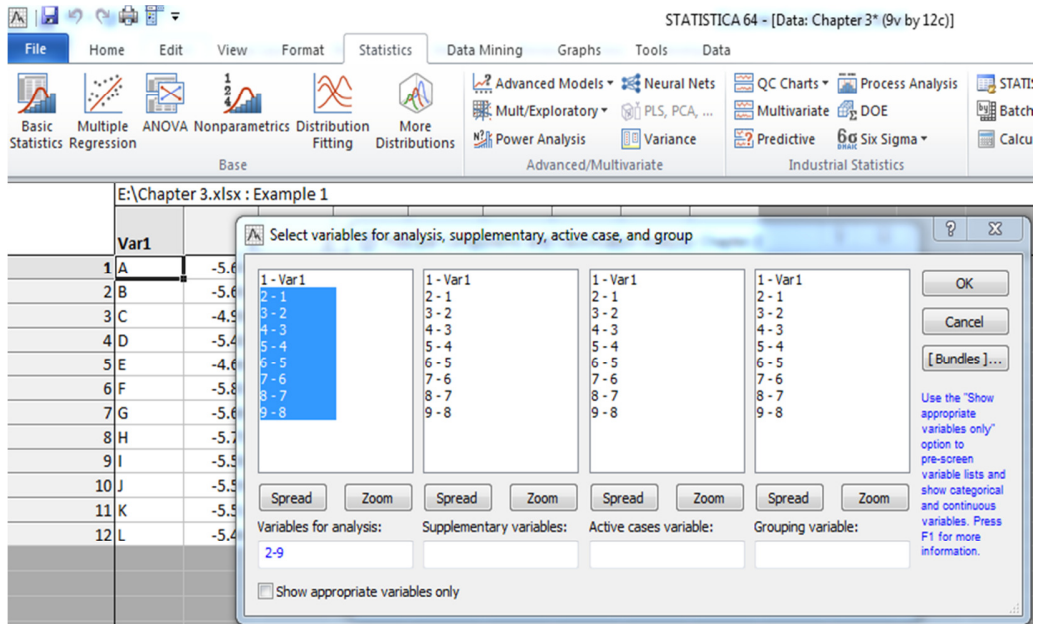


**Figure 3.9:** Variables selected to calculate eigenvalues and % total variance<sup>4</sup>

- ❖ The Eigenvalues tab was selected from the pop-up box. A table with value numbers, eigenvalues, % total variance, cumulative eigenvalue and cumulative % was computed from the correlation matrix as shown in **Figure 3.10**.

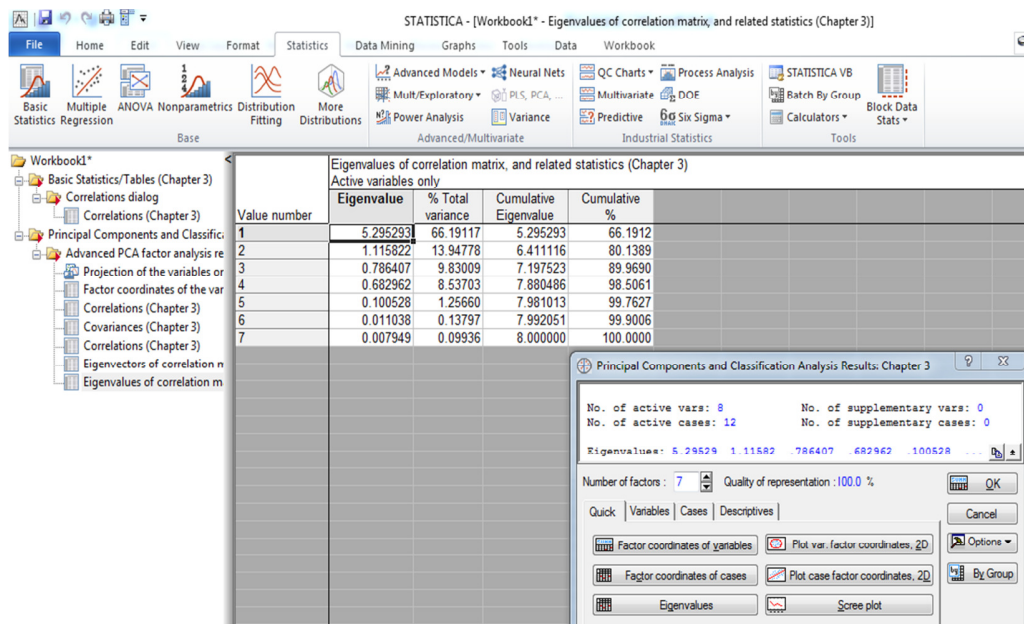


**Figure 3.10:** Eigenvalues and % total variance<sup>4</sup>

The value numbers indicated in **Figure 3.10** represent the principal components that correspond to respective eigenvalues. The first principal component (**PC 1**) with the largest eigenvalue (5.295) describes the most % total variance (66.19%) among the chemical properties, followed by the second principal component (**PC 2**) with a % total variance of 13.95% (**Figure 3.10**, **Table 3.4**). Therefore, **PC 1** and **PC 2** can be used to describe the most variance among the chemical properties. The scores and loadings plots will be calculated by Statistica version 12 along **PC 1** and **PC 2**.

**Table 3.4:** Eigenvalues and % total variance represented by each principal component<sup>4</sup>

	Eigenvalues	% total variance
PC 1	5.295	66.19
PC 2	1.117	13.95
PC 3	0.786	9.83
PC 4	0.683	8.53
PC 5	0.100	1.26
PC 6	0.011	0.14
PC 7	0.008	0.10

#### 3.2.4. Loadings and scores plots

The scores plot is obtained by fitting the relation between the complexes in a two-dimensional axis of the principal components, while the loadings plot can be obtained by fitting the relation between the variables in a two-dimensional axis of the principal components. The computation details used by Statistica version 12, as a module to compute the eigenvalues, % total variance, scores and loadings plots can be analysed in detail from an article written by Jambu<sup>7</sup> in 1991. The relation between data points in a multivariable dataset can be obtained by analysing the scores and loadings plots from PCA.

The scores plots were obtained from Statistica version 12 as follows:

- ❖ The Statistics tab on the tool bar was selected, and then Mult/Exploratory tab was selected to display a list of analysis.
- ❖ Then (Principal Component and Classification) was selected from the list of analyses.

- ❖ The (Plot case factor coordinates, 2D) tab was selected on the pop up box as indicated in **Figure 3.11**.

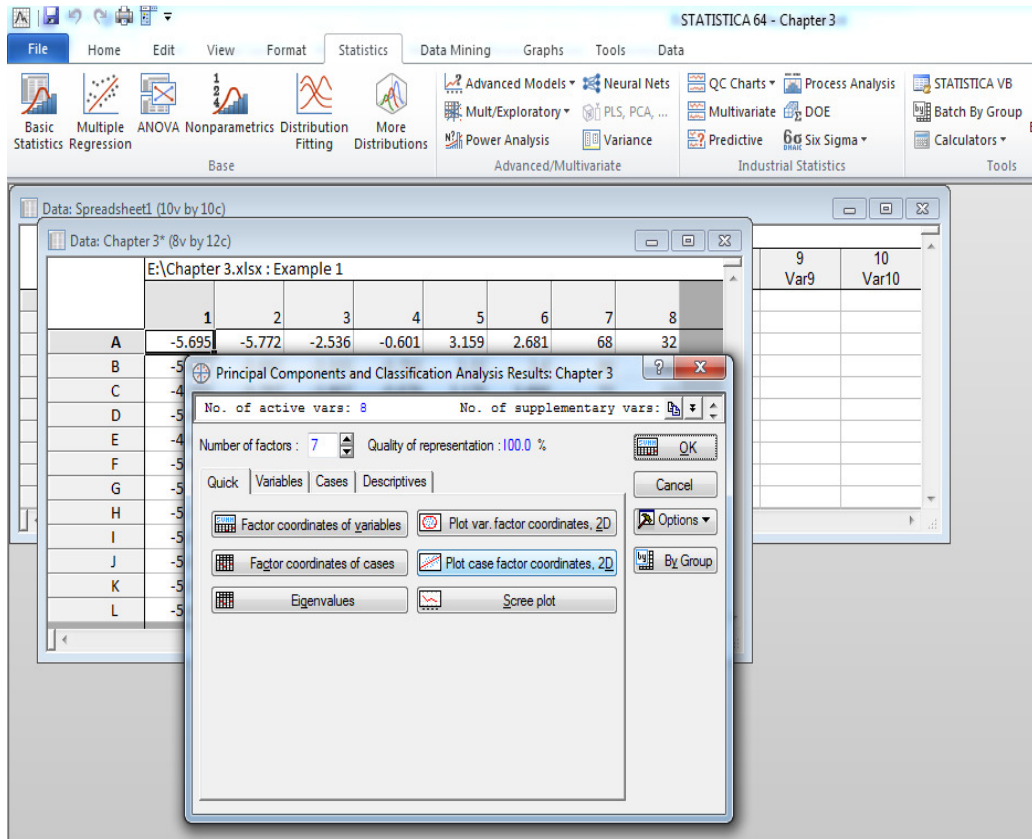


**Figure 3.11:** Case factor coordinates, 2D tab selected in Statistica version 12<sup>4</sup>

- ❖ A pop-up box appears with a prompt to select two factors that can be used to plot the scores plot in a 2D space. Factors 1 and 2 (principal components **PC 1** and **PC 2**) were selected as indicated in **Figure 3.12**.
- ❖ Once the axis, title and background of the plot are edited, the resulting scores plot is obtained as indicated in **Figure 3.13**.

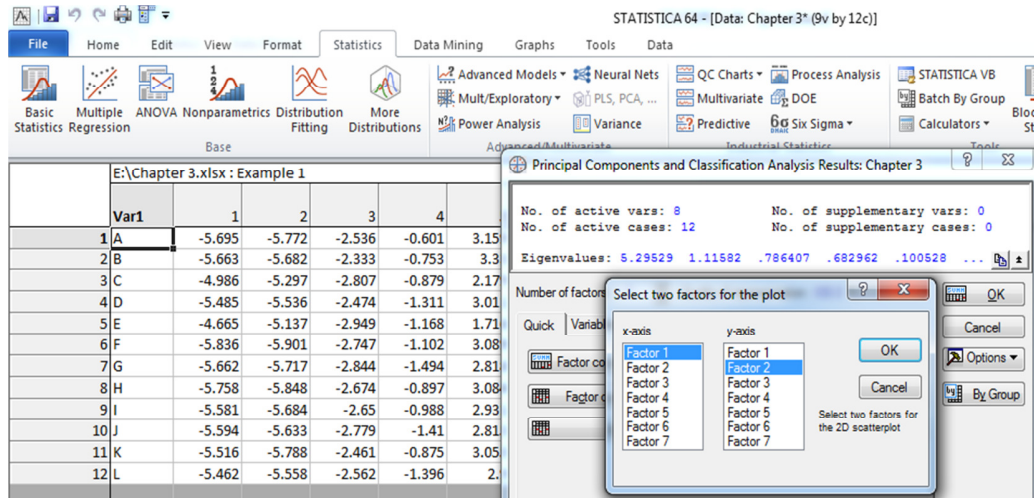


**Figure 3.12:** Factors (principal components) to be used for the 2D scores plots<sup>4</sup>

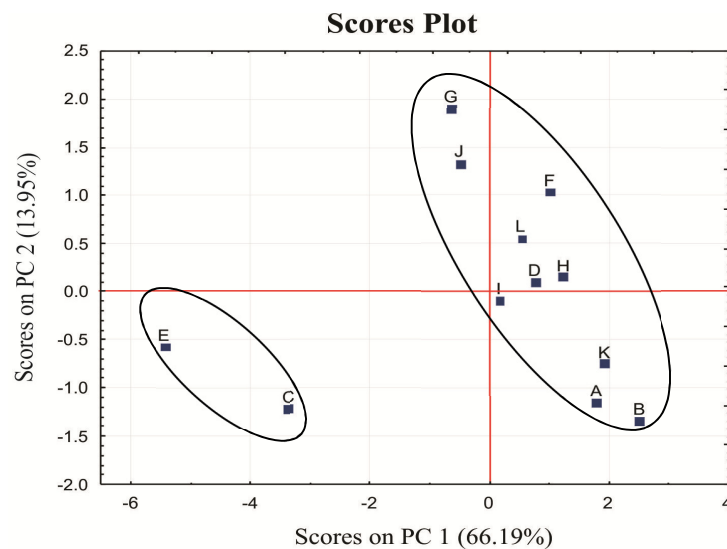


**Figure 3.13:** Scores plot<sup>4</sup>

The following steps were followed in order to obtain the loadings plot from Statistica version 12:

- ❖ The Statistics tab on the tool bar was selected, and then Mult/Exploratory tab was selected to display a list of analysis.
- ❖ The (Principal Component and Classification) option was selected on the list of analysis.
- ❖ The Plot variable factor coordinates (Plot var. factor coordinates, 2D) tab, was selected as indicated in **Figure 3.14**.

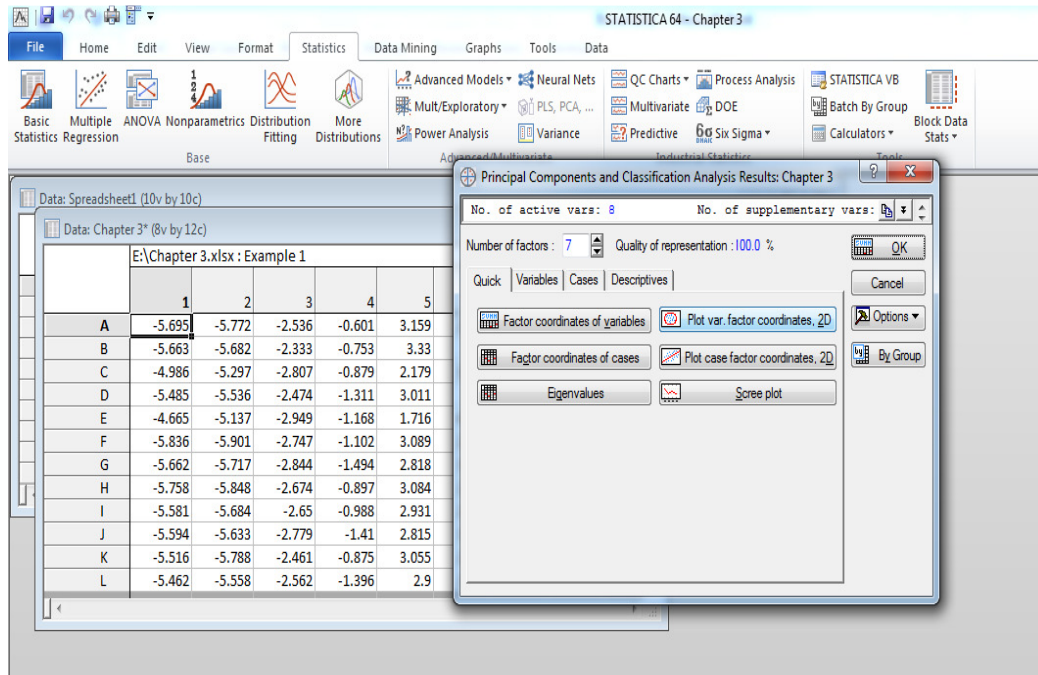


**Figure 3.14:** Plot var. factor coordinates, 2D tab<sup>4</sup>

- ❖ A pop-up box appears with a prompt to select two factors that can be used to plot the variable in a 2D space. Factors 1 and 2 were selected as indicated in **Figure 3.12**.
- ❖ The loadings plot as shown in **Figure 3.15** is obtained.

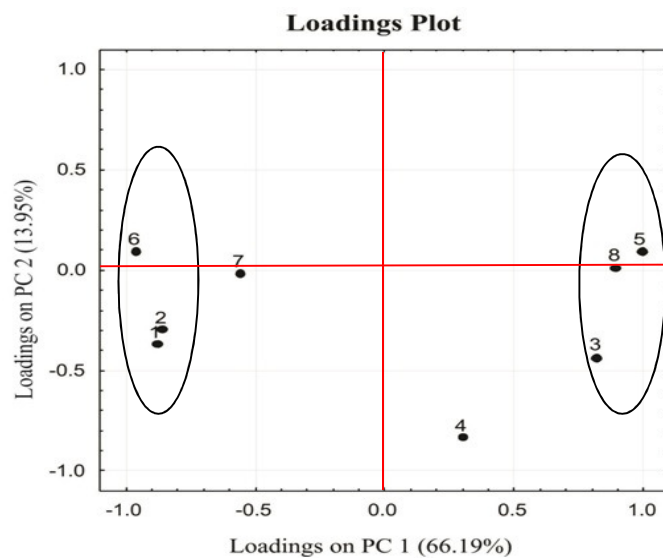


**Figure 3.15:** Loadings plot<sup>4</sup>

The relationship between the complexes can be interpreted from the scores plot (**Figure 3.13**); therefore, these complexes can be divided into two groups when projected along **PC 1** (horizontal axis) of the scores plot. The first group consists of complexes **A, B, D, F, G, H, I, J, K** and **L**, while the second group is made up of complexes **C** and **E**. The chemical properties highlighted in the loadings plot can be used to further classify these complexes.

The chemical properties (1 =  $E_{\text{HOMO}}$  (eV), 2 =  $E_{\text{HOMO}-1}$  (eV), 3 =  $E_{\text{LUMO}}$  (eV), 5 =  $|E_{\text{HOMO}} - E_{\text{LUMO}}|$  energy gap, 6 = Electrophilicity index and 8 = C% contribution to LUMO) are distributed towards the edges of the horizontal scale in the loadings plot (**Figure 3.15**), and therefore they represent the most variance among the chemical properties. Therefore, these chemical properties can be used to distinguish among the complexes in the scores plot when projected along **PC 1**.

### 3.3. Computational method

#### 3.3.1. Geometry optimization

All the complexes listed in **Chart 3.1** and **Chart 3.2** were geometrically optimized using Materials Studio 6.0 DMol<sup>3</sup> DFT module.<sup>8</sup> The generalized gradient approximation, Perdew and Wang's 1991 functional (GGA/PW91)<sup>9</sup> and the double numerical polarized (DNP) basis set was used to accommodate the d- and p-type polarization functions and to describe the valence electron.

All the bi-metallic structures were optimized in a *cis* configuration with respect to both metal fragments, even though some of the synthesized structures were found to be in a *trans* configuration. We decided to optimize all the structures in a similar configuration for better comparison, therefore the influence of *cis* versus *trans* configuration on the chemical properties of these complexes will not be discussed in this study.

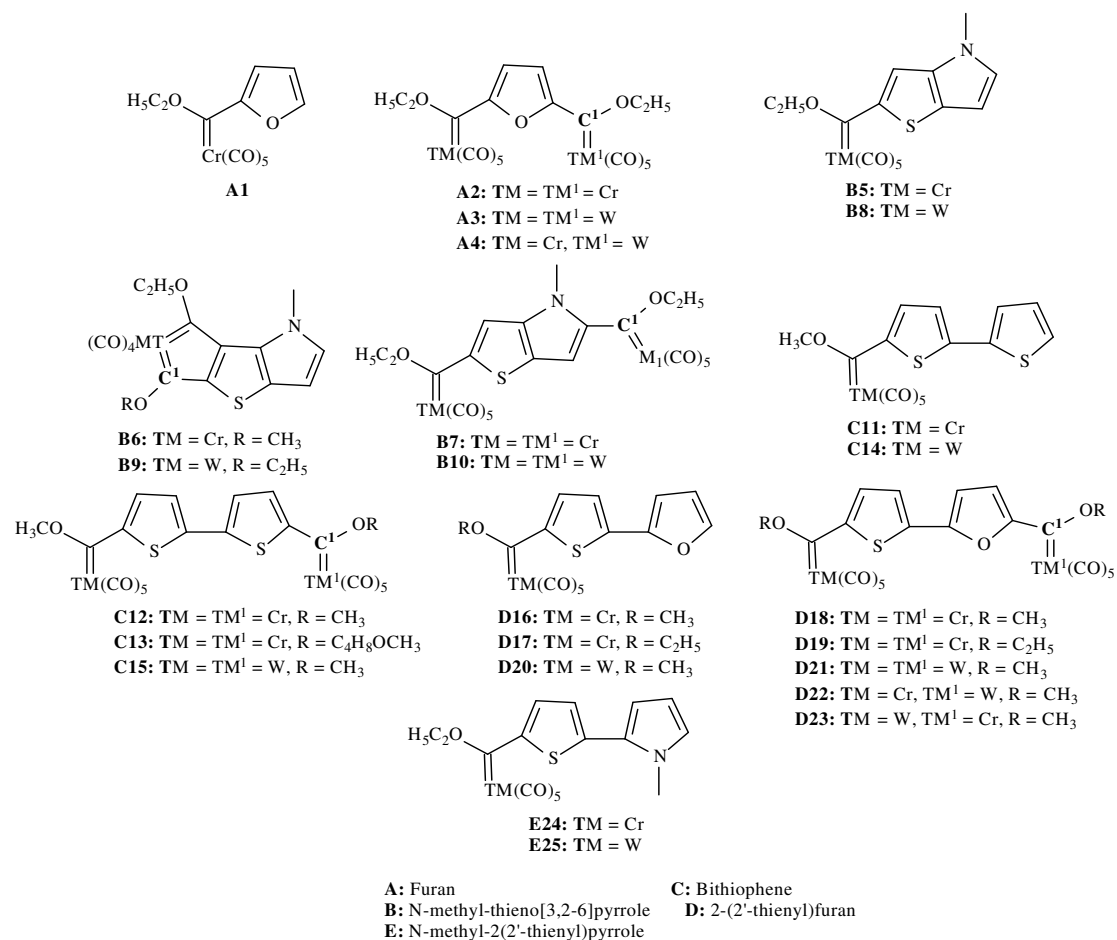
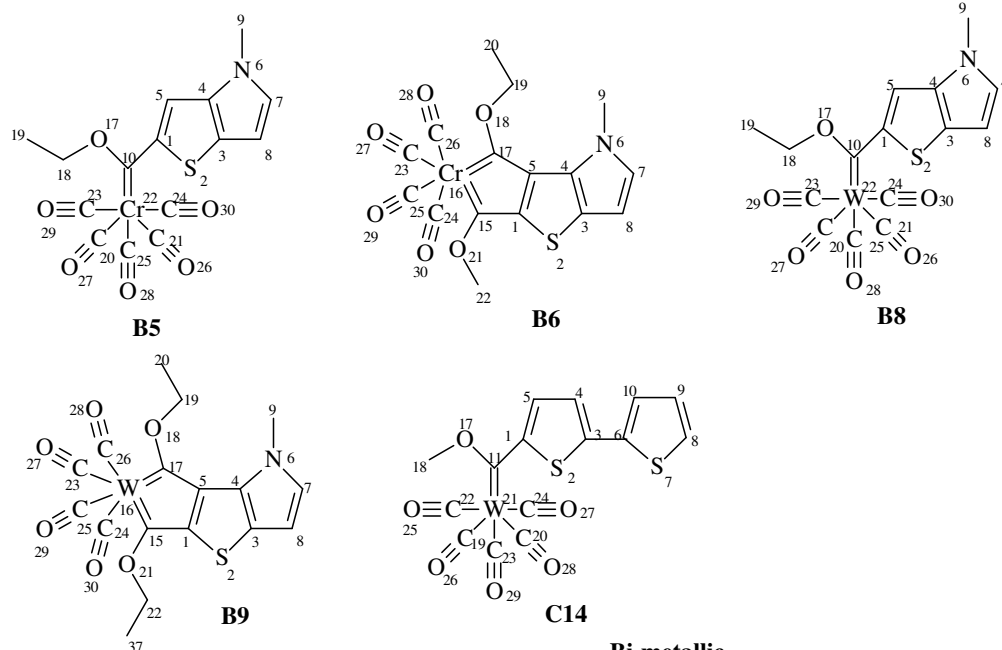


**Chart 3.1:** Fischer type metal carbenes used for principal component analysis

### Mono-metallic



### Bi-metallic

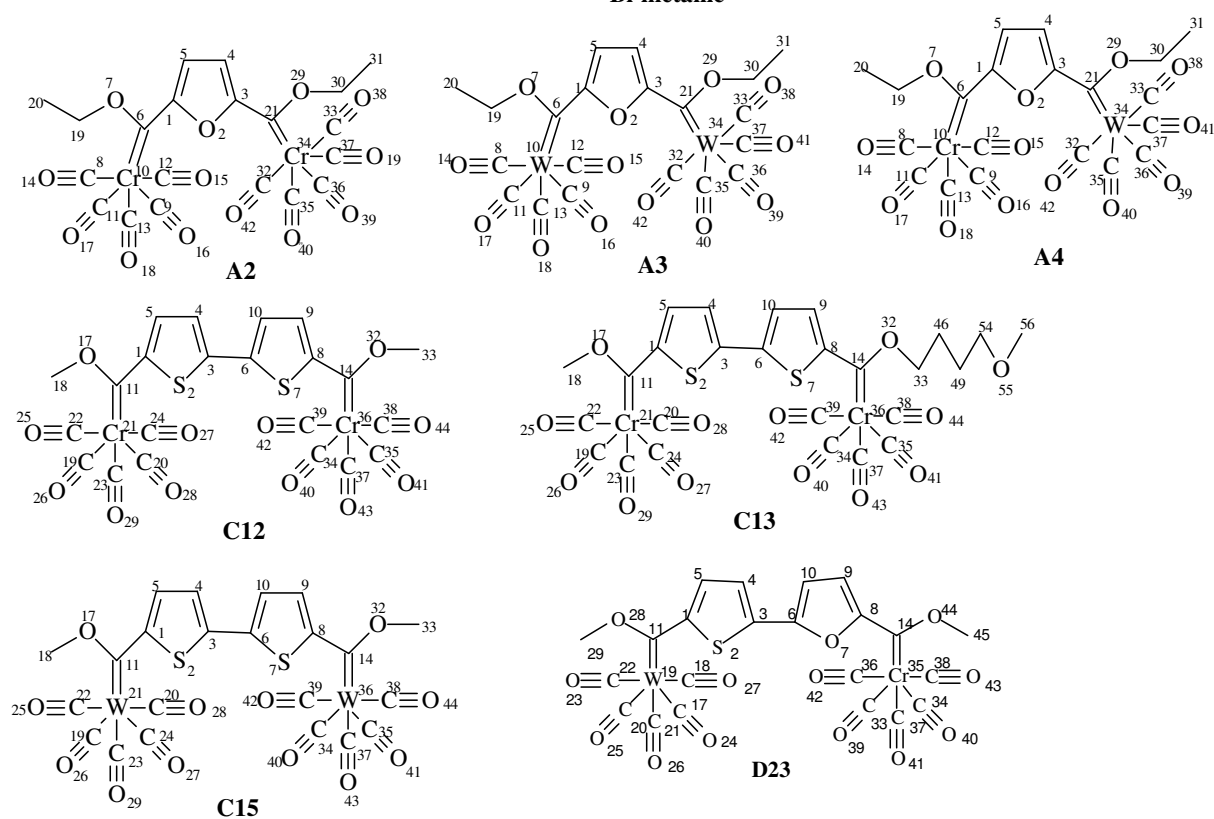


**Chart 3.2:** Atomic numbering of selected mono- and bi-metallic complexes



### 3.3.2. Single-Point energy and property calculations

In order to improve the accuracy of the energy levels the B3LYP<sup>11</sup> (Becke, three-parameter, Lee-Yang-Parr) hybrid functional within Gaussian09<sup>10</sup>, which is known to give more accurate energy levels as compared to GGA/PW91, was used for single-point energy calculations to obtain molecular orbitals. The 6-31G\* basis set was used for C, H, O, N and S, while the Karlsruhe split-valence basis set with polarization functions (def-2SV(P))<sup>12</sup> was used to describe the valence electrons of Cr and W. The core electrons of Cr and W were described by using the Stuttgart/Dresden (SDD)<sup>13</sup> pseudo-potential. Therefore frontier orbital energy levels, *i.e.* E<sub>HOMO</sub> (eV), E<sub>HOMO-1</sub> (eV), E<sub>LUMO</sub> (eV) and E<sub>LUMO+1</sub> (eV) were obtained from the above mentioned calculations.

The electrophilicity index ( $\omega$ ) of the complexes was calculated from the HOMO and LUMO energy levels according to the following equations, as suggested by Parr *et al.*<sup>15</sup>

$$\omega \equiv \mu^2/2\eta \dots\dots\dots(10)$$

$$\mu \approx (\epsilon_{LUMO} + \epsilon_{HOMO})/2 \dots\dots\dots(11)$$

$$\eta \approx \epsilon_{LUMO} - \epsilon_{HOMO} \dots\dots\dots(12)$$

Where  $\mu$  is the chemical potential and  $\eta$  is the hardness.<sup>15,16</sup>

Percentage fragment and atomic orbital coefficient  $\Sigma$ (AOC) which contributions towards the HOMOs and LUMOs (**Table 3.5**) were calculated by Chemissain from data obtained from single-point energy calculations (Gaussian09)<sup>10</sup>. Both of the above-mentioned contributions towards the HOMOs and LUMOs were calculated with Chemissian<sup>14</sup> based on Mulliken-type population analysis.

**Table 3.5:** Chemical properties obtained from Chemissian where TM/TM<sup>1</sup> = transition-metals

Fragment contribution to frontier orbitals	Atomic orbital contribution to frontier orbitals
TM%/TM <sup>1</sup> % contribution to HOMO	Σ(AOC) of HOMO
Carbene C%C <sup>1</sup> % contribution to LUMO	Σ(AOC) of HOMO-1
	Σ(AOC) of LUMO
	Σ(AOC) of LUMO+1

### 3.3.3. Natural bond orbital (NBO)

Gaussian09<sup>10</sup> was also used to analyse orbital occupation, *i.e.* natural population analysis (NPA) and natural bond orbital (NBO) calculations with B3LYP and 6-31G\* basis set for C, H, O, N and S, while (def-2SV(P)) basis set and SDD were used to describe the valence and core electrons of Cr and W, respectively. Hybridization and polarization within the transition metal-carbene (TM-C) bond and donor-acceptor interactions were also calculated using the natural bond orbital (NBO) analysis method.<sup>17-19</sup>

The following properties were calculated from NBO and NPA analysis, where TM-C/TM<sup>1</sup>-C<sup>1</sup> represents the transition metal-carbene bonds: Occupancy of TM-C/TM<sup>1</sup>-C<sup>1</sup> bonds; C%/C<sup>1</sup>% polarization; TM%/TM<sup>1</sup>% polarization; %s orbital hybridization of carbene C/C<sup>1</sup>%; %p orbital hybridization of carbene C/C<sup>1</sup>; %s orbital hybridization of TM/TM<sup>1</sup>; %p orbital hybridization of TM/TM<sup>1</sup>; %d orbital hybridization of TM/TM<sup>1</sup>; NPA charge of carbene carbon C/C<sup>1</sup>; NPA charge of TM/TM<sup>1</sup>; and donor-acceptor stabilization energy (E<sup>2</sup>).

### 3.3.4. Shielding

Solid-G software<sup>20</sup> was used to determine the extent to which the metal fragment is shielded by all the ligated atoms and ligands. The parameters of interest are as follows: G(complex)% is the overall shielding of the complex with all ligands treated as one around the metal; G(M)% is the percentage of the metal's surface shielded by the ligated atoms only. This technique was used to establish the hinderance a reactant might experience as it interacts with the metal atom. The computational details used to calculate these shielding parameters are described in detail by Guzei *et al.*<sup>21</sup>

The following equations serve as a basis for calculating the shielding parameter (G):

$$\Omega = \frac{A}{r^2} \dots\dots\dots (13)$$

$$G = 100 \frac{\Omega}{4\pi} \dots\dots\dots (14)$$

Where  $\Omega$  is a solid angle,  $r^2$  is the square of the sphere radius, A the shadowed area.

A pictorial definition of the geometrical solid angle is given in **Figure 3.16**. This solid angle can be visualized by replacing the metal moiety in an organometallic complex with a light source, thus allowing each ligand to cast a shadow on a sphere surrounding the complex.<sup>21</sup> The numeric value of the solid angle can be calculated from equation 13.

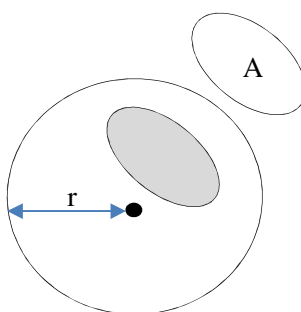


**Figure 3.16:** Definition of the geometrical solid angle<sup>21</sup> ( $\Omega = \frac{A}{r^2}$ )

### 3.3.5. Multivariable data analysis

Statistica version 12<sup>4(a)</sup> was used for principal component analysis (PCA) in order to obtain scores and loadings plots along principal components. This method was used in order to identify the chemical properties that can be used to differentiate among the complexes listed in **Chart 3.1**. Non-redundant chemical properties with a coefficient of determination ( $R^2 \leq 0.9$ )<sup>4</sup> were kept and analysed further. A total of 34 chemical properties (**Table 4.4**) were analysed by PCA in order to find relations between a series of Fischer type carbene complexes.

Firstly, geometry optimization, single point energy, bond occupancy, polarization, hybridization and natural population charges (NPA) calculations were done on the metal carbenes with all ligands attached on both metal moieties *i.e.* TM and TM<sup>1</sup>. The calculations mentioned above were also conducted on the mono- and bi-metallic carbenes, after a CO ligand was dissociated

from metal moiety TM or TM<sup>1</sup> respectively. Then five tables were compiled with the chemical properties studied for each complex as the variables (Supplementary document **S11**). This was finally followed by principal component analysis of the calculated chemical properties of the above-mentioned (**Chart 3.1**) mono- and bi-metallic carbenes respectively.

## References

1. Davis, J.C. *Statistics and Data Analysis in Geology*, 3ed, John Wiley and Sons, Inc., **2002**.
2. Shlens, J. *Tutorial on principal component analysis*. **2005**.  
<http://www.sn1.salk.edu/~shlens/pub/notes/pca.pdf>: date accessed 2015-12-10
3. Introduction to PCA, <http://dml.cs.byu.edu/~cgc/docs/dm/Slides/>: date accessed 2015-12-10.
4. (a) StatSoft, Inc. Statistica version 12, Tulsa, OK, USA. **2013**. (b) Electronic Statistics Textbook; Tulsa, <http://www.statsoft.com/textbook/>: date accessed 2015-05-10.
5. Triola, M. F. *Elementary Statistics*, 12, Pearson Education: Boston. **2014**.
6. Occhipinti, G.; Jensen, V. R. *Organometallics*. **2011**, 30, 3522-3529.
7. Jambu, M. *Exploratory and multivariate data analysis*. Academic Press: Orlando, **1991**.
8. Systèmes, D. BIOVIA Material Studio 6.2016, 16.1.0.21; Accelrys:2015
9. Perdew, J. P. *Electronic Structure of Solids*, Akademie Verlag: Berlin, **1991**, 11.
10. Frisch, M. J.; Trucks, G. W.; Schlegel, H. B.; Scuseria, G. E.; Robb, M. A.; Cheeseman, R. J.; Scalmani, G.; Barone, V.; Mennucci, B.; Petersson, G. A.; Nakatsuji, H.; Caricato, M.; Li, X.; Hratchian, H. P.; Izmaylov, A. F.; Bloino, J.; Zheng, G.; Sonnenberg, J. L.; Hada, M.; Ehara, M.; Toyota, K.; Fukuda, R.; Hasegawa, J.; Ishida, M.; Nakajima, T.; Honda, Y.; Kitao, O.; Nakai, H.; Vreven, T.; Montgomery, J. A.; Peralta, Jr., J. E.; Ogliaro, F.; Bearpark, M.; Heyd, J. J.; Brothers, E.; Kudin, K. N.; Staroverov, V. N.; Kobayashi, R.; Normand, J.; Raghavachari, K.; Rendell, A.; Burant, J. C.; Iyengar, S. S.; Tomasi, J.; Cossi, M.; Rega, N.; Millam, J. M.; Klene, M.; Knox, J. E.; Cross, J. B.; Bakken, V.; Adamo, C.; Jaramillo, J.; Gomperts, R.; Stratmann, R. E.; Yazyev, O.; Austin, A. J.; Cammi, R.; Pomelli, C.; Ochterski, J. W.; Martin, R. L.; Morokuma, K.; Zakrzewski, V. G.; Voth, G. A.; Salvador, P.; Dannenberg, J. J.; Dapprich, S.; Daniels, A. D.; Farkas, Ö.; Foresman, J. B.; Ortiz, J. V.; Cioslowski, J.; Fox, D. J. Gaussian 09, Revision D.01, Gaussian, Inc., Wallingford CT, **2009**. [http://www.gaussian.com/g\\_prod/g09.htm](http://www.gaussian.com/g_prod/g09.htm).

11. Becke, A. D., *J. Chem. Phys.* **1993**, 98, 5648.
12. Weigend, F.; Ahlrichs, R. *Phys. Chem. Chem. Phys.* **2005**, 7, 3297.
13. Fuentealba, W.; Preuss, H.; Stoll, H.; Szentpály, L.V. *Chem. Phys. Lett.* **1982**, 89, 418-422.
14. <http://www.chemissian.com>: date accessed 2015-05-10.
15. Parr, R. G.; v. Szentpály, L.; Liu, S. *J. Am. Chem. Soc.* **1999**, 121, 1922.
16. Kiyooka, S; Kaneno, D; Fujiyama, R. *Tetrahedron Lett.* **2013**, 54, 339 .
17. Foster, J. P.; Weinhold, F. *J. Am. Chem. Soc.* **1980**, 102, 7211.
18. Reed, A. E.; Weinhold, F. *J. Am. Chem. Soc.* **1985**, 83, 1736.
19. Reed, A. E.; Weinstock, R. B.; Weinhold, F. *J. Chem. Phys.* **1985**, 83, 735.
20. Solid, G. Version 0.26, *Program for computing ligand steric effects*; Molecular structure Laboratory: **2004**.
21. Guzei, I. A; Wendt, M. *Dalton Trans.* **2006**, 3991-3999.

## Chapter 4: Results and Discussion

### 4.1. Method validation

The bond lengths and angles obtaining after the geometry optimization as described in Chapter 3 of the following complexes: **A2**, **A3**, **B5**, **B8**, **C12**, **C14** and **D20** were compared with the values obtained from crystal data in order to validate the method used to optimize these complexes. The reactivity profile of these Fischer type carbene complexes depends on the following fragments: the ligands attached to the metal moiety *i.e.* carbonyl, the heteroaromatic ring attached to the carbene carbon and the heteroatom attached to the carbene carbon as mentioned in Section 2.2. Therefore bond lengths and angles between selected atoms attached to the metal moiety and carbene carbons were analyzed. In addition to this, bond lengths and angles within the heteroaromatic rings were also selected for this statistical analysis. The data and statistical analysis of these complexes is given in Supplementary document **S2**. Two complexes with crystal data, **A2** and **B5** will be discussed in the following section as an example of how the method used to optimize these complexes was validated.

The differences between the calculated and crystal data values of bond lengths and angles were determined. Negative values indicate that the bond lengths and angles of the geometry optimized structures are larger than the values obtained from crystal data (**Table 4.1(c)** and **Table 4.2(c)**).

**Table 4.1:** Bond lengths obtained from (a) calculated values and (b) literature values of experimental structures (crystal data);<sup>1</sup> (c) the difference between crystal data and calculated values; atom numbering is shown in **Chart 3.2**

Complex <b>A2</b>				Complex <b>B5</b>			
Atoms	Bond lengths (Å)			Atoms	Bond lengths (Å)		
	(a)	(b) <sup>1</sup>	(c)		(a)	(b) <sup>1</sup>	(c)
Cr(10)-C(8)	1.904	1.899	-0.005	Cr(22)-C(25)	1.884	1.867	-0.017
Cr(10)-C(9)	1.911	1.922	0.011	Cr(22)-C(20)	1.903	1.904	0.001
Cr(10)-C(11)	1.904	1.898	-0.006	Cr(22)-C(21)	1.897	1.897	0.000
Cr(10)-C(12)	1.910	1.913	0.003	Cr(22)-C(23)	1.904	1.904	0.000
Cr(10)-C(13)	1.898	1.908	0.010	Cr(22)-C(24)	1.899	1.897	-0.002
Cr(10)-C(6)	2.058	2.016	-0.042	Cr(22)-C(10)	2.114	2.082	-0.032
C(6)-O(7)	1.343	1.330	-0.013	C(10)-O(17)	1.345	1.332	-0.013
C(6)-C1(1)	1.454	1.470	0.016	C(1)-S(2)	1.791	1.774	-0.017
Cr(34)-C(33)	1.903	1.890	-0.013				
Cr(34)-C(37)	1.907	1.895	-0.012				
Cr(34)-C(35)	1.903	1.904	0.001				
Cr(34)-C(36)	1.896	1.894	-0.002				
Cr(34)-C(32)	1.906	1.921	0.015				
Cr(34)-C(21)	2.076	2.038	-0.038				
C(21)-O(29)	1.334	1.326	-0.008				
C(3)-C(21)	1.453	1.455	0.002				



**Table 4.2:** Bond angles obtained from (a) calculated values and (b) literature values of experimental structures (crystal data);<sup>1</sup> (c) the difference between crystal data and calculated values; atom numbering is shown in **Chart 3.2**

Complex <b>A2</b>				Complex <b>B5</b>			
Atoms	Bond angle (°)			Atoms	Bond angle (°)		
	(a)	(b) <sup>1</sup>	(c)		(a)	(b) <sup>1</sup>	(c)
C(13)-Cr(10)-C(11)	87.04	90.00	2.96	C(25)-Cr(22)-C(24)	89.65	87.46	-2.19
C(13)-Cr(10)-C(9)	88.83	86.80	-2.03	C(25)-Cr(22)-C(21)	88.21	87.46	-0.75
C(13)-Cr(10)-C(8)	88.68	87.00	-1.68	C(24)-Cr(22)-C(21)	91.25	93.95	2.70
C(13)-Cr(10)-C(12)	88.72	88.90	0.18	C(25)-Cr(22)-C(23)	87.30	88.58	1.28
C(6)-Cr(10)-C(11)	93.94	94.70	0.76	C(25)-Cr(22)-C(20)	89.31	88.58	-0.74
C(6)-Cr(10)-C(9)	88.95	90.50	1.55	C(20)-Cr(22)-C(21)	87.20	88.75	1.55
C(6)-Cr(10)-C(8)	93.51	95.80	2.29	C(20)-Cr(22)-C(10)	92.05	97.11	5.06
C(6)-Cr(10)-C(12)	90.32	86.50	-3.82	C(1)-S(2)-C(3)	91.08	91.38	0.30
C(36)-Cr(34)-C(33)	88.05	88.00	-0.05				
C(36)-Cr(34)-C(37)	88.75	90.40	1.65				
C(36)-Cr(34)-C(35)	88.82	89.80	0.99				
C(36)-Cr(34)-C(32)	87.30	87.30	-0.00				
C(21)-Cr(34)-C(37)	90.12	89.80	-0.32				
C(21)-Cr(34)-C(37)	93.56	92.90	-0.66				
C(21)-Cr(34)-C(35)	88.88	86.91	-1.97				
C(21)-Cr(34)-C(32)	94.58	95.00	0.42				

**Table 4.3:** Statistical analysis of the bond length and angle difference<sup>3</sup>

Complex	Bond length (Å)		Bond angle (°)	
	Mean (Å)	Standard deviation (Å)	Mean (°)	Standard deviation (°)
<b>A2</b>	0.005	0.017	0.010	1.825
<b>B5</b>	0.010	0.012	0.903	2.282

The mean values of the absolute difference in the selected bond lengths (**Table 4.3**) are 0.005Å and 0.010Å for complexes **A2** and **B5**, respectively. While the mean values of the absolute difference in the selected bond angles (**Table 4.3**) are 0.010° and 0.903° for complexes **A2** and **B5**, respectively. The standard deviations of the difference in bond lengths are 0.017Å and 0.012Å for complexes **A2** and **B5**, respectively, as indicated in **Table 4.3**. This indicates that there is a marginal difference between the bond lengths of the calculated structures and the literature<sup>1</sup> values of the crystal structures. Higher standard deviations of 1.825° and 2.282 ° for complexes **A2** and **B5** are observed for the difference in bond angles as indicated in **Table 4.3**. This can be ascribed to a few angles which are slightly smaller or larger than those obtained from crystal data. The size of angles obtained from crystal data of C(13)-Cr(10)-C(11), C(13)-Cr(10)-C(9), C(13)-Cr(10)-C(8), C(6)-Cr(10)-C(9), C(6)-Cr(10)-C(8), C(6)-Cr(10)-C(12), C(36)-Cr(34)-C(37) and C(21)-Cr(34)-C(35) appears to be different from those obtained from the geometry optimized structures of complex **A2** (**Table 4.2, Chart 3.2**). The bond angles C(25)-Cr(22)-C(24), C(24)-Cr(22)-C(21), C(25)-Cr(22)-C(23), C(20)-Cr(22)-C(21) and C(20)-Cr(22)-C(10) seem to be slightly different from those obtained from crystal data of complex **B5** (**Table 4.2, Chart 3.2**). Therefore it can be concluded that the modelling method used is reliable even though the calculations were done in gas phase, since most of the bond lengths and angles obtained from calculated structures do not differ much from those obtained from crystal data.

These findings are in agreement with the results of du Toit,<sup>2</sup> where the GGA\PW91 functional and DNP basis set combination was found to be more accurate for bond length and angle calculations than other functional and basis set combinations.

## 4.2. Principal component analysis (PCA)

The chemical properties that were used as data input for the PCAs are listed in **Table 4.4**, while **Chart 3.1** lists the metal carbene complexes investigated in this study.

**Table 4.4:** Chemical properties used in principal component analysis: TM-C bond (TM-C) is used for both mono- and bi-metallic complexes, while  $\text{TM}^1\text{-C}^1$  is used to describe the second TM-C bond in bi-metallic complexes as indicated in **Chart 3.1**.

1. $E_{\text{HOMO}}$ (eV)	19. $\text{C}^1\%$ polarization
2. $E_{\text{HOMO}-1}$ (eV)	20. $\text{TM}^1\%$ polarization
3. $E_{\text{LUMO}}$ (eV)	21. %s orbital hybridization of carbene C
4. $E_{\text{LUMO}+1}$ (eV)	22. %p orbital hybridization of carbene C
5. $ E_{\text{HOMO}} - E_{\text{LUMO}} $ energy gap	23. %s orbital hybridization of metal TM
6. Electrophilicity index	24. %p orbital hybridization of metal TM
7. TM% contribution to HOMO	25. %d orbital hybridization of metal TM
8. $\text{TM}^1\%$ contribution to HOMO	26. %s orbital hybridization of carbene $\text{C}^1$
9. Carbene C% contribution to LUMO	27. %p orbital hybridization of carbene $\text{C}^1$
10. Carbene $\text{C}^1\%$ contribution to LUMO	28. %s orbital hybridization of metal $\text{TM}^1$
11. $\Sigma(\text{AOC})$ of HOMO	29. %p orbital hybridization of metal $\text{TM}^1$
12. $\Sigma(\text{AOC})$ of HOMO-1	30. %d orbital hybridization of metal $\text{TM}^1$
13. $\Sigma(\text{AOC})$ of LUMO	31. NPA charge of carbene C
14. $\Sigma(\text{AOC})$ of LUMO+1	32. NPA charge of metal TM
15. Occupancy of TM-C bond	33. NPA charge of carbene $\text{C}^1$
16. Occupancy of $\text{TM}^1\text{-C}^1$ bond	34. NPA charge of metal $\text{TM}^1$
17. C% polarization	
18. TM% polarization	

The data used for **PCA 1** to **PCA 5** plots is listed in Supplementary document **S12** (Worksheet 1 - Worksheet 5), Worksheet 1 = data used for **PCA 1** (mono-metallic carbenes with all ligands attached); Worksheet 2 = data used for **PCA 2** (mono-metallic carbenes with a *trans*-CO ligand dissociated from TM); Worksheet 3 = data used for **PCA 3** (bi-metallic carbenes with all ligands attached); Worksheet 4 = data used for **PCA 4** (bi-metallic carbenes with a *trans*-CO ligand

dissociated from metal TM) and Worksheet 5 = data used for **PCA 5** (bi-metallic carbenes with a *trans*-CO ligand dissociated from metal TM<sup>1</sup>).

Statistica version 12<sup>4(a)(b)</sup> was used to obtain % total variance and eigenvalues from a correlation matrix. Supplementary document **S3** shows the complete list of principal components with eigenvalues as calculated by Statistica version 12. Only four principal components are listed for **PCA 1** to **PCA 5** (**Table 4.5**); the other principal components represent the least variation among the data set. The first principal component (**PC 1**) with the largest eigenvalue describes the largest percentage variance among the chemical properties when all the chemical properties are projected on it (**Table 4.5**). The second principal component (**PC 2**) is an orthogonal line to **PC 1**. **PC 2** describes the second largest percentage variance (**Table 4.5**). Therefore principal components **PC 1** and **PC 2** describe the largest variance within the dataset from **PCA 1** to **PCA 5** (**Table 4.5**).

**Table 4.5:** Eigenvalues and % total variance of chemical properties used in multivariate analysis in **PCA 1** to **PCA 5**<sup>4(a),5</sup>

	<b>PCA 1</b>		<b>PCA 2</b>		<b>PCA 3</b>	
	Eigenvalues	% Total Variance	Eigenvalues	% Total Variance	Eigenvalues	% Total Variance
PC 1	9.682	44.01	7.8730	37.49	11.179	32.88
PC 2	6.585	29.93	5.6949	27.12	6.600	19.41
PC 3	2.074	9.43	2.6060	12.41	5.076	14.93
PC 4	1.310	5.95	1.5387	7.33	3.883	11.42
	<b>PCA 4</b>		<b>PCA 5</b>			
	Eigenvalues	% Total Variance	Eigenvalues	% Total Variance		
PC 1	10.869	33.97	10.237	31.99		
PC 2	7.528	23.52	8.701	27.19		
PC 3	4.793	14.98	3.965	12.39		
PC 4	3.119	9.75	2.767	8.65		

As the results show in all cases, more than 50% of the total variance is described by the first two principal components, *i.e.* **PC 1** and **PC 2**. Furthermore, **PC 3** only contributes an average of

13.7% to the variance of the data (**PCA 1 - PCA 5**), with **PCA 4** having the largest **PC 3** total variance percentage of 19.6% (**Table 4.5**). Therefore, principal component analysis plots with **PC 1** and **PC 2** will be used to identify chemical properties that can be used to distinguish among the 25 Fischer type metal carbene complexes under investigation (**Chart 3.1**). Redundant chemical properties, *i.e.* properties with a coefficient of determination ( $R^2$ )  $\geq 0.9$ , have been removed from the loadings plots of **PCA 1** to **PCA 5**.

**PCA 1** to **PCA 5** plots are labelled as follows: **PCA 1** (**Figures 4.1** and **4.2**) = mono-metallic carbenes with all ligands attached; **PCA 2** (**Figures 4.3** and **4.4**) = mono-metallic carbenes with a *trans*-CO ligand dissociated from TM; **PCA 3** (**Figures 4.5** and **4.6**) = bi-metallic carbenes with all ligands attached; **PCA 4** (**Figures 4.7** and **4.8**) = bi-metallic carbenes with a *trans*-CO ligand dissociated from metal TM; **PCA 5** (**Figures 4.9** and **4.10**) = bi-metallic carbenes with a *trans*-CO ligand dissociated from metal TM<sup>1</sup>.

The following PCA plots (**Figures 4.1 - 4.10**)<sup>4(a)</sup> with non-redundant chemical properties, *i.e.* properties with a coefficient of determination ( $R^2$ )  $\leq 0.9$ , were used for multivariate analysis.

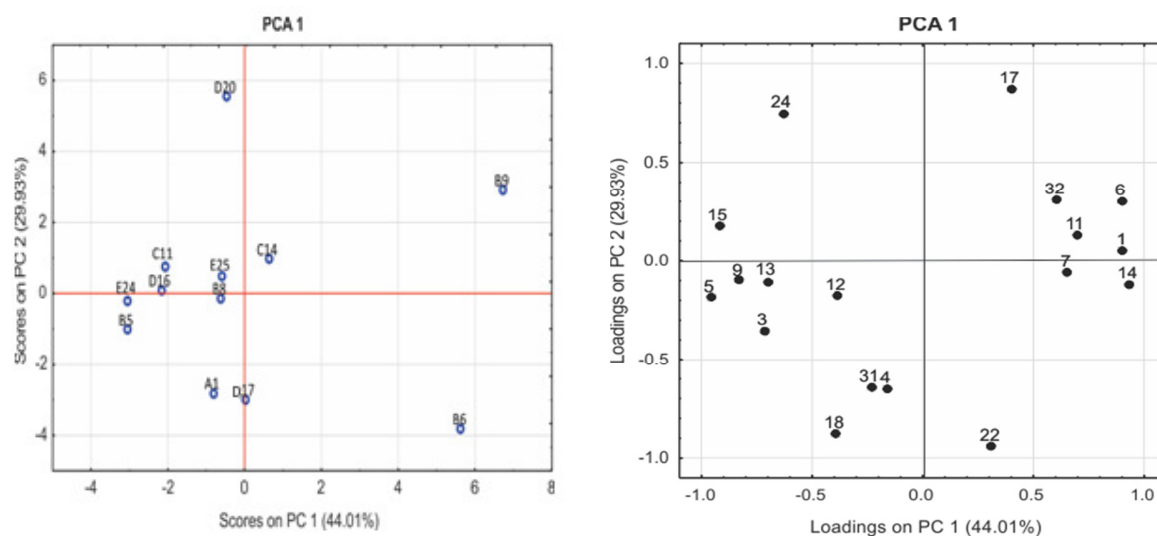


**Figure 4.1: PCA 1 Scores, PC 1 versus PC 2; Figure 4.2: PCA 1 Loadings, PC 1 versus PC 2**

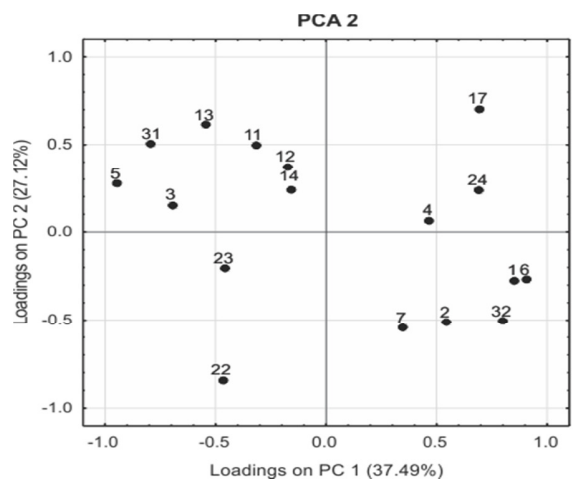
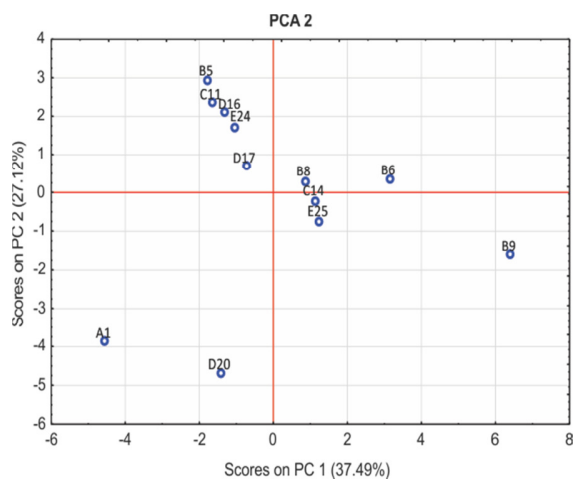


**Figure 4.3: PCA 2 Scores, PC 1 versus PC 2; Figure 4.4: PCA 2 Loadings, PC 1 versus PC 2**

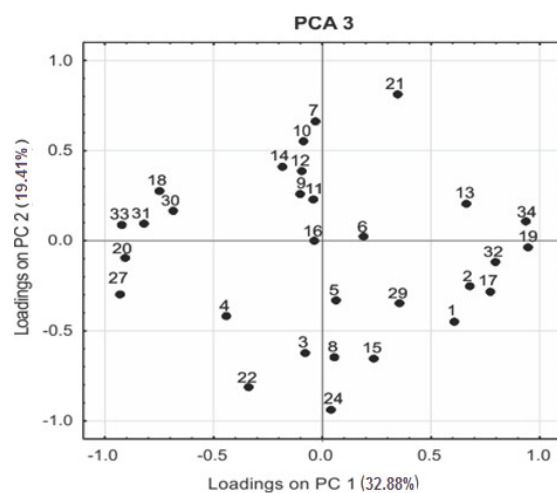
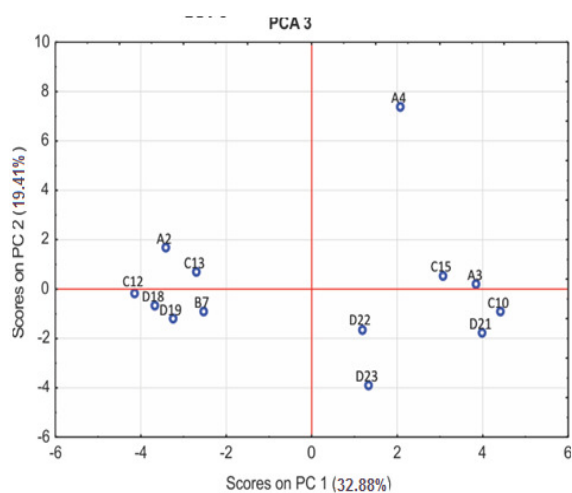


**Figure 4.5: PCA 3 Scores, PC 1 versus PC 2; Figure 4.6: PCA 3 Loadings, PC 1 versus PC 2**

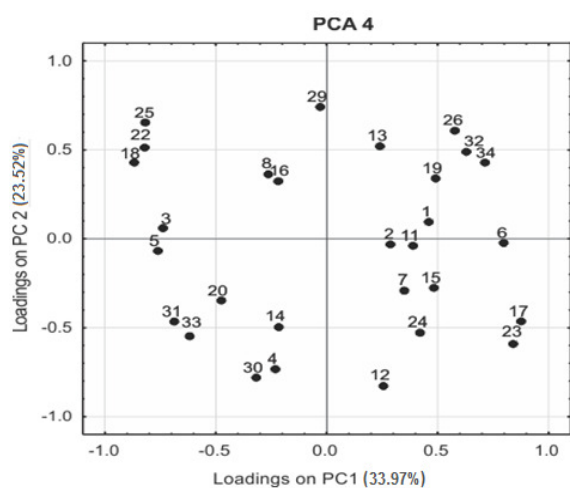
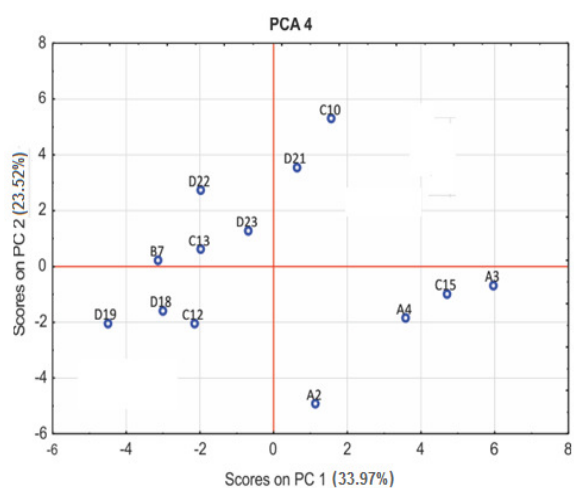


**Figure 4.7: PCA 4 Scores, PC 1 versus PC 2; Figure 4.8: PCA 4 Loadings, PC 1 versus PC 2**

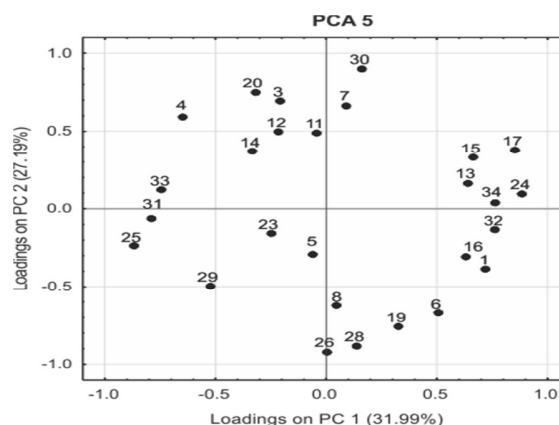
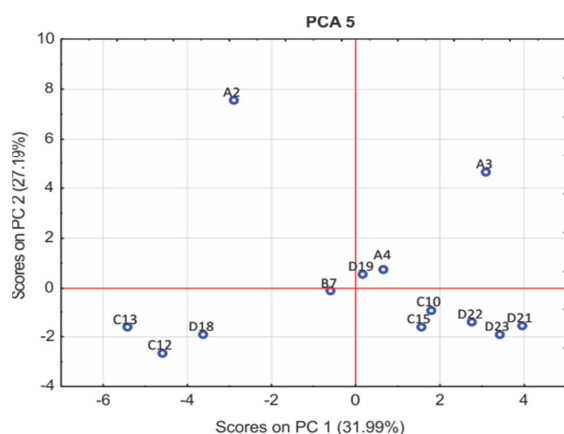


**Figure 4.9: PCA 5 Scores, PC 1 versus PC 2; Figure 4.10: PCA 5 Loadings, PC 1 versus PC 2**

Both **PC 1** and **PC 2** in **Figures 4.1 - 4.10** account for less than 81% total variance, *i.e.*, 80.67% for **PCA 1**; 64.61% for **PCA 2**; 55.38% for **PCA 3**; 57.30% for **PCA 4**; 61.59% for **PCA 5**. These low percentage variances can be attributed to the fact that various groups of the same class, namely five-membered heteroaromatic ring-substituted Fischer type metal carbene complexes are investigated.

The chemical properties, as highlighted from the loadings plots of **PCA 1 - PCA 5**, which represent the most variance among all the properties investigated, will be used to further classify the 25 Fischer type metal carbene complexes (**Chart 3.1**) and are listed in **Table 4.6**.

**Table 4.6:** Chemical properties, which can be used to differentiate complexes within **PCA 1 – PCA 5** when projected along **PC 1** and **PC 2**

	Along <b>PC 1</b>	Along <b>PC 2</b>
<b>PCA 1</b>	1 = $E_{\text{HOMO}}$ (eV) 5 = $ E_{\text{HOMO}} - E_{\text{LUMO}} $ energy gap 6 = Electrophilicity index 9 = Carbene C% contribution to LUMO 15 = occupancy of TM-C bond	17 = C% polarization 18 = TM% polarization 22 = %p orbital hybridization of carbene C 24 = %p orbital hybridization of metal TM
<b>PCA 2</b>	1 = $E_{\text{HOMO}}$ (eV) 5 = $ E_{\text{HOMO}} - E_{\text{LUMO}} $ energy gap 6 = Electrophilicity index 31 = NPA charge of carbene C 32 = NPA charge of carbene TM	13 = $\Sigma(\text{AOC})$ of LUMO 17 = C% polarization 22 = %p orbital hybridization of carbene C
<b>PCA 3</b>	19 = C <sup>1</sup> % polarization 20 = TM <sup>1</sup> % polarization 27 = %p orbital hybridization of carbene C <sup>1</sup> 31 = NPA charge of carbene C 33 = NPA charge of carbene C1 34 = NPA charge of carbene TM <sup>1</sup>	7 = TM% contribution to HOMO 21 = %s orbital hybridization of carbene C 22 = %p orbital hybridization of carbene C 24 = %p orbital hybridization of metal TM
<b>PCA 4</b>	6 = Electrophilicity index 17 = C % polarization 18 = TM% polarization 22 = %p orbital hybridization of carbene C 23 = %s orbital hybridization of metal TM 25 = %d orbital hybridization of metal TM	4 = $E_{\text{LUMO}+1}$ (eV) 12 = $\Sigma(\text{AOC})$ of HOMO-1 22 = %p orbital hybridization of carbene C 25 = %d orbital hybridization of metal TM 26 = %s orbital hybridization of carbene C1 29 = %p orbital hybridization of metal TM1 30 = %d orbital hybridization of metal TM <sup>1</sup> 32 = NPA charge of metal TM
<b>PCA 5</b>	17 = C% polarization 24 = %p orbital hybridization of metal TM 25 = %d orbital hybridization of metal TM 31 = NPA charge of carbene C 32 = NPA charge of metal TM 33 = NPA charge of carbene C1 34 = NPA charge of metal TM <sup>1</sup>	20 = TM <sup>1</sup> % polarization 26 = %s orbital hybridization of carbene C1 28 = %s orbital hybridization of metal TM1 30 = %d hybridization of metal TM1



The various metal carbene complexes, as highlighted from the scores plots of **PCA 1 - PCA 5**, can be clustered into sub-groups according to their properties. **Table 4.7** highlights the sub-groups, as obtained from the scores plots of **PCA 1** to **PCA 5**, projected along **PC 1** and **PC 2**, respectively.

**Table 4.7:** Sub-groups highlighted from the scores plot of **PCA 1** to **PCA 5**, when projected along **PC 1** and **PC 2**

	Along PC 1	Along PC 2
<b>PCA 1</b>	(B6, B9); (A1, B5, B8, C11, C14, D16, D17, D20, E24, E25)	(A1, B6, D17); (B5, B8, C11, C14, D16, E24, E25); B9; D20
<b>PCA 2</b>	A1; (B5, B8, C11, C14, D16, D17, D20, E24, E25); B6; B9	(A1, D20); (B5, B6, B8, B9, C11, C14, D16, D17, E24, E25)
<b>PCA 3</b>	(A2, B7, C12, C13, D18, D19); (A3, A4, C10, C15, D21, D22, D23)	A4; (A2, A3, B7, C10, C12, C13, C15, D18, D19, D21, D22, D23)
<b>PCA 4</b>	(A2, B7, C10, C12, C13, D18, D19, D21, D22, D23); (A3, A4, C15,)	A2; (A3, A4, B7, C10, C12, C13, C15, D18, D19, D21, D22, D23)
<b>PCA 5</b>	(A2, C12, C13, D18); (A3, A4, B7, C10, C15, D19, D21, D22, D23)	A2; A3; (A4, B7, C10, C12, C13, C15, D18, D19, D21, D22, D23)

Two sub-groups are highlighted from **PCA 1** when projected along **PC 1** (**Table 4.7**). Complexes **B6** and **B9** can be isolated from the other mono-metallic Fischer carbenes (**Figure 4.1**). Four sub-groups are highlighted from **PCA 1** when all the mono-metallic complexes are projected on **PC 2** of the scores plot (**Figure 4.1, Table 4.7**). Complexes **A1, B6, B9, D17** and **D20** can be isolated from the other mono-metallic complexes when projected along **PC 2**.

Four sub-groups are highlighted from the scores plot of **PCA 2** (**Figure 4.3, Table 4.7**) when projected along **PC 1**. Complexes **A1, B6** and **B9** can be isolated from the other mono-metallic complexes with a *trans*-CO ligand dissociated from transition metal TM. Complexes **A1** and **D20** can clearly be isolated from the other complexes when projected along **PC 2** (**Figure 4.3**).

Two sub-groups are highlighted from the scores plots of **PCA 3** when projected along **PC 1** (**Table 4.7, Figure 4.5**). Complex **A4** can be isolated from the other bi-metallic complexes when projected along **PC 2**.

Two sub-groups (**Table 4.7**) are highlighted from the scores plots of **PCA 4** (**Figure 4.7**) when projected along **PC 1**. Complex **A2** can be isolated from all the other bi-metallic complexes with a *trans*-CO ligand dissociated from TM when projected along **PC 2**.

Two sub-groups are highlighted from the scores plots of **PCA 5** when projected along **PC 1** (**Figure 4.9, Table 4.7**). Complexes **A2** and **A3** can be isolated from all the other bi-metallic complexes with a *trans*-CO ligand dissociated from TM<sup>1</sup> when projected along **PC 2** (**Figure 4.9**).

The presence of different transition metals (W or Cr) and heteroaromatic ligands in these mono- and bi-metallic carbene complexes does not seem to play a significant role in arranging these complexes into sub-groups based on their chemical properties. This might be due to the fact that all the above-mentioned complexes from group **A** to **E** (**Figure 3.1**) are from the same class of carbene complexes *i.e.* Fischer type carbene complexes. Therefore, all the above complexes have a similar inherent chemical property *i.e.* an electrophilic carbene carbon.

Therefore, the loadings plots (**Figures 4.2, 4.4, 4.6, 4.8 and 4.10**), which highlight the variance within the values of the chemical properties, will be used to give conclusive trends among these complexes. The chemical properties (**Table 4.6**) will be investigated further in Sections 4.3 and 4.4 in order to identify complexes which will be suitable for nucleophilic attack (Section 4.3), benzannulation and metathesis (Section 4.4) reactions.

### 4.3. Complexes which are candidates for nucleophilic attack reactions

Mono-metallic and bi-metallic carbene complexes (**Chart 3.1**) which are possible candidates for nucleophilic attack reactions can be identified by analyzing the electron distribution at the potential site of nucleophilic attack using the electrophilicity indices, the NPA charges, intra- and inter-molecular  $|E_{\text{HOMO}} - E_{\text{LUMO}}|$  energy gaps, polarization, hybridization and atomic orbital coefficients within the TM-C bond.

Complexes with high electrophilicity indices are considered to be the best candidates for nucleophilic attack reactions.<sup>6-8</sup> The method for calculating the electrophilicity indices is discussed in detail by Cases *et al.*<sup>9</sup>

The intra-molecular  $|E_{\text{HOMO}} - E_{\text{LUMO}}|$  energy gap can be used as an indicator of the stability of a molecule. A molecule with a small intra-molecular  $|E_{\text{HOMO}} - E_{\text{LUMO}}|$  energy gap and a high electrophilicity index can be considered to be soft *i.e.* more reactive toward a nucleophilic attack reaction.<sup>6,7</sup> The inverse is also applicable for molecules with a large intra-molecular  $|E_{\text{HOMO}} - E_{\text{LUMO}}|$  energy gap and a low electrophilicity index; such molecules are regarded as hard molecules and are more stable *i.e.* less reactive.

In the case of the inter-molecular  $|E_{\text{HOMO}} - E_{\text{LUMO}}|$  energy gap, the HOMO of the nucleophile interacts with the LUMO of the Fischer type carbene during the nucleophilic attack reaction. For this reason the location of the LUMO as well as the energy of the LUMO are important. For example: the carbene carbon where the LUMO is located and which has a positive NPA charge will most often be the site of nucleophilic attack since the nucleophile has a negative net NPA charge.

Polarization within the TM-C bond is distributed more towards the carbene carbon; this is indicated by the large positive NPA charge on the carbene carbons (Supplementary documents **S8**, **S10**). The hybridization of the bonding molecular orbital of the TM-C bond has a carbene %p orbital and metal %d orbital character (Supplementary document **S10**). Therefore, the p orbital of the carbene carbon will interact with the molecular orbitals located in the HOMO of the nucleophile during nucleophilic attack reactions. The exact carbene p orbital that will interact with the orbitals located in the HOMO of the nucleophiles can be determined by analyzing the atomic orbital coefficients of the various p orbitals and NPA charges of the carbene carbons.

#### 4.3.1. Electrophilicity indices

Mono-metallic carbene complexes with the greatest electrophilicity indices can be arranged as follows (Supplementary document **S5(a)**): **B9** (4.223 eV) > **B6** (3.484 eV) > **E25** (3.228 eV) > **C14** (3.209 eV) > **D20** (3.113 eV), while the five bi-metallic carbene complexes with the greatest electrophilicity indices (Supplementary document **S5 (a)**) are in the following order: **A3** (4.820 eV) > **C15** (4.581 eV) > **A4** (4.573 eV) > **D21** (4.407 eV) > **C12** (4.240 eV).

Complex **B9** (4.223 eV), followed by complex **B6** (3.484 eV), has the highest electrophilicity index among all the mono-metallic complexes in this study. The high electrophilicity indices of complexes **B9** and **B6** can be attributed to the presence of two carbene carbons attached to the

metal moiety, since both carbene carbons have a net positive NPA charge. For example, the high electrophilicity index of complex **B9** can be attributed to the increased net positive charge around tungsten due to the presence of the two carbene carbons, namely C15 (0.3097e) and C17 (0.3279e) (Supplementary document **S8**). Based on the electrophilicity indices complex **B9**, followed by complex **B6**, will be ideal candidates for nucleophilic attack reactions on the carbene carbon, *i.e.* nucleophilic attack with ethenyl methyl ether or methylamine, among others.

Bi-metallic Fischer type metal carbene complexes (Supplementary document **S5** (a)) have higher electrophilicity indices than mono-metallic carbenes. This trend is observed for complexes in groups **A**, **C** and **D** (Chart 3.1, Supplementary document **S5** (a)). Complexes **A3** (4.820 eV), followed by **C15** (4.581 eV) and **A4** (4.573 eV), have the highest electrophilicity indices among all the bi-metallic complexes (Supplementary document **S5** (a)) in this study. Therefore, complexes **A3**, **A4** and **C15** can be considered to be the best candidates for nucleophilic attack reactions among the bi-metallic complexes.

The dissociation of a *trans*-CO ligand from transition metal TM or TM<sup>1</sup> reduces the electrophilicity indices in mono- and bi-metallic complexes. This reduction in the electrophilicity index is accompanied by a reduction in the positive charge on the carbene carbon when a *trans*-CO ligand is dissociated from TM or TM<sup>1</sup>, as indicated in Supplementary document **S8**. Therefore, such molecules cannot be considered good candidates for nucleophilic attack reactions.

NPA charges, intra- and inter-molecular |E<sub>HOMO</sub>-E<sub>LUMO</sub>| energy gaps, polarization, hybridization within the TM-C/TM<sup>1</sup>-C<sup>1</sup> bonds and atomic orbital coefficients will be used in the following sections to strengthen the argument for the carbene complexes, identified by electrophilicity indices, for nucleophilic attack reactions.

#### 4.3.2. NPA charges

Since mono-metallic carbene complexes **B6** and **B9**, as well as bi-metallic carbene complexes **A3**, **A4** and **C15**, have two carbene carbons that are possible sites for nucleophilic attack, site specific electrophilicity can be determined by comparing the NPA charges of carbene carbons C<sub>1</sub> and C<sub>2</sub> in these complexes.

The carbene carbons  $C_1$  and  $C_2$  of complex **B6** (Figure 4.11 (a)) have NPA charges of 0.4668e and 0.4898e, respectively, while Figure 4.11 (b) indicates that carbene carbon  $C_2$  (0.3279e) has a higher positive charge than  $C_1$  (0.3097e) in the case of complex **B9**. Therefore, carbene carbon  $C_2$  will be the site of nucleophilic attack in both complexes **B6** and **B9**.

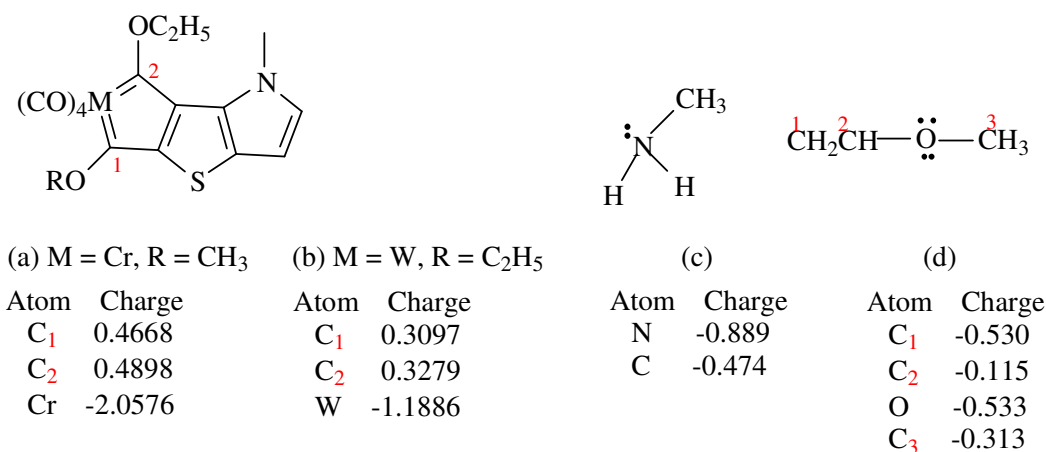


**Figure 4.11:** NPA charges<sup>13</sup> of (a) complex **B6**, (b) complex **B9**, (c) methylamine and (d) ethenyl methyl ether (supplementary document **S8**)

A similar trend is observed for complex **C15** (Figure 4.12), where carbene carbons  $C_1$  and  $C_2$  have positive charges of 0.3269e and 0.3272e, respectively. Therefore, carbene carbon  $C_2$  will be the site of nucleophilic attack for complex **C15**.

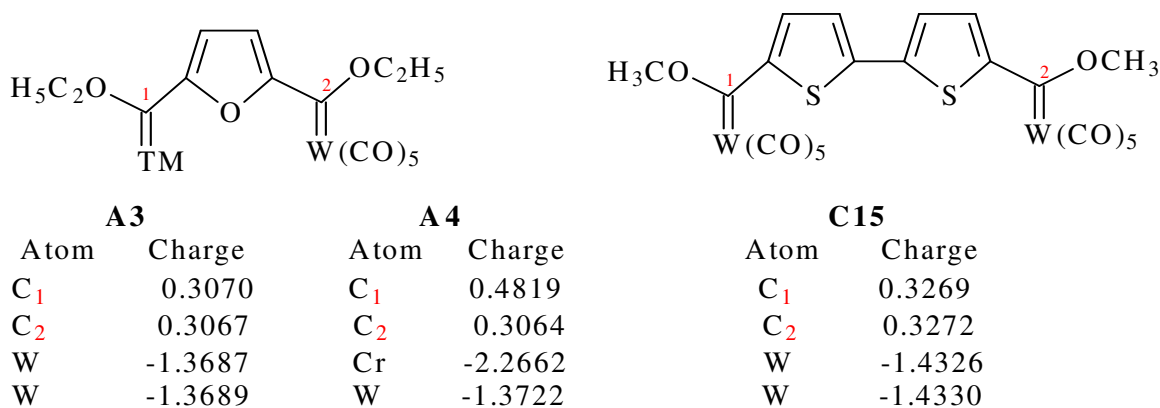


**Figure 4.12:** NPA charges of complex **A3** (TM = W), **A4** (TM = Cr) and **C15**<sup>13</sup> (Supplementary document **S8**)

However, the trend is different for complexes **A3** and **A4**, where carbene carbons  $C_1$  and  $C_2$  (**Figure 4.12**) of complex **A3** both have NPA charges which differ slightly from each other, *i.e.* 0.3070e and 0.3067e, respectively. Carbene carbons  $C_1$  and  $C_2$  (**Figure 4.12**) of complex **A4** have charges of 0.4819e and 0.3064e, respectively. Based on the NPA charges of the carbene carbons of complexes **A3** and **A4**, carbene atom  $C_1$  will be the site of nucleophilic attack in both complexes.

#### 4.3.3. Intra-molecular $|E_{HOMO}-E_{LUMO}|$ energy gap

The HOMO of complexes **B6** and **B9** is located on the metal moiety while the LUMO of both complexes is located predominantly on the carbene carbon (**Figure 4.13**). The frontier orbital energy levels of other Fischer carbene complexes analyzed in this study are given in Supplementary documents **S4**, while the pictorial representation of HOMO and LUMO orbitals are shown in Supplementary document **S6**.

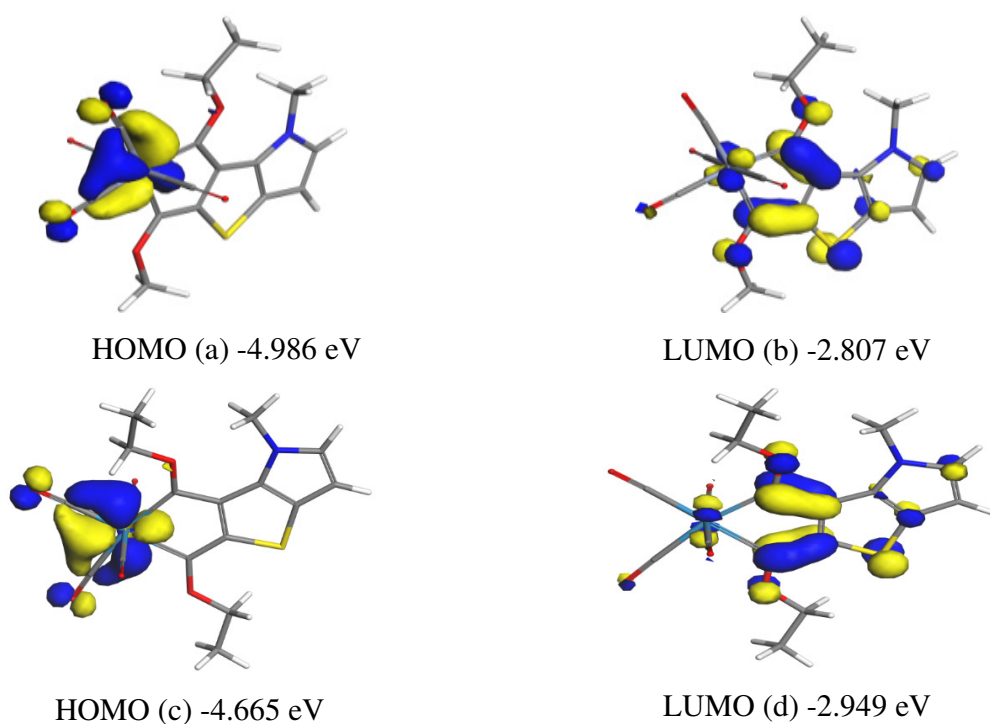


**Figure 4.13:** HOMO ((a) **B6** (TM = Cr), (c) **B9** (TM = W)) and LUMO ((b) **B6** (TM = Cr), (d) **B9** (TM = W)); (Supplementary documents **S4**, **S6**).

The intra-molecular  $|E_{\text{HOMO}} - E_{\text{LUMO}}|$  energy gap of mono-metallic carbene complexes with the highest electrophilicity indices can be arranged as follows: **B9** (1.716 eV) < **B6** (2.179 eV) < **D20** (2.815 eV) < **C14** (2.818 eV) < **E25** (2.867 eV). Complex **B9** and **B6** have the lowest intra-molecular  $|E_{\text{HOMO}} - E_{\text{LUMO}}|$  energy gaps of 1.716 eV and 2.179 eV, respectively (Supplementary document **S5** (a)). Therefore, complexes **B9** and **B6** can be considered to be soft molecules and are thus more reactive for nucleophilic attack reactions. This observation is in agreement with the large electrophilicity indices (Sections 4.3.1) of complexes **B9** (4.223 eV) and **B6** (3.484 eV). The two double bonds between the carbene carbons and the metal moiety reduce the intra-molecular  $|E_{\text{HOMO}} - E_{\text{LUMO}}|$  energy gap. These double bonds are shorter and stronger than single bonds; this can be ascribed to the additional  $\pi$  bond. These  $\pi$  bonds are formed by  $\pi$ -electron back donation from the metal's d orbital to the carbene's p orbital.<sup>9</sup>

The HOMO of bi-metallic compounds **A3**, **A4** and **C15** is located predominately on the transition metal fragment at position TM, while the LUMO of these complexes is located predominately on the carbene carbons. **Figures 4.14** and **4.15** show the location of the HOMO and LUMO orbitals of complexes **A3**, **A4** and **C15** along with their respective energy levels.

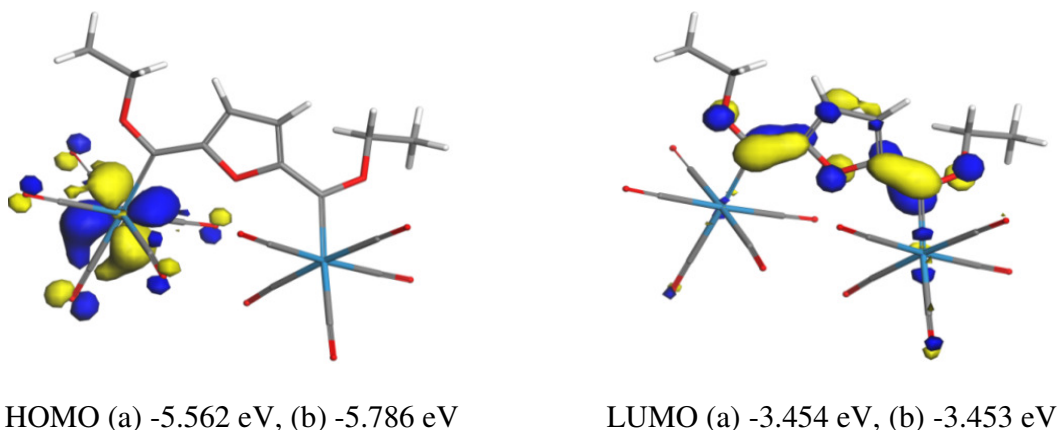


**Figure 4.14:** HOMO and LUMO of complexes: (a) **A3** (TM = TM<sup>1</sup> = W) and (b) **A4** (TM = Cr, TM<sup>1</sup> = W) (Supplementary documents **S4**, **S6**)

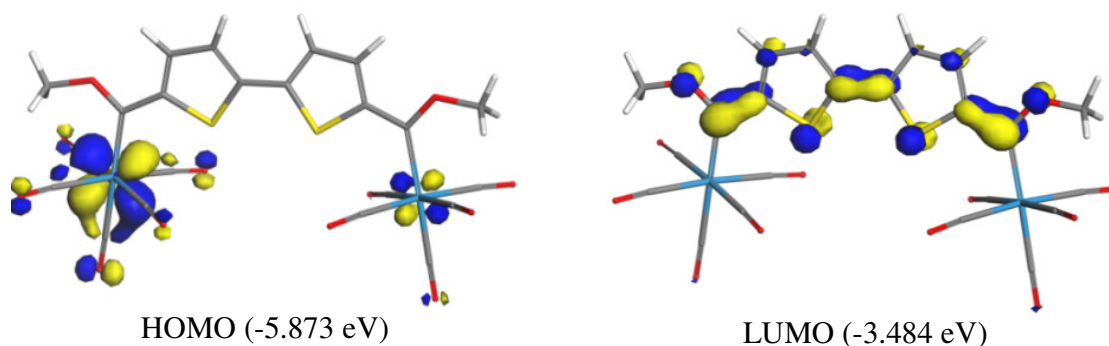


**Figure 4.15:** HOMO and LUMO of complexes: **C15** ( $TM = TM^I = W$ )<sup>13</sup> (Supplementary documents **S4**, **S6**)

As shown in Supplementary document **S5(a)**, the intra-molecular  $|E_{HOMO} - E_{LUMO}|$  energy gaps of bi-metallic carbene complexes with the highest electrophilicity indices can be arranged as follows: **A3** (2.108 eV) < **D21** (2.219 eV) < **A4** (2.333 eV) < **C15** (2.389 eV) < **C12** (2.530 eV). Therefore, complex **A3** has the smallest intra-molecular  $|E_{HOMO} - E_{LUMO}|$  energy gap of all these bi-metallic carbene complexes. This is in agreement with the high electrophilicity index of this complex *i.e.* 4.820eV (Supplementary document **S5** (a)).

#### 4.3.4. Polarization and hybridization within the $TM-C$ and $TM^I-C^I$ bonds

The polarization and hybridization patterns within the  $TM-C$  and  $TM^I-C^I$  bonds of the mono- and bi-metallic carbene complexes with the highest electrophilicity indices (**A3**, **A4**, **B6**, **B9** and **C15**) will be discussed in the following section (**Table 4.8**). A complete list of the polarization and hybridization patterns of all 25 complexes (**Chart 3.1**) is shown in Supplementary document **S10**.

Polarization within the  $TM-C$  bond leans more towards the carbene carbons for both mono-metallic carbene complexes **B6** and **B9**, while the bonding molecular orbital between the transition metal and the carbene carbon has a high carbene %p orbital character (**Table 4.8**). This trend can be observed for both the  $TM-C$  and  $TM-C^I$  bonds of complexes **B6** and **B9**. A similar trend is observed for bi-metallic carbene complexes **A3**, **A4** and **C15**, where the electron density within the  $TM-C$  and  $TM^I-C^I$  bonds is polarized more towards the carbene carbons of each complex. The bonding molecular orbital of  $TM-C$  and  $TM^I-C^I$  bonds in these bi-metallic carbene complexes also have a predominant carbene %p orbital character.



The bond within TM-C is polarized towards either one of the carbene carbon atoms, the % polarization towards the carbene carbon ranges from 69.00% to 77.83% (**Table 4.8**). This is in agreement with the findings of Occhipinti *et al.*<sup>15</sup> The %p orbital character of these TM-C and TM<sup>1</sup>-C<sup>1</sup> bonds is mainly from the contribution of the carbene carbon, while the %d orbital character of these bonds is mainly from the contribution of the metal atom. Therefore, the LUMO to which the p orbital of the carbene carbon contributed will interact with the HOMO of the nucleophile during nucleophilic attack reactions.

**Table 4.8:** Occupancy, % polarization and hybridization<sup>13</sup> within the metal-carbene bond of complexes **A3**, **A4**, **B6**, **B9** and **C15**; atom numbers are shown in **Chart 3.2**

	Bond	Atom	Occup	% Polarization of TM-C and TM <sup>I</sup> -C <sup>I</sup> bonds	Hybridization of TM-C and TM <sup>I</sup> -C <sup>I</sup> bonds		
					%s	%p	%d
<b>A3</b>	C6-W10		1.8466				
		C6 W10		77.10 22.90	45.76 15.71	54.24 46.31	37.84
	C21-W34		1.8465				
		C21 W34		77.14 22.86	45.72 15.70	54.28 46.38	37.92
<b>A4</b>	C6-Cr10		1.8474				
		C6 Cr10		69.00 31.00	42.87 13.97	57.12 46.04	39.98
	C21-W34		1.8466				
		C21 W34		77.10 22.90	45.71 15.65	54.29 46.38	37.84
<b>B6</b>	C15-Cr16		1.8259				
		C15 Cr16		69.42 30.58	40.29 12.75	59.71 46.27	40.96
	C17-Cr16		1.8818				
		C17 Cr16		68.65 31.35	45.14 15.56	54.86 44.35	40.07
<b>B9</b>	C15-W16		1.8270				
		C15 W16		77.83 22.17	43.54 14.55	56.46 47.48	37.82
	C17-W16		1.8835				
		C17 W16		76.20 23.80	47.69 16.26	52.31 45.80	37.79
<b>C15</b>	C11-W21		1.8819				
		C11 W21		77.27 22.73	46.54 17.08	53.46 49.19	33.60
	C14-W36		1.8820				
		C14 W36		77.27 22.73	46.54 17.08	53.47 49.19	33.60

#### 4.3.5. Inter-molecular $|E_{\text{HOMO}}-E_{\text{LUMO}}|$ energy gap

As mentioned previously (Sections 4.3), the HOMO of the nucleophile will interact with the LUMO of the Fischer type carbene during a nucleophilic attack. Therefore, a smaller inter-molecular  $|E_{\text{HOMO}} - E_{\text{LUMO}}|$  energy gap will result in a stronger HOMO/LUMO orbital interaction between the nucleophile and the Fischer type carbene complex. The inter-molecular  $|E_{\text{HOMO}} - E_{\text{LUMO}}|$  energy gaps between the mono- and bi-metallic complexes with the highest electrophilicity indices (**A3**, **A4**, **B6**, **B9**, **C12**, **C14**, **C15**, **D20**, **D21** and **E25**) and the nucleophiles (ethenyl methyl ether or methylamine) are listed in **Table 4.9**.

**Table 4.9:** Inter-molecular  $|E_{\text{HOMO}}-E_{\text{LUMO}}|$  enegy gap (eV) between the mono- and bi- metallic carbene complexes (**A3**, **A4**, **B6**, **B9**, **C12**, **C14**, **C15**, **D20**, **D21** and **E25**) and the nucleophiles; where  $\Delta E_{(a)} = |E_{\text{HOMO}}(\text{CH}_2\text{CHOCH}_3) - E_{\text{LUMO}}(\text{carbene})|$  and  $\Delta E_{(b)} = |E_{\text{HOMO}}(\text{NH}_2\text{CH}_3) - E_{\text{LUMO}}(\text{carbene})|$ <sup>13</sup>

Complex	HOMO (eV)	LUMO (eV)	$\Delta E_{(a)}$	$\Delta E_{(b)}$
<b>A3</b>	-5.562	-3.454	2.526	2.768
<b>A4</b>	-5.786	-3.453	2.527	2.760
<b>B6</b>	-4.986	-2.807	3.173	3.415
<b>B9</b>	-4.665	-2.949	3.031	3.273
<b>C12</b>	-5.897	-3.367	2.613	2.855
<b>C14</b>	-5.662	-2.844	3.136	3.378
<b>C15</b>	-5.873	-3.484	2.496	2.738
<b>D20</b>	-5.594	-2.779	3.201	3.443
<b>D21</b>	-5.532	-3.313	2.667	2.909
<b>E25</b>	-5.736	-2.869	3.111	3.353
NH <sub>2</sub> CH <sub>3</sub>	-6.222	-2.320		
CH <sub>2</sub> CHOCH <sub>3</sub>	-5.980	-1.023		

The inter-molecular  $|E_{\text{HOMO}}-E_{\text{LUMO}}|$  energy gap indicates that the HOMO of ethenyl methyl ether will overlap more readily with the LUMO of complexes **A3**, **A4**, **B6**, **B9**, **C12**, **C14**, **C15**, **D20**, **D21** and **E25**, than with the HOMO of methylamine.

#### 4.3.6. Atomic orbital coefficients

The atomic orbitals  $p_z$  of carbene carbons  $C_1$  and  $C_2$  both contribute equally towards the LUMO, with atomic orbital coefficients of  $\Sigma(\text{AOC}) = 0.12$  and  $0.13$  for complexes **B6** and **B9**, respectively (**Figure 4.16**). The atomic orbital  $p_z$  located in the LUMO of the carbene carbon  $C_2$  of both complexes **B6** and **B9** will interact with the atomic orbital  $p_z$  ( $\Sigma(\text{AOC}) = 0.12$ ) that is located in the HOMO of the ethenyl methyl ether (**Figure 4.16** (a)), since carbene carbon  $C_2$  has been shown to be the possible site of nucleophilic attack based on NPA charges (Section 4.3.2). The  $p_y$  ( $\Sigma(\text{AOC}) = 0.64$ ) atomic orbital located in the HOMO of methylamine will interact with the  $p_z$  atomic orbital located in the LUMO of complexes **B6** and **B9** (**Figure 4.16** (b)).

Therefore, as mentioned previously, the HOMO of the ethenyl methyl ether will overlap more readily with the LUMO of complexes **B6** and **B9** than the HOMO of methylamine with the LUMO of complexes **B6** and **B9** (Section 4.3.5).

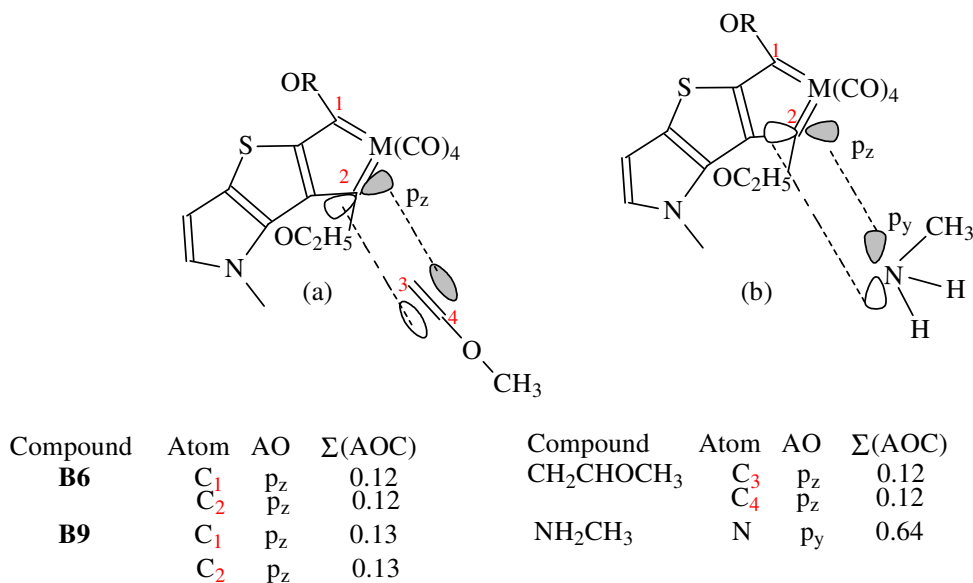


**Figure 4.16:** Orbital interactions of complexes **B6** (TM = Cr, R =  $\text{CH}_3$ ) or **B9** (TM = W, R =  $\text{C}_2\text{H}_5$ ) and (a) ethenyl methyl ether, (b) methylamine

The atomic orbital interactions for the bi-metallic carbene complexes that are likely to occur during the nucleophilic attack reactions are indicated in **Figure 4.17** (a)-(d). Atomic orbital  $p_z$  of carbene carbon  $C_1$  contributes more towards the LUMO than that of carbene carbon  $C_2$  in both complexes **A3** and **A4** (**Figure 4.17** (a)). Therefore, the  $p_z$  atomic orbital of carbene carbon  $C_1$

will interact with the  $p_z$  orbital of carbon atoms  $C_3$  and  $C_4$  of ethenyl methyl ether (**Figure 4.17(a)**). This is in agreement with the observation made in Section 4.3.2, where carbene carbon  $C_1$  was shown to have a greater NPA charge than carbene carbon  $C_2$  for complexes **A3** and **A4**. The  $p_z$  atomic orbital of carbene carbon  $C_1$  on both compound **A3** and **A4** will likely interact with the  $p_y$  orbital of methylamine as indicated in **Figure 4.17(b)**. Ethenyl methyl ether's nucleophilic attack on carbene carbon  $C_2$  is likely to occur as a result of interaction between the  $p_z$  orbital of the carbene carbon on complex **C15** and the  $p_z$  orbital of carbon atoms  $C_3$  and  $C_4$  on ethenyl methyl ether (**Figure 4.17 (c)**). The preference for carbene carbon  $C_2$  over  $C_1$  as the site for nucleophilic attack was based on the NPA charges *i.e.*  $C_2$  (0.3272e) and  $C_1$  (0.3269e), respectively (Section 4.3.2). Nucleophilic attack with methylamine will occur as a result of atomic orbital interaction between the  $p_z$  atomic orbital on the carbene carbon  $C_2$  of complex **C15** and the  $p_y$  atomic orbital on the nitrogen atom of methylamine (**Figure 4.17 (d)**).

This is in agreement with the observation made earlier, based on the inter-molecular  $|E_{\text{HOMO}} - E_{\text{LUMO}}|$  energy gap (**Table 4.9**), that the HOMO of the ethenyl methyl ether will overlap more readily with the LUMO of complexes **A3**, **A4** and **C15**, than the HOMO of methylamine with the LUMO of complexes **A3**, **A4** and **C15**.

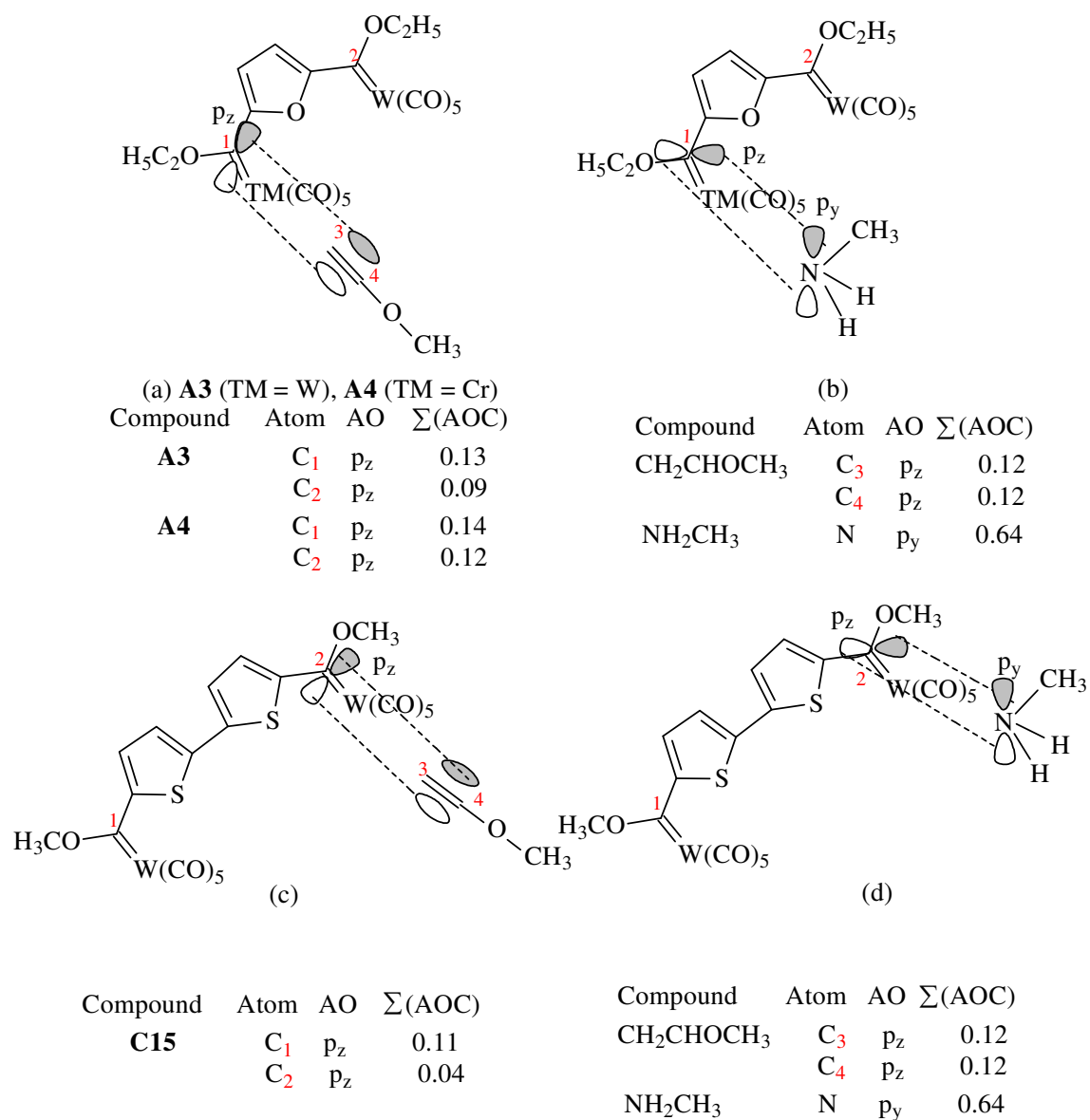


**Figure 4.17:** Orbital interaction between complex **A3** (TM = W), **A4** (TM = Cr) and (a) ethenyl methyl ether, (b) methylamine; complex **C15** and (c) ethenyl methyl ether, (d) methylamine.<sup>13</sup>

#### 4.4. Complexes which are candidates for metathesis and benzannulation reactions

Contrary to nucleophilic attack reactions, which occur as a result of molecular orbital interactions between the LUMO located on the carbene carbon and the HOMO located on the nucleophile (Section 4.3.5), benzannulation and metathesis reactions with Fischer type metal carbenes are facilitated by: the removal of a CO ligand *trans* to the TM-C(carbene) bond; local electrophilicity around the metal moiety; reduction in negative charge on the metal moiety.<sup>2,15-18</sup> Therefore the complexes analyzed in these section were optimized after the removal of a *trans*-CO ligand from the respective metal moiety, this was followed by single point energy, NBO, shielding and NPA charge calculations.

It is also important to note that inter-molecular HOMO/LUMO interactions are the driving force for metathesis reactions with Shrock and Grubbs-type metal carbene complexes.<sup>2</sup> This can be ascribed to the fact that the LUMO of these complexes is located predominately on the positively charged metal moiety and the HOMO is located on the alkene complex.<sup>2</sup> However, the HOMO of the Fischer-type metal carbene complexes investigated in this study is located on the negatively charged transition metal and the LUMO is located on carbene carbon. Supplementary documents **S8** lists the NPA charges of the TM-C/TM<sup>1</sup>-C<sup>1</sup> bonds in all the complexes investigated in this study. Therefore, benzannulation and metathesis reactions with the Fischer-type carbene complexes investigated in this study are driven by the difference in charges, rather than HOMO/LUMO interactions.

In **Chapter 2** it was mentioned that benzannulation and alkene metathesis with chromium-based Fischer type carbene complexes are initiated by the removal of a CO ligand from the metal pentacarbonyl moiety (**Schemes 2.8, 2.9 and 2.10**).<sup>15-18</sup> Furthermore, the carbene carbons attached to chromium are more electrophilic than those attached to tungsten and molybdenum.<sup>17</sup> It was shown that a net positive charge around the chromium facilitates the partial bond formation step between chromium and alkynes or alkenes for benzannulation and metathesis, respectively.<sup>15-18</sup> Therefore it could be concluded that the local electrophilicity around the TM-C bonds facilitates the partial bond formation between the transition metal and alkyne or alkene during benzannulation or metathesis, respectively. Besides the higher electrophilicity of the carbene carbon attached to chromium, chemo- and regioselective products can be obtained by

using chromium-based Fischer type carbene complexes.<sup>15-18</sup> This observation further validates the preference for chromium-based Fischer type carbene complexes.

For this reason the evaluation of the electrophilicity indices and NPA charges of the carbene carbons C and C<sup>1</sup> of mono- and bi-metallic complexes with a *trans*-CO ligand dissociated from TM and TM<sup>1</sup> (**Chart 3.1**, Supplementary document **S8**) could be used to identify carbene complexes that may be active for benzannulation and metathesis. Therefore, in order to get a clear indication of the influence of the metal fragments on the positive charge of the carbene carbon, the NPA charges of the complexes, which differ only by the metal moiety, will be investigated.

**Tables 4.10, 4.11** and **4.12** list the NPA charges of mono- and bi-metallic complexes from groups **A-E** (**Chart 3.1**, Supplementary document **S8**), which differ only by the transition metal at position TM or TM<sup>1</sup>. The NPA charges, as indicated in **Table 4.10**, clearly show that the carbene carbons attached to chromium have a higher positive charge than those attached to tungsten. These results are in agreement with the findings of Block *et al.*<sup>17</sup> Based on these results we can thus conclude that the mono-metallic complexes with a *trans*-CO ligand dissociated from chromium will be favoured even for the Fischer type metal carbenes from groups **A-E** investigated in this study.

A similar trend is observed for bi-metallic complexes with a *trans*-CO ligand dissociated from the transition metal at position TM as indicated in **Table 4.11**, where the carbene carbons attached to chromium have a higher positive charge than those attached to tungsten. Therefore, bi-metallic complexes from groups **A-E** with a *trans*-CO ligand dissociated from chromium at metal position TM will be ideal candidates for benzannulation and metathesis reactions.

**Table 4.12** lists the NPA charges of the TM-C/TM<sup>1</sup>-C<sup>1</sup> bonds of bi-metallic complexes with a *trans*-CO ligand dissociated from the transition metal at metal position TM<sup>1</sup> (**Chart 3.1**, Supplementary document **S8**). The NPA charges from this table (**Table 4.12**) indicated that the carbene carbons attached to chromium at transition metal position TM<sup>1</sup> have a higher positive charge than those attached to tungsten at metal position TM<sup>1</sup>. Therefore, based on the increased local electrophilicity as a result of the positive charge around chromium, bi-metallic complexes



with a *trans*-CO ligand dissociated from chromium at metal position TM<sup>1</sup> can be considered to be possible candidates for benzannulation and metathesis reactions.

**Table 4.10:** NPA charges of the TM-C bond in mono-metallic complexes with *trans*-CO ligand dissociated from TM, atom numbers are shown in Supplementary document **S1** (Supplementary document **S8**)

Cr at metal position TM				W at metal position TM			
	Bond	Atom	NPA charges		Bond	Atom	NPA Charges
<b>B6</b>	C15-Cr16			<b>B9</b>	C15-W16		
		C15	0.3567			C15	0.2364
		Cr16	-1.1732			W16	-0.5039
	C17-Cr16				C17-W16		
		C17	0.4557			C17	0.2930
		Cr16	-1.1732			W16	-0.5039
<b>C11</b>	C11-Cr21			<b>C14</b>	C11-W21		
		C11	0.4699			C11	0.3333
		Cr21	-1.4287			W21	-0.8033
<b>D16</b>	C11-Cr19			<b>D20</b>	C11-W19		
		C11	0.4685			C11	0.3326
		Cr19	-1.4296			W19	-0.8044
<b>E24</b>	C12-Cr23			<b>E25</b>	C12-W23		
		C12	0.4692			C12	0.3407
		Cr23	-1.4284			W23	-0.8215

**Table 4.11:** NPA charges of the TM-C<sup>1</sup>/TM<sup>1</sup>-C<sup>1</sup> bonds, bi-metallic complexes with a *trans*-CO ligand dissociated from TM, atom numbering is shown in Supplementary document **S1** (Supplementary document **S8**).

Cr at metal position TM/TM <sup>1</sup>			W at metal position TM/TM <sup>1</sup>		
	Bond	Atom NPA Charges		Bond	Atom NPA Charges
<b>A2</b>	C6-Cr10	C6	<b>A3</b>	C6-W10	C6
		Cr10			W10
	C21-Cr34	C21		C21-W34	C21
		Cr34			W34
<b>B7</b>	C10-Cr22	C10	<b>B10</b>	C10-W22	C10
		Cr22			W22
	C12-Cr41	C12		C12-W41	C12
		Cr41			W41
<b>C12</b>	C11-Cr21	C11	<b>C15</b>	C11-W21	C11
		Cr21			W21
	C14-Cr36	C14		C14-W36	C14
		Cr36			W36
<b>D18</b>	C11-Cr19	C11	<b>D21</b>	C11-W19	C11
		Cr19			W19
	C14-Cr35	C14		C14-W35	C14
		Cr35			W35

**Table 4.12:** NPA charges of the TM-C<sup>1</sup>/TM<sup>1</sup>-C<sup>1</sup> bonds, bi-metallic complexes with a *trans*-CO ligand dissociated from TM<sup>1</sup>, atom numbering is shown in Supplementary document **S1** (Supplementary document **S8**).

Cr at metal position TM/TM <sup>1</sup>			W at metal position TM/TM <sup>1</sup>		
	Bond	Atom NPA charges		Bond	Atom NPA Charges
<b>A2</b>	C6-Cr10	C6	<b>A3</b>	C6-W10	C6
		Cr10			W10
	C21-Cr34	C21		C21-W34	C21
		Cr34			W34
<b>B7</b>	C10-Cr22	C10	<b>B10</b>	C10-W22	C10
		Cr22			W22
	C12-Cr41	C12		C12-W41	C12
		Cr41			W41
<b>C12</b>	C11-Cr21	C11	<b>C15</b>	C11-W21	C11
		Cr21			W21
	C14-Cr36	C14		C14-W36	C14
		Cr36			W36
<b>D18</b>	C11- Cr19	C11	<b>D21</b>	C11-W19	C11
		Cr19			W19
	C14-Cr35	C14		C14-W35	C14
		Cr35			W35

Therefore, based on the increased local electrophilicity around the metal fragment as a result of the positively charged carbene carbon, chromium-based mono- and bi-metallic carbene complexes with a *trans*-CO ligand dissociated from transition metal TM or TM<sup>1</sup> will be of interest in this section.

#### 4.4.1. Electrophilicity indices

In general, the removal of a *trans*-CO ligand from metal moiety TM or TM<sup>1</sup> reduces the electrophilicity indices of mono- and bi-metallic carbene complexes (Supplementary document **S5** (b),(c)). However, a slight increase in the electrophilicity indices is observed for complexes **B5** (2.400 eV to 2.427 eV) and **B8** (2.630 eV to 2.862 eV) (**Table 4.7** (a)(b)) when a *trans*-CO ligand is removed, thus making these mono-metallic carbene complexes with a *trans*-CO ligand dissociated from transition metal (TM) exceptions to the trend. Although these mono-metallic carbene complexes show an increase in electrophilicity, the electrophilicity indices are still below the ones showing a decrease.

Complexes **B6** (3.050 eV), **B9** (4.003 eV), **C14** (3.124 eV), and **D20** (3.071 eV) (Supplementary document **S5** (b)) have the largest electrophilicity indices among all the mono-metallic carbene complexes with a *trans*-CO ligand dissociated from transition metal TM. As mentioned previously (Section 4.4), chromium-based Fischer type carbenes with a *trans*-CO ligand dissociated from the metal fragment are well-known candidates for benzannulation and metathesis reactions.<sup>17,18</sup> Complex **B6** is the only complex among the above listed mono-metallic carbene complexes with chromium. This limits the possible mono-metallic complex of preference for benzannulation and metathesis to complex **B6** with a dissociated *trans*-CO ligand.

Bi-metallic carbene complexes with a *trans*-CO ligand dissociated from chromium at position TM (**Chart 3.1**) can be considered for both metathesis and benzannulation.<sup>17,18</sup> The bi-metallic carbene complexes with a *trans*-CO ligand dissociated from chromium at metal position TM, with their electrophilicity indices, can be listed as follows: **A2** (3.748 eV), **A4** (4.117 eV), **B7** (3.469 eV), **C12** (3.966 eV), **C13** (4.013 eV), **D18** (3.700 eV), **D19** (3.545 eV) and **D22** (3.608 eV) (**Table 4.7** (a)). Complex **A4** (4.117 eV), followed by complex **C13** (4.013 eV), has the biggest electrophilicity index (Supplementary document **S5** (b)) among the other chromium-based bi-metallic Fischer carbene complexes with a dissociated *trans*-CO ligand at metal

position TM (**Charts 3.1** and **3.2**). Therefore, based on the electrophilicity indices, complexes **A4** and **C13** with a *trans*-CO ligand dissociated from TM can be considered to be candidates for metathesis and benzannulation.

Since all the complexes examined in Supplementary document **S5(c)** are bi-metallic carbenes with a *trans*-CO ligand dissociated from the metal moiety at metal position TM<sup>1</sup> (**Charts 3.1** and **3.2**), all these complexes can be used for benzannulation and metathesis.<sup>17,18</sup> The electrophilicity indices of bi-metallic carbene complexes with a *trans*-CO ligand dissociated from chromium at metal position TM<sup>1</sup> can be arranged as follows: **D23** (4.426 eV) > **C12** (3.958 eV) > **C13** (3.848 eV) > **D18** (3.752 eV) > **D19** (3.651 eV) > **B7** (3.528 eV) > **A2** (3.212 eV). Based on the electrophilicity indices, complexes **D23** (4.426 eV) and **C12** (3.958 eV) are better candidates for benzannulation and metathesis, since these complexes have the biggest electrophilicity indices.

Bi-metallic carbene complex **D22** is an exception to the above-mentioned trend, since the electrophilicity index increases from 4.006 eV to 4.347 eV when a *trans*-CO ligand is dissociated from the transition metal at metal position TM<sup>1</sup> (Supplementary document **S5 (a)(c)**). Nevertheless, complex **D22** has tungsten at transition metal position TM<sup>1</sup>, therefore this complex will not be regarded as an ideal candidate for benzannulation or metathesis reactions. This assumption is based on the findings made earlier where the carbene carbons attached to chromium are observed to have a higher positive charge than those attached to tungsten (Section 4.4).

NPA charges, atomic orbital coefficients, intra-molecular |E<sub>HOMO</sub>-E<sub>LUMO</sub>| energy gaps, polarization and hybridization will be used in the following sections to strengthen the argument for the carbene complexes identified by electrophilicity indices for benzannulation and metathesis.

#### 4.4.2. NPA charges and Atomic orbital coefficients

The electrophilicity around chromium in the mono-metallic carbene complex **B6** is increased by the dissociation of a *trans*-CO ligand. This increased electrophilicity is verified by the reduction in the NPA negative charge on chromium from -2.0576e to -1.1732e (**Figure 4.18** (a) and (b)), while 2-butyne and propene have a net negative charge around the triple and double bond, respectively (**Figure 4.18** (b)-(d)). Therefore, the reduction in negative charge on chromium, the

vacant d orbital created as a result of the removal of the *trans*-CO ligand, and the positive charge on the carbene carbon will facilitate coordination between chromium and 2-butyne or propene for benzannulation (**Figure 4.19** (a)) and metathesis (**Figure 4.19** (b)), respectively.<sup>2,15-18</sup> The orbitals of interest during these reactions are the vacant d orbital on chromium and the highest occupied molecular orbitals located within the triple or double bonds of 2-butyne or propene respectively. The possible orbital interactions that occur during the partial bond formation step of benzannulation and metathesis are illustrated by **Figure 4.19** (a) and (b). Atomic orbital coefficients (AOC) as obtained from Chemissian calculations were used to determine the exact atomic orbital *i.e.* (atomic orbital with the highest  $\sum(\text{AOC})$ ) that will most likely participate in these reactions. Atomic orbital  $d_{xy}$  located on chromium will most likely interact with the molecular orbital (that formed due to overlap of  $p_z$  atomic orbitals) located between carbon C<sub>1</sub> and C<sub>2</sub> of 2-butyne (**Figure 4.19** (a)). The bond formation between chromium and propene is most likely to occur as a result of interaction between the  $d_{xy}$  atomic orbital on chromium and the molecular orbital (that formed due to overlap of  $p_z$  atomic orbitals) between carbene carbon C<sub>4</sub> and C<sub>5</sub> of propene as indicated in **Figure 4.19** (b).

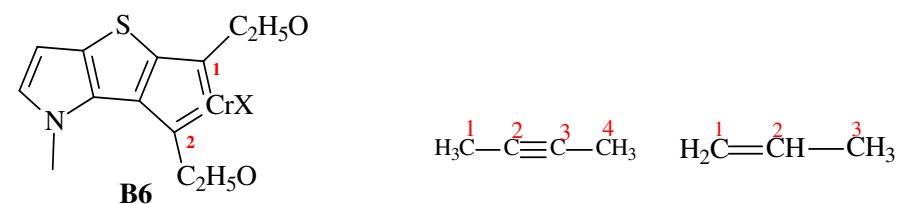
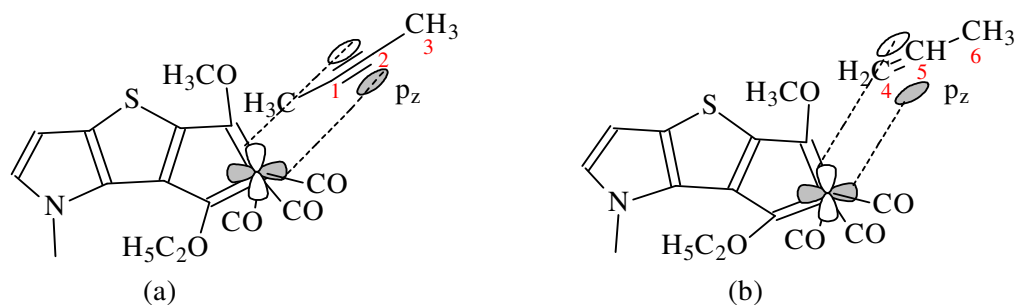


Figure 4.18 displays the NPA charges for various species. The structures shown are: (a) B6 with all ligands attached, (b) B6 with *trans*-CO dissociated, (c) 2-butyne, and (d) propene. The charges are listed in the table below.

(a) X = (CO) <sub>4</sub>		(b) X = (CO) <sub>3</sub>		(c)		(d)	
Atom	Charge	Atom	Charge	Atom	Charge	Atom	Charge
C <sub>1</sub>	0.4668	C <sub>1</sub>	0.3567	C <sub>1</sub>	-0.7376	C <sub>1</sub>	-0.4406
C <sub>2</sub>	0.4898	C <sub>2</sub>	0.4557	C <sub>2</sub>	-0.0271	C <sub>2</sub>	-0.2127
Cr	-2.0576	Cr	-1.1732	C <sub>3</sub>	-0.0266	C <sub>3</sub>	-0.7033
				C <sub>4</sub>	-0.7376		

**Figure 4.18:** NPA charges of (a) **B6** with all ligands attached, (b) **B6** with *trans*-CO dissociated, (c) 2-butyne and (d) propene<sup>13</sup> (Supplementary document S8)



Compound	Atom	AO	$\Sigma(\text{AOC})$
<b>B6</b>	Cr	$d_{xy}$	0.71

Compound	Atom	AO	$\Sigma(\text{AOC})$
2-Butyne	C <sup>1</sup>	$p_z$	0.29
	C <sup>2</sup>	$p_z$	0.29
Propene	C <sup>4</sup>	$p_z$	0.46
	C <sup>5</sup>	$p_z$	0.47

**Figure 4.19:** Orbital interaction between complex **B6** and (a) 2-butyne, (b) propene<sup>13</sup>

In the case of the bi-metallic carbene complex **A4**, the removal of a *trans*-CO ligand is accompanied by the reduction in the NPA negative charge on chromium from -2.2662e to -1.3788e (**Figure 4.20** (a) and (b)). A similar reduction in negative charge from -2.2749e to -1.3965e on Cr can be observed when a *trans*-CO ligand is removed from complex **C13** (**Figure 4.20** (c) and (d)). This reduction in negative charge and the presence of a vacant d orbital on chromium facilitate the coordination between the chromium and 2-butyne or propene for benzannulation (**Figure 4.21** (a),(c)) or metathesis (**Figure 4.21** (b),(d)), respectively.

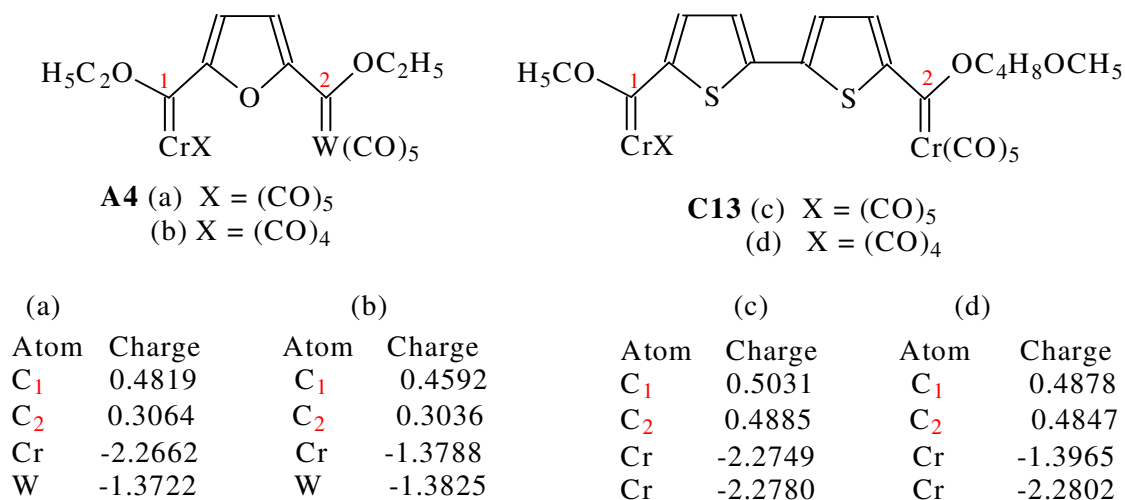


**Figure 4.20:** NPA charges of complex **A4** with (a) all ligands attached, (b) *trans*-CO ligand dissociated from TM; (c) **C13** with all ligands attached, (d) *trans*-CO ligand dissociated from TM (Supplementary document **S8**).

The negative NPA charge on the chromium atom at position TM<sup>1</sup> decreases from -2.2753e to -1.3982e with the removal of a *trans*-CO ligand from complex **C12** (Figure 4.22 (a) and (b)). A different trend is observed for complex **D23**, where a slight increase in negative charge (-1.3735e to -1.3904e) is observed with the removal of a *trans*-CO ligand from chromium at metal position TM<sup>1</sup> (Figure 4.22 (c) and (d)). Nevertheless the negative charge on chromium (TM<sup>1</sup>) with a *trans*-CO ligand dissociated from complex **C13** is within the range of the other bi-metallic complexes with a *trans*-ligand dissociated from TM or TM<sup>1</sup>.

Therefore, the reduction in the negative charge on chromium and the vacant d orbital due to the removal of a CO ligand facilitates the formation of a partial bond between chromium and either 2-butyne or propene. The possible orbital interactions that occur during the partial bond formation step in both benzannulation and metathesis are illustrated by Figure 4.23. Figure 4.23 (a) shows the orbital interaction that occurs between the d<sub>z</sub><sup>2</sup> atomic orbital on the chromium of complex **C12** and the molecular orbital (that forms due to the overlap of p<sub>z</sub> atomic orbitals) between carbon atoms C<sub>1</sub> and C<sub>2</sub> of 2-butyne. Bond formation between the d<sub>z</sub><sup>2</sup> atomic orbital on the chromium of complex **C12** and the molecular orbital (that formed due to overlap of p<sub>z</sub> orbitals) between carbon atoms C<sub>4</sub> and C<sub>5</sub> of propene is indicated in Figure 4.23 (b). The orbital interactions that occur between the d<sub>xz</sub> orbital on the chromium of complex **D23** and the



molecular orbital (that formed due to overlap of  $p_z$  orbitals) of 2-butyne and propene are indicated in **Figure 4.23(c)** and (d), respectively.

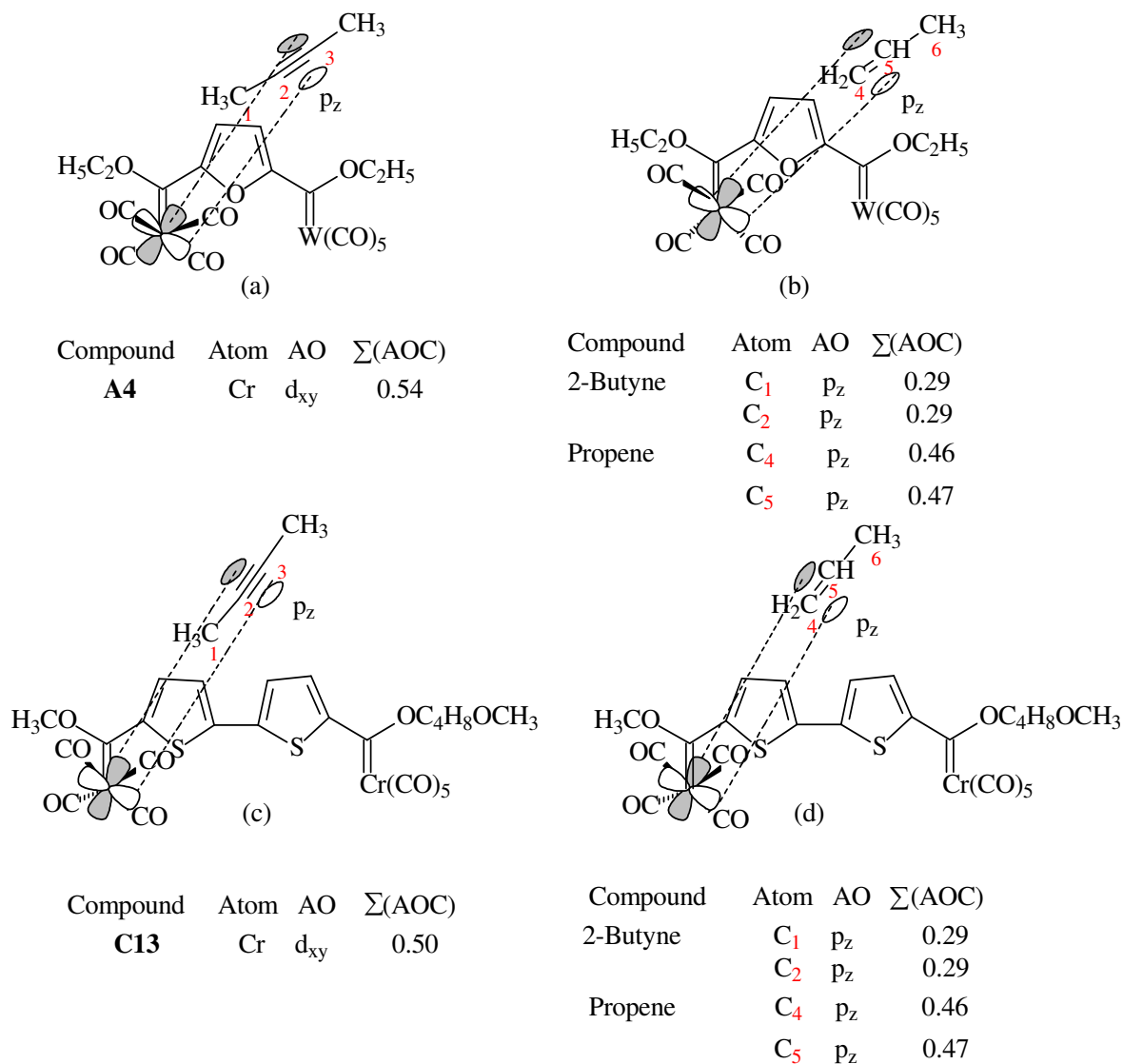


**Figure 4.21:** Orbital interactions between complex **A4** and (a) 2-butyne, (b) propene; complex **C13** and (c) 2-butyne, (d) propene<sup>13</sup>

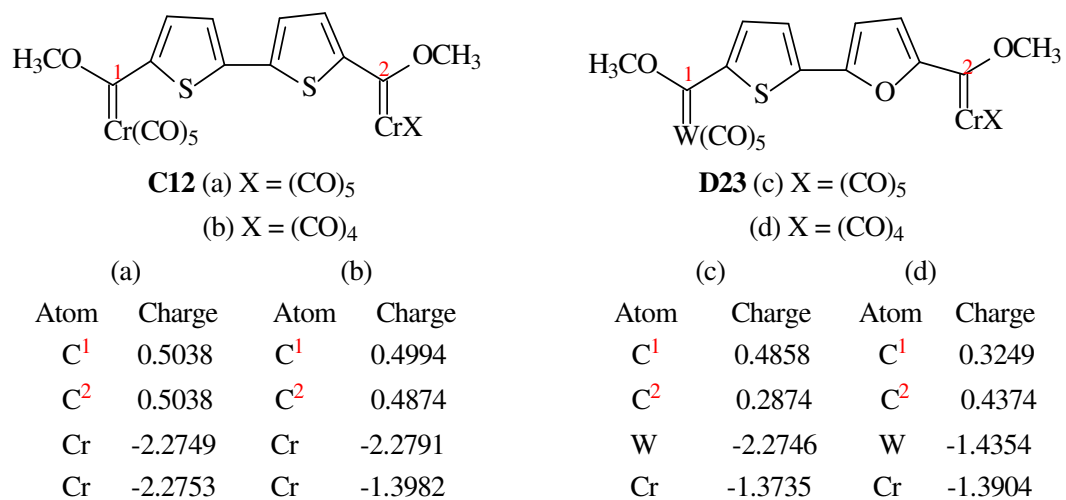


**Figure 4.22:** NPA charges<sup>13</sup> of complex **C12** with (a) all ligands attached, (b) *trans*-CO ligand dissociated from TM<sup>1</sup>; (c) **D23** with all ligands attached, (d) *trans*-CO ligand dissociated from TM<sup>1</sup>

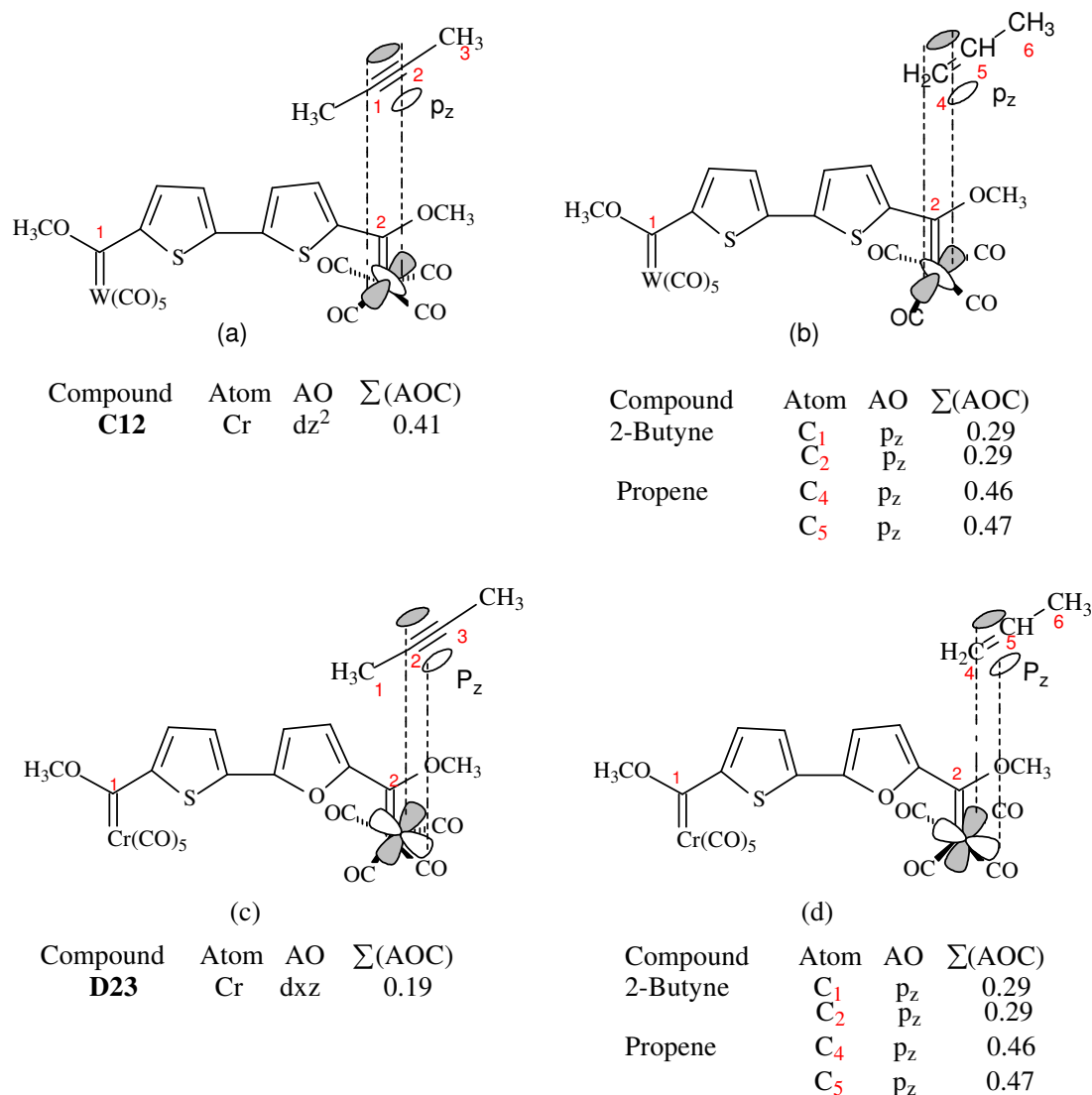


**Figure 4.23:** Orbital interactions between complex **C12** and (a) 2-butyne, (b) propene; complex **D23** and (c) 2-butyne, (d) propene<sup>1</sup>

#### 4.4.3. Intra-molecular $|E_{\text{HOMO}} - E_{\text{LUMO}}|$ energy gap

The intra-molecular  $|E_{\text{HOMO}} - E_{\text{LUMO}}|$  energy gap decreases with the dissociation of a *trans*-CO ligand from transition metal TM or TM<sup>I</sup> of mono- and bi-metallic carbene complexes, respectively (Supplementary document S5(a)-(c)).

**Table 4.13** lists the intra-molecular  $|E_{\text{HOMO}} - E_{\text{LUMO}}|$  energy gap, HOMO and LUMO energy of complexes **A4**, **B6**, **C12**, **C13** and **D23** with all ligands attached and with a *trans*-CO ligand

dissociated from chromium at metal position TM and TM<sup>1</sup>, respectively. In the case of **B6** the CO *trans* to the bond Cr16-C15 (**Chart 3.2**) was dissociated.

Bi-metallic complexes **A4** and **C13** have a *trans*-CO ligand dissociated from chromium at metal position TM, while complexes **C12** and **D23** have a *trans*-CO ligand dissociated from chromium at metal position TM<sup>1</sup>.

**Table 4.13:** HOMO<sup>(a)</sup> = all ligands attached, HOMO<sup>(b)</sup> = *trans*-CO dissociated, LUMO<sup>(a)</sup> = all ligands attached, LUMO<sup>(b)</sup> = *trans*-CO dissociated,  $\Delta E^{(a)}$  = all ligands attached,  $\Delta E^{(b)}$  = *trans*-CO dissociated for complexes **A4**, **B6**, **C12**, **C13** and **D23**; where  $\Delta E$  = intra-molecular  $|E_{\text{HOMO}} - E_{\text{LUMO}}|$  energy gap, all values are listed in eV

	HOMO <sup>(a)</sup>	HOMO <sup>(b)</sup>	LUMO <sup>(a)</sup>	LUMO <sup>(b)</sup>	$\Delta E^{(a)}$	$\Delta E^{(b)}$
<b>A4</b>	-5.786	-5.483	-3.453	-3.196	2.333	2.287
<b>B6</b>	-4.986	-4.576	-2.807	-2.515	2.179	2.061
<b>C12</b>	-5.897	-5.491	-3.367	-3.139	2.530	2.352
<b>C13</b>	-5.882	5.471	-3.358	-3.154	2.524	2.317
<b>D23</b>	-6.023	-4.938	-3.558	-3.109	2.465	1.829

The results shown in **Table 4.13** indicate that the intra-molecular  $|E_{\text{HOMO}} - E_{\text{LUMO}}|$  energy gap, the energy of the HOMO and the energy of the LUMO decrease with the dissociation of a *trans*-CO ligand from TM or TM<sup>1</sup> for complexes (**A4**, **B6**, **C12**, **C13** and **D23**) which were identified as ideal candidates for benzannulation and metathesis. This slight decrease in the intra-molecular  $|E_{\text{HOMO}} - E_{\text{LUMO}}|$  energy gap makes these complexes unstable, therefore making them even more reactive towards alkynes and alkenes for benzannulation and metathesis, respectively.

However, an increase in the intra-molecular  $|E_{\text{HOMO}} - E_{\text{LUMO}}|$  energy gap is observed for complexes **D21** (2.219 eV to 2.281 eV) and **D22** (2.390 eV to 2.485 eV) with a *trans*-CO ligand dissociated from TM (Supplementary document **S5** (a) and (b)). Therefore, these bi-metallic carbene complexes with a *trans*-CO ligand dissociated from the transition metal moiety at position TM (**Chart 3.1**) are exceptions to the trend. Bi-metallic carbene complexes **A2**, **A3**, **A4** and **C13** are exceptions to the trend, since the dissociation of a *trans*-CO ligand from the transition metal at position TM<sup>1</sup> increases the intra-molecular  $|E_{\text{HOMO}} - E_{\text{LUMO}}|$  energy gap. This

increase in energy gap (Supplementary document **S5** (a) and (c)) can be listed as follows: **A2** (2.497 eV to 2.814 eV), **A3** (2.108 eV to 2.375 eV), **A4** (2.333 eV to 2.521 eV) and **C13** (2.524 eV to 2.529 eV). The overall electrophilicity of the above-mentioned bi-metallic complexes also decreases with the removal of the *trans*-CO ligand from TM<sup>1</sup> (Supplementary document **S5**(a)-(c)). However, this slight increase in the intra-molecular |E<sub>HOMO</sub>-E<sub>LUMO</sub>| energy gap of the above-mentioned complexes (**A2**, **A3**, **A4** and **C13**, **D21** and **D22**) does not seem to have a great effect on the trend of electrophilicity indices.

#### 4.4.4. Polarization and hybridization within the TM-C and TM<sup>1</sup>-C<sup>1</sup> bonds

Mono-metallic complex **B6** without a CO ligand *trans* to carbene carbon C<sup>1</sup> (**Chart 3.1**) was identified earlier to be a possible candidate for benzannulation and metathesis reactions. The polarization within the TM-C<sup>1</sup> (**Chart 3.1**) bond shifts more toward chromium with the removal of a CO ligand *trans* to carbene carbon C<sup>1</sup> (C17) (**Table 4.14 and 4.15**). The bonding molecular orbital within TM-C<sup>1</sup> (**Chart 3.1**) *i.e.* Cr16-C17, adopts a predominant metal %d orbital and a carbene %p orbital character with the removal of a *trans*-CO ligand from chromium. This trend is observed for most of the mono-metallic complexes with a *trans*-CO ligand dissociated from TM, with the exception of mono-metallic complexes **B8**, **C14** and **E25**.

In the case of bi-metallic carbene complexes **A4** and **C13**, the removal of a *trans*-CO ligand from chromium at metal position TM shifts the polarization within the TM-C bond towards chromium at position TM. The bonding molecular orbital between the transition metal and the carbene carbon adopts a predominant metal %d orbital and a carbene %p orbital character.

The dissociation of the *trans*-CO ligand from chromium shifts the polarization within the TM<sup>1</sup>-C<sup>1</sup> bond more towards chromium at metal position TM<sup>1</sup> (**Table 4.14 and 4.15**). This trend can be observed for most of the bi-metallic complexes with a *trans*-CO ligand dissociated from position TM<sup>1</sup> (Supplementary document **S10**), with complex **D23** being an exception (**Table 4.14 and 4.15**). This observation is consistent with the slight increase in negative charge on chromium with the removal of the *trans*-CO ligand from complex **D23** *i.e.* -1.3735e to -1.3904e.

The bonding molecular orbital between chromium and the carbene carbon adopts a predominant metal %d orbital and a carbene %p orbital character for most bi-metallic carbene complexes with

a *trans*-CO ligand dissociated from TM<sup>1</sup> (Supplementary document **S10**), with the exception of complex **D23** (**Table 4.15**).

Therefore, polarization within the TM-C/TM<sup>1</sup>-C<sup>1</sup> in both mono- and bi-metallic complexes is shown to shift more towards the metal moiety with the dissociation of a *trans*-CO ligand. The bonding molecular orbital of TM-C/TM<sup>1</sup>-C<sup>1</sup> is observed to adopt a predominant metal %d orbital and a carbene %p orbital character with the dissociation of a *trans*-CO ligand from TM/TM<sup>1</sup> of mono- and bimetallic complexes, respectively.

This shift in polarization from the carbene carbon towards the metal moiety with a *trans*-CO ligand dissociated from TM or TM<sup>1</sup> is in agreement with the decrease in negative NPA charge of the metal moiety with the removal of a *trans*-CO ligand (Section 4.4.2, Supplementary document **S8**). This reduction in negative NPA charge facilitates the formation of the partial bond between the metal moiety and 2-butyne/propene during benzannulation or metathesis, respectively.

**Table 4.14:** Occupancy, % polarization and hybridization<sup>13</sup> within the TM-C and TM<sup>1</sup>-C<sup>1</sup> bonds of complexes **B6**, **A4** and **C13**, with all ligands attached; **C12** and **D23** with all ligands attached. Atom numbering is shown in **Chart 3.2**

	Bond	Atom	Occup	% Polarization of TM-C and TM <sup>1</sup> -C <sup>1</sup> bond	Hybridization of TM-C and TM <sup>1</sup> -C <sup>1</sup> Bond		
					%s	%p	%d
<b>A4</b>	C6-Cr10		1.8474				
		C6 Cr10		69.00 31.00	42.87 13.97	57.12 46.04	39.98
	C21-W34		1.8466				
		C21 W34		77.10 22.90	45.71 15.65	54.29 46.38	37.84
<b>B6</b>	C15-Cr16		1.8259				
		C15 Cr16		69.42 30.58	40.29 12.75	59.71 46.27	40.96
	C17-Cr16		1.8818				
		C17 Cr16		68.65 31.35	45.14 15.56	54.86 44.35	40.07
<b>C13</b>	C11-Cr21		1.8503				
		C11 Cr21		69.59 30.41	42.34 13.93	57.66 46.76	39.30
	C14-Cr36		1.8879				
		C14 Cr36		70.44 29.56	43.96 15.12	56.03 48.38	36.49
<b>C12</b>	C11-Cr21		1.8503				
		C11 Cr21		68.58 33.54	42.36 14.73	57.64 48.56	39.00
	C14-Cr36		1.8505				
		C14 Cr36		69.60 30.40	42.33 13.93	57.66 46.76	39.30
<b>D23</b>	C11-W19		1.8895				
		C11 W19		70.38 29.62	44.32 15.28	55.67 48.36	36.35
	C14-Cr35		1.8470				
		C14 Cr35		77.65 22.35	44.99 15.64	55.01 47.54	36.69

**Table 4.15:** Occupancy, % polarization and hybridization<sup>13</sup> within the TM-C and TM<sup>I</sup>-C<sup>I</sup> bonds of complexes **B6**, **A4** and **C13**, with *trans*-CO ligand dissociated from TM; **C12** and **D23** with a *trans*-CO ligand dissociated from TM<sup>I</sup>. Atom numbering is shown in **Chart 3.2**

	Bond	Atom	Occup	% Polarization of TM-C and TM <sup>I</sup> -C <sup>I</sup> bond	Hybridization of TM-C and TM <sup>I</sup> -C <sup>I</sup> Bond		
					%s	%p	%d
<b>A4</b>	C6-Cr10		1.6817				
		C6 Cr10		30.70 69.30	0.32 0.24	99.68 2.79	96.97
	C21-W34		1.8460				
		C21 W34		77.53 22.47	45.02 15.59	54.98 47.46	36.82
<b>B6</b>	C15-Cr16		1.8231				
		C15 Cr16		73.81 26.19	38.44 15.59	61.56 48.01	36.37
	C17-Cr16		1.6080				
		C17 Cr16		33.31 66.69	0.00 0.00	99.98 0.60	99.40
<b>C13</b>	C11-Cr21		1.6800				
		C11 Cr21		24.38 75.62	0.21 0.10	99.70 3.03	96.87
	C14-Cr36		1.8900				
		C14 Cr36		70.52 29.48	43.62 15.03	56.37 48.44	36.52
<b>C12</b>	C11-Cr21		1.8500				
		C11 Cr21		69.81 30.19	41.95 13.91	58.04 47.07	39.00
	C14-Cr36		1.6839				
		C14 Cr36		28.09 71.91	0.26 0.15	99.73 2.99	96.86
<b>D23</b>	C11-W19		1.8816				
		C11 W19		77.30 22.70	46.27 17.05	53.72 49.28	33.55
	C14-Cr35		1.8931				
		C14 Cr35		64.95 35.05	41.80 13.77	58.20 47.19	39.02

Donor-acceptor interactions of natural bonding orbitals and shielding parameters can be used further to explain the influence that the removal of a *trans*-CO ligand has on the charge distribution, electrophilicity indices and polarization within the TM-C bond.



#### 4.4.5. Donor-acceptor interactions of natural bonding orbitals (NBO) in TM-C and TM<sup>I</sup>-C<sup>I</sup> bonds

Donor-acceptor NBO interactions give an indication of how much energy is required to remove the *trans*-CO ligand (Supplementary document **S11**) from the metal carbene complexes.

The energetic importance of the donor-acceptor natural bond orbitals (NBOs), which contribute to the formation of the TM-C bond, can be estimated by using the second order perturbation theory, *i.e.* stabilization energies ( $E^2$ ) greater than 20 kJ/mol.<sup>19</sup> **Table 4.16** lists the donor-acceptor molecular orbital stabilization energy ( $E^2$ ) of complexes with the greatest electrophilicity index *i.e.* **A4**, **B6**, **C12**, **C13** and **D23**. NBOs formed by hybridization between the carbene carbon and the metal fragment play a significant role in the formation of the donor natural bond orbital (NBO), while the NBOs formed by hybridization between the metal fragment and the carbon atom of the CO-ligand *trans* to the carbene carbon contribute extensively towards the formation of the acceptor NBOs (**Table 4.16**, **Figure 4.24**). These observations are in agreement with the Dewar-Chatt-Duncanson model<sup>20</sup>, which suggests that the TM-C bond is formed predominately by  $\sigma$ -electron donation from the carbene carbon to the metal fragment.

Since CO ligands are strong electron withdrawing groups, the anti-bonding (BD\*) NBO formed between the metal and the carbon of the CO ligand *trans* to the carbene carbon, acts as an acceptor NBO.

Removing the *trans*-CO ligand from the metal fragment will result in an increase in  $\pi$ -electron back donation<sup>20</sup> from the occupied d orbitals of the metal to the carbene carbon, thus reducing the electrophilicity on this carbon. This effect can be proven by the apparent decrease in positive charge on the carbene carbon (Supplementary document **S8**), accompanied by the decrease in the negative charge on the metal fragment with the removal of the *trans*-CO ligand as indicated in **Figure 4.18** (a),(b); **Figure 4.20** (a)-(d) and **Figure 4.22** (a)-(d).

**Table 4.16:** Donor-acceptor stabilization energy ( $E^2$ )<sup>13,20</sup> of **A4**, **B6**, **C12**, **C13** and **D23** (all ligands attached), where BD = bonding orbital, BD\* = anti-bonding orbital;  $E^2$  is the stabilization energy;  $E(j)-E(i)$  are diagonal elements;  $F(i,j)$  represents the off-diagonal NBO Fock matrix element<sup>15</sup>; atom numbering is shown in **Chart 3.2**

Complex	Donor NBO (i)	Acceptor NBO (j)	$E^2$ kJ/mol	$E(j)-E(i)$ a.u.	$F(i,j)$ a.u.
<b>A4</b>	BD C6-Cr10	BD* Cr10-C13	58.99	0.92	0.104
	BD C21-W34	BD* W34-C36	87.86	1.35	0.152
<b>B6</b>	BD C15-Cr16	BD* Cr16-C23	68.07	0.89	0.110
	BD C17-Cr16	BD* Cr16-C23	58.95	1.21	0.129
<b>C12</b>	BD C11-Cr21	BD* Cr21-C23	58.24	0.92	0.104
	BD C14 -Cr36	BD* Cr36-C37	58.15	0.90	0.104
<b>C13</b>	BD C11-Cr21	BD* Cr21-C23	58.19	0.92	0.104
	BD C14-Cr36	BD* Cr36-C37	53.59	0.93	0.099
<b>D23</b>	BD C11-W19	BD* W19-C21	53.51	0.94	0.099
	BD C14-Cr35	BD* Cr35-C37	57.94	0.92	0.103

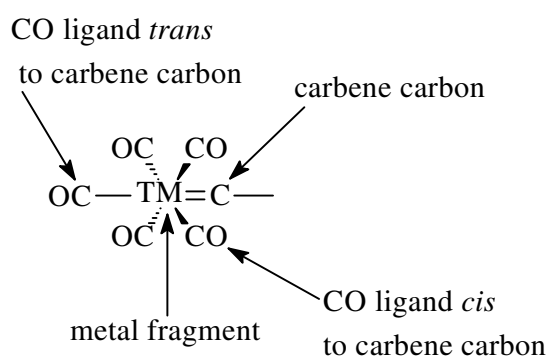


**Figure 4.24:** Transition metal-carbene bond with *trans*-CO ligands attached to the metal fragment

#### 4.4.6. Shielding

Shielding parameters  $\%G(\text{complex})$  and  $\%G(\text{M})$  indicate that the removal of a *trans*-CO ligand from the metal moiety reduces the hindrance that the alkene or alkyne might experience while interacting with the metal fragment (Supplementary document **S9**).

**Table 4.17** lists the  $G(\text{complex})\%$  and  $G(\text{TM})\%$ <sup>22</sup> of the complexes (**A4**, **B6**, **C12**, **C13** and **D23**) that were identified as good candidates for metathesis and benzannulation. These shielding parameters will be listed for the above-mentioned complexes with and without a *trans*-CO ligand. Where  $G(\text{complex})\%$  is the overall shielding of the complex with all ligands treated as one around the metal,  $G(\text{TM})\%$  is the percentage of the metal's surface shielded by the ligated atoms only. As observed from **Table 4.17**, shielding parameters  $G(\text{complex})\%$  and  $G(\text{TM})\%$  decrease slightly with the removal of a *trans*-CO ligand from the metal at position TM and TM<sup>1</sup>. Therefore, dissociation of a *trans*-CO ligand from the metal moiety creates a vacant d orbital and reduces sterical hindrance. Solid-G software was used to visualize the steric effect of the various ligands on the surface of the metal moiety.<sup>22</sup> Each ligand is indicated in a specific color on the sphere surrounding the complex (Figure 4.25), thus giving us an idea of the extent of the steric hindrance around this complex.

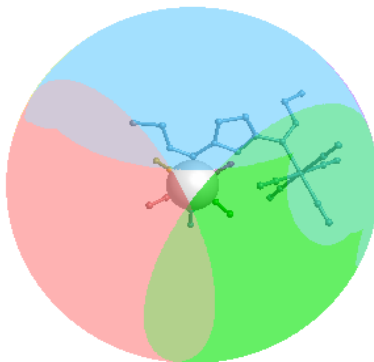


**Figure 4.25:** Solid angle visualized for complex **A4** (with all ligands attached)

**Table 4.17:.**  $G(\text{complex})\%$  and  $G(\text{TM})\%^{22}$  of complexes **A4**, **B6**, **C12**, **C13** and **D23**, where  $G(\text{complex})^a\%$  = is the overall shielding of the complex (all ligands attached),  $G(\text{TM})^a\%$  = shielding of metal with all ligands attached;  $G(\text{complex})^b\%$  = % overall shielding of the complex (*trans*-CO ligand dissociated from TM and  $\text{TM}^1$ ),  $G(\text{TM})^b\%$  = % shielding of metal with (*trans*-CO ligand dissociated from TM and  $\text{TM}^1$ ); atom numbering is shown in **Chart 3.2** (Supplementary document **S9**)

Complex	Metal	$G(\text{complex})^a\%$	$G(\text{TM})^a\%$	$G(\text{complex})^b\%$	$G(\text{TM})^b\%$
<b>A4</b>	Cr10	99.76	99.53	86.89	86.60
	W34	93.34	91.40	79.50	78.38
<b>B6</b>	Cr16	99.55	98.91	85.98	85.15
<b>C12</b>	Cr21	99.75	99.48	87.03	86.74
	Cr36	99.77	99.48	87.11	86.81
<b>C13</b>	Cr21	99.76	99.47	86.99	86.73
	Cr36	99.62	99.01	88.22	87.61
<b>D23</b>	W19	87.19	84.78	88.09	87.58
	Cr35	99.75	99.58	86.83	86.64

## 4.5. Conclusion

### 4.5.1. Principal component analysis

The scores plots (**Figures 4.1, 4.3, 4.5, 4.7, 4.9**) of principal component analysis (PCA) could not be used to arrange the complexes in this study into sub-groups based on their chemical properties. This is due to the fact that all the complexes investigated in this study have an electrophilic carbene carbon. This bestows these complexes with an inherent electrophilicity regardless of the heteroaromatic substituents attached to the carbene carbon. Therefore the scores plots of PCA can be used effectively to differentiate among complexes which differ significantly with respect to their reactivity profile *i.e.* electrophilic and nucleophilic complexes. This assumption is based on the results obtained by Occhipinti *et. al*<sup>15</sup>, where the scores plot of PCA was used to clearly distinguish among the Fischer-, Schrock- and Grubbs-type metal carbenes.

The loadings plots (**Figures 4.1, 4.3, 4.5, 4.7, 4.9**) were successfully used to highlight chemical properties which showed the most variance among all these complexes. The properties of great interest as highlighted by the loadings plot are listed in **Table 4.6**.

#### 4.5.2. Mono-and bi-metallic complexes with all ligands attached

Bi-metallic complexes examined in this study have a higher electrophilicity index than mono-metallic complexes (Supplementary document **S5** (a)). Furthermore, the transition metals are observed to have a negative NPA charge, while the carbene carbon is shown to have a positive NPA charge (Supplementary document **S8**). Polarization within the TM-C bonds in mono- and bi-metallic complexes with all ligands attached to the transition metal leans more towards the carbene carbon (supplementary document **S10**). Molecular orbital hybridization results indicate that the bonding molecular orbital between the transition metal and the carbene carbon adopts a predominant metal %d orbital and a carbene %p orbital character (Supplementary document **S10**).

The LUMO of the mono- and bi-metallic complexes investigated in this study is located predominantly on the carbene carbon, while the HOMO on the other hand is located on the transition metal fragment (Supplementary document **S6**). Therefore, the LUMO of the carbene carbon will interact with the HOMO of the nucleophile during nucleophilic attack reactions. Based on the inter-molecular  $|E_{\text{HOMO}} - E_{\text{LUMO}}|$  energy gap, the LUMO of complexes **A3, A4, B6, B9** and **C15** will interact more readily with the HOMO of ethenyl methyl ether than with that of methylamine (**Table 4.9**).

#### 4.5.3. Mono-and bi-metallic complexes with a trans-CO dissociated from TM or TM<sup>I</sup>

The carbene carbon atom in the Cr-C bond with a *trans*-CO ligand dissociated is generally more electrophilic than that in the W-C bond, as indicated by NPA charges (Supplementary document **S8**). This confirms the results suggested by Landman *et al.*<sup>23</sup> and Casey *et al.*<sup>17</sup>, where Mulliken charges were used to indicate that the carbene carbons attached to chromium had a higher positive charge than those attached to tungsten.

Natural bond orbital (NBO) analysis results indicate that the  $\pi$ -character of the transition metal-carbene double bond is polarized more towards the carbene carbon in both mono- and bi-metallic

carbene complexes when all ligands are attached (Supplementary document **S10**). This is in agreement with the results of Occhipinti *et al.*<sup>15</sup> and the fact that the carbene carbon is electrophilic in nature. A shift in polarization is also observed when a CO ligand *trans* to the carbene carbon is removed from the metal fragment. The dissociation of a *trans*-CO ligand shifts the polarization within the  $\pi$ -bond more towards the metal fragment. This shift in polarization is accompanied by an increase in the TM% contribution towards the HOMO (Supplementary document **S7**). NPA charges (Supplementary document **S8**) also indicate a reduction in the negative charge on the metal moiety with the removal of a *trans*-CO ligand, which is consistent with the shift in polarization.

Shielding parameters %G(complex) and %G(M) indicate that the removal of a *trans*-CO ligand from transition metal TM or TM<sup>1</sup> reduces the steric hindrance that 2-butyne or propene might experience while interaction with the Fischer type carbene complexes during benzannulation or metathesis reactions, respectively (Supplementary document **S9**).

#### 4.5.4. Complexes identified for nucleophilic attack, benzannulation and metathesis reactions

Based on the chemical properties of the various complexes from groups **A-E** the following table (**Table 4.18**) can be compiled with suggested complexes for various reactions.

**Table 4.18:** Suggested complexes for various reactions

Fischer type carbene	Reactants	Reactions
<b>B6</b> and <b>B9</b>	CH <sub>2</sub> CHOCH <sub>3</sub> /NH <sub>2</sub> CH <sub>3</sub>	Nucleophilic attack reactions
<b>B6</b>	H <sub>3</sub> CC≡CCH <sub>3</sub> /H <sub>2</sub> C=CHCH <sub>3</sub>	Benzannulation/metathesis
<b>A3</b> , <b>A4</b> and <b>C15</b>	CH <sub>2</sub> CHOCH <sub>3</sub> /NH <sub>2</sub> CH <sub>3</sub>	Nucleophilic attack reactions
<b>A4</b> and <b>C13</b>	H <sub>3</sub> CC≡CCH <sub>3</sub> /H <sub>2</sub> C=CHCH <sub>3</sub>	Benzannulation/metathesis
<b>C12</b> and <b>D23</b>	H <sub>3</sub> CC≡CCH <sub>3</sub> /H <sub>2</sub> C=CHCH <sub>3</sub>	Benzannulation/metathesis

## References

1. Crause, C. *Synthesis and application of carbene complexes with heteroaromatic substituents*, PhD, University of Pretoria; South Africa, **2004**.
2. Du Toit, J. I. *'n Modelleringsondersoek na die meganisme van die homogene alkeenmetatesereaksie*, MSc, North West University: South Africa, **2009**.
3. [www.originlab.com/doc/Tutorials/Box-Plot](http://www.originlab.com/doc/Tutorials/Box-Plot) date accessed 2015 09 30.
4. (a) StatSoft, Inc. Statistica version 12, Tulsa, OK, USA, **2013**. (b) Electronic Statistics Textbook; Tulsa; <http://www.statsoft.com/textbook/> date accessed 2015 05 10.
5. Du Toit, J. I.; van Sittert, C. G. C. E.; Vosloo, H. C. M. *Monatshefte für Chemie*, 147, 7, 1115-1129, **2015**.
6. Demircioğlu, Z; Kastas, Ç. A; Büyükgöngör, O. *J. Mol. Struct.* **2015**, 1091, 183-195.
7. Parr, R.G.; Pearson, R.G. *J. Am. Chem. Soc.* **1983**, 105, 7512–7516.
8. Parr, R.G.; Yang, W. *J. Am. Chem. Soc.* **1984**, 106, 4048–4049.
9. Cases, M.; Frenking, G.; Duran, G.; Sola, M. *Organometallics*. **2002**, 21, 4182-4191.
10. (a) Parr, R. G.; Yang, W. *Density-Functional Theory of Atoms and Molecules*; Oxford University Press: New York, 1989.
11. Pearson, R. G. *Chemical Hardness*; Wiley-VCH: Oxford, 1997.
12. Parr, R. G.; v. Szentpály, L.; Liu, S. *J. Am. Chem. Soc.* **1999**, 121, 1922.
13. Frisch, M. J.; Trucks, G. W.; Schlegel, H. B.; Scuseria, G. E.; Robb, M. A.; Cheeseman, R. J.; Scalmani, G.; Barone, V.; Mennucci, B.; Petersson, G. A.; Nakatsuji, H.; Caricato, M.; Li, X.; Hratchian, H. P.; Izmaylov, A. F.; Bloino, J.; Zheng, G.; Sonnenberg, J. L.; Hada, M.; Ehara, M.; Toyota, K.; Fukuda, R.; Hasegawa, J.; Ishida, M.; Nakajima, T.; Honda, Y.; Kitao, O.; Nakai, H.; Vreven, T.; Montgomery, J. A.; Peralta, Jr., J. E.; Ogliaro, F.; Bearpark, M.; Heyd, J. J.; Brothers, E.; Kudin, K. N.; Staroverov, V. N.; Kobayashi, R.; Normand, J.; Raghavachari, K.; Rendell, A.; Burant, J. C.; Iyengar, S. S.; Tomasi, J.;

- Cossi, M.; Rega, N.; Millam, J. M.; Klene, M.; Knox, J. E.; Cross, J. B.; Bakken, V.; Adamo, C.; Jaramillo, J.; Gomperts, R.; Stratmann, R. E.; Yazyev, O.; Austin, A. J.; Cammi, R.; Pomelli, C.; Ochterski, J. W.; Martin, R. L.; Morokuma, K.; Zakrzewski, V. G.; Voth, G. A.; Salvador, P.; Dannenberg, J. J.; Dapprich, S.; Daniels, A. D.; Farkas, Ö.; Foresman, J. B.; Ortiz, J. V.; Cioslowski, J.; Fox, D. J. Gaussian 09, Revision D.01, Gaussian, Inc., Wallingford CT, **2009**. [http://www.gaussian.com/g\\_prod/g09.htm](http://www.gaussian.com/g_prod/g09.htm), date accessed 2015 05 10.
14. Kiyooka, S; Kaneno, D; Fujiyama, R. *Tetrahedron Lett.* **2013**, 54, 337-342.
  15. Occhipinti, G.; Jensen, V. R. *Organometallics*. **2011**, 30, 3522-3529.
  16. de Frémont, P.; Marion, N.; Nolan, S. *Coord. Chem. Rev.* **2009**, 253, 862-892
  17. Block, T. T.; Fenske, R. F.; Casey, C. P. *J. Am. Chem. Soc.* **1976**, 98, 441.
  18. Crause, C.; Görls, H.; Lotz, S. *Dalton Trans.* **2005**, 1649-1657.
  19. Weinhold, F.; Landis, C.R. *Discovering Chemistry with Natural Bond Orbitals*, Wiley: New York, **2012**, 319.
  20. Dewar, M. J. S. *Bull. Soc. Chim. Fr.* **1951**, C79.
  21. <http://www.chemissian.com>, date accessed 2015-05-10.
  22. Solid, G. Version 0.26, *Program for computing ligand steric effects*; Molecular structure Laboratory: 2004.
  23. Lotz, S.; Landman, M.; Görls, H.; Crause, C.; Nienaber, H.; Olivier, A. *Naturforsch. B*, **2007**, 62b, 419-426.



## Chapter 5: Conclusions and recommendations

### 5.1. Conclusions

The success of this study will be evaluated in the following section by inspecting whether the objectives, as outlined in **Chapter 1** section 1.3 have been accomplished.

#### *5.1.1. A comprehensive literature review on metal carbene complexes, especially Fischer type metal carbene complexes*

The reactivity profile of Fischer type metal carbene complexes was investigated in **Chapter 2**, section 2. This evaluation was based on reviewing articles that describe the transition metal-carbene (TM-C) bond and the influence of the heteroatoms and the cycloaromatic ring on these complexes. From these articles, it was found that the heteroatom substituents stabilize the electron-deficient carbene carbon, while the transition metal is usually stabilized by strong  $\pi$ -acceptor ligands, such as phosphine, cyclopentadienyl or carbonyl.<sup>1</sup> Furthermore, the presence of a heteroatom in the conjugated carbon ring improves charge transfer properties within the Fischer type metal carbene complexes.<sup>2</sup> The presence of different transition metals in bi-metallic Fischer type carbene complexes improves the polarization of electron density from one metal to the other.<sup>2</sup>

A concise literature study was successfully done, which highlights some of the important reactions where Fischer type metal carbene complexes have been used. These reactions include nucleophilic attack reactions with anionic and neutral electrophiles, alkene metathesis and benzannulation reactions (**Chapter 2**, section 2.3). The findings from this study indicate that Fischer type metal carbene complexes are sometimes referred to as isolobal analogues of esters, due to similarities in the reaction profiles of these complexes to that of  $\alpha,\beta$ -unsaturated esters.<sup>2</sup> Furthermore, benzannulation and metathesis reactions with Fischer type metal carbene complexes were found to be favoured for complexes with chromium metal fragments.<sup>3</sup> This can be attributed to the increased electrophilicity of the carbene carbon bonded to chromium. Block *et al.*<sup>3</sup> used Mulliken charges to prove that carbene carbons bonded to chromium are more positive than those attached to tungsten. Alkene metathesis with Fischer type carbene complexes occurs through a Chauvin dissociation mechanism.<sup>4</sup> Benzannulation and alkene metathesis are both initiated by the dissociation of a carbonyl ligand from a metal fragment.

### 5.1.2. *Verification of the molecular modelling method with the aid of crystal data and statistical techniques*

The molecular modelling method was validated by comparing the difference in bond angle and length between the geometrically optimized structures as calculated by the Material Studio 6.0 DMol<sup>3</sup> DFT model and those obtained from crystal data (**Chapter 4**, section 4.1).<sup>2,5</sup> A box plot statistical method was used to obtain the standard deviation and the mean difference between the calculated values and the values obtained from crystal structures. From this evaluation, it was concluded that the modelling method was reliable, even though the bond angles and lengths of the calculated structure were obtained in the gas phase (Supplementary document **S2**).

### 5.1.3. *Evaluating the influence of various transition metals (single or double; the same or different) and various ligands on chemical properties*

Single point energy calculations, as calculated by Gaussian09,<sup>6</sup> indicate that the HOMO is predominantly located on the metal fragments, *i.e.* W and Cr, respectively, while the LUMO is predominantly located on the carbene carbon and across the five-membered heteroaromatic substituents (Supplementary document **S6**). The %TM contribution towards the HOMO increases with the removal of a *trans*-CO from the metal moiety (W or Cr); this trend is observed for both mono- and bi-metallic Fischer carbene complexes (Supplementary document **S7**).

Shielding parameters G(complex)% and G(TM)%, as calculated by Solid-G software,<sup>7</sup> were used to calculate the steric hindrance that reactants might experience when interacting with the metal fragments. Therefore, the removal of a *trans*-CO ligand from the metal moiety reduces the amount of shielding around the metal fragments; this facilitates bond formation during benzannulation and metathesis reactions (Supplementary document **S9**).

Furthermore, the removal of a *trans*-CO ligand shifts polarization more towards the metal atom, as indicated by NBO calculations.<sup>6</sup> The TM-C bond has a carbene carbon p orbital character and metal d orbital character as indicated by NBO calculations (Supplementary document **S10**).<sup>6</sup>

Bi-metallic Fischer carbene complexes are found to have larger electrophilicity indices than mono-metallic complexes (Supplementary document **S5**). The carbene carbon attached to a

chromium atom is more electrophilic than that attached to tungsten, as indicated by NPA charges (Supplementary document **S8**).

*5.1.4. Employing multivariate statistical analysis to identify chemical properties that can be used to classify these Fischer type metal carbenes*

Since a total of 34 chemical properties were calculated for all the Fischer type carbene complexes in this study, finding trends and identifying chemical properties that are worth investigating further was a tedious process. Therefore, Statistica version 12<sup>7</sup> was used to identify chemical properties that can be used to further classify these Fischer type metal carbene complexes, since some of the properties might be redundant or show less variance among all the complexes. Eigenvalues and % total variance were calculated from a correlation matrix in order to obtain principal components that will be used for scores and loadings plots (**Chapter 4**). The relation between the chemical properties is highlighted in the loadings plots (**Chapter 4, Figures 4.2, 4.4, 4.6, 4.8 and 4.10**); while the relation between the complexes is highlighted in the scores plots (**Chapter 4, Figures 4.1, 4.3, 4.5, 5.7 and 5.9**).

The following chemical properties represent the most variance among all the other properties as identified by Statistica version 12:

- Intra-molecular  $|E_{\text{HOMO}} - E_{\text{LUMO}}|$  energy gap;
- Electrophilicity indices;
- Polarization within the TM-C/TM<sup>1</sup>-C<sup>1</sup> bonds;
- Molecular orbital hybridization within the TM-C/TM<sup>1</sup>-C<sup>1</sup> bonds; and
- The NPA charges of the TM-C/TM<sup>1</sup>-C<sup>1</sup> bonds.

*5.1.5. Identifying complexes that can be used for various reactions, i.e. nucleophilic attack reactions, benzannulation and metathesis, based on their chemical properties*

Based on the chemical properties of the various complexes from groups **A** to **E** (**Chapter 3, Chart 3.1**), the following table can be compiled with suggested complexes for various reactions.

**Table 5.1:** Suggested complexes for various reactions

Fischer type carbene	Reactants	Reactions
<b>B6</b> and <b>B9</b>	$\text{CH}_2=\text{CHOCH}_3/\text{NH}_2\text{CH}_3$	Nucleophilic attack reactions
<b>B6</b>	$\text{H}_3\text{CC}\equiv\text{CCH}_3/\text{H}_2\text{C}=\text{CHCH}_3$	Benzannulation/metathesis
<b>A3</b> , <b>A4</b> and <b>C15</b>	$\text{CH}_2=\text{CHOCH}_3/\text{NH}_2\text{CH}_3$	Nucleophilic attack reactions
<b>A4</b> and <b>C13</b>	$\text{H}_3\text{CC}\equiv\text{CCH}_3/\text{H}_2\text{C}=\text{CHCH}_3$	Benzannulation/metathesis
<b>C12</b> and <b>D23</b>	$\text{H}_3\text{CC}\equiv\text{CCH}_3/\text{H}_2\text{C}=\text{CHCH}_3$	Benzannulation/metathesis

The complexes (**A4**, **C12**, **C13** and **D23**) identified for Benzannulation reactions are from the furyl-, bitheiny- and 2-(2'-thienyl)furyl-substituted Fischer type carbene groups (**Chart 3.1**) this confirms the use of these complexes for benzannulation reactions as indicated in **Table 1.1** of **Chapter 1**.

Since the objectives required to achieve the aim of this study (as highlighted in **Chapter 1** section 1.3) were accomplished, we can conclude that the study was successful.

## 5.2. Recommendations

Since all the bi-metallic complexes studied in **Chapter 4** were in the *cis* configuration with respect to both metal fragments, further investigations should be conducted to evaluate the effect of a *trans* configuration on energetic properties, NPA charges, NBO analysis, and the shielding of these complexes. NBO resonance calculations should also be conducted on these complexes to evaluate electron transfer properties within these complexes. Furthermore, the following reactions should be examined experimentally: benzannulation and metathesis with complexes **A4**, **B6**, **C12**, **C13** and **D23**; as well as nucleophilic attack reactions using complexes **A3**, **A4**, **B6**, **B9** and **C15**. Therefore, the efficiency of these complexes for the above-mentioned reactions should be examined in terms of product yield and energy efficiency.

## References

1. Jacobsen, H.; Ziegler, T. *Inorg. Chem.*, **1996**, *35*, 775-783.
2. Crause, C. *Synthesis and application of carbenecomplexes with heteroaromatic substituents*, *PhD*, University of Pretoria, **2004**.
3. Block, T.F.; Fenske, R.F.; Casey, C.P. *J. Am. Chem. Soc.*, **1976**, *98*, 441.
4. Murray, C.K.; Yang, D.C.; Wulff, W.D. *J. Am. Chem. Soc.*, **1990**, *112*, 5660.
5. Systèmes, D. BIOVIA Material Studio 2016, 16.1.0.21; Accelrys:2015
6. <http://accelrys.com/products/collaborative-science/biovia-materials-studio/>
7. Frisch, M.J.; Trucks, G.W.; Schlegel, H.B.; Scuseria, G.E.; Robb, M.A.; Cheeseman, R.J.; Scalmani, G.; Barone, V.; Mennucci, B.; Petersson, G.A.; Nakatsuji, H.; Caricato, M.; Li, X.; Hratchian, H.P.; Izmaylov, A.F.; Bloino, J.; Zheng, G.; Sonnenberg, J.L.; Hada, M.; Ehara, M.; Toyota, K.; Fukuda, R.; Hasegawa, J.; Ishida, M.; Nakajima, T.; Honda, Y.; Kitao, O.; Nakai, H.; Vreven, T.; Montgomery, J.A.; Peralta, Jr., J.E.; Ogliaro, F.; Bearpark, M.; Heyd, J.J.; Brothers, E.; Kudin, K.N.; Staroverov, V.N.; Kobayashi, R.; Normand, J.; Raghavachari, K.; Rendell, A.; Burant, J.C.; Iyengar, S.S.; Tomasi, J.; Cossi, M.; Rega, N.; Millam, J.M.; Klene, M.; Knox, J.E.; Cross, J.B.; Bakken, V.; Adamo, C.; Jaramillo, J.; Gomperts, R.; Stratmann, R.E.; Yazyev, O.; Austin, A.J.; Cammi, R.; Pomelli, C.; Ochterski, J.W.; Martin, R.L.; Morokuma, K.; Zakrzewski, V.G.; Voth, G.A.; Salvador, P.; Dannenberg, J.J.; Dapprich, S.; Daniels, A.D.; Farkas, Ö.; Foresman, J.B.; Ortiz, J.V.; Cioslowski, J.; Fox, D.J. *Gaussian 09*, Revision D.01, Gaussian, Inc., Wallingford CT, **2009**.  
[http://www.gaussian.com/g\\_prod/g09.htm](http://www.gaussian.com/g_prod/g09.htm): accessed on 2015 05 10.
8. Solid G. Version 0.26, *Program for computing ligand steric effects*; Molecular structure Laboratory: **2004**.
9. StatSoft, Inc. Statistica version 12, *Electronic Statistics Textbook*; Tulsa, <http://www.statsoft.com/textbook/>: accessed on 2015 05 10.



## Acknowledgements

I would like to thank the following people for their support, patience and guidance:

1. My wonderful parents, Mr Mosiuwa Mofokeng and Dr Mantoa Mofokeng;
2. My dearest wife Mrs Nkele Mofokeng;
3. My Brother Thabiso and his wife;
4. My little sister Lebohang;
5. My extended family members;
6. Mma (Mme Puseletso Mosenene), Oupa Green (Ntate Moholo: Mojaosi Raau) may their souls rest in peace;
7. My family in-law, especially Mme Angie (Angelina Machaba);

My research supervisors:

1. Dr C.G.C.E van Sittert
2. Prof M. Landman
3. Dr J.I du Toit

Language editing:

1. Mrs Hendrine Krieg
2. Mrs Cecile van Zyl

I would also like to show my gratitude to the following institutions for their financial support:

1. Chemical Resource Beneficiation (CRB), NWU
2. National Research Foundation (NRF)

The almighty God (Modimo, Ramasedi) who gave me the strength, wisdom, patience and passion to explore and appreciate “His” creation.

"Then we shall... be able to take part in the discussion of the question of why it is that we and the universe exist. If we find the answer to that, it would be the ultimate triumph of human reason - for then we would know the mind of God." *Stephen Hawking*



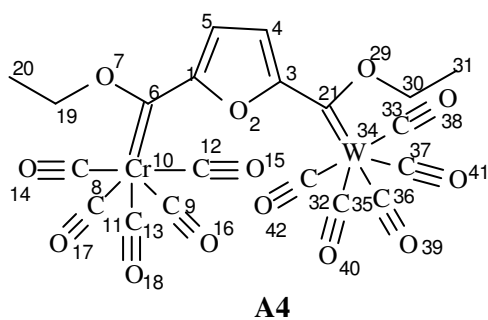
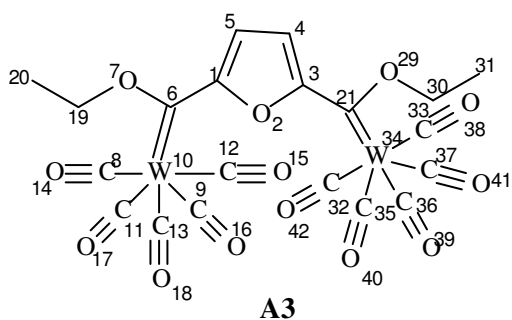
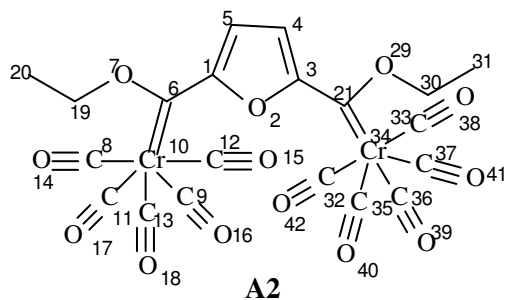
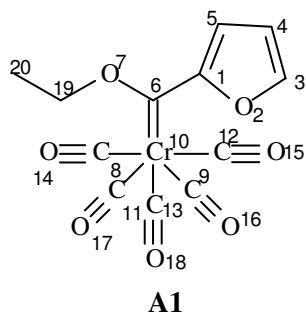


## Supplementary Material

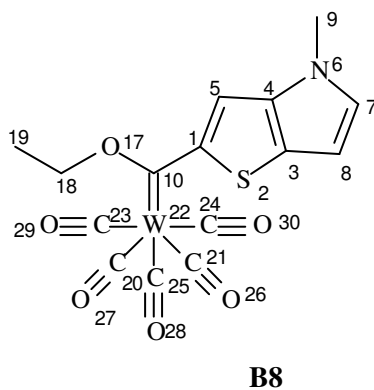
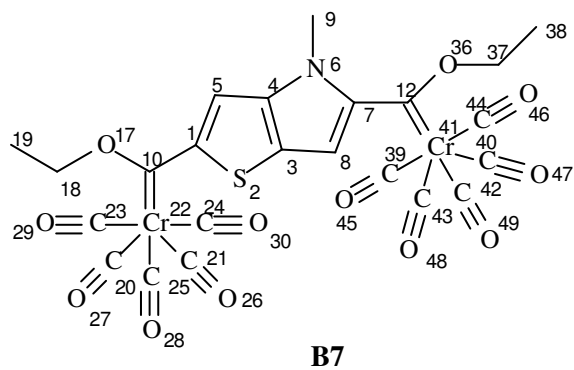
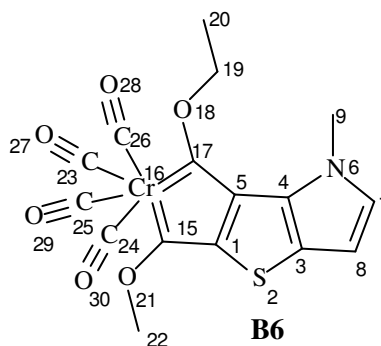
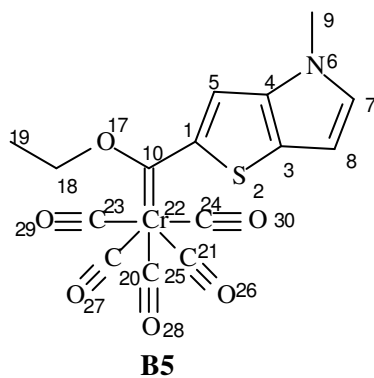
<b>Supplementary document S1:</b> List of Complexes.....	114-117
<b>Supplementary document S2:</b> Method validation, bond lengths(Å) and angles (°) .....	118-126
<b>Supplementary document S3:</b> Eigenvalues and %Total variance for PCA 1 to PCA 5..	127-130
<b>Supplementary document S4:</b> Frontier orbital energies .....	131-132
<b>Supplementary document S5:</b> Intra-molecular $E_{\text{HOMO}}-E_{\text{LUMO}}$ energy gap and electrophilicity index ( $\omega$ ) .....	133-134
<b>Supplementary document S6:</b> Pictorial representation of HOMO and LUMO.....	135-143
<b>Supplementary document S7:</b> Fragment contribution to HOMO and LUMO .....	144-154
<b>Supplementary document S8:</b> Natural Population Charges .....	155-159
<b>Supplementary document S9:</b> Shielding Parameters.....	160-161
<b>Supplementary document S10:</b> Hybridization of the transition metal-carbene bond (NBO analysis) .....	162-170
<b>Supplementary document S11:</b> Donor-Acceptor interactions (NBO analysis).....	171-172
<b>Supplementary document S12:</b> PCA worksheets .....	173-181

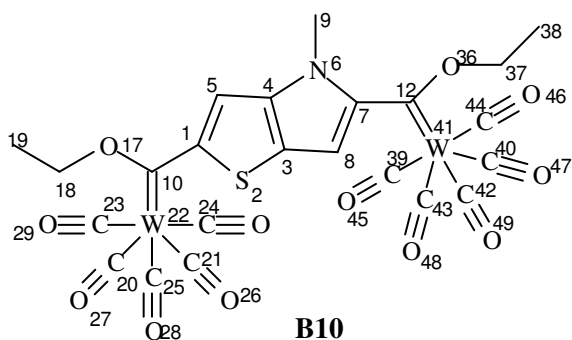
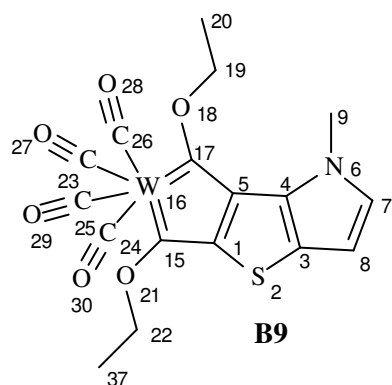
**Supplementary document S1 : List of complexes**

**Group A = Furan**

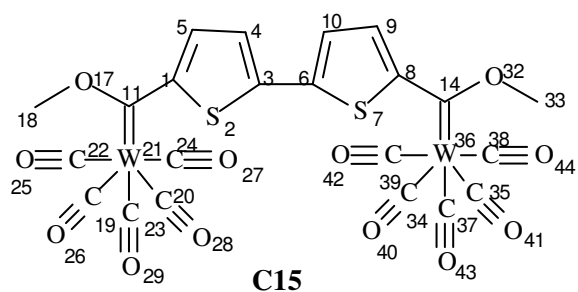
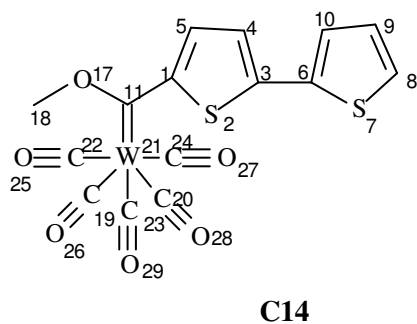
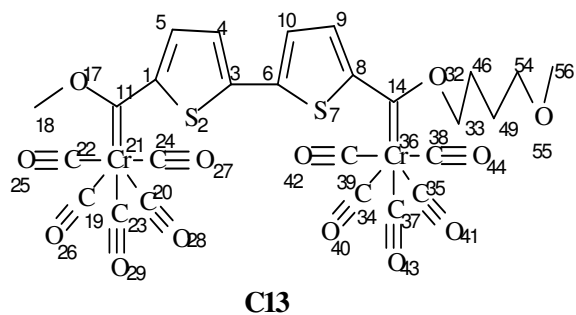
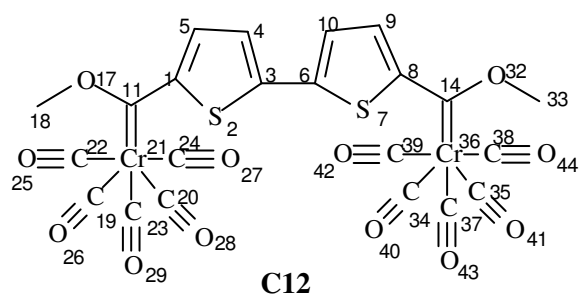
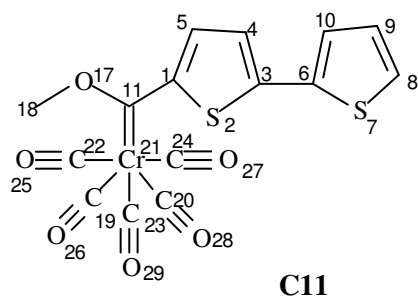


**Group B = N-methyl-thieno[3,2-b]pyrrole**

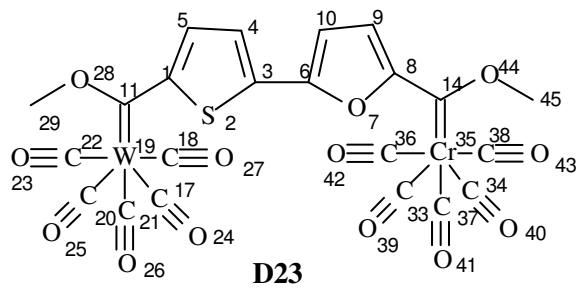
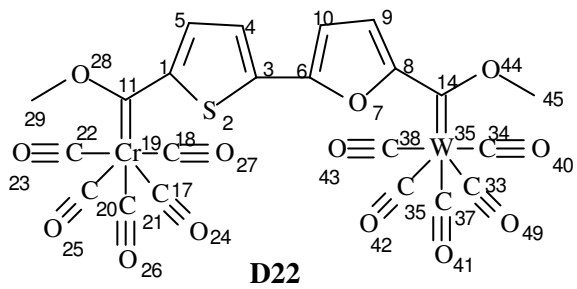
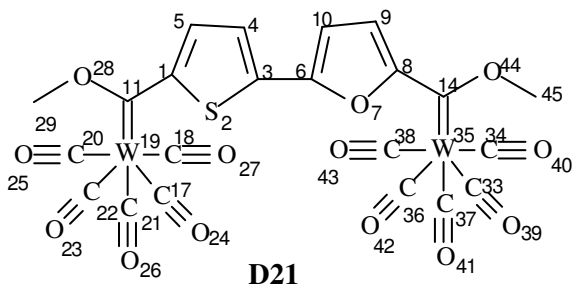
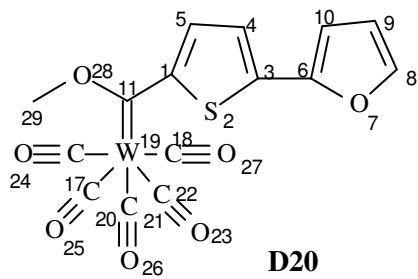
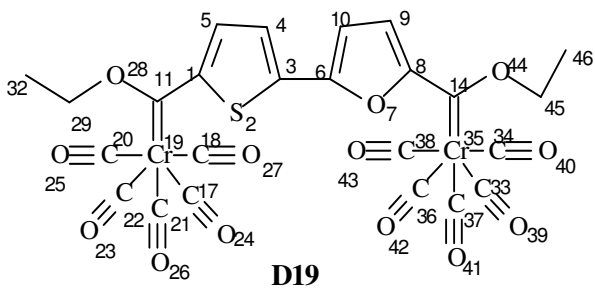
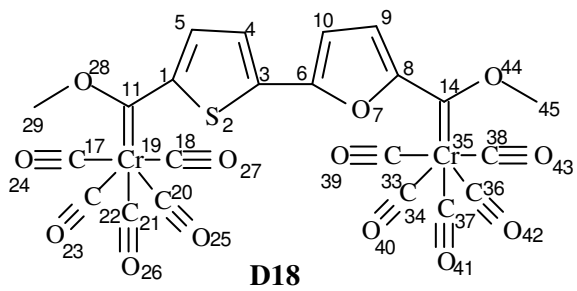
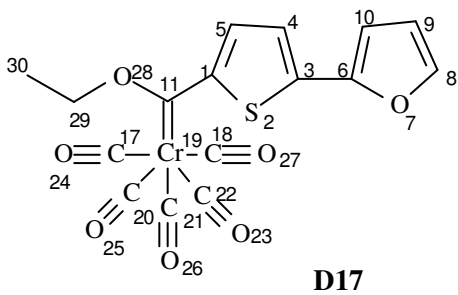
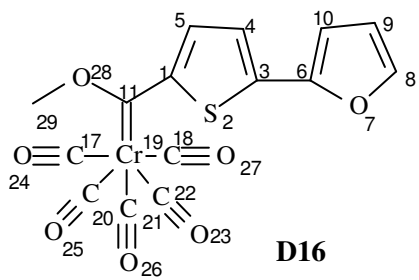




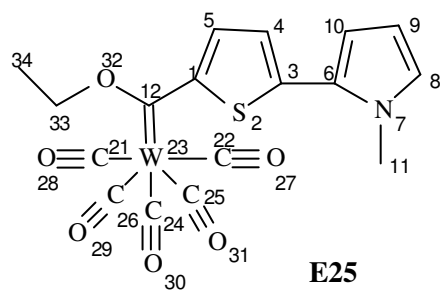
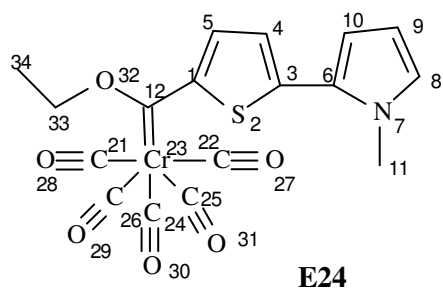
### Group C = Bithiophene



**Group D = 2-(2'-thienyl) furan**



**Group E = N-methyl-2-(2'-thienyl) pyrrole**



**Supplementary document S2:** Method validation, bond lengths(Å) and angles (°)<sup>2:</sup>

**Complex A2**

	Calculated <sup>1</sup>	Crystal Structure	Difference between crystal and calculated values
<i>Bond lengths (Å)</i>			
Cr(10)-C(8)	1.904	1.899	-0.005
Cr(10)-C(9)	1.911	1.922	0.011
Cr(10)-C(11)	1.904	1.898	-0.006
Cr(10)-C(12)	1.910	1.913	0.003
Cr(10)-C(13)	1.898	1.908	0.010
Cr(10)-C(6)	2.058	2.016	-0.042
C(6)-O(7)	1.343	1.330	-0.013
C(6)-C(1)	1.454	1.470	0.016
Cr(34)-C(33)	1.903	1.890	-0.013
Cr(34)-C(37)	1.907	1.895	-0.012
Cr(34)-C(35)	1.903	1.904	0.001
Cr(34)-C(36)	1.896	1.894	-0.002
Cr(34)-C(32)	1.906	1.921	0.015
Cr(34)-C(21)	2.076	2.038	-0.038
C(21)-O(29)	1.334	1.326	-0.008
C(3)-C(21)	1.453	1.455	0.002
<i>Angles (°)</i>			
C(13)-Cr(10)-C(11)	87.04	90.00	2.96
C(13)-Cr(10)-C(9)	88.83	86.80	-2.03
C(13)-Cr(10)-C(8)	88.68	87.00	-1.68
C(13)-Cr(10)-C(12)	88.72	88.90	0.18
C(6)-Cr(10)-C(11)	93.94	94.70	0.76
C(6)-Cr(10)-C(9)	88.95	90.50	1.55
C(6)-Cr(10)-C(8)	93.51	95.80	2.29
C(6)-Cr(10)-C(12)	90.32	86.50	-3.82
C(36)-Cr(34)-C(33)	88.05	88.00	-0.05
C(36)-Cr(34)-C(37)	88.75	90.40	1.65
C(36)-Cr(34)-C(35)	88.82	89.80	0.99
C(36)-Cr(34)-C(32)	87.30	87.30	-0.00

C(21)-Cr(34)-C(37)	90.12	89.80	-0.32
C(21)-Cr(34)-C(37)	93.56	92.90	-0.66
C(21)-Cr(34)-C(35)	88.88	86.91	-1.97
C(21)-Cr(34)-C(32)	94.58	95.00	0.42

### Complex A3

Atoms	Calculated	Crystal structure	Difference between crystal and calculated values
<i>Bond lengths (Å)</i>			
W(10)-C(8)	2.109	2.041	-0.068
W(10)-C(9)	2.116	2.032	-0.084
W(10)-C(11)	2.112	2.032	-0.08
W(10)-C(12)	2.093	2.041	-0.052
W(10)-C(13)	2.107	2.046	-0.061
W(10)-C(6)	2.232	2.139	-0.093
C(19)-O(7)	1.471	1.47	-0.001
C(6)-O(7)	1.337	1.343	0.006
W(34)-C(32)	2.097	2.031	-0.066
W(34)-C(33)	2.109	2.072	-0.037
W(34)-C(35)	2.102	2.031	-0.071
W(34)-C(36)	2.098	2.044	-0.054
W(34)-C(37)	2.116	2.072	-0.044
W(34)-C(21)	2.267	2.166	-0.101
C(1)-O(2)	1.380	1.370	-0.010
C(3)-O(2)	1.391	1.393	0.002
<i>Angles (°)</i>			
C(13)-W(10)-C(11)	88.251	87.22	-1.031
C(13)-W(10)-C(9)	91.185	87.22	-3.965
C(13)-W(10)-C(8)	92.073	89.47	-2.603
C(13)-W(10)-C(12)	89.601	89.47	-0.131
C(6)-W(10)-C(11)	87.631	94.03	6.399
C(6)-W(10)-C(9)	86.837	94.04	7.203
C(6)-W(10)-C(8)	89.975	89.23	-0.745
C(6)-W(10)-C(12)	94.492	89.23	-5.262
C(36)-W(34)-C(32)	87.951	88.13	0.179
C(36)-W(34)-C(33)	90.847	89.83	-1.017
C(36)-W(34)-C(35)	89.527	88.13	-1.397

C(36)-W(34)-C(37)	91.478	89.83	-1.648
C(21)-W(34)-C(32)	91.574	87.35	-4.224
C(37)-W(34)-C(33)	88.655	89.50	0.845
C(21)-W(34)-C(35)	91.707	87.35	-4.357
C(32)-W(34)-C(35)	91.979	92.10	0.121

### Complex B5

Atoms	Calculated	Crystal structure <sup>1</sup>	Difference between crystal and calculated values
<i>Bond lengths (Å)</i>			
Cr(22)-C(25)	1.884	1.867	-0.017
Cr(22)-C(20)	1.903	1.904	0.001
Cr(22)-C(21)	1.897	1.897	0.000
Cr(22)-C(23)	1.904	1.904	0.000
Cr(22)-C(24)	1.899	1.897	-0.002
Cr(22)-C(10)	2.114	2.082	-0.032
C(10)-O(17)	1.345	1.332	-0.013
C(1)-S(2)	1.791	1.774	-0.017
<i>Angles (°)</i>			
C(25)-Cr(22)-C(24)	89.65	87.46	-2.19
C(25)-Cr(22)-C(21)	88.21	87.46	-0.75
C(24)-Cr(22)-C(21)	91.25	93.95	2.70
C(25)-Cr(22)-C(23)	87.30	88.58	1.28
C(25)-Cr(22)-C(20)	89.31	88.58	-0.74
C(20)-Cr(22)-C(21)	87.20	88.75	1.55
C(20)-Cr(22)-C(10)	92.05	97.11	5.06
C(1)-S(2)-C(3)	91.08	91.38	0.30



### Complex B8

Atoms	Calculated	Crystal structure	Difference between crystal and calculated values
<i>Bond lengths (Å)</i>			
W(22)-C(25)	2.078	2.004	-0.074
W(22)-C(20)	2.104	2.044	-0.06
W(22)-C(21)	2.097	2.019	-0.078
W(22)-C(23)	2.102	2.036	-0.066
W(22)-C(24)	2.097	2.063	-0.034
W(22)-C(10)	2.305	2.221	-0.084
C(10)-O(17)	1.344	1.320	-0.024
C(1)-S(2)	1.789	1.789	0.000
<i>Angles (°)</i>			
C(25)-W(22)-C(24)	88.371	92.70	4.329
C(25)-W(22)-C(21)	88.855	87.50	-1.355
C(24)-W(22)-C(21)	91.64	92.70	1.060
C(25)-W(22)-C(23)	87.763	82.90	-4.863
C(25)-W(22)-C(20)	87.613	93.51	5.897
C(20)-W(22)-C(21)	87.822	87.07	-0.752
C(20)-W(22)-C(10)	94.091	87.74	-6.351
C(1)-S(2)-C(3)	90.995	91.20	0.205

### Complex C12

Atoms	Calculated	Crystal structure	Difference between crystal and calculated values
<i>Bond lengths (Å)</i>			
Cr(21)-C(19)	1.904	1.898	-0.006
Cr(21)-C(20)	1.903	1.900	-0.003
Cr(21)-C(22)	1.892	1.893	0.001
Cr(21)-C(23)	1.892	1.879	-0.013
Cr(21)-C(24)	1.902	1.913	0.011
Cr(21)-C(11)	2.088	2.059	-0.029
S(2)-C(1)	1.759	1.737	-0.022
S(2)-C(3)	1.732	1.714	-0.018
Cr(36)-C(34)	1.902	1.900	-0.002
Cr(36)-C(35)	1.904	1.898	-0.006
Cr(36)-C(37)	1.891	1.879	-0.012
Cr(36)-C(38)	1.904	1.893	-0.011
Cr(36)-C(39)	1.902	1.913	0.011
Cr(36)-C(14)	2.088	2.059	-0.029
S(7)-C(6)	1.733	1.714	-0.019
S(7)-C(8)	1.759	1.737	-0.022
<i>Angles (°)</i>			
C(23)-Cr(21)-C(19)	89.843	88.90	-0.943
C(23)-Cr(21)-C(20)	87.703	88.80	1.097
C(23)-Cr(21)-C(22)	87.169	86.90	-0.269
C(23)-Cr(21)-C(24)	89.716	89.40	-0.316
C(11)-Cr(21)-C(19)	91.03	93.60	2.57
C(11)-Cr(21)-C(20)	90.128	91.40	1.272
C(11)-Cr(21)-C(22)	95.017	92.90	-2.117
C(11)-Cr(21)-C(24)	89.398	88.10	-1.298
C(37)-Cr(36)-C(34)	90.451	88.80	-1.651
C(37)-Cr(36)-C(35)	86.906	88.90	1.994
C(37)-Cr(36)-C(38)	89.354	86.90	-2.454
C(37)-Cr(36)-C(39)	87.112	89.40	2.288
C(14)-Cr(36)-C(34)	89.988	91.40	1.412
C(14)-Cr(36)-C(35)	95.107	93.60	-1.507

C(14)-Cr(36)-C(38)	90.187	92.90	2.713
C(37)-Cr(36)-C(39)	90.876	88.10	-2.776

### Complex C14

Atoms	Calculated	Crystal structure	Difference between crystal and calculated values
<i>Bond lengths (Å)</i>			
W(21)-C(19)	2.102	2.040	-0.062
W(21)-C(20)	2.098	2.045	-0.053
W(21)-C(22)	2.102	2.041	-0.061
W(21)-C(23)	2.083	2.006	-0.077
W(21)-C(24)	2.101	2.013	-0.088
W(21)-C(11)	2.297	2.205	-0.092
C(1)- S(2)	1.765	1.746	-0.019
C(3)-S(2)	1.731	1.716	-0.015
<i>Angles (°)</i>			
C(23)-W(21)-C(19)	88.173	88.10	-0.073
C(23)-W(21)-C(20)	87.713	86.90	-0.813
C(23)-W(21)-C(22)	86.139	87.60	1.461
C(23)-W(21)-C(24)	89.699	87.70	-1.999
C(11)-W(21)-C(19)	91.861	94.40	2.539
C(11)-W(21)-C(20)	91.775	92.40	0.625
C(11)-W(21)-C(22)	94.393	93.20	-1.193
C(11)-W(21)-C(24)	90.252	89.90	-0.352

### Complex D20

Atoms	Calculated	Crystal structure	Difference between crystal and calculated values
<i>Bond lengths (Å)</i>			
W(19)-C(17)	2.101	2.042	-0.059
W(19)-C(18)	2.098	2.046	-0.052
W(19)-C(20)	2.102	2.042	-0.0602
W(19)-C(21)	2.083	2.034	-0.049
W(19)-C(22)	2.105	2.046	-0.059
W(19)-C(11)	2.298	2.225	-0.073
C(1)- S(2)	1.764	1.739	-0.025
C(3)-S(2)	1.728	1.711	-0.017
<i>Angles (°)</i>			
C(21)-W(19)-C(17)	88.989	87.70	-1.289
C(21)-W(19)-C(18)	86.821	89.40	2.579
C(21)-W(19)-C(20)	85.963	87.70	1.737
C(21)-W(19)-C(22)	89.313	89.40	0.087
C(11)-W(19)-C(17)	92.677	94.10	1.423
C(11)-W(19)-C(18)	92.497	88.90	-3.597
C(11)-W(19)-C(20)	94.734	94.10	-0.634
C(11)-W(19)-C(22)	89.02	88.90	-0.120

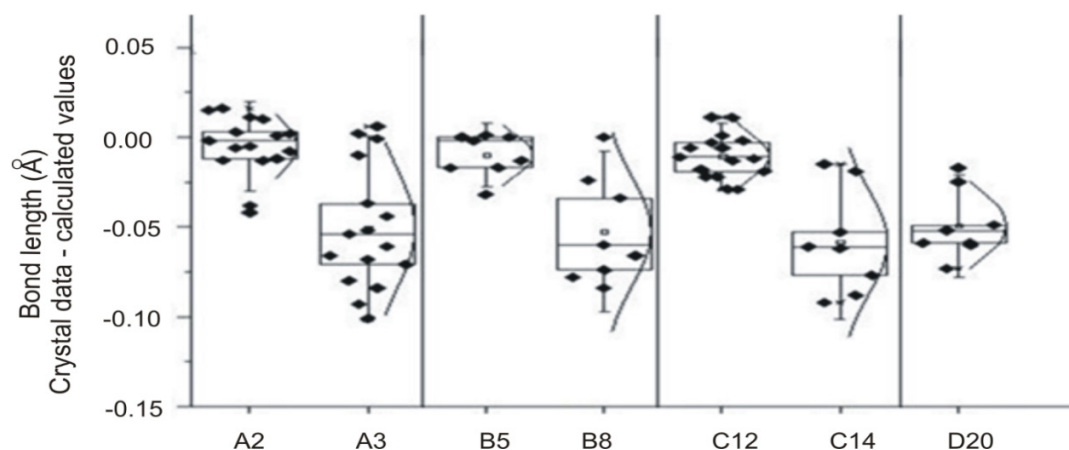


**Figure S2.1:** Crystal data – Experimental data (Bond lengths)

**Table S2.1:** Statistical analysis on the bond length difference data point<sup>3</sup>

Complex	Mean(Å)	Standard deviation	Min(Å)	Max(Å)
A2	0.005	0.017	-0.042	0.016
A3	0.051	0.034	-0.101	0.006
B5	0.010	0.012	-0.032	0.001
B8	0.052	0.029	-0.084	0.000
C12	0.011	0.012	-0.029	0.011
C14	0.058	0.029	-0.092	-0.015
D20	0.049	0.019	-0.073	-0.017

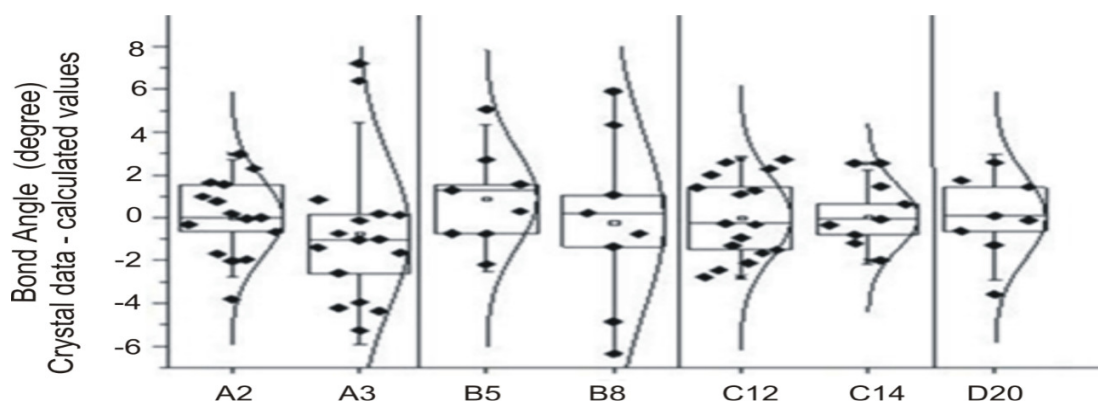


**Figure S2.2:** Crystal data – Experimental data (Bond angles)

**Table S2.2:** Statistical analysis on the angle difference data point<sup>3</sup>

Complex	Mean (°)	Standard deviation	Min(°)	Max(°)
<b>A2</b>	0.010	1.825	-3.82	2.958
<b>A3</b>	0.727	3.459	-5.262	7.203
<b>B5</b>	0.903	2.282	-2.19	5.064
<b>B8</b>	0.220	4.151	-6.351	5.897
<b>C12</b>	0.9E-3	1.896	-2.776	2.713
<b>C14</b>	0.024	1.472	-1.999	2.539
<b>D20</b>	0.023	1.953	-3.597	2.579

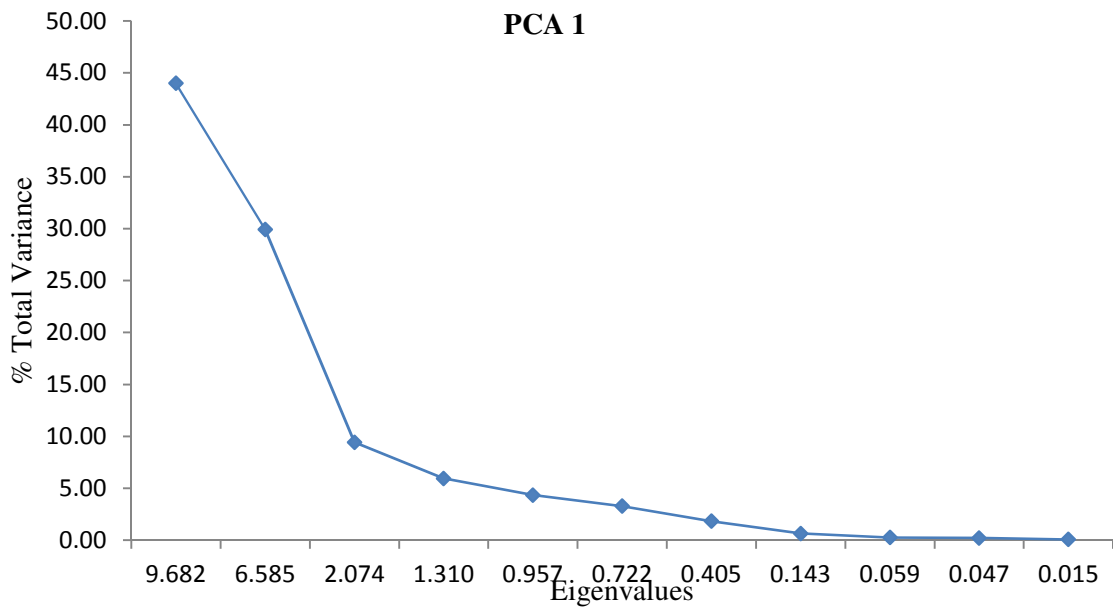
1. Accelrys Software Inc, *Materials Studio 6.0*, **2011**.  
<http://accelrys.com/products/collaborative-science/biovia-materials-studio/>: date accessed 2016-04-29
2. Crause, C. *Synthesis and application of carbene complexes with heteroaromatic substituents*, Phd, University of Pretoria: South Africa, **2004**.
3. [www.originlab.com/doc/Origin-Help/PCA](http://www.originlab.com/doc/Origin-Help/PCA): date accessed 10 May 2015.

**Supplementary document S3: Eigenvalues and %Total variance for PCA 1 to PCA 5<sup>1</sup>**

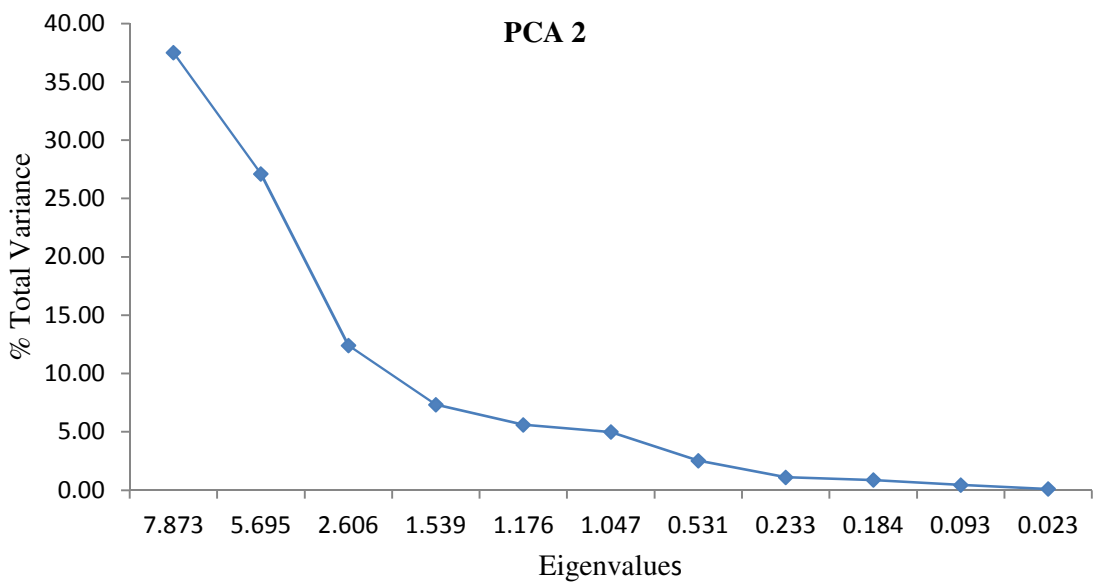
PCA 1			PCA 2		PCA 3	
	Eigenvalues	% Total Variance	Eigenvalues	% Total Variance	Eigenvalues	% Total Variance
PC1	9.682	44.01	7.8730	37.49	11.179	32.88
PC2	6.585	29.93	5.6949	27.12	6.600	19.41
PC3	2.074	9.43	2.6060	12.41	5.076	14.93
PC4	1.310	5.95	1.5387	7.33	3.883	11.42
PC5	0.957	4.35	1.1763	5.60	2.600	7.65
PC6	0.722	3.28	1.0475	4.99	2.123	6.24
PC7	0.405	1.84	0.5310	2.53	1.154	3.40
PC8	0.143	0.65	0.2330	1.11	0.554	1.63
PC9	0.059	0.27	0.1838	0.88	0.292	0.86
PC10	0.047	0.21	0.0931	0.44	0.199	0.59
PC11	0.015	0.07	0.0226	0.11	0.185	0.54

PCA 4			PCA 5	
	Eigenvalues	% Total Variance	Eigenvalues	% Total Variance
PC1	10.869	33.97	10.237	31.99
PC2	7.528	23.52	8.701	27.19
PC3	4.793	14.98	3.965	12.39
PC4	3.119	9.75	2.767	8.65
PC5	1.800	5.63	1.988	6.21
PC6	1.399	4.37	1.163	3.63
PC7	0.926	2.89	0.939	2.94
PC8	0.692	2.16	0.866	2.71
PC9	0.365	1.14	0.614	1.92
PC10	0.304	0.95	0.362	1.13
PC 11	0.134	0.42	0.314	0.98



**Figure S3.1:** % Total variance v/s Eigenvalues



**Figure S3.2:** % Total variance v/s Eigenvalues



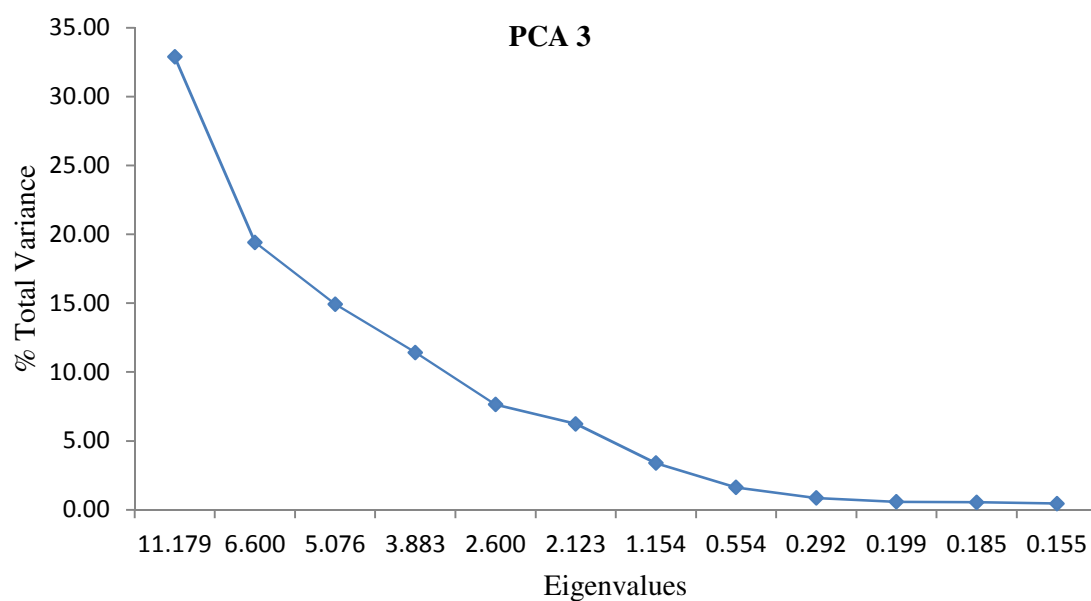


**Figure S3.3:** % Total variance v/s Eigenvalues

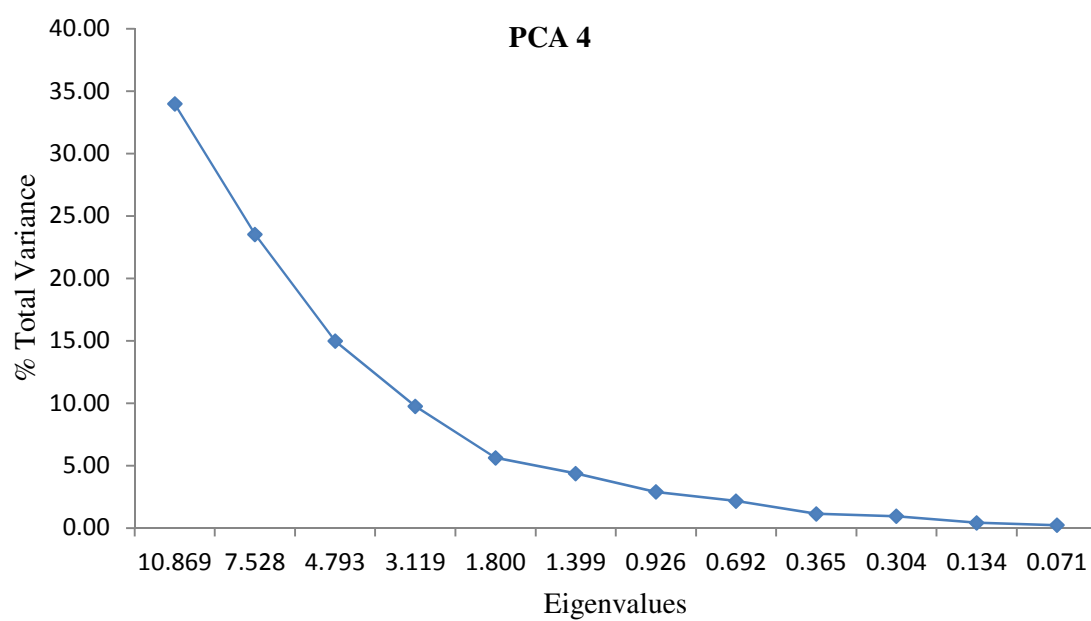


**Figure S3.4:** % Total variance v/s Eigenvalues

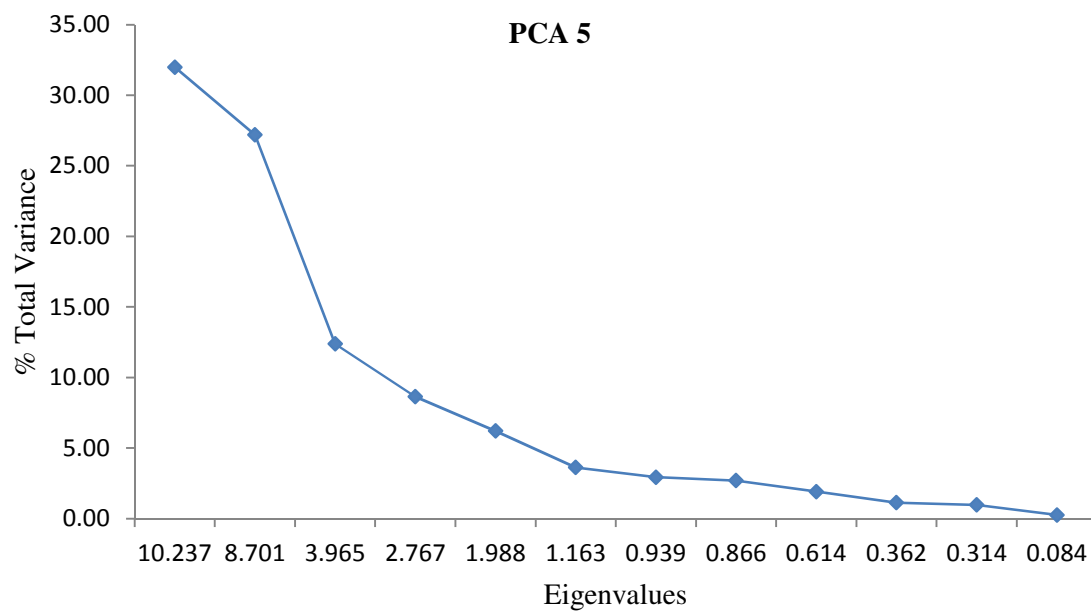


**Figure S3.5:** % Total variance v/s Eigenvalues

1. (a) StatSoft, Inc. *Statistica version 12, Tulsa, OK, USA, 2013*. (b) *Electronic Statistics Textbook*; Tulsa. <http://www.statsoft.com/textbook/>: date accessed 10 May 2015.

**Supplementary document S4:** Frontier orbital energies (all energies are expressed in eV)<sup>1</sup>

Mono- and Bi-metallic compound (all ligands attached)					Mono compound ( <i>trans</i> -CO ligand dissociated from TM)				
	HOMO	HOMO-1	LUMO	LUMO+1		HOMO	HOMO-1	LUMO	LUMO+1
<b>A1</b>	-5.695	-5.772	-2.536	-0.601	<b>A1</b>	-5.151	-5.200	-2.128	-2.113
<b>A2</b>	-5.800	-5.849	-3.303	-2.011	<b>B5</b>	-5.186	-5.761	-2.300	-2.005
<b>A3</b>	-5.562	-5.686	-3.454	-2.162	<b>B6</b>	-4.576	-5.017	-2.515	-1.495
<b>A4</b>	-5.786	-5.871	-3.453	-2.111	<b>B8</b>	-4.991	-5.119	-2.524	-2.185
<b>B5</b>	-5.663	-5.682	-2.333	-0.753	<b>B9</b>	-4.134	-4.931	-2.683	-1.797
<b>B6</b>	-4.986	-5.297	-2.807	-0.879	<b>C11</b>	-5.397	-5.975	-2.499	-2.462
<b>B7</b>	-5.864	-6.016	-3.074	-1.876	<b>C14</b>	-5.193	-5.316	-2.700	-2.604
<b>B8</b>	-5.485	-5.536	-2.474	-1.311	<b>D16</b>	-5.338	-5.362	-2.470	-2.377
<b>B9</b>	-4.665	-5.137	-2.949	-1.168	<b>D17</b>	-5.106	-5.213	-2.335	-2.166
<b>B10</b>	-5.705	-5.790	-3.273	-2.068	<b>D20</b>	-5.13	-5.251	-2.66	-2.52
<b>C11</b>	-5.836	-5.901	-2.747	-1.102	<b>E24</b>	-5.132	-5.241	-2.362	-2.17
<b>C12</b>	-5.897	-5.969	-3.367	-2.397	<b>E25</b>	-5.063	-5.099	-2.587	-2.32
<b>C13</b>	-5.882	-6.006	-3.358	-2.30					
<b>C14</b>	-5.662	-5.717	-2.844	-1.494					
<b>C15</b>	-5.873	-5.886	-3.484	-2.465					
<b>D16</b>	-5.758	-5.848	-2.674	-0.897					
<b>D17</b>	-5.581	-5.684	-2.65	-0.988					
<b>D18</b>	-5.765	-5.864	-3.24	-2.314					
<b>D19</b>	-5.768	-5.845	-3.188	-2.184					
<b>D20</b>	-5.594	-5.633	-2.779	-1.41					
<b>D21</b>	-5.532	-5.713	-3.313	-2.388					
<b>D22</b>	-5.571	-5.72	-3.181	-2.293					
<b>D23</b>	-6.023	-6.117	-3.558	-2.960					
<b>E24</b>	-5.516	-5.788	-2.461	-0.875					
<b>E25</b>	-5.736	-5.804	-2.869	-1.748					

Bi-metallic compound ( <i>trans</i> -CO ligand dissociated from TM)					Bi-metallic compound ( <i>trans</i> -CO ligand dissociated from TM <sup>1</sup> )				
	HOMO	HOMO-1	LUMO	LUMO+1		HOMO	HOMO-1	LUMO	LUMO+1
<b>A2</b>	-5.396	-5.424	-3.029	-2.337	<b>A2</b>	-5.659	-5.783	-2.845	-2.68
<b>A3</b>	-5.150	-5.424	-3.251	-2.594	<b>A3</b>	-5.408	-5.439	-3.033	-2.866
<b>A4</b>	-5.483	-5.503	-3.196	-2.419	<b>A4</b>	-5.453	-5.651	-2.932	-2.826
<b>B7</b>	-5.634	-5.705	-2.968	-2.748	<b>B7</b>	-5.615	-5.678	-2.991	-2.706
<b>C10</b>	-5.382	-5.554	-3.076	-2.904	<b>C10</b>	-5.377	-5.565	-3.100	-2.892
<b>C12</b>	-5.897	-5.969	-3.367	-2.397	<b>C12</b>	-5.491	-5.617	-3.139	-2.524
<b>C13</b>	-5.471	-5.601	-3.154	-2.492	<b>C13</b>	-5.676	-5.844	-3.147	-2.753
<b>C15</b>	-5.463	-5.608	-3.309	-2.943	<b>C15</b>	-5.475	-5.606	-3.308	-2.944
<b>D18</b>	-5.446	-5.581	-3.023	-2.464	<b>D18</b>	-5.377	-5.485	-3.025	-2.339
<b>D19</b>	-5.551	-5.622	-2.983	-2.657	<b>D19</b>	-5.370	-5.446	-2.982	-2.332
<b>D21</b>	-5.411	-5.463	-3.130	-2.901	<b>D21</b>	-5.109	-5.407	-3.132	-2.551
<b>D22</b>	-5.477	-5.572	-2.992	-2.728	<b>D22</b>	-5.139	-5.396	-3.159	-2.566
<b>D23</b>	-5.164	-5.388	-3.136	-3.020	<b>D23</b>	-4.938	-5.006	-3.109	-2.092

1. Frisch, M. J.; Trucks, G. W.; Schlegel, H. B.; Scuseria, G. E.; Robb, M. A.; Cheeseman, R. J.; Scalmani, G.; Barone, V.; Mennucci, B.; Petersson, G. A.; Nakatsuji, H.; Caricato, M.; Li, X.; Hratchian, H. P.; Izmaylov, A. F.; Bloino, J.; Zheng, G.; Sonnenberg, J. L.; Hada, M.; Ehara, M.; Toyota, K.; Fukuda, R.; Hasegawa, J.; Ishida, M.; Nakajima, T.; Honda, Y.; Kitao, O.; Nakai, H.; Vreven, T.; Montgomery, J. A.; Peralta, Jr., J. E.; Ogliaro, F.; Bearpark, M.; Heyd, J. J.; Brothers, E.; Kudin, K. N.; Staroverov, V. N.; Kobayashi, R.; Normand, J.; Raghavachari, K.; Rendell, A.; Burant, J. C.; Iyengar, S. S.; Tomasi, J.; Cossi, M.; Rega, N.; Millam, J. M.; Klene, M.; Knox, J. E.; Cross, J. B.; Bakken, V.; Adamo, C.; Jaramillo, J.; Gomperts, R.; Stratmann, R. E.; Yazyev, O.; Austin, A. J.; Cammi, R.; Pomelli, C.; Ochterski, J. W.; Martin, R. L.; Morokuma, K.; Zakrzewski, V. G.; Voth, G. A.; Salvador, P.; Dannenberg, J. J.; Dapprich, S.; Daniels, A. D.; Farkas, Ö.; Foresman, J. B.; Ortiz, J. V.; Cioslowski, J.; Fox, D. J. Gaussian 09, Revision D.01, Gaussian, Inc., Wallingford CT, **2009**. [http://www.gaussian.com/g\\_prod/g09.htm](http://www.gaussian.com/g_prod/g09.htm): date accessed 10 May **2015**.

**Supplementary document S5:** Intra-molecular  $|E_{\text{HOMO}} - E_{\text{LUMO}}|^1$  energy gap and electrophilicity index ( $\omega$ )<sup>2</sup>

Intra-molecular  $|E_{\text{HOMO}} - E_{\text{LUMO}}|$  energy gap and electrophilicity index ( $\omega$ ) of mono- and bi-metallic carbene complexes, (a) all ligands attached; (b) *trans*-CO ligand dissociated from metal TM; (c) *trans*-CO ligand dissociated from metal TM<sup>1</sup>; all values are expressed in eV. Transition metal positions TM and TM<sup>1</sup> are indicated in **Chart 3.1**. Detailed calculations are shown in Chapter 3, section 3.2.2.

	(a)		(b)		(c)	
	$\Delta E$	( $\omega$ )	$\Delta E$	( $\omega$ )	$\Delta E$	( $\omega$ )
<b>A1</b>	3.159	2.681	3.023	2.191		
<b>A2</b>	2.497	4.148	2.367	3.748	2.814	3.212
<b>A3</b>	2.108	4.820	1.899	4.646	2.375	3.750
<b>A4</b>	2.333	4.573	2.287	4.117	2.521	3.486
<b>B5</b>	3.330	2.400	2.886	2.427		
<b>B6</b>	2.179	3.484	2.061	3.050		
<b>B7</b>	2.790	3.579	2.666	3.469	2.624	3.528
<b>B8</b>	3.011	2.630	2.467	2.862		
<b>B9</b>	1.716	4.223	1.451	4.003		
<b>B10</b>	2.432	4.143	2.306	3.878	2.277	3.945
<b>C11</b>	3.089	2.981	2.898	2.689		
<b>C12</b>	2.530	4.240	2.342	3.966	2.352	3.958
<b>C13</b>	2.524	4.228	2.317	4.013	2.529	3.848
<b>C14</b>	2.818	3.209	2.493	3.124		
<b>C15</b>	2.389	4.581	2.154	4.465	2.167	4.450
<b>D16</b>	3.084	2.882	2.868	2.657		
<b>D17</b>	2.931	2.889	2.771	2.498		
<b>D18</b>	2.525	4.014	2.423	3.700	2.352	3.752
<b>D19</b>	2.580	3.886	2.568	3.545	2.388	3.651
<b>D20</b>	2.815	3.113	2.470	3.071		
<b>D21</b>	2.219	4.407	2.281	3.998	1.977	4.294
<b>D22</b>	2.390	4.006	2.485	3.608	1.980	4.347
<b>D23</b>	2.465	4.655	2.028	4.246	1.829	4.426
<b>E24</b>	3.055	2.604	2.770	2.534		
<b>E25</b>	2.867	3.228	2.476	2.954		

1. Frisch, M. J.; Trucks, G. W.; Schlegel, H. B.; Scuseria, G. E.; Robb, M. A.; Cheeseman, R. J.; Scalmani, G.; Barone, V.; Mennucci, B.; Petersson, G. A.; Nakatsuji, H.; Caricato, M.; Li, X.; Hratchian, H. P.; Izmaylov, A. F.; Bloino, J.; Zheng, G.; Sonnenberg, J. L.; Hada, M.; Ehara, M.; Toyota, K.; Fukuda, R.; Hasegawa, J.; Ishida, M.; Nakajima, T.; Honda, Y.; Kitao, O.; Nakai, H.; Vreven, T.; Montgomery, J. A.; Peralta, Jr., J. E.; Ogliaro, F.; Bearpark, M.; Heyd, J. J.; Brothers, E.; Kudin, K. N.; Staroverov, V. N.; Kobayashi, R.; Normand, J.; Raghavachari, K.; Rendell, A.; Burant, J. C.; Iyengar, S. S.; Tomasi, J.; Cossi, M.; Rega, N.; Millam, J. M.; Klene, M.; Knox, J. E.; Cross, J. B.; Bakken, V.; Adamo, C.; Jaramillo, J.; Gomperts, R.; Stratmann, R. E.; Yazyev, O.; Austin, A. J.; Cammi, R.; Pomelli, C.; Ochterski, J. W.; Martin, R. L.; Morokuma, K.; Zakrzewski, V. G.; Voth, G. A.; Salvador, P.; Dannenberg, J. J.; Dapprich, S.; Daniels, A. D.; Farkas, Ö.; Foresman, J. B.; Ortiz, J. V.; Cioslowski, J.; Fox, D. J. Gaussian 09, Revision D.01, Gaussian, Inc., Wallingford CT, **2009**.[http://www.gaussian.com/g\\_prod/g09.htm](http://www.gaussian.com/g_prod/g09.htm): date accessed 10 May **2015**.
2. Cases, M.; Frenking, G.; Duran, G.; Sola, M. *Organometallics*. **2002**, *21*, 4182-4191.

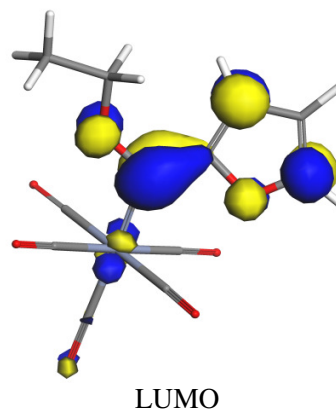
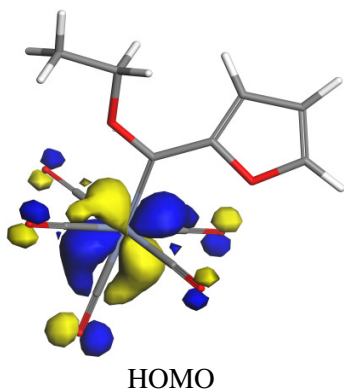
**Supplementary document S6: Pictorial representation of HOMO and LUMO**

---

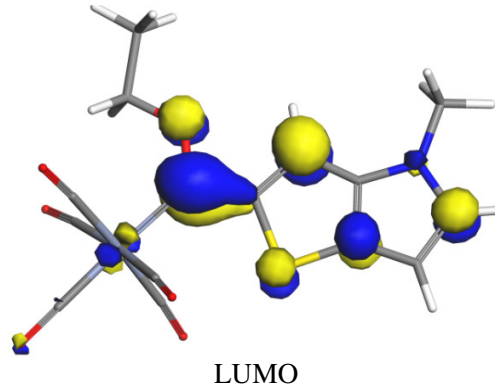
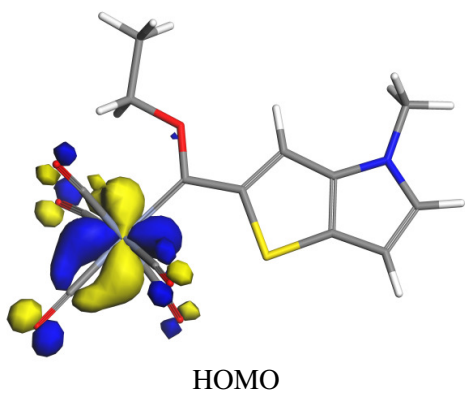
**Mono-metallic carbenes (All metal ligands attached)**

---

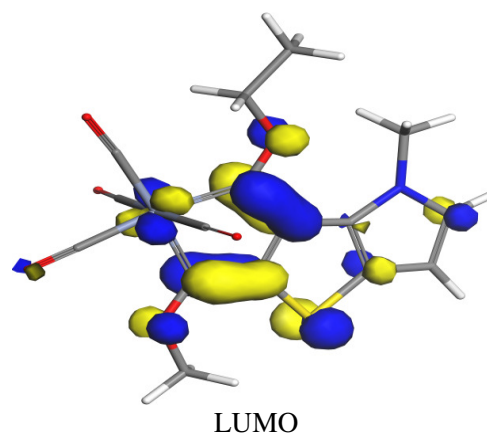
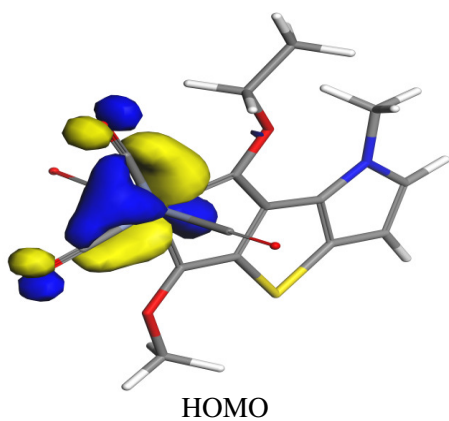
**A1**



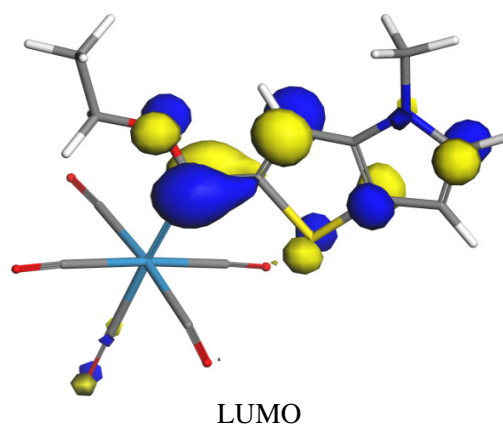
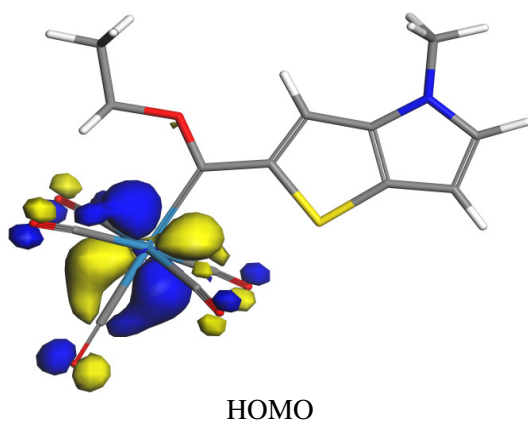
**B5**



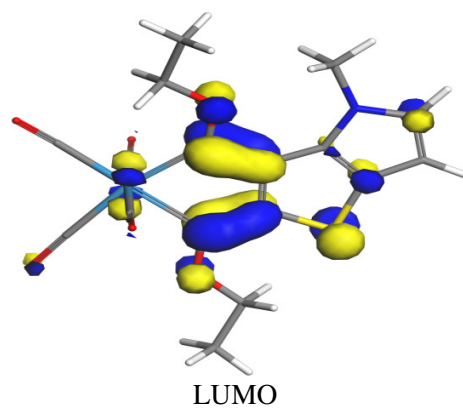
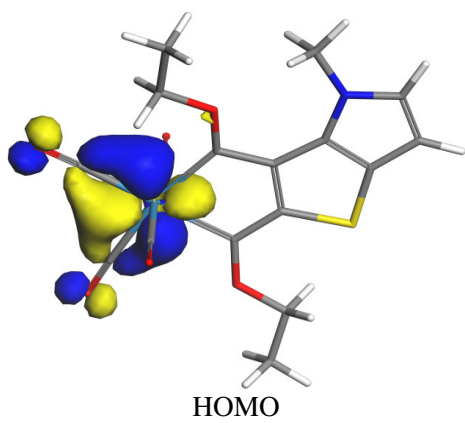
**B6**



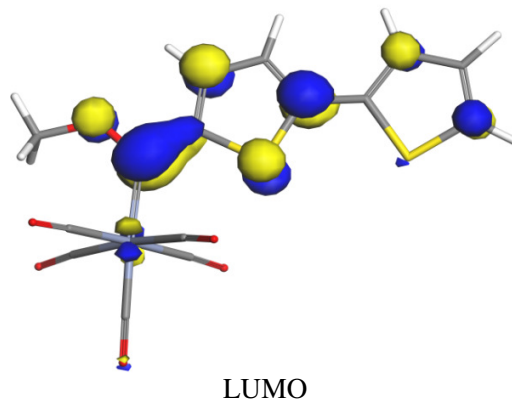
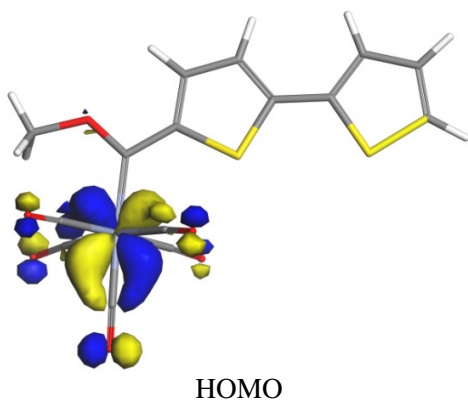
**B8**



**B9**

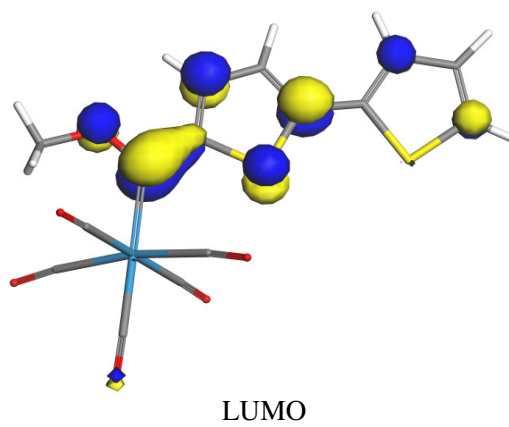
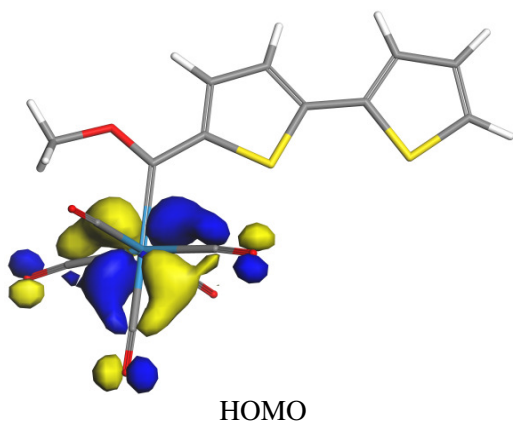


**C11**

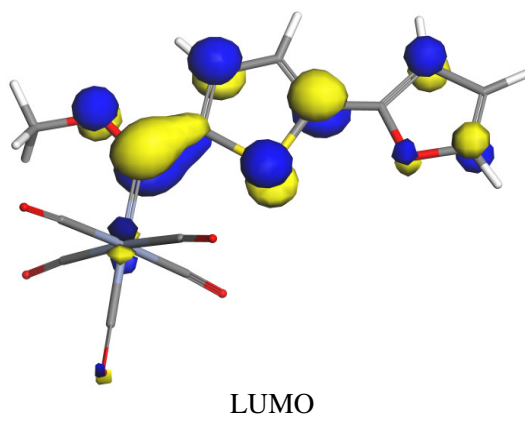
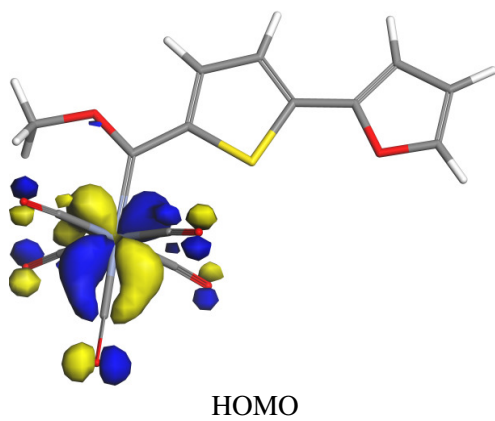




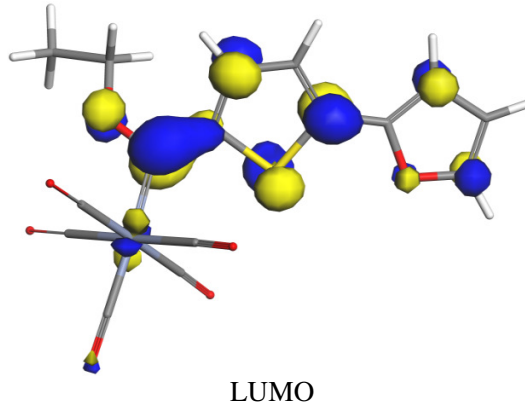
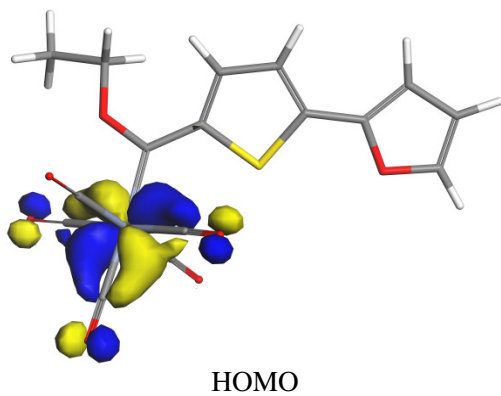
**C14**

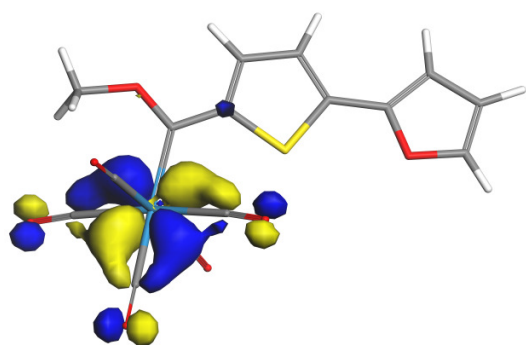


**D16**



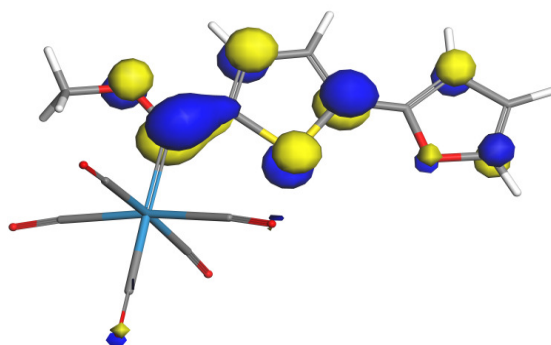
**D17**



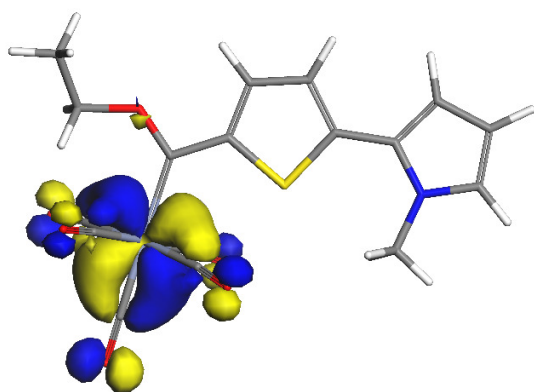


HOMO

**D20**

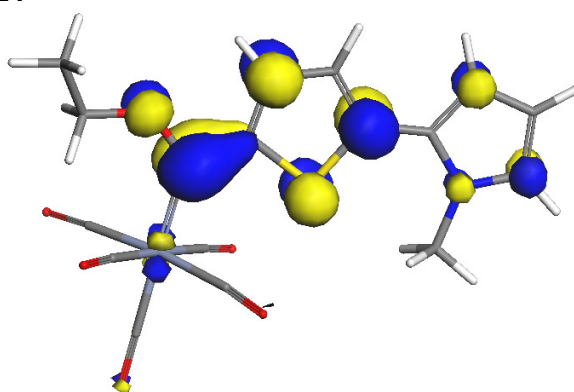


LUMO

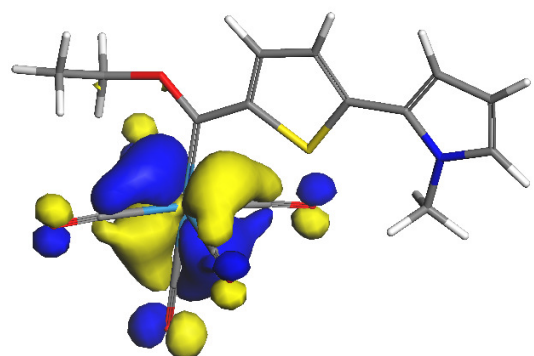


HOMO

**E24**

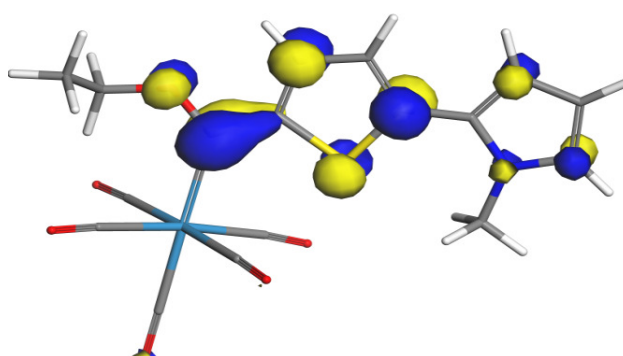


LUMO



HOMO

**E25**



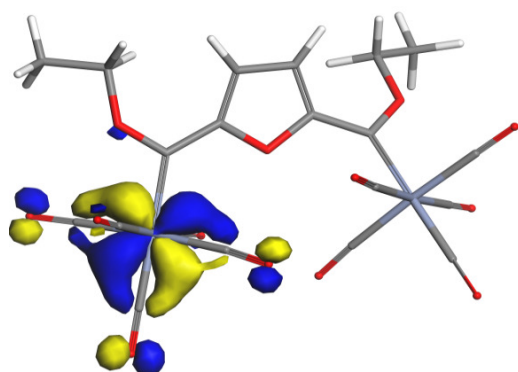
LUMO

---

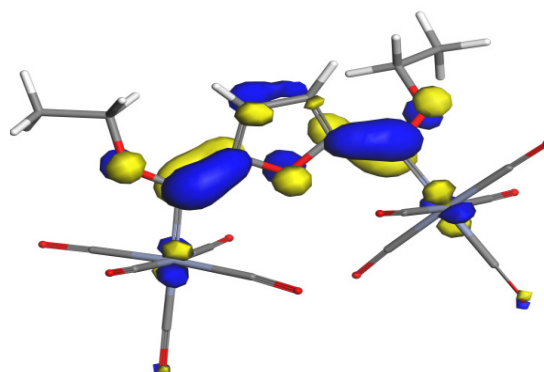
Bi-metallic Carbenes (All metal ligands attached)

---

A2

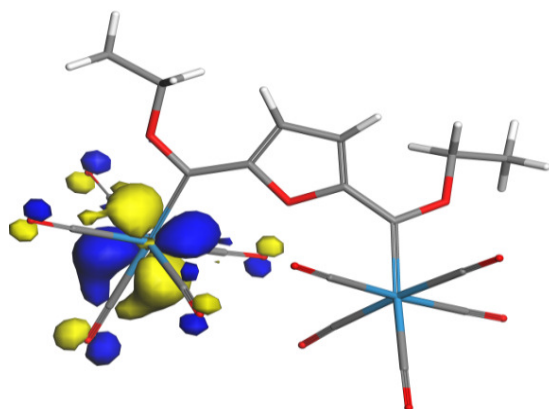


HOMO

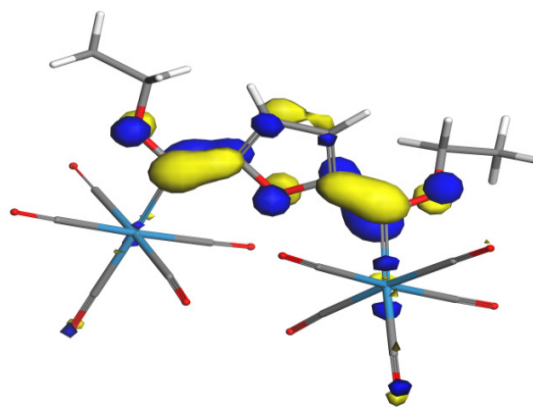


LUMO

A3

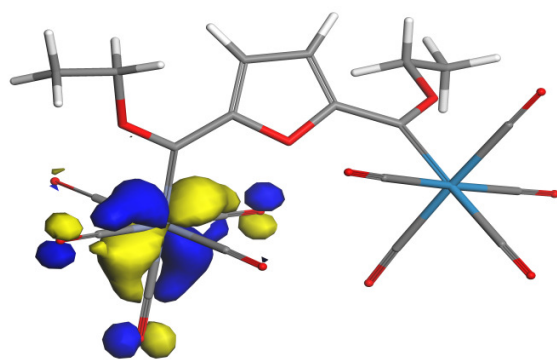


HOMO

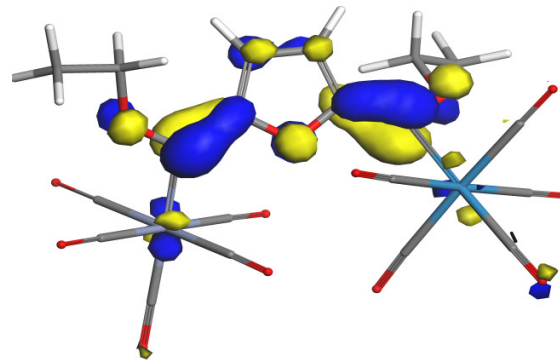


LUMO

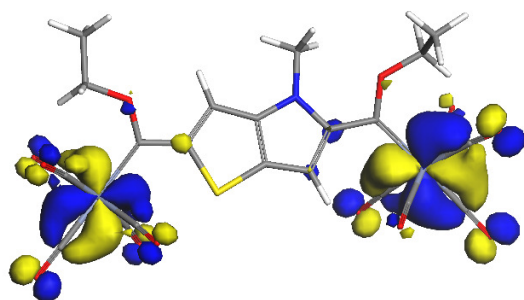
A4



HOMO

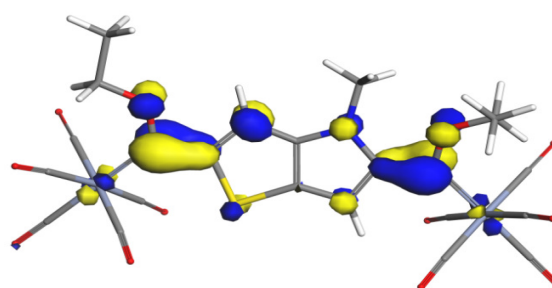


LUMO

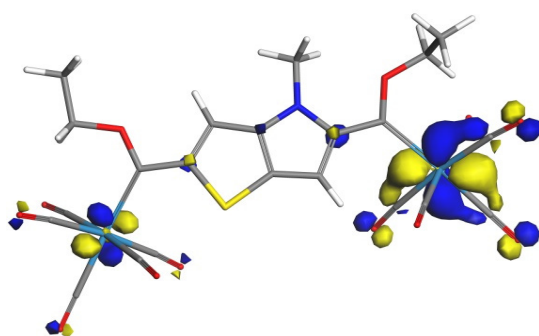


HOMO

**B7**

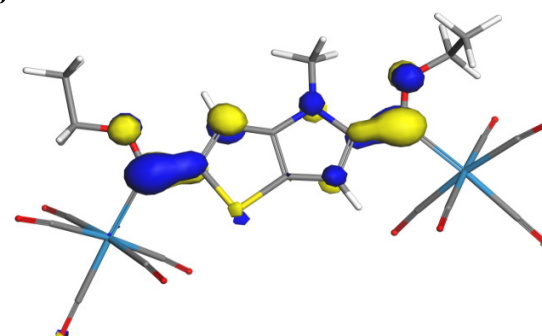


LUMO

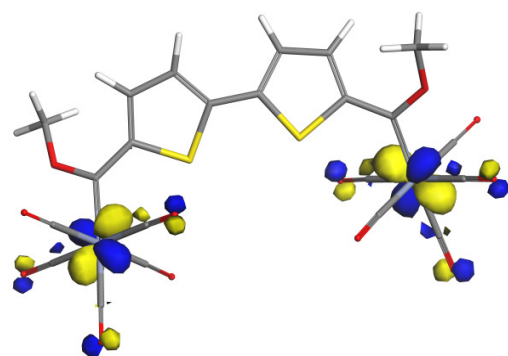


HOMO

**B10**

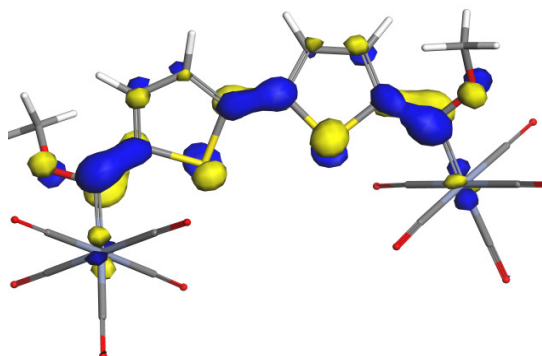


LUMO



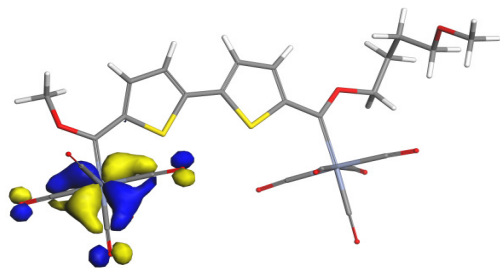
HOMO

**C12**

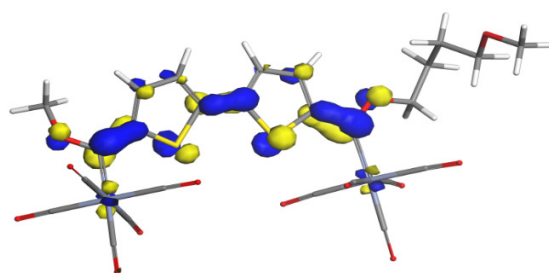


LUMO

**C13**

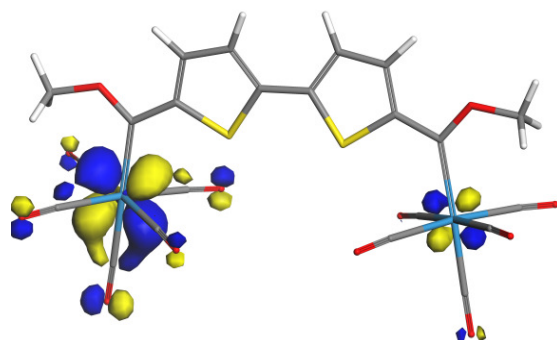


HOMO

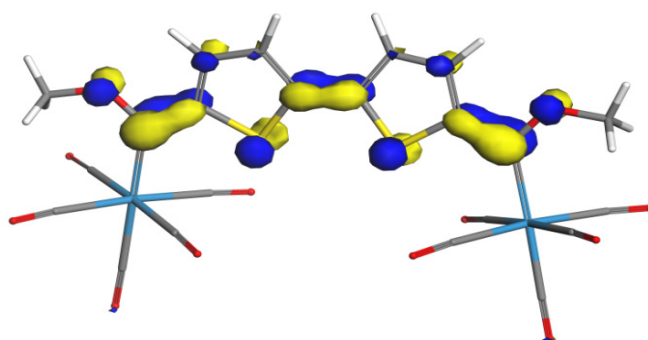


LUMO

**C15**

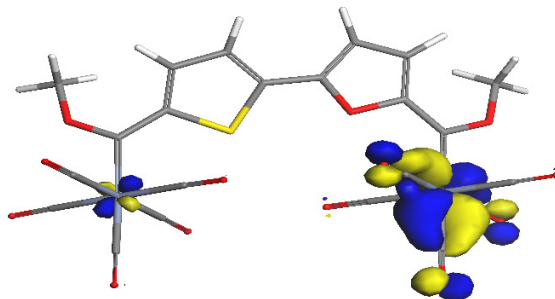


HOMO

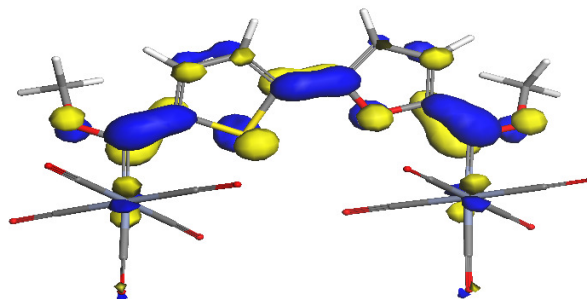


LUMO

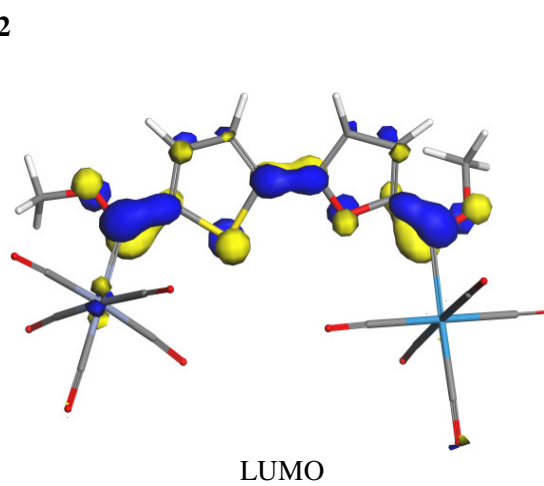
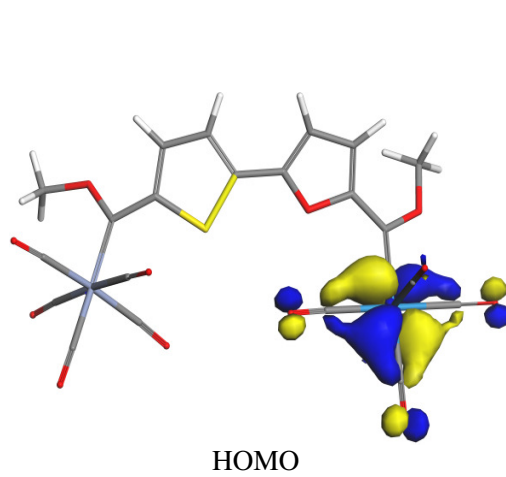
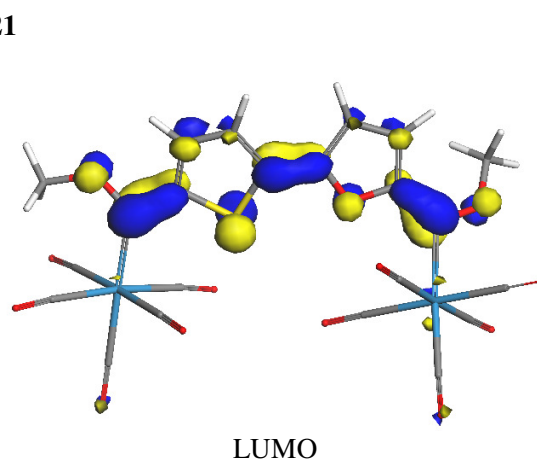
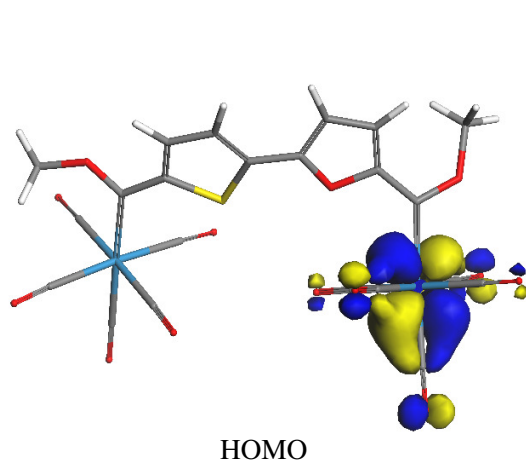
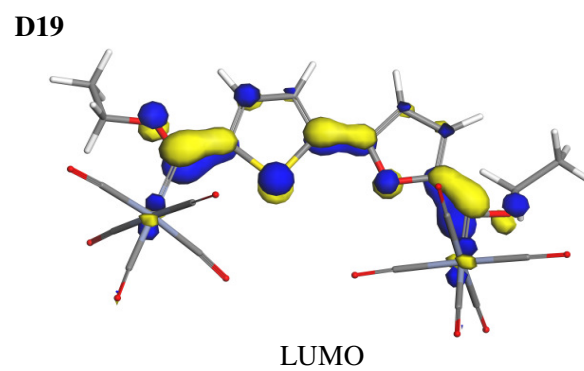
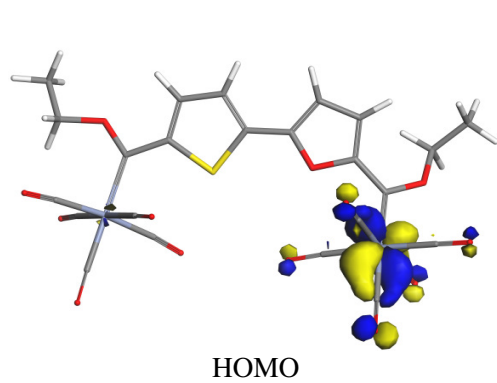
**D18**



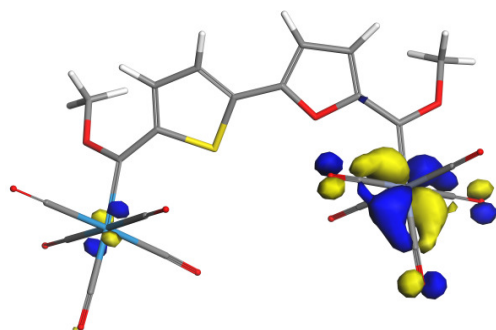
HOMO



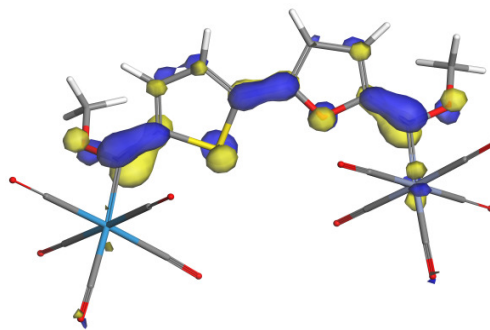
LUMO



D23



HOMO



LUMO

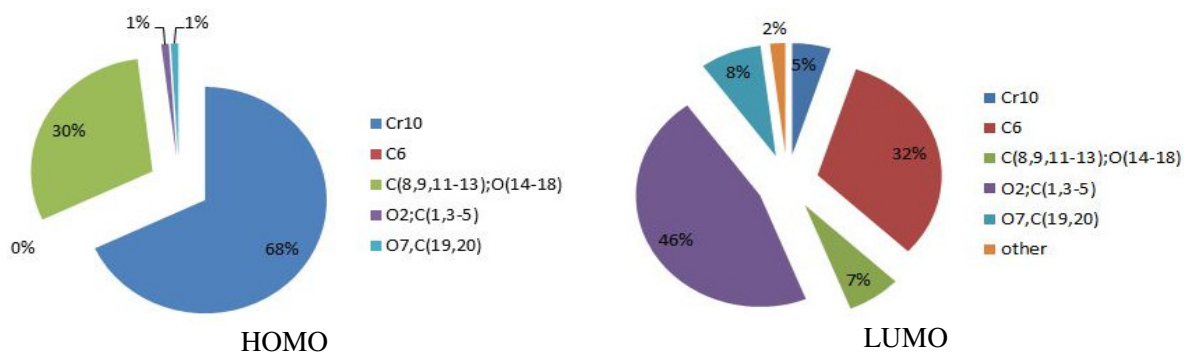
- 
1. Accelrys Software Inc, *Materials Studio 6.0*, 2011. <http://accelrys.com/products/collaborative-science/biovia-materials-studio/>: date accessed 2016-04-29



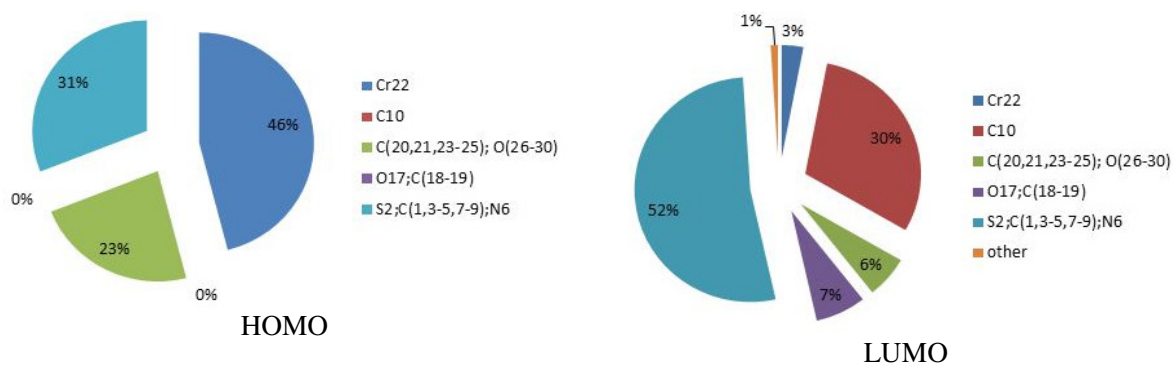
**Supplementary document S7: Fragment contribution to HOMO and LUMO<sup>1,2</sup>**

Mono-metallic (All ligands attached)

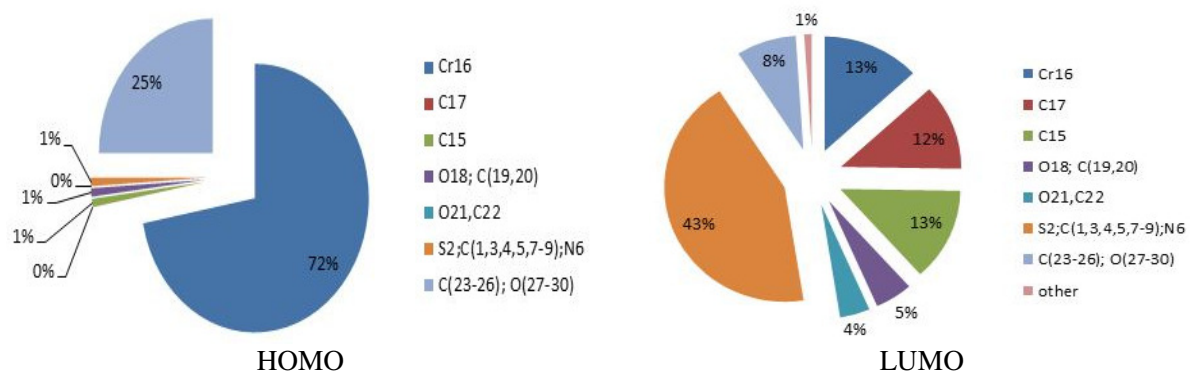
**A1**



**B5**

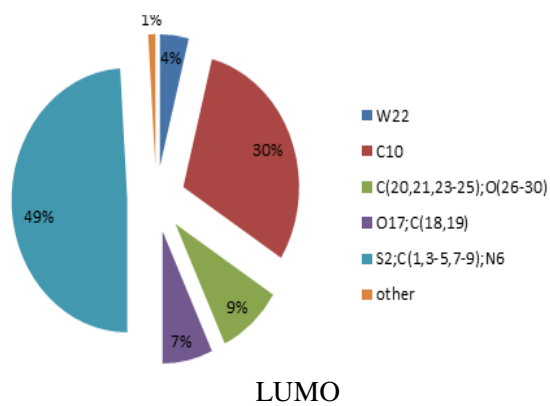
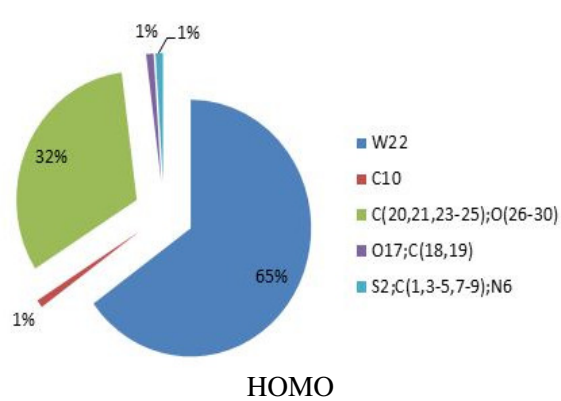


**B6**

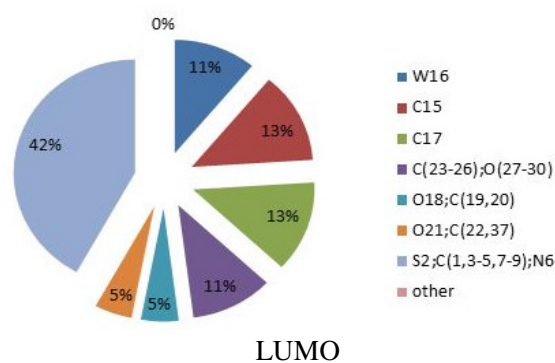
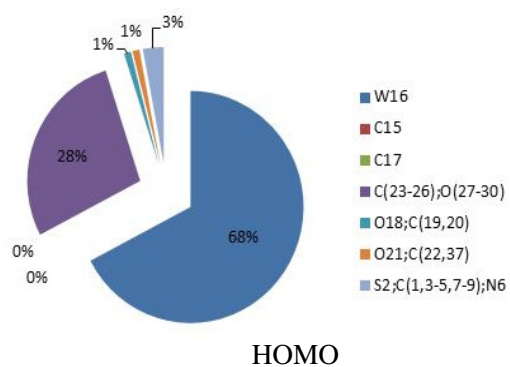




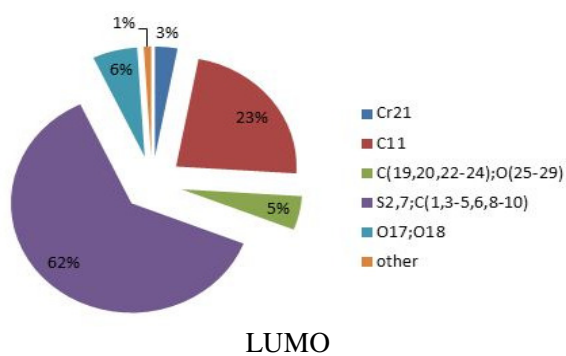
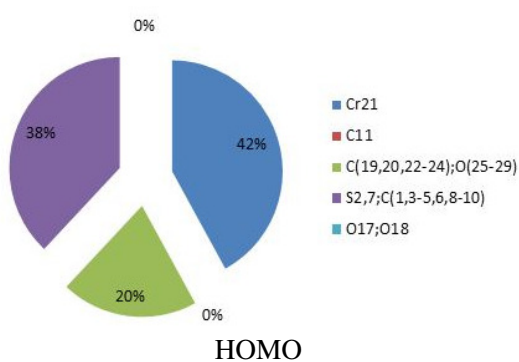
**B8**



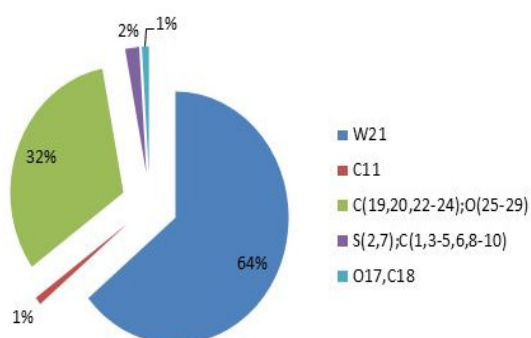
**B9**



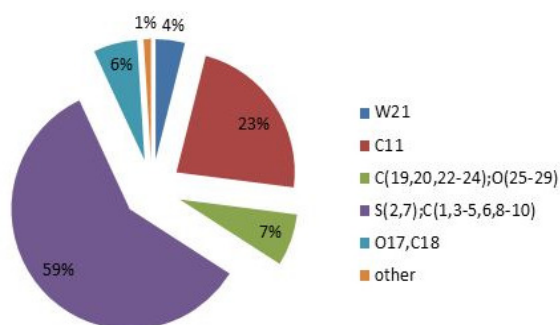
**C11**



# C14

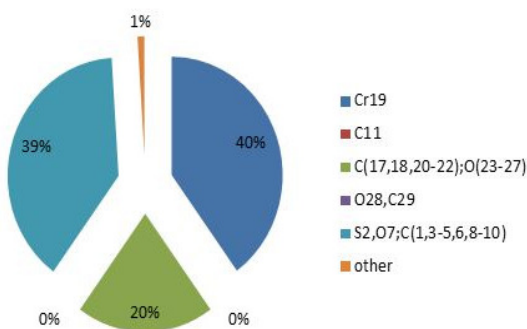


HOMO

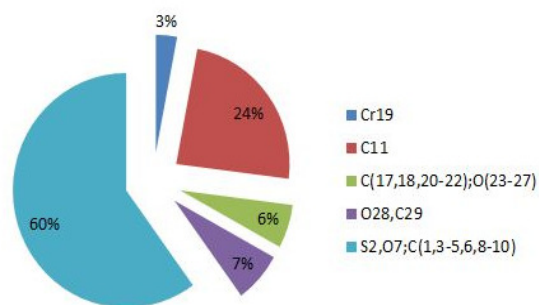


LUMO

# D16

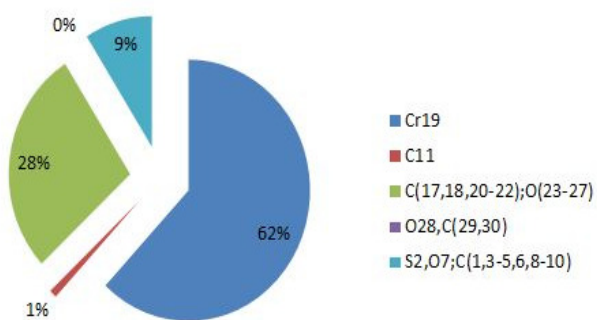


HOMO

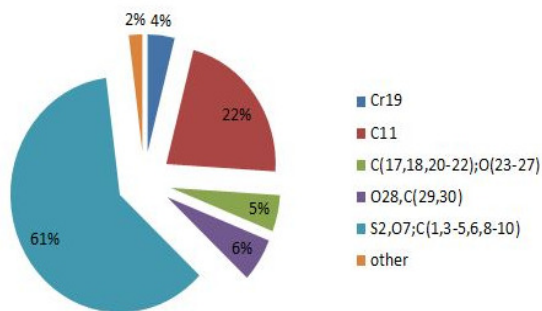


LUMO

# D17

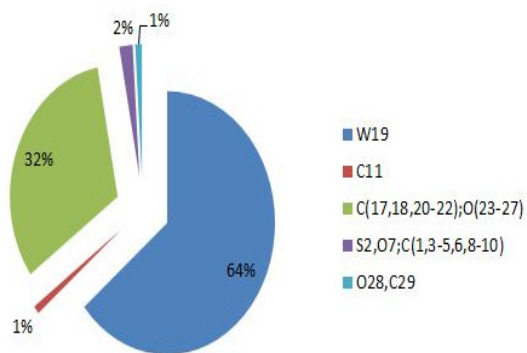


HOMO

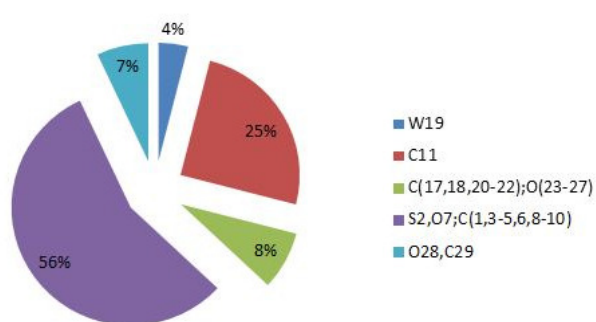


LUMO

# D20

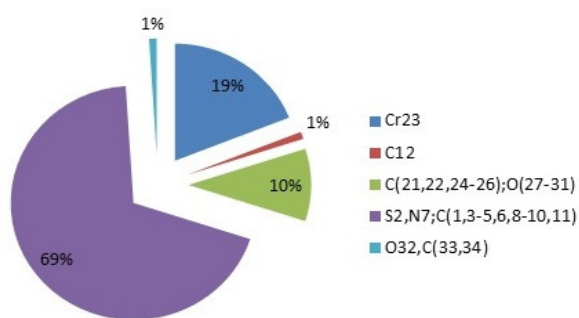


HOMO

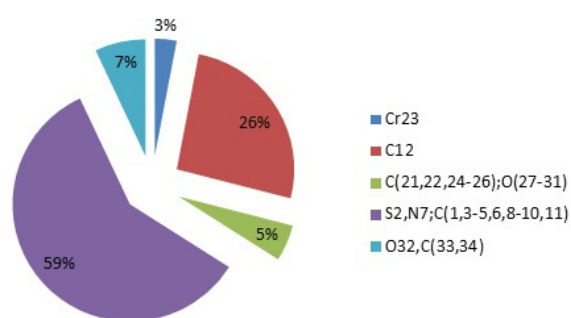


LUMO

# E24

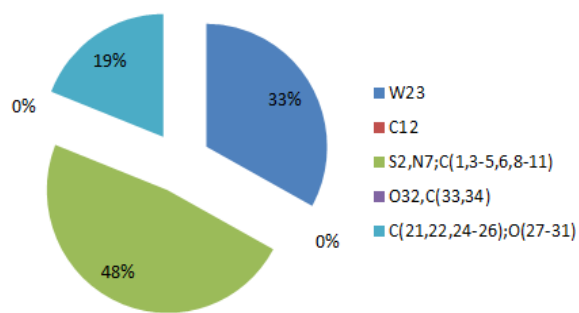


HOMO

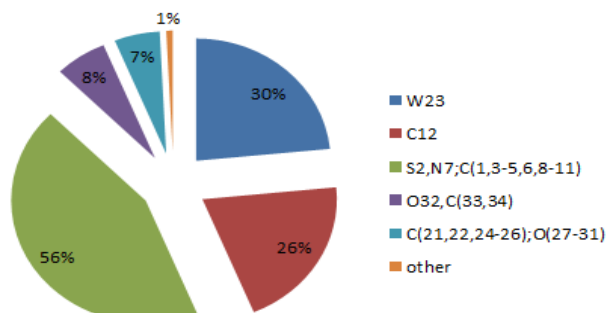


LUMO

# E25



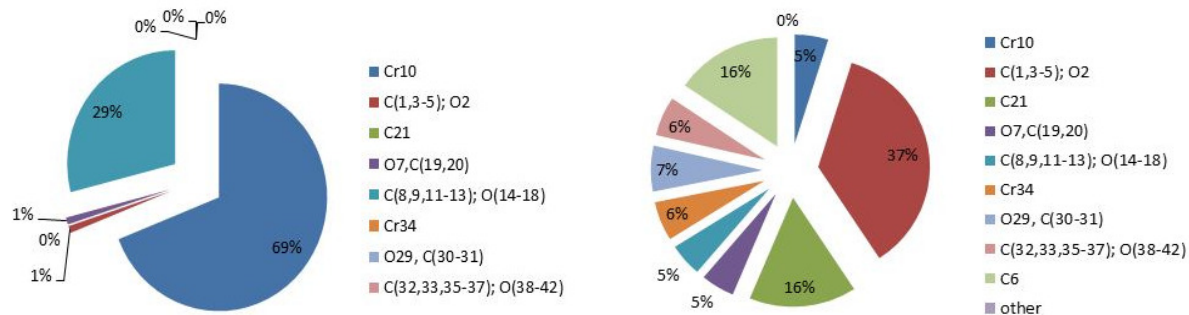
HOMO



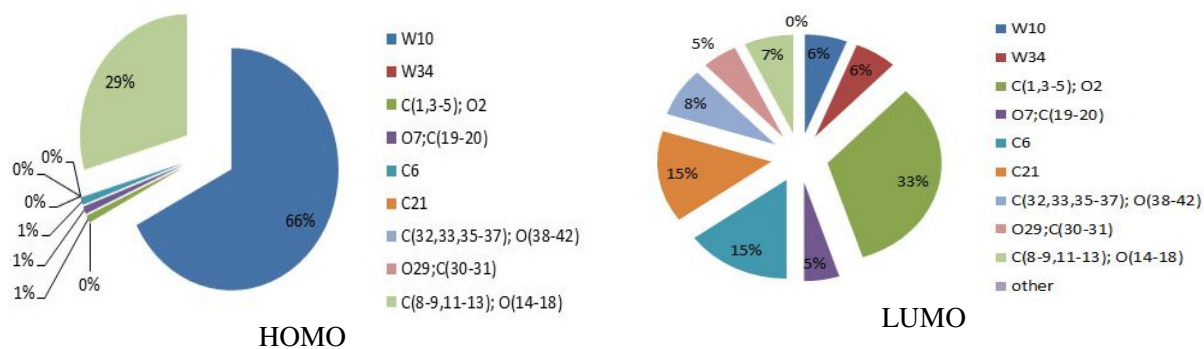
LUMO

## Bi-metallic carbenes (All ligands attached)

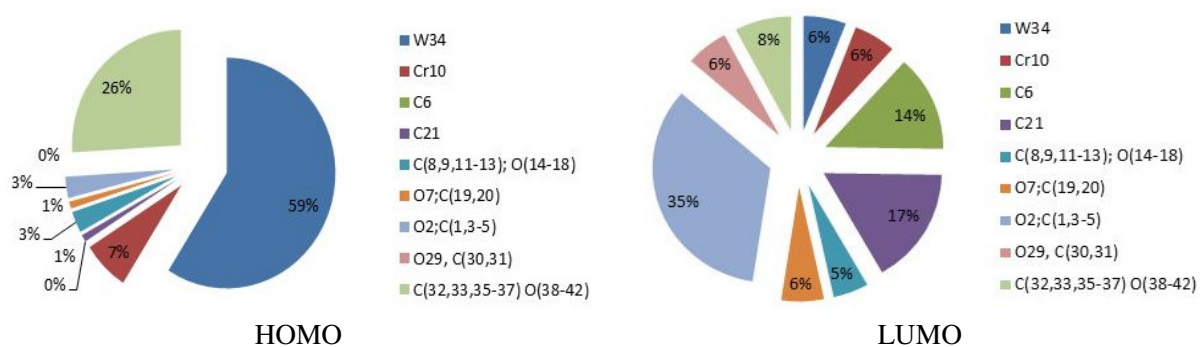
**A2**



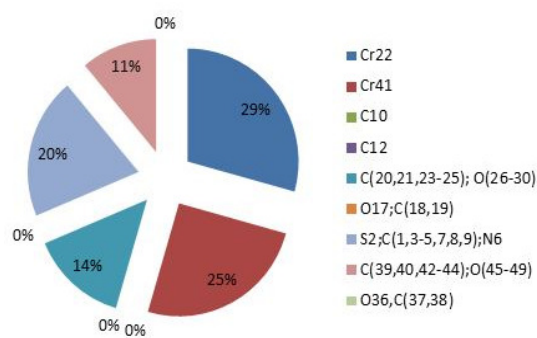
**A3**



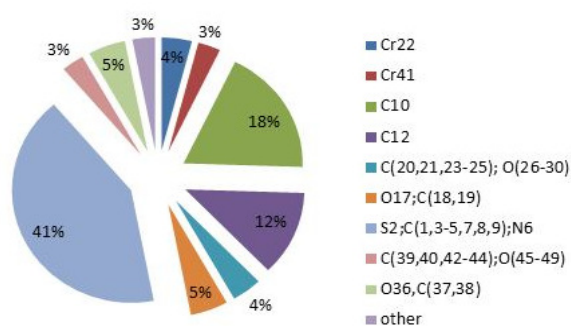
**A4**



## B7

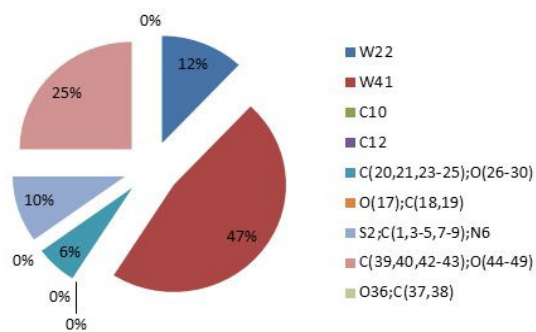


HOMO

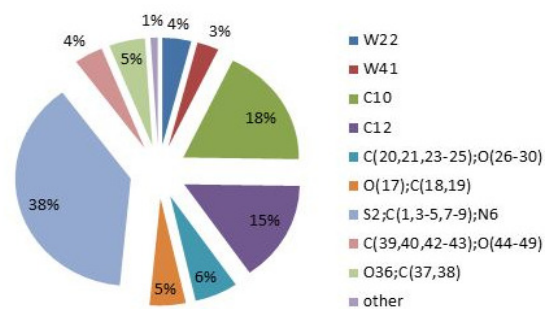


LUMO

## B10

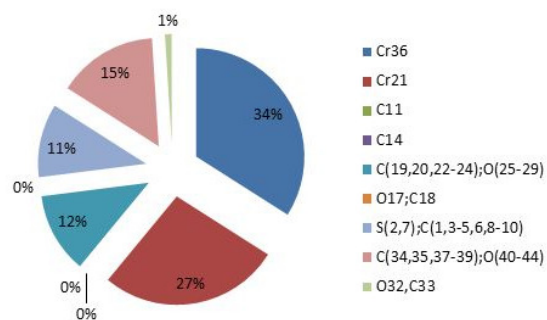


HOMO

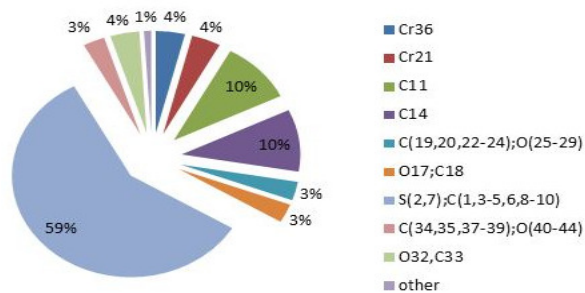


LUMO

## C12



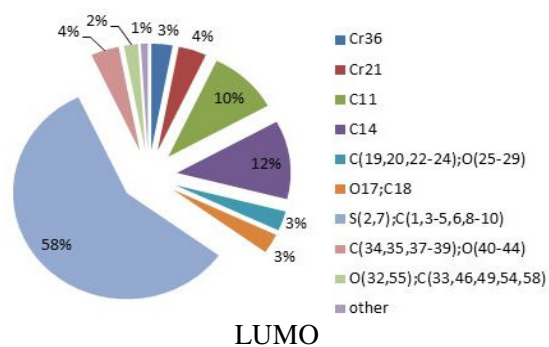
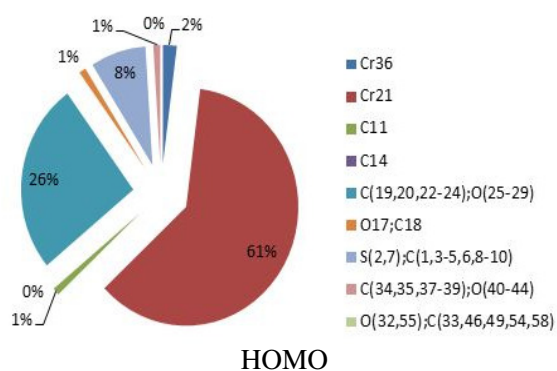
HOMO



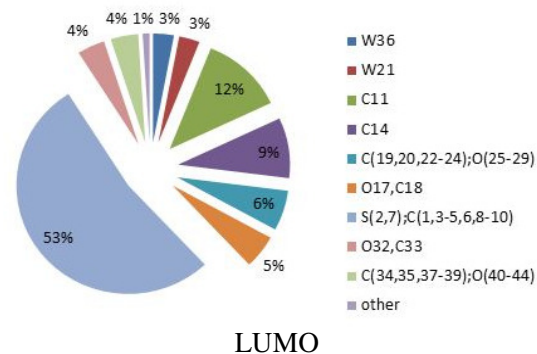
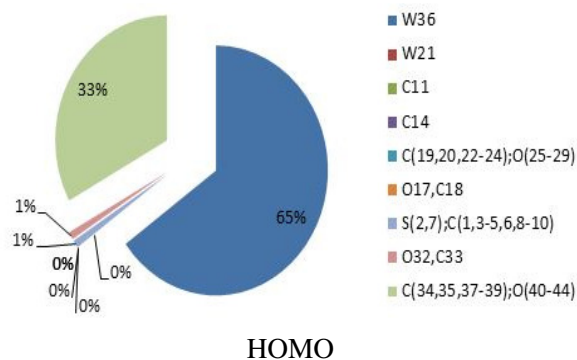
LUMO



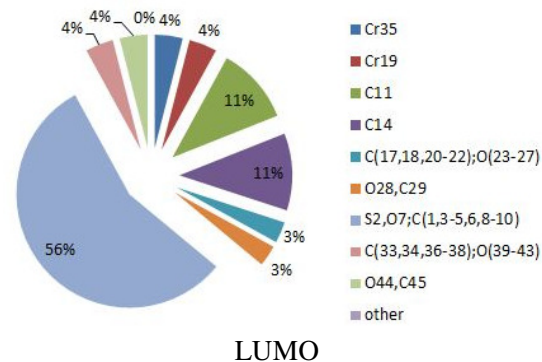
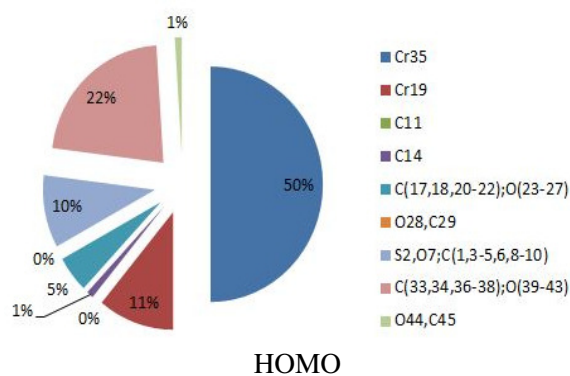
### C13



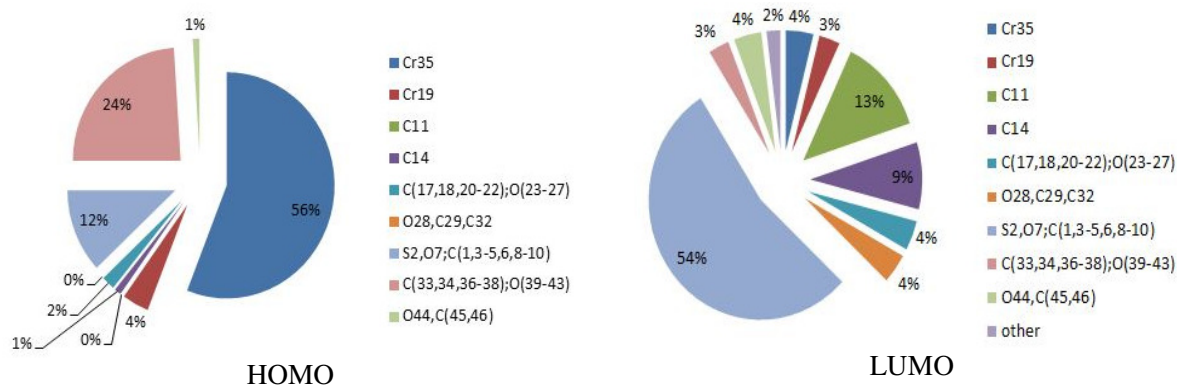
### C15



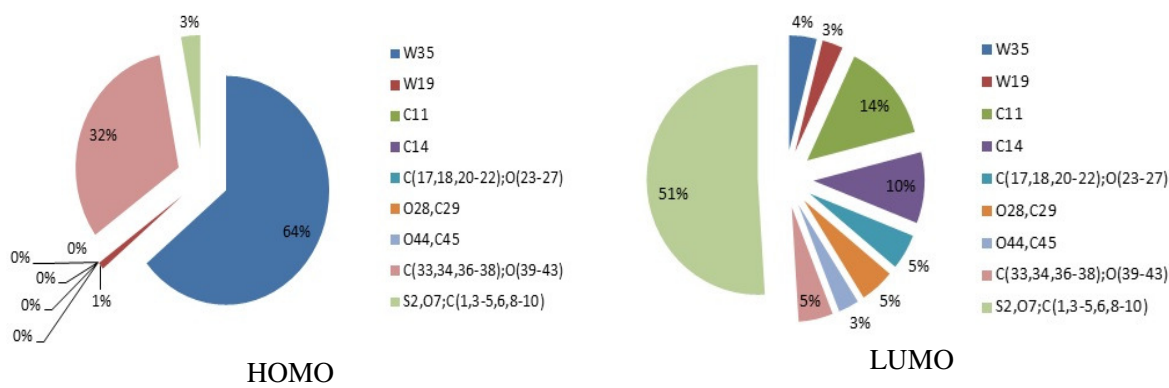
### D18



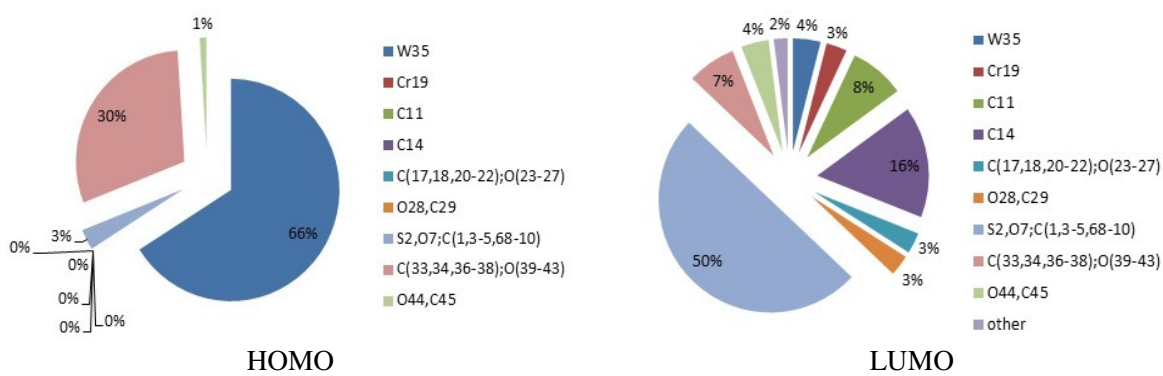
# D19



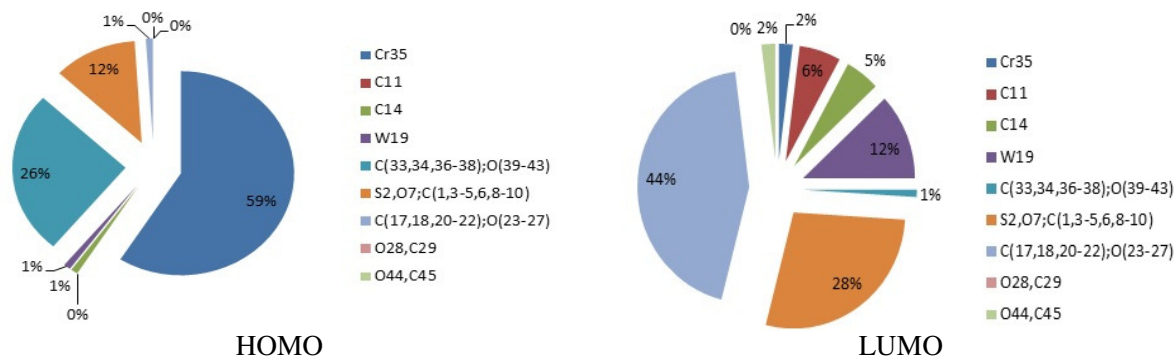
# D21



# D22



## D23



S6.1. Mono-metallic (*trans*-CO ligand dissociated from metal); metal and carbene %contribution only

Complex	HOMO (TM%)	LUMO (C%)
A1	73	16
B5	54	1
B6	72	13
B8	70	3
B9	74	15
C11	73	2
C14	69	3
D16	49	1
A17	65	19
D20	70	3
E24	39	1
E25	70	0



S6.2. Bi-metallic (a) *trans*-CO ligand dissociated from TM, (b) *trans*-CO ligand dissociated from TM<sup>1</sup>; metals (M, M<sup>1</sup>) and carbenes (C, C<sup>1</sup>) % contribution (identity of TM, TM<sup>1</sup>, C and C<sup>1</sup> is as shown in **Chart 3.1**)

(a) *trans*-CO ligand dissociated from TM

Complexes	HOMO		LUMO	
	TM%	TM <sup>1</sup> %	C%	C <sup>1</sup> %
<b>A2</b>	56	4	12	8
<b>A3</b>	71	0	12	20
<b>A4</b>	56	8	11	21
<b>B7</b>	60	4	14	17
<b>C10</b>	66	2	1	0
<b>C12</b>	66	1	2	0
<b>C13</b>	66	1	6	14
<b>C15</b>	70	0	9	13
<b>D18</b>	50	10	10	13
<b>D19</b>	50	10	10	13
<b>D21</b>	46	18	10	13
<b>D22</b>	5	55	8	16
<b>D23</b>	8	48	5	1

(b) *trans*-CO ligand dissociated from TM<sup>1</sup>

Complexes	HOMO		LUMO	
	TM%	TM <sup>1</sup> %	C%	C <sup>1</sup> %
<b>A2</b>	18	48	7	0
<b>A3</b>	61	4	13	6
<b>A4</b>	7	60	7	5
<b>B7</b>	5	56	0	1
<b>C10</b>	2	63	18	12
<b>C12</b>	2	66	0	2
<b>C13</b>	13	42	12	9
<b>C15</b>	0	71	13	9
<b>D18</b>	1	67	6	7
<b>D19</b>	1	67	16	7
<b>D21</b>	0	71	0	1
<b>D22</b>	0	71	15	8
<b>D23</b>	0	62	19	6

1. Frisch, M. J.; Trucks, G. W.; Schlegel, H. B.; Scuseria, G. E.; Robb, M. A.; Cheeseman, R. J.; Scalmani, G.; Barone, V.; Mennucci, B.; Petersson, G. A.; Nakatsuji, H.; Caricato, M.; Li, X.; Hratchian, H. P.; Izmaylov, A. F.; Bloino, J.; Zheng, G.; Sonnenberg, J. L.; Hada, M.; Ehara, M.; Toyota, K.; Fukuda, R.; Hasegawa, J.; Ishida, M.; Nakajima, T.; Honda, Y.; Kitao, O.; Nakai, H.; Vreven, T.;

Montgomery, J. A.; Peralta, Jr., J. E.; Ogliaro, F.; Bearpark, M.; Heyd, J. J.; Brothers, E.; Kudin, K. N.; Staroverov, V. N.; Kobayashi, R.; Normand, J.; Raghavachari, K.; Rendell, A.; Burant, J. C.; Iyengar, S. S.; Tomasi, J.; Cossi, M.; Rega, N.; Millam, J. M.; Klene, M.; Knox, J. E.; Cross, J. B.; Bakken, V.; Adamo, C.; Jaramillo, J.; Gomperts, R.; Stratmann, R. E.; Yazyev, O.; Austin, A. J.; Cammi, R.; Pomelli, C.; Ochterski, J. W.; Martin, R. L.; Morokuma, K.; Zakrzewski, V. G.; Voth, G. A.; Salvador, P.; Dannenberg, J. J.; Dapprich, S.; Daniels, A. D.; Farkas, Ö.; Foresman, J. B.; Ortiz, J. V.; Cioslowski, J.; Fox, D. J. Gaussian 09, Revision D.01, Gaussian, Inc., Wallingford CT, **2009**.[http://www.gaussian.com/g\\_prod/g09.htm](http://www.gaussian.com/g_prod/g09.htm): date accessed 10 May 2015

2. [www.chemissionian.com/ch20](http://www.chemissionian.com/ch20): date accessed 10 May 2015

**Supplementary document S8.** Natural Population Charges<sup>1</sup>; atom numbering is shown in Supplementary document **S1**

Mono-metallic							
	Bond	Atom	NPA Charges		Bond	Atom	NPA Charges
A1	C6-Cr10	C6	0.4703	C14	C11-W21	C11	0.3250
		Cr10	-2.2894			W21	-1.4374
B5	C10-Cr22	C10	0.4736	D16	C11-Cr19	C11	0.5074
		Cr22	-2.2775			Cr19	-2.2735
B6	C15-Cr16	C15	0.4668	D17	C11-Cr19	C11	0.4947
		Cr16	-2.0576			Cr19	-2.2837
	C17-Cr16	C17	0.4898	D20	C11-W19	C11	0.3234
		Cr16	-2.0576			W19	-1.4371
B8	C10-W22	C10	0.4859	E24	C12-Cr23	C12	0.4708
		W22	-2.2699			Cr23	
B9	C15-W16	C15	0.3097	E25	C12-W23	C12	0.3207
		W16	-1.1886			W23	-1.4480
	C17-W16	C17	0.3279				
		W16	-1.1886				
C11	C11-Cr21	C11	0.4796				
		Cr21	-2.2824				
Bi-metallic							
	Bond	Atom	NPA Charges		Bond	Atom	NPA Charges
A2	C6-Cr10	C6	0.4816	B10	C10-W22	C10	0.3279
		Cr10	-2.2694			W22	-1.4281
	C21-Cr34	C21	0.4812		C12-W41	C12	0.3219
		Cr34	-2.2681			W41	-1.4313
A3	C6-W10	C6	0.3070	C12	C11-Cr21	C11	0.5038
		W10	-1.3687			Cr21	-2.2749
	C21-W34	C21	0.3067		C14-Cr36	C14	0.5038

<b>A4</b>	C6-Cr10	W34	-1.3689	<b>C13</b>	C11-Cr21	Cr36	-2.2753
		C6	0.4819			C11	0.5031
		Cr10	-2.2662			Cr21	-2.2749
		C21-W34				C14-Cr36	
<b>B7</b>	C10-Cr22	C21	0.3064	<b>C15</b>	C11-W21	C14	0.4885
		W34	-1.3722			Cr36	-2.2780
		C10	0.4858			C11	0.3269
		Cr22	-2.2699			W21	-1.4326
<b>D18</b>	C11-Cr19	C12-Cr41		<b>D22</b>	C11-Cr19	C14-W36	
		C12	0.4700			C14	0.3272
		Cr41	-2.2837			W36	-1.4330
		C11	0.5074			C11	0.4863
<b>D19</b>	C14-Cr35	Cr19	-2.2735	<b>D23</b>	C11-W19	Cr19	-2.2750
		C14	0.4571			C14	0.2870
		Cr35	-2.2774			W35	-1.3736
		C11	0.4885			C11	0.4858
<b>D21</b>	C11-W19	Cr19	-2.2751	<b>D20</b>	C11-W19	W19	-2.2746
		C14	0.4662			C14	0.2874
		Cr35	-2.2792			Cr35	-1.3735
		C11	0.3278				
		W19	-1.4321				
		C14-W35					
		C14	0.2886				
		W35	-1.3726				

Mono-metallic with a <i>trans</i> -CO ligand dissociated from TM							
	Bond	Atom	NPA Charges		Bond	Atom	NPA Charges
<b>A1</b>	C6-Cr10	C6		<b>C14</b>	C11-W21	C11	0.3333
		Cr10	-1.4123			W21	-0.8033
<b>B5</b>	C10-Cr22	C10	0.4671	<b>D16</b>	C11-Cr19	C11	0.4685
		Cr22	-1.4256			Cr19	-1.4296
<b>B6</b>	C15-Cr16	C15	0.3567	<b>D17</b>	C11-Cr19	C11	0.4864
		Cr16	-1.1732			Cr19	-1.4095
	C17-Cr16	C17	0.4557		C11-W19	C11	0.3326

<b>B8</b>	C10-W22	Cr16	-1.1732	<b>E24</b>	C12-Cr23	W19	-0.8044
		C10	0.3350			C12	0.4692
		W22	-0.8080			Cr23	-1.4284
<b>B9</b>	C15-W16	C15	0.2364	<b>E25</b>	C12-W23	C12	0.3407
		W16	-0.5039			W23	-0.8215
		C17-W16					
<b>C11</b>	C11-Cr21	C17	0.2930				
		W16	-0.5039				
		C11	0.4699				
		Cr21	-1.4287				

Bi-metallic with <i>trans</i> -CO ligand dissociated from TM							
	Bond	Atom	NPA Charges		Bond	Atom	NPA Charges
<b>A2</b>	C6-Cr10	C6	0.4594	<b>C13</b>	C11-Cr21	C11	0.4878
		Cr10	-1.3809			Cr21	-1.3965
	C21-Cr34	C21	0.4744		C14-Cr36	C14	0.4847
		Cr34	-2.2823			Cr36	-2.2802
<b>A3</b>	C6-W10	C6	0.2915	<b>C15</b>	C11-W21	C11	0.4878
		W10	-0.7206			W21	-1.3965
	C21-W34	C21	0.3037		C14-W36	C14	0.4847
		W34	-1.3790			W36	-2.2802
<b>A4</b>	C6-Cr10	C6	0.4592	<b>D18</b>	C11-Cr19	C11	0.4940
		Cr10	-1.3788			Cr19	-1.3924
	C21-W34	C21	0.3036		C14-Cr35	C14	0.4503
		W34	-1.3825			Cr35	-2.2842
<b>B7</b>	C10-Cr22	C10	0.4710	<b>D19</b>	C11-Cr19	C11	0.4612
		Cr22	-1.4149			Cr19	-1.4160
	C12-Cr41	C12	0.4623		C14-Cr35	C14	0.4613
		Cr41	-2.2856			Cr35	-2.2833
<b>B10</b>	C10-W22	C10	0.3278	<b>D22</b>	C11-Cr19	C11	0.4689
		W22	-0.7846			Cr19	-1.4143
	C12-W41	C12	0.3169		C14-W35	C14	0.2855

<b>C12</b>	C11-Cr21	W41	-1.4336	<b>D23</b>	C11-W19	W35	-1.3789
		C11	0.4883			C11	0.3256
		Cr21	-1.3968			W19	-0.7858
		C14-Cr36				C14-Cr35	
<b>D21</b>	C11-W19	C14	0.4990			C14	0.4526
		Cr36	-2.2795			W35	-2.2812
		C11	0.3245				
		W19	-0.7842				
	C14-W35	C14	0.2851				
		W35	-1.3782				

Bi-metallic with <i>trans</i> -CO ligand dissociated from TM <sup>1</sup>							
	Bond	Atom	NPA Charges		Bond	Atom	NPA Charges
<b>A2</b>	C6-Cr10	C6	0.4747	<b>B7</b>	C10-Cr22	C10	0.4781
		Cr10	-2.2823			Cr22	-2.2734
	C21-Cr34	C21	0.4588		C12-Cr41	C12	0.4643
		Cr34	-1.3813			Cr41	-1.4189
<b>A3</b>	C6-W10	C6	0.3028	<b>B10</b>	C10-W22	C10	0.3226
		W10	-1.3782			W22	-1.4321
	C21-W34	C21	0.2894		C12-W41	C12	0.2561
		W34	-0.7193			W41	-0.7892
<b>A4</b>	C6-Cr10	C6	0.4734	<b>C12</b>	C11-Cr21	C11	0.4994
		Cr10	-2.2792			Cr21	-2.2791
	C21-W34	C21	0.2885		C14-Cr36	C14	0.4874
		W34	-0.7219			Cr36	-1.3982
<b>C13</b>	C11-Cr21	C11	0.4996	<b>D21</b>	C11-W19	C11	0.3250
		Cr21	-2.2784			W19	-1.4352
	C14-Cr36	C14	0.4742		C14-W35	C14	0.2791
		Cr36	-1.4180			W35	-0.7232
<b>C15</b>	C11-W21	C11	0.3251	<b>D22</b>	C11-Cr19	C11	0.4809
		W21	-1.4348			Cr19	-2.2787
	C14-W36	C14	0.3271		C14-W35	C14	0.2788

<b>D18</b>	C11-Cr19	W36	-0.7892	<b>D23</b>	C11-W19	W35	-0.7240
		C11	0.5012			C11	0.3249
		Cr19	-2.2783			W19	-1.4354
		C14-Cr35				C14-Cr35	
		C14	0.4342			C14	0.4374
<b>D19</b>	C11-Cr19	Cr35	-1.3879			Cr35	-1.3904
		C11	0.4832				
		Cr19	-2.2777				
		C14-Cr35					
		C14	0.4426				
		Cr35	-1.3930				

---

1. Frisch, M. J.; Trucks, G. W.; Schlegel, H. B.; Scuseria, G. E.; Robb, M. A.; Cheeseman, R. J.; Scalmani, G.; Barone, V.; Mennucci, B.; Petersson, G. A.; Nakatsuji, H.; Caricato, M.; Li, X.; Hratchian, H. P.; Izmaylov, A. F.; Bloino, J.; Zheng, G.; Sonnenberg, J. L.; Hada, M.; Ehara, M.; Toyota, K.; Fukuda, R.; Hasegawa, J.; Ishida, M.; Nakajima, T.; Honda, Y.; Kitao, O.; Nakai, H.; Vreven, T.; Montgomery, J. A.; Peralta, Jr., J. E.; Ogliaro, F.; Bearpark, M.; Heyd, J. J.; Brothers, E.; Kudin, K. N.; Staroverov, V. N.; Kobayashi, R.; Normand, J.; Raghavachari, K.; Rendell, A.; Burant, J. C.; Iyengar, S. S.; Tomasi, J.; Cossi, M.; Rega, N.; Millam, J. M.; Klene, M.; Knox, J. E.; Cross, J. B.; Bakken, V.; Adamo, C.; Jaramillo, J.; Gomperts, R.; Stratmann, R. E.; Yazyev, O.; Austin, A. J.; Cammi, R.; Pomelli, C.; Ochterski, J. W.; Martin, R. L.; Morokuma, K.; Zakrzewski, V. G.; Voth, G. A.; Salvador, P.; Dannenberg, J. J.; Dapprich, S.; Daniels, A. D.; Farkas, Ö.; Foresman, J. B.; Ortiz, J. V.; Cioslowski, J.; Fox, D. J. Gaussian 09, Revision D.01, Gaussian, Inc., Wallingford CT, **2009**. [http://www.gaussian.com/g\\_prod/g09.htm](http://www.gaussian.com/g_prod/g09.htm): date accessed 10 May **2015**.

**Supplementary document S9. Shielding parameters.<sup>1</sup>****G(complex)% and G(M)% of mono-metallic carbenes (all ligands attached)**

Complexes	Metal fragment	G(complex) %	G(Metal) %
<b>A1</b>	Cr10	99.79	99.58
<b>B5</b>	Cr22	99.76	99.53
<b>B6</b>	Cr16	99.55	98.91
<b>B8</b>	W22	93.81	89.92
<b>B9</b>	W16	92.52	89.64
<b>C11</b>	Cr21	88.64	86.01
<b>C14</b>	W21	93.89	89.94
<b>D16</b>	Cr19	99.57	98.91
<b>D17</b>	Cr19	99.75	99.44
<b>D20</b>	W19	93.87	89.96
<b>E24</b>	Cr23	99.60	98.29
<b>E25</b>	W23	93.97	89.97

**G(complex)% and G(M)% of bi-metallic carbenes (all ligands attached)**

Complex	Metal fragment	G(complex) %	G(Metal) %
<b>A2</b>	Cr10	99.78	99.52
	Cr34	99.60	99.32
<b>A3</b>	W10	99.78	99.52
	W34	99.60	99.32
<b>A4</b>	Cr10	99.76	99.53
	W34	93.34	91.40
<b>B7</b>	Cr22	99.61	98.97
	Cr41	99.62	99.07
<b>B10</b>	W22	93.81	89.92
	W41	94.31	89.00
<b>C12</b>	Cr21	99.75	99.48
	Cr36	99.77	99.48
<b>C13</b>	Cr21	99.76	99.47
	Cr36	99.62	99.01
<b>C15</b>	W21	93.82	90.21
	W36	93.76	90.09
<b>D18</b>	Cr19	99.76	99.50
	Cr35	99.77	99.59
<b>D19</b>	Cr19	99.65	99.14
	Cr35	99.78	99.63
<b>D21</b>	W19	93.81	90.12
	W35	93.30	91.36
<b>D22</b>	Cr19	99.58	99.10
	W35	92.04	91.27
<b>D23</b>	W19	87.19	84.78
	Cr35	99.75	99.58



**G(complex) and G(M) % of mono-metallic carbenes (*trans*-CO ligand dissociated from TM)**

Complex	Metal fragment	G(complex) %	G(Metal) %
<b>A1</b>	Cr10	86.83	86.63
<b>B5</b>	Cr22	88.13	87.45
<b>B6</b>	Cr16	85.98	85.15
<b>B8</b>	W22	77.62	75.58
<b>B9</b>	W16	77.36	74.31
<b>C11</b>	Cr21	88.11	87.49
<b>C14</b>	W21	79.70	75.84
<b>D16</b>	Cr19	88.18	87.56
<b>D17</b>	Cr19	86.98	86.69
<b>D20</b>	W19	79.56	75.57
<b>E24</b>	W23	87.95	87.38
<b>E25</b>	W23	79.56	75.53

**G(complex) and G(M) % of bi-metallic carbenes (*trans*-CO ligand dissociated from TM and TM<sup>1</sup> respectively )**

Complex	Metal fragment	G(complex) %	G(Metal) %
<b>A2</b>	Cr10	99.79	99.62
	Cr34	99.81	99.65
<b>A3</b>	W10	88.86	76.13
	W34	92.42	80.34
<b>A4</b>	Cr10	86.89	86.60
	W34	79.50	78.38
<b>B7</b>	Cr22	88.18	87.58
	Cr41	87.87	87.34
<b>B10</b>	W22	85.96	75.74
	W41	79.69	75.74
<b>C12</b>	Cr21	87.03	86.74
	Cr36	87.11	86.81
<b>C13</b>	Cr21	86.99	86.73
	Cr36	88.22	87.61
<b>C15</b>	W21	79.65	75.93
	W36	79.59	75.95
<b>D18</b>	Cr19	87.02	86.80
	Cr35	86.55	86.41
<b>D19</b>	Cr19	88.08	87.55
	Cr35	86.58	86.51
<b>D21</b>	W19	79.34	75.80
	W35	77.33	76.20
<b>D22</b>	Cr19	87.99	87.50
	W35	77.04	76.27
<b>D23</b>	W19	88.09	87.58
	Cr35	86.83	86.64

1. Solid, G. Version 0.26, *Program for computing ligand steric effects*; Molecular structure Laboratory: **2004**.

**Supplementary document S10.** Hybridization of the transition metal-carbene bond (NBO analysis); Complex, Occupancy, Polarization (%) and Hybridization (%) of the transition metal-carbene (TM-C) bond; bonding (BD) orbitals<sup>1</sup>

Mono-metallic all ligands attached								
Complex	Bond	Atom	Occup	Polarization (%) TM-C bond	Hybridization of TM-C bond			
					%s	%p	%d	%f
<b>A1</b>	C6-Cr10		1.8515					
		C6		69.99	41.80	58.20	0.01	
		Cr10		30.01	13.68	47.15	39.16	0.01
<b>B5</b>	C10-Cr22		1.8860					
		C10		70.71	43.00	56.99	0.01	
		Cr22		29.29	15.03	48.42	36.54	0.01
<b>B6</b>	C15-Cr16		1.8259					
		C15		69.42	40.29	59.71		
		Cr16		30.58	12.75	46.27	40.96	0.01
	C17-Cr16		1.8818					
		C17		68.65	45.14	54.86		
		Cr16		31.35	15.56	44.35	40.07	0.02
<b>B8</b>				Missing from output file				
<b>B9</b>	C15-W16		1.8270					
		C15		77.83	43.54	56.46		
		W16		22.17	14.55	47.48	37.82	0.15
	C17-W16		1.8835					
		C17		76.20	47.69	52.31		
		W16		23.80	16.26	45.80	37.79	0.14
<b>C11</b>	C11-Cr21		1.8876					
		C11		70.51	43.57	56.43	0.01	
		Cr21		29.49	15.07	48.48	36.44	0.01
<b>C14</b>	C11-W21							
		C11		Missing from output file				
		W21						
<b>D16</b>	C11-Cr19		1.8874					
		C11		70.54	43.46	56.53	0.01	
		Cr19		29.46	15.04	48.50	36.46	0.01
<b>D17</b>	C11-Cr19		1.8514					
		C11		70.01	41.47	58.53	0.01	
		Cr19		29.99	13.72	47.17	39.09	0.01
<b>D20</b>	C11-W19							
		C11		Missing from output file				
		W19						
<b>E24</b>	C12-Cr23		1.9251					
		C12		68.15	68.98	31.02		
		Cr23		31.85	17.38	49.57	33.03	0.02
<b>E25</b>	C12-W23							
		C12		Missing from output file				
		W23						

**Mono-metallic (*trans*-CO dissociated from TM)**

Complex	Bond	Atom	Occup	Polarization (%)	Hybridization of TM-C bonds		
				TM-C bonds	%s	%p	%d
<b>A1</b>	C6-Cr10		1.6845				
		C6 Cr10		25.99 74.01	0.09 0.00	99.90 0.05	0.01 96.92
<b>B5</b>	C10-Cr22		1.6529				
		C10 Cr22		20.50 79.50	0.00 0.00	99.99 2.93	
<b>B6</b>	C15-Cr16		1.8231				
		C15 Cr16		73.81 26.19	38.44 15.59	61.56 48.01	
	C17-Cr16		1.6080				
		C17 Cr16		33.31 66.69	0.00 0.00	99.98 0.60	0.02 99.40
<b>B8</b>	C10-W22		1.9626				
		C10 W22		67.91 32.09	42.85 27.55	57.14 5.79	0.01 66.59
<b>B9</b>	C15-W16		1.8284				
		C15 W16		80.32 19.68	41.43 16.98	58.57 47.33	
	C17-W16		1.6709				
		C17 W16		37.34 62.66	0.22 0.11	99.76 2.60	
<b>C11</b>	C11-Cr21		1.6577				
		C11 Cr21		21.61 78.39	0.00 0.00	99.99 3.50	
<b>C14</b>	C11-W21		1.9637				
		C11 W21		67.84 32.16	43.23 27.57	56.76 5.80	
<b>D16</b>	C11-Cr19		1.65773				
		C11 Cr19		21.41 78.59	0.00 0.00	99.99 3.40	
<b>D17</b>	C11-Cr19		1.6726				
		C11 Cr19		25.72 74.28	0.18 0.09	99.81 2.60	
<b>D20</b>	C11-W19		1.6303				
		C11 W19		28.59 71.41	0.00 0.00	99.99 4.74	
<b>E24</b>	C12-Cr23		1.6534				
		C12 Cr23		20.15 79.85	0.00 0.00	99.99 2.69	
<b>E25</b>	C12-W23		1.9615				
		C12 W23		68.19 31.81	42.98 27.57	57.01 5.96	

**Bi-metallic (all ligands attached)**

Complex	Bond	Atom	Occup	Polarization (%)	Hybridization of TM-C/TM <sup>I</sup> -C <sup>I</sup> bonds		
				TM-C/TM <sup>I</sup> -C <sup>I</sup> bonds	%s	%p	%d
<b>A2</b>	C6-Cr10		1.8478				
		C6 Cr10		69.06 30.94	42.84 13.93	57.15 46.12	39.94
	C21-Cr34		1.8479				
		C21 Cr34		69.04 30.96	42.84 13.95	57.16 46.08	39.96
<b>A3</b>	C6-W10		1.8466				
		C6 W10		77.10 22.90	45.76 15.71	54.24 46.31	37.84
	C21-W34		1.8465				
		C21 W34		77.14 22.86	45.72 15.70	54.28 46.38	
<b>A4</b>	C6-Cr10		1.8474				
		C6 Cr10		69.00 31.00	42.87 13.97	57.12 46.04	39.98
	C21-W34		1.8466				
		C21 W34		77.10 22.90	45.71 15.65	54.29 46.38	37.84
<b>B7</b>	C10-Cr22		1.8885				
		C10 Cr22		70.41 29.59	43.95 15.31	56.04 48.27	36.41
	C12-Cr41		1.8814				
		C12 Cr41		70.97 29.03	43.62 14.74	56.38 48.42	0.01 36.83
<b>B10</b>	C10-W22		1.8810				
		C10 W22		77.31 22.69	46.37 17.17	53.63 49.19	33.51
	C12-W41		1.8746				
		C12 W41		77.67 22.33	46.21 16.61	53.78 49.29	33.98
<b>C12</b>	C11-Cr21		1.8503				
		C11		68.58	42.36	57.64	
	C14-Cr36		1.8505				
		C14 Cr36		69.60 30.40	42.33 13.93	57.66 46.76	39.30
<b>C13</b>	C11-Cr21		1.8503				
		C11 Cr21		69.59 30.41	42.34 13.93	57.66 46.76	39.30
	C14-Cr36		1.8879				
		C14 Cr36		70.44 29.56	43.96 15.12	56.03 48.38	0.01 36.49
<b>C15</b>	C11-W21		1.8819				
		C11 W21		77.27 22.73	46.54 17.08	53.46 49.19	33.60
	C14-W36		1.8819				

<b>D18</b>	C11-Cr19	C14	77.27	46.54	53.46	
		W36	22.73	17.08	49.19	33.60
			1.8496			
		C11	69.44	42.52	57.48	
<b>D19</b>	C14-Cr35	Cr19	30.56	13.96	46.58	39.45
			1.8509			
		C14	69.77	42.11	57.88	
		Cr36	30.23	13.82	46.90	39.27
<b>D21</b>	C11-Cr19		1.8889			
		C11	70.43	44.13	55.87	0.01
		Cr19	29.57	15.22	48.39	36.38
			1.8488			
<b>D22</b>	C14-Cr35	C14	69.52	42.17	57.83	
		Cr35	30.48	13.76	46.68	39.55
			1.8822			
		C11	77.28	46.69	53.30	
<b>D23</b>	C11-W19	W19	22.72	17.12	49.15	33.60
			1.8469			
		C14	77.60	45.06	54.94	
		W35	22.40	15.67	47.49	36.71
<b>D22</b>	C11-Cr19		1.8894			
		C11	70.35	44.35	55.65	
		Cr19	29.65	15.29	48.35	36.35
			1.8407			
<b>D23</b>	C14-W35	C14	77.66	44.97	55.03	
		W35	22.34	15.64	47.56	36.66
			1.8895			
		C11	70.38	44.32	55.67	
<b>D23</b>	C11-W19	W19	29.62	15.28	48.36	36.35
			1.8470			
		C14	77.65	44.99	55.01	
		Cr35	22.35	15.64	47.54	36.69

---

**Bi-metallic (*trans*-CO dissociated from TM)**

Complex	Bond	Atom	Occup	Polarization (%)	Hybridization of TM-C/TM <sup>1</sup> -C <sup>1</sup>		
				TM-C/TM <sup>1</sup> -C <sup>1</sup> bonds	%s	bonds %p	%d
<b>A2</b>	C6-Cr10		1.6827				
		C6 Cr10		30.61 69.39	0.31 0.23	99.68 2.78	0.01 96.98
	C21-Cr34		1.8471				
		C21 Cr34		69.9 30.4	42.09 13.81	57.9 46.98	39.2
<b>A3</b>	C6-W10		1.6840				
		C6 W10		36.63 63.37	0.10 0.15	99.89 3.30	96.53
	C21-W34		1.8462				
		C21 W34		77.49 22.51	44.98 15.6	55.02 47.2	37.08
<b>A4</b>	C6-Cr10		1.6818				
		C6 Cr10		30.70 69.30	0.32 0.24	99.68 2.79	96.97
	C21-W34		1.8461				
		C21 W34		77.53 22.47	45.02 15.59	54.98 47.46	36.82
<b>B7</b>	C10-Cr22		1.9305				
		C10 Cr22		23.64 76.36	0.00 0.00	99.99 3.88	0.01 96.12
	C12-Cr41		1.8807				
		C12 Cr41		71.17 28.83	43.18 14.6	56.81 48.56	0.0 36.83
<b>C10</b>	C10-W22		1.9631				
		C10 W22		30.80 69.20	0.00 0.00	99.99 5.19	94.8
	C12-W41		1.8734				
		C12 W41		77.78 22.22	45.72 16.46	54.28 49.48	33.93
<b>C12</b>	C11-Cr21		1.8868				
		C11 Cr21		28.16 71.84	0.25 0.15	99.74 2.83	97.03
	C14-Cr36		1.8501				
		C14 Cr36		69.83 30.17	41.94 13.91	58.05 47.1	38.98
<b>C13</b>	C11-Cr21		1.6800				
		C11 Cr21		24.38 75.62	0.21 0.10	99.70 3.03	96.87
	C14-Cr36		1.8900				
		C14 Cr36		70.52 29.48	43.62 15.03	56.37 48.44	36.52
<b>C15</b>	C11-W21		1.9638				
		C11 W21		67.78 32.22	43.61 27.54	56.38 5.78	66.61

	C14-W36		Missing form output file				
		C14 W36					
<b>D18</b>	C11-Cr19		1.8800				
		C11 Cr19		28.07 71.93	0.02 0.00	99.98 2.64	97.32
	C14-Cr35		1.8506				
		C14 Cr35		70.11 29.89	41.57 13.71	58.43 47.25	39.03
<b>D19</b>	C11-Cr19		1.6570				
		C11 Cr19		23.56 76.44	0.00 0.00	99.99 3.76	96.24
	C14-Cr35		1.8481				
		C14 Cr35		69.79 30.21	41.76 13.72	58.23 47.08	39.18
<b>D21</b>	C11-W19		1.6163				
		C11 W19		29.06 70.90	0.00 0.00	99.98 1.09	95.71
	C14-W35		1.8466				
		C14 W35		77.80 22.19	45.06 15.67	54.94 47.49	36.71
<b>D22</b>	C11-Cr19		1.6591				
		C11 Cr19		24.09 75.90	0.00 0.00	99.99 1.09	95.71
	C14-W35		1.8465				
		C14 W35		77.80 22.21	44.63 15.59	55.37 47.88	36.41
<b>D23</b>	C11-W19		1.6446				
		C11 W19		30.86 69.10	0.00 0.00	99.98 4.71	95.28
	C14-Cr35		1.8506				
		C14 Cr35		70.00 30.02	41.80 13.77	58.20 47.19	39.02

**Bi-metallic (trans-CO dissociated from TM<sup>1</sup>)**

Complex	Bond	Atom	Occup	Polarization (%)	Hybridization of TM-C/TM <sup>1</sup> -C <sup>1</sup>		
				TM-C/TM <sup>1</sup> -C <sup>1</sup> bonds	% s	%p	%d
<b>A2</b>	C6-Cr10		1.8470				
		C6 Cr10		69.60 30.40	42.11 13.81	57.89 46.97	39.20
	C21-Cr34		1.6834				
		C21 Cr34		30.58 69.42	0.31 0.22	99.68 2.76	0.01 97.02
<b>A3</b>	C6-W10		1.8464				
		C6 W10		77.46 22.54	45.03 15.60	54.97 47.16	37.10
	C21-W34		1.6836				
		C21 W34		36.86 63.14	0.10 0.16	99.89 3.60	96.23
<b>A4</b>	C6-Cr10		1.8467				
		C6 Cr10		69.55 30.45	42.07 13.83	57.92 46.93	39.22
	C21-W34		1.8460				
		C21 W34		36.92 63.08	0.09 0.15	99.89 3.41	0.01 96.42
<b>B7</b>	C10-Cr22		1.8870				
		C10 Cr22		70.60 15.14	43.45 48.49	56.55 36.36	0.01 0.01
	C12-Cr41		1.6664				
		C12 Cr41		23.11 76.89	0.01 0.01	99.99 2.63	97.36
<b>C10</b>	C10-W22		1.6498	Missing from output file			
		C10 W22					
	C12-W41		1.6498				
		C12 W41		30.43 69.57	0.00 0.01	99.98 4.72	95.27
<b>C12</b>	C11-Cr21		1.8500				
		C11 Cr21		69.81 30.19	41.95 13.91	58.04 47.08	39.00
	C14-Cr36		1.6839				
		C14 Cr36		28.09 71.91	0.26 0.15	99.73 2.99	0.01 96.86
<b>C13</b>	C11-Cr21		1.8498				
		C11 Cr21		69.79 30.21	41.98 13.92	58.01 47.07	39.00
	C14-Cr36		1.6546				
		C14 Cr36		23.04 76.96	0.00 0.00	99.99 3.51	0.01 96.49
<b>C15</b>	C11-W21		1.9639	Missing from output file			
		C11 W21					
	C14-W36		1.9639				



<b>D18</b>	C11-Cr19	C14		67.80	43.61	56.39	
		W36	1.8498	32.20	27.55	5.79	66.66
		C11		69.75	42.07	57.93	
		Cr19		30.25	13.95	47.06	38.98
<b>D19</b>	C11- Cr19	C14-Cr35	1.6768				
		C14		28.34	0.16	99.84	
		Cr35	1.8879	71.66	0.09	2.81	97.10
<b>D21</b>	C11-W19	C11		70.55	43.70	56.30	0.01
		Cr19	1.6756	29.45	15.10	48.47	36.42
		C14-Cr35					
<b>D22</b>	C11-W35	C14		27.07	0.24	99.69	
		Cr35	1.8815	72.93	0.12	4.47	95.41
		C11		77.32	46.25	53.75	
<b>D23</b>	C11- W19	W19	1.9413	22.68	17.05	49.31	33.52
		C14-W35					
		C14		67.27	42.61	57.38	
<b>D22</b>	C11-Cr19	W35	1.8883	32.73	27.16	4.48	68.29
		C11		70.46	43.86	56.14	
		Cr19	1.6744	29.54	15.16	48.43	36.39
<b>D23</b>	C11- W19	C14		35.65	0.07	99.91	
		W35	1.8816	64.35	0.07	3.39	96.52
		C11		77.30	46.27	53.72	
<b>D23</b>	C14-Cr35	W19	1.8931	22.70	17.05	49.28	33.55
		C14		64.95	41.8	58.20	
		Cr35		35.05	13.77	47.19	39.02

1. Frisch, M. J.; Trucks, G. W.; Schlegel, H. B.; Scuseria, G. E.; Robb, M. A.; Cheeseman, R. J.; Scalmani, G.; Barone, V.; Mennucci, B.; Petersson, G. A.; Nakatsuji, H.; Caricato, M.; Li, X.; Hratchian, H. P.; Izmaylov, A. F.; Bloino, J.; Zheng, G.; Sonnenberg, J. L.; Hada, M.; Ehara, M.; Toyota, K.; Fukuda, R.; Hasegawa, J.; Ishida, M.; Nakajima, T.; Honda, Y.; Kitao, O.; Nakai, H.; Vreven, T.; Montgomery, J. A.; Peralta, Jr., J. E.; Ogliaro, F.; Bearpark, M.; Heyd, J. J.; Brothers, E.; Kudin, K. N.; Staroverov, V. N.; Kobayashi, R.; Normand, J.; Raghavachari, K.; Rendell, A.; Burant, J. C.; Iyengar, S. S.; Tomasi, J.; Cossi, M.; Rega, N.; Millam, J. M.; Klene, M.; Knox, J. E.; Cross, J. B.; Bakken, V.; Adamo, C.; Jaramillo, J.; Gomperts, R.; Stratmann, R. E.; Yazyev, O.; Austin, A. J.; Cammi, R.;

Pomelli, C.; Ochterski, J. W.; Martin, R. L.; Morokuma, K.; Zakrzewski, V. G.; Voth, G. A.; Salvador, P.; Dannenberg, J. J.; Dapprich, S.; Daniels, A. D.; Farkas, Ö.; Foresman, J. B.; Ortiz, J. V.; Cioslowski, J.; Fox, D. J. Gaussian 09, Revision D.01, Gaussian, Inc., Wallingford CT, **2009**. [http://www.gaussian.com/g\\_prod/g09.htm](http://www.gaussian.com/g_prod/g09.htm): date accessed 10 May **2015**.

**Supplementary document S11.** Donor-Acceptor interactions (NBO analysis)

**Mono-metallic (all ligands attached)**

	Donor NBO (i)		Acceptor NBO (j)		E <sup>2</sup> Kcal/mol	E(j) -E(i) a.u.	F(i,j) a.u.
<b>C1</b>	BD	C6-Cr10	BD*	Cr10-C13	57.48	0.91	0.103
<b>B5</b>	BD	C10-Cr22	BD*	Cr22-C25	52.59	0.92	0.098
<b>B6</b>	BD	C15-Cr16	BD*	Cr16-C23	68.07	0.89	0.110
	BD	C17-Cr16	BD*	Cr16-C23	58.95	1.21	0.129
<b>B8</b>	BD	C10-W22	BD*	W22-C25	69.45	1.21	0.129
<b>B9</b>	BD	C15-W16	BD*	W16-C23	69.45	1.21	0.129
	BD	C17-W16	BD*	W16-C23	115.17	1.37	0.175
<b>C11</b>	BD	C11-Cr21	BD*	Cr21-C23	53.26	0.93	0.099
<b>C14</b>	BD	C11-W21	BD*	W21-C23	52.71	0.95	0.099
<b>D16</b>	BD	C11-Cr19	BD*	Cr19-C21	53.26	0.93	0.099
<b>D17</b>	BD	C11-Cr19	BD*	Cr19-C21	57.11	0.91	0.102
<b>E24</b>	BD	C12-Cr23	BD*	Cr23-C24	53.01	0.92	0.098
<b>E25</b>	BD	C12-W23	BD*	W23-C24	Missing from output file		

**Bi-metallic (all ligands attached)**

	Donor NBO (i)		Acceptor NBO (j)		E <sup>2</sup> Kcal/mol	E(j) -E(i) a.u.	F(i,j) a.u.
<b>B2</b>	BD	C6-Cr10	BD*	Cr10-C13	59.07	0.92	0.104
	BD	C21-Cr34	BD*	Cr34-C36	59.15	0.92	0.104
<b>A3</b>	BD	C6-W10	BD*	W10-C13	92.21	1.37	0.157
	BD	C21-W34	BD*	W34-C36	87.52	1.35	0.152
<b>A4</b>	BD	C6-Cr10	BD*	Cr10-C13	58.99	0.92	0.104
	BD	C21-W34	BD*	W34-C36	87.86	1.35	0.152
<b>B7</b>	BD	C10-Cr22	BD*	Cr22-C25	53.30	0.93	0.099
	BD	C12-Cr41	BD*	Cr41-C42	51.75	0.92	0.097
<b>B10</b>	BD	C10-W22	BD*	W22-C25	Missing From output file		
	BD	C12-W41	BD*	W41-C42	103.04	1.30	0.161
<b>C12</b>	BD	C11-Cr21	BD*	Cr21-C23	58.24	0.92	0.104
	BD	C14-Cr36	BD*	Cr36-C37	58.15	0.90	0.104
<b>C13</b>	BD	C11-Cr21	BD*	Cr21-C23	58.19	0.92	0.104
	BD	C14-Cr36	BD*	Cr36-C37	53.59	0.93	0.099
<b>C15</b>	BD	C11-W21	BD*	W21-C23	Missing from output file		
	BD	C14-W36	BD*	W36-C37	95.47	1.31	0.155
<b>D18</b>	BD	C11-Cr19	BD*	Cr19-C21	58.57	0.92	0.141
	BD	C14-Cr35	BD*	Cr35-C37	57.78	0.92	0.103
<b>D19</b>	BD	C11-Cr19	BD*	Cr19-C21	56.57	8.07	0.91
	BD	C14-Cr35	BD*	Cr35-C37	58.36	0.92	0.104
<b>D21</b>	BD	C11-W19	BD*	W19-C21	95.85	1.30	0.155
	BD	C14-W35	BD*	W35-C37	79.91	1.34	0.145
<b>D22</b>	BD	C11-Cr19	BD*	Cr19-C21	53.51	0.94	0.0991
	BD	C14-W35	BD*	W35-C37	79.53	1.33	0.144
<b>D23</b>	BD	C11-W19	BD*	W19-C21	53.51	0.94	0.099
	BD	C14-Cr35	BD*	Cr35-C37	57.94	0.92	0.103

1. Frisch, M. J.; Trucks, G. W.; Schlegel, H. B.; Scuseria, G. E.; Robb, M. A.; Cheeseman, R. J.; Scalmani, G.; Barone, V.; Mennucci, B.; Petersson, G. A.; Nakatsuji, H.; Caricato, M.; Li, X.; Hratchian, H. P.; Izmaylov, A. F.; Bloino, J.; Zheng, G.; Sonnenberg, J. L.; Hada, M.; Ehara, M.; Toyota, K.; Fukuda, R.; Hasegawa, J.; Ishida, M.; Nakajima, T.; Honda, Y.; Kitao, O.; Nakai, H.; Vreven, T.; Montgomery, J. A.; Peralta, Jr., J. E.; Ogliaro, F.; Bearpark, M.; Heyd, J. J.; Brothers, E.; Kudin, K. N.; Staroverov, V. N.; Kobayashi, R.; Normand, J.; Raghavachari, K.; Rendell, A.; Burant, J. C.; Iyengar, S. S.; Tomasi, J.; Cossi, M.; Rega, N.; Millam, J. M.; Klene, M.; Knox, J. E.; Cross, J. B.; Bakken, V.; Adamo, C.; Jaramillo, J.; Gomperts, R.; Stratmann, R. E.; Yazyev, O.; Austin, A. J.; Cammi, R.; Pomelli, C.; Ochterski, J. W.; Martin, R. L.; Morokuma, K.; Zakrzewski, V. G.; Voth, G. A.; Salvador, P.; Dannenberg, J. J.; Dapprich, S.; Daniels, A. D.; Farkas, Ö.; Foresman, J. B.; Ortiz, J. V.; Cioslowski, J.; Fox, D. J. Gaussian 09, Revision D.01, Gaussian, Inc., Wallingford CT, **2009**. [http://www.gaussian.com/g\\_prod/g09.htm](http://www.gaussian.com/g_prod/g09.htm): date accessed 10 May **2015**.

**Supplementary document S12.** PCA worksheets

**Worksheet 1** = Mono-metallic compounds with all ligands attached (**PCA 1**)

	1	2	3	4	5	6	7	8	9	10	11	12
<b>A1</b>	-5.695	-5.772	-2.536	-0.601	3.159	2.681	68	32	0.46	0.37	0.30	0.07
<b>B5</b>	-5.663	-5.682	-2.333	-0.753	3.330	2.400	46	30	0.38	0.60	0.28	0.05
<b>B6</b>	-4.986	-5.297	-2.807	-0.879	2.179	3.484	72	13	0.65	0.50	0.08	0.29
<b>B8</b>	-5.485	-5.536	-2.474	-1.311	3.011	2.63	65	30	0.62	0.46	0.28	0.06
<b>B9</b>	-4.665	-5.137	-2.949	-1.168	1.716	4.223	68	13	0.60	0.37	0.13	0.27
<b>C11</b>	-5.836	-5.901	-2.747	-1.102	3.089	2.981	42	23	0.35	0.64	0.22	0.07
<b>C14</b>	-5.662	-5.717	-2.844	-1.494	2.818	3.209	64	23	0.61	0.45	0.30	0.05
<b>D16</b>	-5.758	-5.848	-2.674	-0.897	3.084	2.882	40	24	0.29	0.56	0.19	0.05
<b>A17</b>	-5.581	-5.684	-2.65	-0.988	2.931	2.889	62	22	0.33	0.26	0.28	0.05
<b>D20</b>	-5.594	-5.633	-2.779	-1.410	2.815	3.113	64	25	0.53	0.25	0.21	0.05
<b>E24</b>	-5.516	-5.788	-2.461	-0.875	3.055	2.604	19	26	0.17	0.64	0.25	0.02
<b>E25</b>	-5.462	-5.558	-2.562	-1.396	2.900	2.775	33	26	0.30	0.65	0.25	0.06
	13	14	15	16	17	18	19	20	21	22		
<b>A1</b>	1.8515	69.99	30.01	41.80	58.2	13.68	47.15	39.16	0.4703	-2.2894		
<b>B5</b>	1.8860	70.71	29.29	43.00	56.99	15.03	48.42	36.54	0.4736	-2.2775		
<b>B6</b>	1.8259	69.42	30.58	40.29	59.71	12.75	46.27	40.96	0.4669	-2.0576		
<b>B8</b>	1.8631	71.90	28.09	42.86	57.13	14.58	47.95	37.42	0.4859	-2.2699		
<b>B9</b>	1.8270	77.83	22.17	43.54	56.46	14.55	47.48	37.82	0.3097	-1.1886		
<b>C11</b>	1.8877	70.51	29.49	43.57	56.43	15.07	48.48	36.44	0.4796	-2.2824		
<b>C14</b>	1.8631	71.91	28.09	42.86	57.13	14.59	47.95	37.42	0.3251	-1.4374		
<b>D16</b>	1.8874	70.54	29.46	43.46	56.53	15.04	48.50	36.45	0.5074	-2.2735		
<b>A17</b>	1.8514	70.01	29.99	41.47	58.53	13.72	47.17	39.09	0.8328	-2.2837		
<b>D20</b>	1.8655	77.46	22.54	45.70	54.30	16.54	49.51	33.84	0.3234	-2.2792		
<b>E24</b>	1.8855	70.68	29.32	42.94	57.06	14.91	48.59	36.49	0.4708	-2.2830		
<b>E25</b>	1.8631	71.91	28.09	42.86	57.13	14.59	47.95	37.42	0.3207	-1.4480		

**Worksheet 2 = Mono-metallic compounds (*trans*-CO dissociated from M) PCA 2**

	1	2	3	4	5	6	7	8	9	10	11	12
<b>A1</b>	-5.151	-5.200	-2.128	-2.113	3.023	2.191	73	0.41	0.54	0.10	0.14	1.6845
<b>B5</b>	-5.186	-5.761	-2.300	-2.005	2.886	2.427	54	0.51	0.71	0.20	0.26	1.9247
<b>B6</b>	-4.576	-5.017	-2.515	-1.495	2.061	3.050	77	0.49	0.71	0.09	0.20	1.8231
<b>B8</b>	-4.991	-5.119	-2.524	-2.185	2.467	2.862	70	0.35	0.58	0.15	0.24	1.9626
<b>B9</b>	-4.134	-4.931	-2.683	-1.797	1.451	4.003	74	0.30	0.31	0.07	0.12	1.8284
<b>C11</b>	-5.397	-5.975	-2.499	-2.462	2.898	2.689	73	0.67	0.44	0.20	0.18	1.9290
<b>C14</b>	-5.193	-5.316	-2.700	-2.604	2.493	3.124	69	0.38	0.50	0.06	0.20	1.9637
<b>D16</b>	-5.338	-5.362	-2.470	-2.377	2.868	2.657	49	0.56	0.36	0.20	0.17	1.9288
<b>D17</b>	-5.106	-5.213	-2.335	-2.166	2.771	2.498	65	0.25	0.33	0.16	0.18	1.8903
<b>D20</b>	-5.130	-5.251	-2.660	-2.520	2.470	3.071	70	0.34	0.29	0.14	0.20	1.6304
<b>E24</b>	-5.132	-5.241	-2.362	-2.170	2.770	2.534	39	0.38	0.73	0.20	0.14	1.9248
<b>E25</b>	-5.063	-5.099	-2.587	-2.320	2.476	2.954	70	0.32	0.11	0.13	0.16	1.9615
	13	14	15	16	17	18	19	20	21			
<b>A1</b>	25.99	74.01	0.09	99.90	74.01	0.05	96.92	0.4509	-1.4123			
<b>B5</b>	66.55	33.45	42.31	57.68	22.35	17.91	59.73	0.4671	-1.4256			
<b>B6</b>	73.81	26.19	38.44	61.56	15.59	48.01	36.37	0.3567	-1.1732			
<b>B8</b>	67.91	32.09	42.85	57.14	27.55	5.79	66.59	0.3350	-0.8080			
<b>B9</b>	80.32	19.68	41.43	58.57	16.98	47.33	35.48	0.2364	-0.5040			
<b>C11</b>	66.35	33.65	42.83	57.17	22.54	17.81	59.64	0.4699	-1.4288			
<b>C14</b>	67.84	32.16	43.23	56.76	27.57	5.80	66.56	0.3333	-0.8033			
<b>D16</b>	66.38	33.62	42.76	57.24	22.52	17.84	59.62	0.4685	-1.4296			
<b>D17</b>	65.24	34.76	40.73	59.27	21.92	15.68	62.39	0.4864	-1.4095			
<b>D20</b>	28.59	71.41	0.00	99.99	0.00	4.74	95.25	0.3326	-0.8044			
<b>E24</b>	66.55	33.45	42.34	57.66	22.31	17.94	59.73	0.4693	-1.4284			
<b>E25</b>	68.19	31.81	42.98	57.01	27.57	5.96	66.41	0.3407	-0.8215			

**Worksheet 3 = Bi-metallic compounds with all ligands attached (PCA 3)**

	1	2	3	4	5	6	7	8	9	10	11	12	13		
A2	-5.800	-5.849	-3.303	-2.011	2.497	4.148	69	0	16	16	0.56	0.40	0.140		
A3	-5.562	-5.686	-3.454	-2.162	2.108	4.820	66	0	6	6	0.63	0.07	0.140		
A4	-5.786	-5.871	-3.453	-2.111	2.333	4.573	59	7	14	17	0.28	0.63	0.140		
B7	-5.864	-6.016	-3.074	-1.876	2.790	3.579	29	25	18	12	0.20	0.26	0.070		
C10	-5.705	-5.790	-3.273	-2.068	2.432	4.143	12	41	18	15	0.25	0.44	0.160		
C12	-5.897	-5.969	-3.367	-2.397	2.530	4.240	34	27	10	10	0.37	0.23	0.040		
C13	-5.882	-6.006	-3.358	-2.300	2.524	4.228	61	2	10	12	0.37	0.27	0.060		
C15	-5.873	-5.886	-3.484	-2.465	2.389	4.581	65	0	12	9	0.40	0.10	0.070		
D18	-5.765	-5.864	-3.240	-2.314	2.525	4.014	11	50	11	11	0.20	0.26	0.060		
D19	-5.768	-5.845	-3.188	-2.184	2.580	3.886	45	56	13	9	0.39	0.42	0.080		
D21	-5.532	-5.713	-3.313	-2.388	2.219	4.407	55	64	14	10	0.23	0.20	0.140		
D22	-5.571	-5.720	-3.181	-2.293	2.390	9.604	45	66	8	16	0.29	0.21	0.080		
D23	-5.516	-5.788	-2.461	-0.875	3.055	2.604	45	59	6	5	0.22	0.46	0.110		
	14	15	16	17	18	19	20	21	22	23	24	25	26	27	28
A2	0.200	1.848	1.848	69.06	30.94	69.04	30.96	42.84	57.15	13.93	46.12	39.94	42.84	57.16	13.95
A3	0.160	1.847	1.847	77.10	22.90	77.14	22.86	45.76	54.24	15.71	46.31	37.84	45.72	54.28	15.70
A4	0.170	1.847	1.847	69.00	31.00	77.10	22.90	77.10	22.90	46.04	39.98	0.01	45.71	54.29	15.65
B7	0.180	1.889	1.881	70.41	29.59	70.97	29.03	43.95	56.04	15.31	48.27	36.41	43.62	56.38	14.74
C10	0.180	1.881	1.875	77.31	22.69	77.67	22.33	46.37	53.63	17.17	49.19	33.51	46.21	53.78	16.61
C12	0.100	1.850	1.851	68.58	30.42	69.60	30.40	42.36	57.64	13.93	46.71	39.34	42.33	57.66	13.93
C13	0.200	1.850	1.888	69.59	30.41	70.44	29.56	42.34	57.66	13.93	46.76	39.30	43.96	56.03	15.12
C15	0.160	1.868	1.882	71.58	28.34	77.27	22.73	46.89	53.10	17.74	47.01	34.04	46.54	53.46	17.08
D18	0.200	1.850	1.851	69.44	30.56	69.77	30.23	42.52	57.48	13.96	46.58	39.45	42.11	57.88	13.82
D19	0.170	1.889	1.849	70.43	29.57	69.52	30.48	44.13	55.87	15.22	48.39	36.38	42.17	57.83	13.76
D21	0.150	1.882	1.847	77.28	22.72	77.60	22.40	46.69	53.30	17.12	49.15	33.60	45.06	54.94	15.67
D22	0.170	1.889	1.841	70.35	29.65	77.66	29.65	44.35	55.65	15.29	48.35	36.35	44.97	55.03	15.28
D23	0.020	1.890	1.847	70.38	29.62	77.65	22.35	44.32	55.67	15.28	48.36	36.35	44.99	55.01	15.64

	29	30	31	32	33	34
<b>A2</b>	46.08	39.96	0.482	-2.269	0.481	-2.268
<b>A3</b>	46.38	37.92	0.307	-1.369	0.307	-1.369
<b>A4</b>	46.38	37.84	0.482	-2.266	0.306	-1.372
<b>B7</b>	48.42	36.83	0.486	-2.270	0.470	-2.284
<b>C10</b>	49.29	33.98	0.328	-1.428	0.322	-1.431
<b>C12</b>	46.76	39.30	0.504	-2.275	0.504	-2.275
<b>C13</b>	48.38	36.49	0.503	-2.275	0.489	-2.278
<b>C15</b>	49.19	33.60	0.327	-1.433	0.327	-1.433
<b>D18</b>	46.90	39.27	0.507	-2.274	0.457	-2.277
<b>D19</b>	46.68	39.55	0.489	-2.275	0.466	-2.279
<b>D21</b>	47.49	36.71	0.328	-1.432	0.289	-1.373
<b>D22</b>	48.36	36.35	0.486	-2.275	0.287	-1.374
<b>D23</b>	47.54	36.69	0.486	-2.275	0.287	-1.374



**Worksheet 4 = Bi-metallic compounds (*trans*-CO dissociated from M) PCA 4**

	1	2	3	4	5	6	7	8	9	10	11	12	
A2	-5.396	-5.424	-3.029	-2.337	3.748	3.748	56	4	0.490	0.680	0.07	0.21	
A3	-5.150	-5.424	-3.251	-2.594	4.646	4.646	71	0	0.470	0.640	0.07	0.16	
A4	-5.483	-5.503	-3.196	-2.419	4.117	4.117	56	8	0.350	0.540	0.07	0.21	
B7	-5.634	-5.705	-2.968	-2.748	3.469	3.469	60	4	0.510	0.560	0.06	0.20	
C10	-5.382	-5.554	-3.076	-2.904	3.878	3.878	66	2	0.540	0.130	0.24	0.13	
C12	-5.481	-5.595	-3.139	-2.506	3.966	3.966	66	1	0.610	0.580	0.05	0.20	
C13	-5.471	-5.601	-3.154	-2.492	4.013	4.013	66	1	0.500	0.380	0.06	0.20	
C15	-5.463	-5.608	-3.309	-2.943	4.465	4.465	70	0	0.690	0.430	0.08	0.16	
D18	-5.446	-5.581	-3.023	-2.464	3.700	3.700	50	10	0.420	0.460	0.08	0.20	
D19	-5.446	-5.581	-3.023	-2.464	2.982	3.700	50	10	0.220	0.310	0.06	0.19	
D21	-5.411	-5.463	-3.130	-2.901	3.998	3.998	46	18	0.410	0.230	0.06	0.16	
D22	-5.477	-5.572	-2.992	-2.728	3.608	3.608	5	55	0.300	0.180	0.05	0.20	
D23	-5.164	-5.388	-3.136	-3.020	4.246	4.246	8	48	0.410	0.250	0.08	0.06	
	13	14	15	16	17	18	19	20	21	22	23	24	25
A2	1.883	1.847	64.150	35.850	69.900	30.400	41.430	58.570	22.320	15.130	62.54	42.09	57.90
A3	1.937	1.846	67.080	32.920	77.490	22.510	42.950	57.040	27.240	4.420	68.27	44.98	55.02
A4	1.882	1.846	64.140	35.860	77.530	22.470	41.420	58.570	22.330	15.130	62.53	45.02	54.98
B7	1.931	1.881	23.640	76.360	71.170	28.830	0.000	99.990	0.000	3.880	96.12	43.18	56.81
C10	1.963	1.873	30.800	69.200	77.780	22.220	0.000	99.990	0.000	5.190	94.80	45.72	54.28
C12	1.887	1.850	28.160	71.840	69.830	30.170	0.250	99.740	0.150	2.830	97.03	41.94	58.05
C13	1.684	1.887	24.380	75.620	70.520	29.480	0.210	99.700	0.100	3.030	96.87	43.62	56.37
C15	1.964	1.856	67.780	32.220	68.928	31.097	43.610	56.380	27.540	5.780	66.61	43.41	56.58
D18	1.878	1.851	28.070	71.930	70.110	29.890	0.020	99.980	0.000	2.640	97.32	41.57	58.43
D19	1.657	1.848	23.560	76.440	17.230	82.770	0.000	99.990	0.000	3.760	96.24	41.76	58.23
D21	1.616	1.847	29.060	70.940	77.810	22.190	0.000	99.980	0.000	1.090	95.71	44.63	55.37
D22	1.659	1.847	24.090	75.910	77.790	22.210	0.000	99.990	0.000	3.830	96.17	44.65	55.35
D23	1.645	1.851	30.860	69.140	69.980	30.020	0.000	99.980	0.000	4.710	95.28	41.80	58.20

	26	27	28	29	30	31	32
<b>A2</b>	13.81	46.98	39.20	0.459	-1.381	0.474	-2.282
<b>A3</b>	15.60	47.20	37.08	0.292	-0.721	0.304	-1.379
<b>A4</b>	15.59	47.46	36.82	0.459	-1.379	0.304	-1.383
<b>B7</b>	14.60	48.56	36.83	0.471	-1.415	0.462	-2.286
<b>C10</b>	16.46	49.48	33.93	0.328	-0.785	0.317	-1.434
<b>C12</b>	13.91	47.10	38.98	0.488	-1.397	0.499	-2.279
<b>C13</b>	15.03	48.44	36.52	0.488	-1.396	0.485	-2.280
<b>C15</b>	14.87	47.71	37.45	0.327	-0.789	0.325	-1.435
<b>D18</b>	13.71	47.25	39.03	0.494	-1.392	0.450	-2.284
<b>D19</b>	13.72	47.08	39.18	0.473	-1.416	0.461	-2.283
<b>D21</b>	16.62	47.90	36.35	0.325	-0.784	0.285	-1.378
<b>D22</b>	15.59	47.88	36.41	0.469	-1.414	0.285	-1.379
<b>D23</b>	13.77	47.19	39.02	0.326	-0.786	0.453	-2.281

**Worksheet 5 = Bi-metallic compounds (*trans*-CO dissociated from M<sup>1</sup>) PCA 5**

	1	2	3	4	5	6	7	8	9	10	11	12
A2	-5.659	-5.783	-2.845	-2.68	2.814	3.212	18	48	0.42	0.59	0.15	0.26
A3	-5.408	-5.439	-3.033	-2.866	2.375	3.750	61	4	0.44	0.22	0.15	0.05
A4	-5.453	-5.651	-2.932	-2.826	2.521	3.486	7	60	0.25	0.59	0.05	0.13
B7	-5.615	-5.678	-2.991	-2.706	2.624	3.528	5	56	0.19	0.24	0.07	0.12
C10	-5.377	-5.565	-3.100	-2.892	2.277	3.945	2	63	0.38	0.15	0.22	0.11
C12	-5.491	-5.617	-3.139	-2.524	2.352	3.958	2	66	0.35	0.20	0.07	0.11
C13	-5.676	-5.844	-3.147	-2.753	2.529	3.848	13	42	0.20	0.35	0.07	0.11
C15	-5.475	-5.606	-3.308	-2.944	2.167	4.450	0	71	0.35	0.44	0.13	0.14
D18	-5.377	-5.485	-3.025	-2.339	2.352	3.752	1	67	0.33	0.22	0.08	0.18
D19	-5.37	-5.446	-2.982	-2.332	2.388	3.651	1	67	0.48	0.5	0.16	0.21
D21	-5.109	-5.407	-3.132	-2.551	1.977	4.294	0	71	0.15	0.15	0.16	0.14
D22	-5.139	-5.396	-3.159	-2.566	1.98	4.347	0	71	0.28	0.22	0.15	0.14
D23	-4.938	-5.006	-3.109	-2.092	1.829	4.426	0	62	0.27	0.27	0.18	0.08

	13	14	15	16	17	18	19	20	21	22	23	24	25
A2	1.8828	1.6834	64.15	35.85	30.58	69.42	41.42	58.57	22.34	15.15	62.50	0.31	99.68
A3	1.8465	1.9381	77.46	22.54	66.99	33.01	45.03	54.97	15.60	47.16	37.10	0.10	99.89
A4	1.8467	1.9387	69.55	30.45	66.96	33.04	42.07	57.92	13.83	46.93	39.22	42.92	57.08
B7	1.8870	1.9166	70.60	29.40	66.46	33.54	43.45	56.55	15.14	48.49	36.36	43.23	56.77
C10	1.8231	1.9568	57.18	42.82	67.85	32.15	32.03	67.96	21.02	32.15	55.87	43.84	56.15
C12	1.6007	1.8876	17.04	82.96	64.76	35.24	0.11	99.89	99.89	0.13	99.85	41.22	58.78
C13	1.6005	1.6546	17.20	82.80	66.19	33.81	0.11	99.89	0.030	0.13	99.84	43.10	56.90
C15	1.8231	1.9639	57.18	42.82	67.80	32.20	32.03	67.96	21.02	32.15	55.87	43.61	56.39
D18	1.8500	1.8908	17.40	82.60	65.30	34.70	0.11	99.89	0.030	0.16	99.81	41.19	58.81
D19	1.8880	1.8946	70.55	29.45	63.36	36.64	43.70	56.30	15.10	48.47	36.42	41.27	58.73
D21	1.8816	1.9413	77.32	22.68	67.27	32.73	46.25	53.75	17.05	49.31	33.52	42.61	57.38
D22	1.8884	1.9407	70.46	29.54	67.24	32.76	43.86	56.14	15.16	48.43	36.39	42.53	57.47
D23	1.8816	1.8931	77.30	22.70	64.95	35.05	46.27	53.72	17.05	49.28	33.55	41.42	58.58

	26	27	28	29	30	31	32
<b>A2</b>	0.22	2.76	97.02	0.4747	-2.28234	0.4588	-1.3814
<b>A3</b>	0.16	3.60	96.23	0.3029	-1.3782	0.2894	-0.7193
<b>A4</b>	27.25	4.39	68.29	0.4734	-2.2792	0.2885	-0.7215
<b>B7</b>	22.39	17.96	59.64	0.4781	-2.2734	0.4643	-1.4190
<b>C10</b>	27.59	5.73	66.62	0.3226	-1.4321	0.3266	-0.7892
<b>C12</b>	22.13	15.35	62.50	0.4994	-2.2791	0.4874	-1.3982
<b>C13</b>	22.57	17.69	59.73	0.4996	-2.2785	0.4742	-1.4180
<b>C15</b>	27.55	5.79	66.59	0.3252	-1.4348	0.3272	-0.7892
<b>D18</b>	22.08	16.04	61.87	0.5012	-2.2783	0.4342	-1.3879
<b>D19</b>	22.69	14.57	62.72	0.4832	-2.2777	0.4426	-1.3930
<b>D21</b>	27.16	4.48	68.29	0.3250	-1.4352	0.2792	-0.7233
<b>D22</b>	27.30	4.45	68.19	0.4809	-2.2787	0.2788	-0.7241
<b>D23</b>	21.93	15.71	62.35	0.3250	-1.4355	0.4374	-1.3904

**Table S11.1.** Chemical properties used in principal component analysis; TM-C bond (TM-C) is used for both mono-and bi-metallic complexes, while TM<sup>1</sup>-C<sup>1</sup> is used to describe the second TM-C bond in bi-metallic complexes as indicated in **Chart 3.1**.

1. E <sub>HOMO</sub> (eV)	19. C <sup>1</sup> % polarization
2. E <sub>HOMO-1</sub> (eV)	20. TM <sup>1</sup> % polarization
3. E <sub>LUMO</sub> (eV)	21. %s orbital hybridization of carbene C
4. E <sub>LUMO+1</sub> (eV)	22. %p orbital hybridization of carbene C
5.  E <sub>HOMO</sub> – E <sub>LUMO</sub>   energy gap	23. %s orbital hybridization of metal TM
6. Electrophilicity index	24. %p orbital hybridization of metal TM
7. TM% contribution to HOMO	25. %d orbital hybridization of metal TM
8. TM <sup>1</sup> % contribution to HOMO	26. %s orbital hybridization of carbene C <sup>1</sup>
9. Carbene C% contribution to LUMO	27. %p orbital hybridization of carbene C <sup>1</sup>
10. Carbene C <sup>1</sup> % contribution to LUMO	28. %s orbital hybridization of metal TM <sup>1</sup>
11. Σ(AOC) of HOMO	29. %p orbital hybridization of metal TM <sup>1</sup>
12. Σ(AOC) of HOMO-1	30. %d orbital hybridization of metal TM <sup>1</sup>
13. Σ(AOC) of LUMO	31. NPA charge of carbene C
14. Σ(AOC) of LUMO+1	32. NPA charge of metal TM
15. Occupancy of TM-C bond	33. NPA charge of carbene C <sup>1</sup>
16. Occupancy of TM <sup>1</sup> -C <sup>1</sup> bond	34. NPA charge of metal TM <sup>1</sup>
17. C% polarization	
18. TM% polarization	